



**Nye County Nuclear Waste Repository Project Office
Independent Scientific Investigations Program Final Report,
Fiscal Years 2002 – 2006**

NWRPO-2010-01

Prepared for:
U.S. Department of Energy

Prepared by
Nuclear Waste Repository Project Office, Grant No. DE-FC28-02RW-12163

September 2010

DISCLAIMER

This report was prepared by the Nye County Nuclear Waste Repository Project Office, pursuant to a Cooperative Agreement funded by the U.S. Department of Energy, and neither Nye County nor any of its contractors or subcontractors nor the U.S. Department of Energy, nor any person acting on behalf of either, assumes any liabilities with respect to the use of, or for damages resulting from the use of, any information, apparatus, method, or process disclosed in this report. Reference herein to any specific commercial product, process, or service by trade name, trademark, manufacturer, or otherwise, does not necessarily constitute or imply its endorsement, recommendation, or favoring by the U.S. Department of Energy or Nye County. The views and opinions of authors expressed herein do not necessarily state or reflect those of the U.S. Department of Energy.

CONTENTS

1.0 INTRODUCTION	15
Background.....	15
Program Purpose and Objectives.....	16
1.3 Quality Assurance Requirements.....	17
1.4 Publication of Data and Analyses	18
1.5 Report Organization	18
2.0 DRILLING, CORING, SAMPLING, LOGGING, WELL CONSTRUCTION, AND TESTING	18
2.1 Overview of Drilling and Coring Methods	19
2.1.1 Description of Drilling Methods	20
2.1.1.1 Small Diameter Air Rotary-Reverse Circulation Methods	20
2.1.1.2 Intermediate Diameter Air Rotary-Reverse Circulation Methods	21
2.1.1.3 Casing Advance Methods	22
2.1.1.4 Dual Rotary-Casing Advance Methods	23
2.1.1.5 Flooded Mud Methods.....	24
2.1.1.6 Mud Rotary Methods	24
2.1.1.7 Air Rotary Methods.....	24
2.1.2 Description of Coring Methods	24
2.1.2.1 Drive Core Methods	24
2.1.2.2 Sonic Core Methods	25
2.2 Geologic Sampling, Logging, and Testing	26
2.2.1 Geologic Sampling.....	26
2.2.1.1 Drill Cuttings.....	26
2.2.1.2 Drive Core	27
2.2.1.3 Sonic Core	28
2.2.2 Geologic and Photographic Logging.....	29
2.2.3 Laboratory and Field Results	30
2.2.3.1 Phase III.....	30
2.2.3.2 Phase IV	31
2.2.3.3 Phase V.....	33
2.3 Well Completion and Development.....	35
2.3.1 Well Completion Overview.....	35
2.3.1.1 Completion Procedures Used in the Majority of Phase III Wells and all Phase IV and V Boreholes.....	36
2.3.1.2 Completion of Phase III Boreholes 10P, 18P, and 22PA	37
2.3.1.3 Completion of Westbay® Packer and Instrument Monitoring Systems in Phase III Monitor Wells	38
2.3.2 Well Development.....	38
2.3.2.1 Development of Multiple-Screen Monitor Wells 10S, 19IM1, and 22S.....	39
2.3.2.2 Development of Piezometers 23P and 28P	39
2.4 Borehole Lithology	39
2.4.1 Summary Lithologic Logs	39
2.4.1.1 Phase III	39
2.4.1.2 Phase IV	40

2.4.1.3	Phase V	41
2.4.2	Borehole Geophysics	43
2.4.3	Cross Sections.....	45
2.4.3.1	Phase III	45
2.4.3.2	Phase IV	46
2.4.3.2.1	Phase IV Cross Section A–A’	47
2.4.3.2.2	Phase IV Conceptual Cross Section B–B’	47
2.4.3.2.3	Phase IV Conceptual Cross Section C–C’	48
2.4.3.2.4	Phase IV Cross Section Interpretation.....	48
2.4.3.3	Phase V	49
2.4.3.3.1	Phase V Cross Section A-A’	50
2.4.3.3.2	Phase V Cross Section B-B’	53
2.4.3.3.3	Phase V Cross Section Interpretations	55
3.0	REGIONAL GEOLOGIC CHARACTERIZATION	57
3.1	Surface Geophysics.....	57
3.2	Structural Investigation of Western Rock Valley, Specter Range Region, and Northern Spring Mountains	57
3.2.1	Introduction and Overview of Results.....	57
3.2.2	Field Mapping and Reconnaissance	59
3.2.3	Results and Discussion from Field Studies and Analyses.....	59
3.2.3.1	Folds	60
3.2.3.2	Stratigraphic Detachments	61
3.2.3.3	Brecciation.....	62
3.2.3.4	Thrust Faults.....	62
3.2.3.5	Left-Lateral Strike-Slip Faults.....	62
3.2.3.6	Rock Valley Fault and Associated Normal Faults	63
3.2.3.7	Mount Shader Basin	63
3.2.3.8	Mesozoic Features	63
3.2.3.9	Development of the Yucca Mountain Pull-Apart.....	64
3.2.3.10	Sequence of Deformation	64
3.2.4	Summary and Conclusions	64
4.0	WATER LEVEL MONITORING	66
4.1	Introduction and Background	66
4.2	Devils Hole Workshops	66
4.3	Data Collection	66
4.4	Growth and Decay of Groundwater Mounds.....	67
4.5	Regional Potentiometric Map	68
4.6	Groundwater Discharge in Amargosa Desert	69
5.0	GROUNDWATER CHEMISTRY	70
5.1	Groundwater Sampling and Analysis	70
5.2	Results and Trend Analyses.....	70
5.2.1	Tertiary Diagram Trends in EWDP Data	71
5.2.2	Principle Component Factor Analysis Method	71
5.2.3	PCFA Statistical Results	72

5.2.4	Supporting Data and Analyses	73
Chloride and TDS		73
Carbon-14		73
Oxygen-18 and Hydrogen-2		74
5.2.5	Conclusions from Analysis of Groundwater Chemistry	75
5.3	Engineered Barrier System Groundwater Chemistry Modeling	75
6.0	AQUIFER TESTING.....	76
6.1	Methods and Procedures	77
6.1.1	Monitoring Instrumentation and Pump Spinner Logging Methods	77
6.1.2	Data Analysis Methods	78
6.1.3	Site 22 Test Wells and Approach	78
6.1.4	Site 19 Test Wells and Approach	79
6.1.5	Site 10 Test Wells and Approach	80
6.2	Test Results	80
6.2.1	Static Spinner Logging	80
6.2.2	Pump Spinner Logging	80
6.2.3	Constant Discharge Rate Pump Tests	81
7.0	TRACER TESTING	82
7.1	Overview of Tracer Test Methods and Procedures	82
7.1.1	Single-Well Tests	83
7.1.2	Cross-Hole Well Tests.....	84
7.2	Tracer Testing Results	85
7.2.1	Cross-Hole Well Test Results	85
7.2.2	Single-Well Tests Results	88
8.0	VENTILATION RELATED MODELING STUDIES.....	89
8.1	Task 1: A Numerical Verification Test of the Correctness of MULTIFLUX (FY02)	89
8.1.1	Task 1 Purpose and Procedures.....	90
8.1.2	Task 1 Results and Conclusions.....	90
8.2	Task 2: A Preliminary MULTIFLUX Study of Temperature and Relative Humidity Variations in a Conceptual Yucca Mountain Repository Design (FY02)	91
8.2.1	Task 2 Purpose and Procedures.....	91
8.2.2	Task 2 Results and Conclusions.....	91
8.3	Task 3: Preliminary MULTIFLUX Sensitivity Studies (FY02)	92
8.3.1	Task 3 Purpose and Procedures.....	92
8.3.2	Task 3 Results and Conclusions.....	92
8.4	Task 4: Model Update and Baseline Case Simulation (FY03 - FY04).....	92
8.4.1	Task 4 Purpose and Procedures.....	92
8.4.2	Task 4 Results and Conclusions.....	92
8.5	Task 5: Pre-Closure Time Study (FY03 - FY04).....	93
8.5.1	Task 5 Purpose and Procedures.....	93
8.5.2	Task 5 Results and Conclusions.....	93
8.6	Task 6: Barometric Pressure Pumping Study (FY03 - FY04)	94
8.6.1	Task 6 Purpose and Procedures.....	94
8.6.2	Task 6 Results and Conclusions.....	94

8.7	Task 7: Fate of Condensation Study (FY03 - FY04)	95
8.7.1	Task 7 Purpose and Procedures	95
8.7.2	Task 7 Results and Conclusions	95
8.8	Task 8: Laboratory Test Preparation (FY03 - FY04)	95
8.9	Task 9: Examine the Potential Significance of Water Vapor Migration Between the Network of Drifts for the Baseline Repository Design (FY05 - FY06)	96
8.9.1	Model update	96
8.9.2	One-directional air flow studies	96
8.9.3	Recirculation air flow studies	96
8.9.4	Task 9 Conclusions	99
8.10	Task 10: Barometric Pressure Fluctuation Studies with a Refined Model (FY05 – FY06)	99
8.10.1	The Effect of Revised Model Assumptions on Moisture Influx and Condensation	99
8.10.2	Task 10 Conclusions	100
8.11	Task 11: Long-Term, Forced Ventilation Studies (FY05 – FY06)	101
8.11.1	Task 11 Modeling Procedures and Results	101
8.11.2	Task 11 Conclusions	101
8.12	Task 12: In-rock Vapor Flow Studies (FY05 – FY06)	102
8.12.1	Task 12 Description of Modeling and Results	102
8.12.2	Task 12 Conclusions	103
9.0	SUMMARY OF MAJOR FINDINGS AND RECOMMENDATIONS	104
9.1	Drilling, Sampling, Logging, Well Construction, and Testing	104
9.1.1	Major Findings	104
9.1.1.1	Drilling	104
9.1.1.2	Geologic and Borehole Logging	106
9.1.1.3	Laboratory Measurements on Geologic Samples and Drilling and Sampling Impacts	108
9.1.1.3.1	Laboratory Tests on Alluvial Core Samples: PSD's, Hydrometer and Atterberg Limit Data	108
9.1.1.3.2	Laboratory Tests on Drill Cuttings: PSD's, Hydrometer and Atterberg Limit Data	109
9.1.1.3.3	Gravimetric Water Content Data	111
9.1.1.3.5	Dry Bulk Density and Porosity Tests on Core Runs	112
9.1.1.3.6	Field Saturated Hydraulic Conductivity Tests at Site 19	114
9.1.1.4	Trends in Lithostratigraphy	114
9.1.1.4.3	Summary Lithology Log – Phase V	116
	Sonic corehole 19PB, located approximately 3 miles downstream from 22PC in the Fortymile Wash flow system, shows similar trends in gravel and sand units (NWRPO, 2009) as described above for 22PC	117
9.1.1.5	Borehole Geophysical Logging	117
9.1.1.5.1	Gravity and Magnetic Features – Phase IV	118
9.1.1.6	Geologic Interpretations from Drilling and Geophysical Data Phase IV	118
9.1.1.7	Geologic Interpretations from Drilling and Geophysical Data Phase V	119
9.1.2	Recommendations	119
9.1.2.1	Phase III	119

9.1.2.2	Phase IV	120
9.1.2.3	Phase V	121
9.2	Regional Geologic Characterization Major Findings and Recommendations	122
9.3	Water Level Monitoring Major Findings and Recommendations	122
9.4	Water Chemistry	123
9.4.1	Major Findings	123
9.4.2	Recommendations	124
9.5	Aquifer Testing	124
9.5.1	Major Findings	124
9.5.2	Recommendations	125
9.6	Tracer Testing	125
9.6.1	Major Findings	125
9.6.2	Recommendations	126
9.7	Ventilation Studies	126
9.7.1	Major Findings	126
9.7.2	Recommendations	127
10.0	REFERENCES	128

FIGURES

- 1.1-1 Early Warning Drilling Program Region
- 2.0-1 Early Warning Drilling Program Well Locations by Phase
- 2.3-1 Typical Monitor Well Completion Diagram
- 2.3-2 Schematic Single-String Piezometer Completion Diagram for 16P
- 2.3-3 Dual-String Piezometer Completion Diagram for 22PC
- 2.3-4 Triple-String Piezometer Completion Diagram for 32P
- 2.3-5 Typical Piezometer Well Completion Diagram
- 2.4-1 Geologic Map of the Yucca Mountain Area
- 2.4-2 Phase V Geologic Cross Section A-A'
- 2.4-3 Phase V Geologic Cross Section B-B'
- 3.2-1 Generalized regional geologic map of southern Nevada data modified from Raines and others, (1996) geology modified from Stewart and Carlson, (1974)
- 3.2-2 Photograph of Crater Flat region that shows Early Warning Drilling Program well sites
- 3.2-3 Hydrogeologic map of the bedrock aquifer in southern Nevada
- 3.2-4 Hydrogeologic cross-section across the northern Spring Mountains
- 3.2-5 Field photos of the major detachment in the northern Spring Mountains: (A) hanging wall, (B) fault contact, and (C) footwall
- 3.2-6 Stratigraphic columns that show: a) stratigraphic units, lithologies, and thicknesses of Paleozoic and Neoproterozoic strata in the Northern Spring Mountains and the Specter Range b) the thicknesses of units missing (shown in gray) among detachments c) stratigraphic column showing the detachments within the study area
- 3.2-7 Nopah breccia samples from the hanging wall of the major detachment in the Spring Mountains
- 3.2-8 Index map of 2001 structural investigations east of Yucca Mountain along Jackass Flats Road
- 3.2-9 Aerial photo depicting folds in Tertiary strata of Pavits Spring east of Yucca Mountain along Jackass Flats Road
- 3.2-10 Photo showing brecciated Nopah Formation along the Point of Rocks detachment
- 3.2-11 Working cross-section of folds in Tertiary strata of Pavits Spring east of Yucca Mountain from south to north
- 3.2-12 Schematic block diagram of part of study area
- 3.2-13 Structure map of northeastern Specter Range
- 3.2-14 Geologic Map with major faults of the southwestern part of the Nevada Test Site: Northern Spring Mountains, Jackass Flats, Crater Flat, Bare Mountain and southeastern Amargosa Valley

- 3.2-15 Diagrams showing the uninterpreted (top) and interpreted (middle) detail of the most easterly segment of the USGS seismic line AV-1
- 3.2-16 Stratigraphic column showing a measured section of exposed Miocene deposits within the eastern subbasin of the Mt. Shader basin
- 3.2-17 Photographs that show outcrops of Miocene basin deposits (A and B); and rocks sampled from Miocene basin units (C, D and E)
- 3.2-18 Equal area lower hemisphere stereogram of poles to bedding, folds, and slickenlines from the northern Spring Mountains
- 4.5-1 Regional Potentiometric Map with 100 meter contour interval
- 4.5-2 Nye County 2004 Baseline Potentiometric Map with 328 ft (100 m) contour interval
- 4.5-3 Pahrump Valley Potentiometric Maps
- 5.2-1 Piper Plot of Nye County Well Data
- 5.2-2 Contours of concentration in milligrams per liter with a thick contour at the dataset average and with maroon contours over Fortymile Wash. a) Ground water total dissolved solids; b) Ground water chloride
- 5.2-3 Principal component analysis biplot with samples grouped into seven hydrochemical facies and relevant major ions
- 5.2-4 Factor 1 contours shown with well groupings and potential flow paths
- 5.2-5 ^{14}C age dates adjusted with ^{13}C data
- 5.2-6 $\delta^{18}\text{O}$ data contoured over the Digital Elevation Model
- 5.2-7 ^2H versus ^{18}O groundwater values beneath Fortymile Wash, the Amargosa River, and the junction of the two, plotted against the GMWL
- 5.3-1 Flow separation of anions
- 6.0-1 Location of Sites 19, 10, and 22 in relation to other nearby EDWP wells and the proposed Yucca Mountain repository site
- 6.1-1 Site 22 Layout for Aquifer Tests
- 6.1-2 Location of Pump and Observation Wells at the Site 19 ATC
- 6.1-3 Location of Pump (10S) and Observation (10P) Wells at Site 10
- 7.1-1 Surface layout for tracer tests at Site 22
- 7.2-1 Alternative calculated injected tracer mass normalized tracer response curves for injection in 22PA Zone 2
- 7.2-2 Mass normalized tracer response curves for injection in 22PC Zone 2
- 7.2-3 Aerial view of Site 22 and the channel system observed in nearby Fortymile Wash
- 7.2-4 MODFLOW model geometry for Zone 2 at Site 22 in map view
- 7.2-5 Calibration match obtained for 2,6-DFBA (cross-hole test 2)
- 7.2-6 Mass normalized tracer response curves indicating oxidizing conditions at Site 22

- 7.2-7 Nearly identical mass normalized tracer recovery curves indicate no diffusion into stagnant layers
- 7.2-8 Calibration match obtained for iodide on first single-well push/pull tracer test
- 8.1-1 Wall temperature history comparison for Solutions 1 through 4 at 1m, 250m and 500m distance along the airway
- 8.2-1 A three-drift section of an emplacement panel of 26 drifts with the peripheral tunnels, the intake and exhaust shafts, and the surrounding rockmass.
- 8.2-2 Pre- and post-closure wall temperature (a) and wall relative humidity (b) distributions in time and space
- 8.4-1 Rockmass domain around an emplacement drift in Panel 2
- 8.4-2 Computational fluid dynamics model configuration in the airway showing repeated sequence of eight waste packages in an emplacement drift (a), schematic diagram of pre-closure powered ventilation (b), and schematic diagram of post-closure natural air movement with axial dispersion (c)
- 8.4-3 Drift wall temperature (a) and relative humidity distributions (b) in time and space
- 8.4-4 Axial Distribution of Drift Wall Condensation Rate and Temperature at Selected Post-Closure Time Divisions
- 8.5-1 Drift wall temperature (a) and relative humidity distributions (b) in time and space with 300-year pre-closure
- 8.5-2 Axial Distribution of Drift Wall Condensation Rate and Temperature at Selected Time Divisions for 300-Year Pre-Closure Ventilation
- 8.6-1 Effect of Barometric Pressure Fluctuation on Drift Moisture Inflow (a) and Condensation Rate (b) and Maximum and Minimum Temperature (c)
- 8.7-1 Comparison of drift wall moisture fluxes
- 8.9-1 Air flow variation with time, used in the one-dimensional air flow studies
- 8.9-2 Temperature and relative humidity variations at year 500 under two different air flow directions in the emplacement drift
- 8.9-3 Definition of horizontal and vertical velocity components at a given cross section under the drip shield
- 8.9-4 Definition of horizontal and vertical velocity components at a given cross section outside the drip shield
- 8.9-5 Drift-scale natural air flow patterns in one emplacement drift
- 8.9-6 Air flow velocity variation in the horizontal circulation direction along the emplacement drift (a) inside and (b) outside the drip shield at year 1000
- 8.9-7 Vertical in-drift velocities along the drift length (a)inside and (b)outside the drip shield at year 1000
- 8.9-8 Equivalent dispersion coefficient at three time periods

- 8.9-9 Temperature, relative humidity, and rate of condensation distributions along the drift length for selected post-closure time periods at the roof segment of the drift wall
- 8.9-10 Temperature, relative humidity, and rate of condensation distributions along the drift length for selected post-closure time periods at the sidewall segment of the drift wall
- 8.9-11 Temperature, relative humidity, and rate of condensation distributions along the drift length for selected post-closure time periods at the floor segment of the drift wall over the invert
- 8.9-12 Temperature, relative humidity, and rate of condensation distributions along the drift length for the floor segment of the drift wall for two post-closure time periods: year 1000 (a); and year 5000 (b)
- 8.9-13 Sensitivity study of input friction loss coefficient, used in the air flow model, (a)inside and (b)outside the drip shield
- 8.9-14 Sensitivity study of input kinetic shock loss factor, used in the air flow model, inside (a) and outside (b) the drip shield
- 8.10-1 Barometric pressure fluctuation effects on relative humidity and condensation rate, FY03 – FY04 model results
- 8.10-2 Barometric pressure fluctuation effects on relative humidity and condensation rate, updated FY06 model results at the roof segment of the drift wall
- 8.10-3 Barometric pressure fluctuation effects on relative humidity and condensation rate, updated FY06 model results at the sidewalls segment of the drift wall
- 8.10-4 Barometric pressure fluctuation effects on relative humidity and condensation rate, updated FY06 model results at the floor segment of the drift wall, over the invert
- 8.11-1 Long-term, forced ventilation studies (300 years), baseline results
- 8.11-2 Variable, optimized post-closure heat load per unit length for individual WPs at year 600 (solid line), and line-averaged load equivalent (smooth surface) (a); temperature variation of a double-capacity, low-temperature, conceptual repository (b)
- 8.12-1 In-rock (via drift) vapor flow studies, drift wall temperature (a) and wall relative humidity (b) distribution in time and space
- 8.12-2 Water condensation rate at the emplacement drift wall (a); W/D water attraction ratio (b); chloride accumulation over the drift width D (c); as a hypothesis from the model results
- 8.12-3 Water pore velocity in the rock mass surrounding the emplacement drift in liquid phase (left column, a, c, e) and gas phase (right column, b, d, f) at year 600 (a, b); year 1500 (c, d); and year 2000 (e, f); solid line indicates 96 °C contour, the boiling temperature at Yucca Mountain

TABLES

- 2.1-1 Drilling, Coring, and Completion Summary for EWDP Phase III
- 2.1-2 Drilling, Coring, and Completion Summary for EWDP Phase IV
- 2.1-3 Drilling, Coring, and Completion Summary for EWDP Phase V
- 2.4-1 Summary of Phase III Geophysical Logs
- 2.4-2 Summary of Phase IV Geophysical Logs
- 2.4-3 Summary of Phase V Geophysical Logs
- 4.1-1 Summary Table of Nye County Monitoring Wells
- 5.1-1 Well Sampling History
- 6.0-1 Test Zone Intervals in Multiple Screen Pump Wells and Observation Wells
- 6.2-1 Allocation of Constant Rate Pump Test Transmissivity to Zone Intervals Based on Pump Spinner Logging
- 6.2-2 Constant Rate Pump Test Data and Analysis Results
- 7.1-1 Tracer Test Injection and Pumping Summary
- 7.2-1 Summary of Final Calibration Parameters for Tracer Tests at Site 22

ACRONYMS

AR	air rotary
APH-RC	air-percussion hammer reverse circulation
AR-RC	air-rotary reverse circulation
ASTM	American Society of Testing and Materials
ATC	Alluvial Tracer Complex
bgs	below ground surface
BHA	bottom hole assembly
CA	Correspondence Analysis
CFD	computational fluid dynamics
DEM	digital elevation model
DOE	U.S. Department Of Energy
DR-CA	dual-rotary casing-advance
DVRGFS	Death Valley Regional Groundwater Flow System
EBS	Engineered Barrier System
EWDP	Early Warning Drilling Program
FM	flooded mud
ft	feet
GMWL	Global Meteoric Water Line
gpm	gallons per minute
HFM	Hydrologic Framework Model
HCl	hydrochloric acid
hr	hour
in	inch
ISIP	Independent Scientific Investigations Program
Ksat	saturated hydraulic conductivity
LANL	Los Alamos National Laboratory
LDTH	Line-averaged-heat-source Drift-scale Thermal-Hydrological
LVVSZ	Las Vegas Valley shear zone
MT3DMS	Modular 3-D Transport model, multi-species
MR	mud rotary
MSTH	Multi-Scale Thermal Hydrologic
NRC	Nuclear Regulatory Commission
NTS	Nevada Test Site
NWIS	National Water Information System
NWRPO	Nuclear Waste Repository Project Office

NUFT	Nonisothermal Unsaturated-saturated Flow and Transport
OD	outside diameter
OSTI	Office of Scientific and Technical Information
PCFA	Principle Component Factor Analysis Method
PSD	particle size distribution
QA	quality assurance
QARC	Quality Assurance Records Center
PFBA	Pentafluorobenzoic acid
RC	reverse circulation
REEC _o	Reynolds Electrical and Engineering Co., Inc
RID	record index designator
RMS	root-mean-square
SAR	Square-array direct-current resistivity
SMF	Sample Management Facility
SNL	Sandia National Laboratory
TD	total depth
TDS	total dissolved solids
TeFBA	tetrafluorobenzoic acid
TP	technical procedure
TPN	test plan
TSPA	Total System Performance Assessment
UIC	Underground Injection Control
UGTA	Underground Test Area
USCS	Unified Soil Classification System
USGS	U.S. Geological Survey
WP	work plan
YMP	Yucca Mountain Project

1.0 INTRODUCTION

This report focuses on the major activities and findings of the Independent Scientific Investigations Program (ISIP) conducted by the Nye County Nuclear Waste Repository Project Office (NWRPO) for the 5-year period beginning in fiscal year 2002 and ending in fiscal year 2006. Funding for this program has come solely from the U.S. Department of Energy (DOE) Yucca Mountain Project (YMP). The main goal of the ISIP has been, and will continue to be, the independent evaluation of selected site characterization, repository design, and performance issues potentially affecting human health, safety, and the environment in Nye County.

1.1 Background

Nye County is the host of the proposed DOE YMP, high-level radioactive waste repository. Because Nye County retains limited local jurisdiction over the proposed repository site, the County has rights of participation, funding, and on-site representation in YMP policies and activities. Nye County began to exercise these rights in 1987 by creating the NWRPO. Major goals of this office have and continue to be providing independent evaluation and review of activities and policies related to the transport, disposal, and storage of nuclear waste within Nye County and supplementing federal studies of the potential impacts of the proposed Yucca Mountain repository.

To begin supplementing federal studies, the NWRPO in 1994 obtained a technical grant from DOE to initiate the ISIP. The specific objectives of this program are the independent evaluation of selected site characterization, repository design, and performance issues potentially affecting human health, safety, and the environment in southern Nye County. Since 1994, several additional grants have been obtained from DOE to continue the ISIP, including the 1998 Early Warning Drilling Program (EWDP) grant, which funded the work described in this report.

The EWDP is a subregional-scale hydrogeologic study and monitoring program designed to help protect Nye County's water supply interests. It has and will continue to focus primarily on the area between the proposed repository at Yucca Mountain and the populated areas of Amargosa Valley in southern Nye County, located approximately 12 miles southeast of Yucca Mountain and downgradient along potential groundwater flow paths. Figure 1.1-1 shows the location of these geographic features, as well as the Nevada Test Site (NTS), private land ownership areas, and the principal population centers within southern Nye County. Lathrop Wells is the closest Amargosa Valley community to Yucca Mountain.

A major Nye County concern is whether future Yucca Mountain nuclear waste management activities have potential to impact the groundwater and surface water supplies within the Amargosa Valley and, in turn, potential to impact human health and the environment. Although Amargosa Valley is currently sparsely populated and largely undeveloped, future significant economic development and population growth will likely occur. Amargosa Valley also encompasses important sensitive natural environments and habitats, including Ash Meadows National Wildlife Refuge, Devils Hole, the Amargosa River, and various springs and their associated wetlands.

The first three phases of the EWDP, conducted from October 1998 through March 2002, were funded through DOE cooperative grant DE-FC08-98NV-12083. This report presents the results of additional characterization work conducted from April 2002 through March 2007 under DOE grant, DE-FC28-02RW-12163.

1.2 Program Purpose and Objectives

The purpose of the EWDP is to provide essential data needed to: (1) better define the potential risk to Amargosa Valley drinking water supplies from high-level radioactive waste handling and disposal at the proposed Yucca Mountain high-level radioactive waste repository, and (2) design an appropriate “early warning” groundwater monitoring network between the repository and the existing and potential future populations in the Amargosa Valley area. A better understanding of the hydrogeologic system, including baseline hydrologic conditions, is a necessary first step toward achieving these goals and therefore has been the focus of the early phases of the EWDP.

Prior to initiating the EWDP, an evaluation of existing hydrogeologic data revealed a significant data gap encompassing part of Southern Jackass Flats, southern Crater Flat, western Rock Valley, and the northern Amargosa Desert. In short, there were few or no subsurface hydrogeologic data in these areas. The EWDP has and continues to target basic hydrogeologic data deficiencies in this region, including obtaining further information about the origin of the spring deposits, geologic and hydraulic properties of valley-fill sediments, distribution and rates of recharge, groundwater depths, gradients, and flow patterns, and baseline water chemistry.

The specific objectives of the EWDP are to provide:

- Flow and transport parameters needed to refine and reduce uncertainty in groundwater models and in performance assessment models that incorporate groundwater modeling results.
- Baseline water chemistry and water level data and the capability to monitor trends in these data over time in strategically placed wells.
- A better understanding of the flow paths between tuff and alluvium, the nature and continuity of alluvial textural layers, the hydrogeologic units underlying the alluvium, and hydraulic gradients within and between units.

Phases I and II, completed in 2000 and 2001, respectively, provided hydrogeologic and baseline water chemistry data south of the proposed repository and along U.S. Highway 95, which traverses the northern edge of Amargosa Valley. Phase III focused on filling data gaps along Fortymile Wash, within and outside of the NTS. Work outside the NTS included establishing further testing and monitoring capabilities at the Alluvial Tracer Complex (ATC) site. The ATC was established for cooperative studies conducted by the DOE, U.S. Geological Survey (USGS), Los Alamos National Laboratory (LANL), the University of Nevada, Las Vegas, and Nye County to locally characterize the hydraulic and transport properties of the saturated alluvium near the southwest boundary of the NTS.

Phase III, completed in 2002, focused on filling data gaps for the region along the lower reaches of Fortymile Wash within and outside the NTS. Work in the region outside the NTS included establishing further testing and monitoring capabilities at the ATC (Site 19) located just west of the present day braided channel area of Fortymile Wash approximately a mile north of Highway

95. The ATC was established for cooperative studies conducted by the DOE YMP; USGS; LANL; University of Nevada, Las Vegas; and Nye County to characterize the hydraulic and transport properties of the saturated alluvium near the southwestern boundary of the NTS.

Phase IV, completed in August 2003, targeted southerly flow paths from Yucca Mountain in the drainage immediately to the west of Fortymile Wash, named Flat Tire flat in NWRPO (2005a), and along the western edge of Fortymile Wash. In addition, it included a sonic corehole at Site 19.

Phase V activities were concluded in April 2006 and involved constructing 6 boreholes, 5 of which were completed as piezometers to help fill data gaps in hydrogeology along the southeastern edge of Crater Flat and in the area south of Highway 95 in the general area of Fortymile Wash, and to support on-going groundwater tracer testing in both alluvium and fractured tuff. Phase V activities included borehole drilling, drill cuttings and core collection, geologic logging and laboratory testing of selected samples, borehole geophysical logging, completion of single-screen and multiple string (i.e. nested) piezometers, water chemistry and water level monitoring, and limited aquifer testing.

1.3 Quality Assurance Requirements

The scientific data generated during the course of the ISIP have been collected under the Nye County NWRPO Quality Assurance (QA) Program. More specifically, ISIP data have been gathered under the constraints and controls of the *NWRPO Quality Assurance Program Plan* (QAPP) (NWRPO, 2003e). Constraints and controls necessary to produce valid data include QA Program elements such as design control, calibration of equipment, adequate training, use of formal procedures, a records and data management system, control of nonconforming items, corrective action, audits, and surveillances.

The NWRPO QAPP has been evaluated and audited by the staff of the U.S. Nuclear Regulatory Commission (NRC). The NRC's evaluation took the form of a formal acceptance evaluation, which resulted in the following statement: NRC staff finds that the Nye County QAPP is in conformance with the relevant criteria of Title 10 of the Code of Federal Regulations (10 CFR) Part 60, Subpart G, and 10 CFR Part 50, Appendix B. Accordingly, NRC staff finds the Nye County QAPP acceptable for the type of activities to be conducted for the early warning drilling program (Reamer, 1999).

The QA Program is based on the interpretation of federal regulations and industry standards (10 CFR Part 50, Appendix B; ANSI/ASME NQA-1) for nuclear power plants, adapted for geologic waste repository research. All NWRPO personnel and contractors who perform or manage quality-affecting functions work under the procedures outlined in the QAPP. These procedures include QA administrative procedures, as well as technical procedures and work plans that specify all necessary controls to ensure conformance with the requirements. In summary, the NWRPO QA Program helps to ensure that ISIP investigations yield valid data that can be used by the scientific and engineering community to support nuclear waste repository site characterization, performance assessment, and design.

1.4 Publication of Data and Analyses

Samples, data collected, and analyses performed under the ISIP directly support Nye County NWRPO efforts to protect the health and safety of Nye County residents. These data and analyses also support ongoing studies by the DOE YMP. Accordingly, the timely distribution and access to ISIP data and analyses are important objectives of the ISIP.

As part of the NWRPO's effort to provide information in a timely manner, ISIP data and analyses have been published in annual program summary reports and numerous reports on specific topics. These reports will be referenced, as needed, in the following sections. In addition, summaries of methods, data, and analyses of major ISIP studies have been communicated by NWRPO staff and contractors to the scientific community through numerous presentations. Recipients of these presentations have included the Nuclear Waste Technical Review Board, NRC Technical Exchanges, the Devils Hole Workshop, Death Valley Regional Groundwater Flow Model Technical Interactions, and the Nevada Test Site's Community Advisory Board, among others.

In order to broaden the public and scientific community's access to ISIP data and analyses, a Nye County NWRPO web site (www.nyecounty.com) (NWRPO, 2007a) was developed. Several key reports and a significant portion of the QA-qualified data collected under the ISIP are available on the web site. Efforts to add key data and analyses to the web site are ongoing and will continue as part of Nye County's participation in the NRC's Licensing Support Network.

1.5 Report Organization

Section 1.0 of this report provides pertinent background information and describes the purpose and scope of ISIP activities. Section 2.0 summarizes field drilling, sampling, logging, laboratory testing methods, procedures and results, and well construction activities. Section 3.0 describes regional geologic characterization. Section 4.0 presents the results of water level monitoring, Section 5.0 the water chemistry sampling and analysis, Section 6.0 the results of aquifer testing, and Section 7.0 presents results from tracer testing. Engineered barrier and repository design-related studies are presented in Section 8.0. Lastly, Section 9.0 summarizes major findings and recommendations.

2.0 DRILLING, CORING, SAMPLING, LOGGING, WELL CONSTRUCTION, AND TESTING

This section summarizes the following activities conducted as part of Phases III, IV, and V of the EWDP: drilling, coring, and well construction; sampling and testing of geologic samples; geologic and geophysical logging; and lithology including cross-sections. These activities including methods used and resulting data and information have been previously described in greater detail in NWRPO technical reports NWRPO (2003a), NWRPO (2005a), and NWRPO (2009) for Phases III, IV, and V, respectively.

NWRPO QA procedures for collecting, processing, and storing information and data from these work phases are also listed in the above cited technical reports. Copies of these QA procedures

as well as original data and information are available from the NWRPO Quality Assurance Records Center (QARC) in Pahrump, NV.

Phases III, IV, and V were conducted from 2001 through 2006. The locations of boreholes drilled during these phases, as well as during Phases I and II from 1998 to 2001, are shown in Figure 2.0-1. Note that in this figure and in the text and tables of this report the formal prefix for Nye County EWDP well names (NC-EWDP-) is not used. For example, NC-EWDP-24P is referred to as 24P herein.

The EWDP is a subregional-scale hydrogeologic study and monitoring program designed to help protect Nye County water supply interests. The program focuses primarily on the region between the Yucca Mountain repository and populated areas of the Town of Amargosa Valley, referred to as Amargosa Valley in this report, in southern Nye County. A major Nye County concern is whether future Yucca Mountain nuclear waste management activities have the potential to impact the groundwater and surface water supplies within the Amargosa Valley and, in turn, human health and the environment.

EWDP Phase III concentrated on filling in hydrogeology data gaps in the area of lower Fortymile Wash north of U.S. Highway 95. Phase IV focused on the hydrogeology of the western edge of lower Fortymile Wash and a north-south trending drainage (referred to as “Flat Tire Flat” in this report) located immediately to the west of Fortymile Wash. Phase V was designed to fill gaps in hydrogeology along the southeastern edge of Crater Flat and the area south of Highway 95 within the Fortymile Wash drainage. In addition, Phase V constructed wells to support on-going groundwater tracer testing in both alluvium and fractured tuff in lower Fortymile Wash north of Highway 95.

As part of EWDP Phases III, IV, and V nearly 30,000 ft of borehole was drilled and approximately 650 ft of core was cut using a number of different drilling and coring methods. Both drilling and coring methods affect the degree to which geologic samples (drill cuttings and core) are representative of in situ formation conditions, as well as the degree to which the formation is disturbed in the vicinity of the borehole or corehole. A description of these drilling and coring methods as well as their impact on geologic sample and formation material is presented below.

2.1 Overview of Drilling and Coring Methods

The drilling methods used in Phases III, IV, and V include: air rotary-reverse circulation (AR-RC), casing advance (CA), dual rotary-casing advance (DR-CA), flooded mud (FM), air rotary (AR) and mud rotary (MR). Coring methods were limited to drive coring and sonic coring of alluvium.

Drilling methods and drilling fluids were selected for drilling boreholes in Phase III, IV, and V based on a number of criteria including their ability to: yield drill cuttings that were as representative as possible of in situ formation rock, minimize the disturbance of the formation rock and groundwater chemistry, and produce boreholes suitable for completing single- and multiple-screen monitor wells and piezometers. Coring methods were selected to yield geologic samples that were as representative as reasonably possible from saturated and unsaturated alluvium, and that did not significantly disturb the formation alluvium or groundwater chemistry.

Drilling and coring methods together with well construction details are summarized for each borehole in Tables 2.1-1, 2.1-2, and 2.1-3 for Phases III, IV, and V, respectively. Drilling fluids and related additives used in Phases III, IV, and V boreholes are listed in Appendix A of NWRPO (2003a), NWRPO (2005a), and NWRPO (2009), respectively. Some important facts regarding drilling and coring and their impact on geologic samples and the formation materials are described in the following sections.

2.1.1 Description of Drilling Methods

2.1.1.1 *Small Diameter Air Rotary-Reverse Circulation Methods*

Relatively small diameter AR-RC drilling (drill bits generally < 6.75 inches in diameter) was the primary method used to advance boreholes for the collection of geologic samples and the completion of piezometers in Phases III, IV, and V (Tables 2.1-1, 2.1-2, and 2.1-3). AR-RC methods are commonly used in mineral exploration and were used by Nye County to provide reasonably representative drill cuttings for geologic logging; produce boreholes suitable for geophysical logging; and for completion of single, dual, and triple piezometer strings at a reasonable cost.

In AR-RC drilling, the contact of compressed-air drilling fluid with the formation is minimized by routing air flow down the dual-wall drill pipe annulus to the drill bit and up the center of the drill pipe to the ground surface. This reverse circulation airflow design minimizes the erosion of borehole walls by the compressed air. Moreover, the relatively small-diameter of the drill bits (< 6.75-inches) used in combination with 4.0 to 5.5-inch diameter drill pipe also works to increase borehole stability and limit borehole wall caving. Limiting borehole wall erosion and caving minimizes the chance of getting the drill string stuck in the borehole; and results in less mixing of drill cuttings from different regions of the borehole, which in turn facilitates collection of representative drill cuttings samples and identification of lithostratigraphic unit changes.

Nye County required that AR-RC method use compressed air exclusively as the drilling fluid. Generally, compressed air minimizes the disturbance to formation rock permeability and water chemistry. However, even in AR-RC drilling, compressed air can erode borehole walls and create caving conditions, especially in unsaturated alluvium. In these cases, drilling mud (i.e., sodium bentonite and/or polymers and/or foamers) was used to stabilize the unsaturated borehole walls of AR-RC drilled boreholes. The method involved halting drilling, injecting drilling fluid using conventional circulation (down the center of the dual wall tube, through the bit, and out into the formation) and drying the borehole walls with conventionally circulated compressed air before continuing the advancement of the borehole. This borehole conditioning method allowed AR-RC dry drilling to proceed to depths of 500 ft below ground surface (bgs) or more in unconsolidated unsaturated alluvium and valley-fill deposits using only approximately 20 to 60 ft of surface casing. Where necessary, similar drilling fluids were used below the water table in saturated alluvium and valley-fill deposits to condition borehole walls and facilitate reaching depths of nearly 3,000 ft in some cases. At the same time, use of organic drilling fluids and additives, including foams and polymers, were minimized to the extent possible to avoid affecting oxidation-reduction conditions in the vicinity of the borehole walls.

AR-RC methods in Phase III, IV, and V produced drill cuttings with particle size distributions (PSDs) that were approximately representative of in situ formation conditions with one

exception; that is, in saturated alluvium, which produced significant amounts of water during drilling. Data presented in NWRPO (2003a) demonstrated that the grinding of clasts of relatively soft nonwelded tuff below the water table reduces a high percentage of gravel-sized particles to sand-sized, and significantly disturbs the PSD of alluvial drill cuttings. NWRPO (2003a, 2005a, and 2009) show that particle size reduction caused by AR-RC drilling is not as significant in the uppermost part of the saturated zone, where only small quantities of water are produced at the drill bit; and in the unsaturated zone, where free water is not available to facilitate grinding. However, this lack of water in the unsaturated zone resulted in both drilling-created and naturally occurring small (e.g., silt- and clay-sized) particles to be lost as dust from the sample collection system (cyclone separator) at the ground surface. In future EWDP phases using AR-RC methods, improvements will be made to the above ground dust capture system.

In unsaturated alluvium, AR-RC generally produces drill cuttings where the total percent of fine particle sizes (silt plus clay) and the total percent of coarse particle sizes (sand plus gravel) are not significantly altered from in situ conditions. However, the method generally significantly reduces the gravel fraction and increases the sand fraction percentages compared to in situ conditions, while the percentages of silt and clay generally remain similar to in situ conditions (NWRPO, 2003a, 2005a, and 2009). It is hypothesized that fines lost as dust during dry drilling of unsaturated alluvium were replaced by fines created by the dry drilling process.

2.1.1.2 Intermediate Diameter Air Rotary-Reverse Circulation Methods

The last two piezometers drilled as part of Phase III, 22PB and 23P, were drilled using an 8.5-inch bit, 4.5-inch diameter dual-wall drill pipe, and AR-RC methods. This drilling/completion effort was essentially an experiment to determine if intermediate diameter AR-RC boreholes would remain open and stable long enough to complete open-hole geophysical logging and the installation of nested piezometers. The larger drill bit was required to provide sufficient annular space for emplacement of sandpacks and grout plugs with a tremmie pipe at appropriate depth intervals around 2 piezometer strings.

Some caving of borehole 22PB occurred, and it was necessary to spend time cleaning the hole of these cuttings after every 20 ft to a total depth of nearly 1,200 ft bgs. In addition, drilling rates were significantly slower than rates achieved with the smaller diameter AR-RC systems described in Section 2.1.1.1. However, open-hole geophysical logs and the installation of dual nested piezometers were successfully completed without major caving problems.

In contrast, major caving problems were encountered in 23P despite using large amounts of bentonite/polymer drilling fluids to stabilize borehole walls. At a depth of 1,340 ft bgs, the bottom hole assembly (BHA) of the drill string became stuck and could not be pulled back above 1,050 ft bgs. As a result it was necessary to sever the drill pipe above the BHA with an explosive charge and abandon approximately 65 ft of this assembly in the borehole. Following this severing process, the borehole caved to 712 ft bgs. A dual nested piezometer string was then completed in the remaining uncaved portion of the borehole.

In summary, the large annular space between the 4.5-inch diameter dual-wall inner drill string and the borehole wall cut by the 8.5-inch drill bit appeared to be a factor in causing significantly more caving than with the smaller diameter AR-RC system described in Section 2.1.1.1. This caving may also be related to the much slower drilling rate achieved with the larger diameter

system. Finally, there is some evidence that this slower drilling in the larger diameter AR-RC boreholes may also disturb drill cuttings from in situ conditions to a greater extent than drill cuttings obtained from the smaller diameter AR-RC boreholes.

2.1.1.3 Casing Advance Methods

CA drilling methods were used in EWDP Phase III to drill two intermediate sized boreholes (10P and 22PA) with diameters ranging from approximately 7 to 10 inches in the lower and upper regions of boreholes, respectively (Table 2.1-1). CA air-drilling methods were selected for drilling several intermediate-diameter Phase III boreholes for many of the same reasons that AR-RC methods were selected for use in all EWDP Phases III, IV, and V. In addition, these methods were selected to permit the use of drive coring methods to collect minimally disturbed core samples from both the unsaturated and saturated zones.

CA drilling systems are called by various names including Odex™, Tubex™, and Stradex™. The components of each of these CA systems are similar and are designed to advance the drill casing as the borehole is deepened. The borehole is usually advanced and the casing driven downward with a downhole air-percussion hammer attached to a pilot/eccentric reamer bit. This advancement approach effectively seals off (in most cases) the borehole above the drill bit, thereby virtually eliminating borehole wall erosion and caving and the resulting mixing of drill cuttings from different borehole regions. In addition, the central drill string can be removed from CA boreholes, leaving behind the drill casing that is open at the bottom to the underlying formation. This permits collecting drive-core samples of unconsolidated formation rock beneath the drill casing or using another drilling method below the drill casing. Finally, the drill casing, if removed in stages, facilitates completing wells in unstable formation materials.

Similar to AR-RC drilling of alluvium as described in Section 2.1.1.1, it is likely that the grinding action of CA drilling also disturbs the PSDs of non-welded tuff alluvium drill cuttings below the water table. However, geologic sample collection problems in CA Phase III boreholes precluded collecting the necessary evidence to prove this hypothesis.

Evidence supporting the selection of CA methods for Phase III borehole drilling and geologic sample collection include data from the Nevada Test Site where CA drilling produced drill cuttings from tuffaceous alluvium, which exhibited PSDs that were representative of in situ formation materials (Reynolds Electrical and Engineering Co., Inc., 1994). The CA drilling system used on the Nevada Test Site included dual-wall reverse circulation drill pipe that permitted the achievement of drilling fluid velocities necessary to efficiently remove drill cuttings from the boreholes.

Dual-wall reverse-circulation drill pipe was not included in the CA drill system used in EWDP Phase III. Instead a single wall inner drill pipe was used with standard air circulation; that is, air flow went down the small diameter inner string and up the large volume annular space between the drill pipe and the larger diameter drill casing. Drilling fluid velocities were not large enough in the large annular space to efficiently remove drill cuttings from these boreholes. As a result there was significant recirculation and additional mixing of drill cutting in the return flow between the drill bit and the ground surface. Further, the drillers found it difficult to clean the drill cuttings from the drill bit and the drill cuttings were further disturbed from in situ conditions by the grinding action of the bit.

2.1.1.4 Dual Rotary-Casing Advance Methods

Conventional DR-CA drilling methods and the recently developed Symmetrix™ version of DR-CA methods were used in several Phase V boreholes to enlarge previously drilled AR-RC boreholes and case-off as much as 460 ft of unconsolidated alluvium; and in some cases several tens of ft of volcanic rock underlying the alluvium (Table 2.1-3). The casing-off of these units (especially the unconsolidated alluvium) permitted further borehole advancement using AR-RC or sonic coring methods.

The conventional DR-CA method uses an outer drill casing with a fixed shoe bit and is advanced by rotating while the cuttings are “drilled-out” from inside the casing with tri-cone rotary bits or percussion hammer bits attached to a separate drill string. This separate inner drill string is independently rotated and advanced using one of several circulation methods including: dual-wall reverse-circulation and conventional circulation. The drilling fluid circulation is controlled with the inner drill string and top head drive system.

The Symmetrix™ version of the DR-CA method is similar to the conventional DR-CA method, but employs a freely rotating bushed casing shoe bit and locking down-hole air percussion hammer that advances and rotates both bits while advancing drill casing. In addition, the air percussion hammer is deployed on dual-wall reverse-circulation drill pipe providing efficient and rapid return of drill cuttings to surface. This method has been proven to be reasonably successful at moderate depths (<500 ft bgs) in alluvium, but is less effective in consolidated or bedrock units.

With the exception of two Phase V boreholes (24PA and 22PC), DR-CA methods were used only for borehole enlargement and not for advancing a new borehole and collecting geologic drill cuttings. In the unsaturated interval of alluvium from approximately 57 to 153 ft bgs in 22PA where DR-CA (Symmetrix version) was used to advance the new borehole, the PSDs of drill cuttings were similar to drill cuttings collected by AR-RC methods in a nearby borehole located 37 ft away.

The PSDs of the coarse (sand and gravel) fractions in unsaturated alluvial drill cuttings collected by conventional DR-CA drilling methods from 0 to 460 ft in 22PC agree reasonably closely with the PSDs of the coarse fractions in sonic core samples collected from 460 to approximately 763 ft in the same borehole. Both DR-CA drill cuttings and sonic core PSD data sets show that the percentage of gravel often predominates over the percentage of sand. This is in contrast to drill cuttings produced by small-diameter AR-RC methods in 22PA and other Phase III and IV boreholes (NWRPO, 2003a and 2005a) where the percentage of sand in most depth intervals significantly exceeded the percentage of gravel. These findings suggest that DR-CA methods have the potential to produce more representative coarse fractions in unsaturated alluvium in Fortymile Wash than AR-RC methods. Moreover, if the loss of fines as dust from unsaturated DR-CA drill cuttings samples in 22PC could have been reduced by an enhanced capture system, the fines size fraction in the DR-CA drill cuttings would also likely have been in reasonable agreement with the fines in the sonic core and the formation alluvium. In summary, DR-CA methods appear to have the potential to produce drill cuttings from unsaturated alluvium with PSDs that are in reasonable agreement with sonic core and in situ formation materials.

2.1.1.5 Flooded Mud Methods

FM drilling methods were used in Phase III to drill four relatively large-diameter (14.75 in.) boreholes (10S, 19IM1, 19IM2, and 22S) to depths ranging from approximately 966 to 1197 ft bgs (Table 2.1-1). Each of these boreholes was completed with multiple well screens in a single monitor well casing. Drill cuttings were not collected from these boreholes for geologic logging or laboratory testing. Instead, geologic samples were collected and logged from small diameter AR-RC boreholes that were previously drilled at the same locations as the FM boreholes (Table 2.1-1). Following geophysical logging, these AR-RC boreholes were abandoned.

The FM method was selected primarily because it had been used successfully in Phase II to drill similar large-diameter, plumb, straight, and relatively stable boreholes. Borehole wall stability is enhanced by filling (i.e., flooding) the hole with bentonite mud drilling fluid during drilling and keeping the borehole partially full of mud during well completion activities. Drill cuttings are moved from the drill bit to the ground surface through the inside of the drill pipe using an air-lift tube positioned within the drill pipe. This upward flow within the drill pipe helps to minimize borehole erosion effects and the mixing of drill cuttings with eroded formation materials.

2.1.1.6 Mud Rotary Methods

Conventional MR methods were used only to drill a large diameter (approximately 12-inches in diameter) Phase IV borehole (19PB) to a depth 350 ft bgs in unsaturated alluvium. An 8-inch diameter conductor casing was cemented in place in this borehole and served to seal off unstable alluvial layers and permitted sonic coring of approximately the lower 18.5 ft of unsaturated alluvium and the upper approximately 265.5 ft of saturated alluvium. Drill cuttings collected from this borehole were not considered to be as representative of AR-RC drill cuttings collected from 2 boreholes located less than 100 ft away from the MR borehole. As a result MR drill cuttings were not geologically logged.

2.1.1.7 Air Rotary Methods

Consolidated rock penetrated from 45 to 900 ft bgs in 18P was drilled using open-hole conventional AR methods with a 7.875-inch drill bit and compressed air as the primary drilling fluid. However, due to the high instability and/or permeability of some formation intervals, it was necessary to use other drilling fluids and additives to restore circulation in several depth intervals located primarily above the approximately 780 ft deep water table. The drill cuttings produced from this borehole, especially the interval of volcanic sandstone from 515 to 810 ft bgs and the underlying moderately welded tuff from 810 to 890 ft bgs were ground into very small particles making it very difficult to geologically log these samples. Because the AR method produced poor quality samples for geologic description and intervals of unstable borehole, this method will not be used in future EWDP phases where geologic sampling is required.

2.1.2 Description of Coring Methods

2.1.2.1 Drive Core Methods

Obtaining representative core from coarse-grained alluvium is difficult and costly. Numerous coring methods have been attempted without success in the vicinity of Yucca Mountain,

including split barrel (i.e., split spoon) sampling with a drop weight; hollow-stem auger with push-tube sampler; double- or triple-tube rotary coring; and Pitcher[®] or similar spring-loaded core barrel methods. In contrast, drive core methods have been shown to provide good core recovery with minimal disturbance of hydrologic conditions and physical properties of the core and the coarse grained alluvial and unconsolidated basin fill formation sediments (Hammermeister and others, 1986; Reynolds Electrical and Engineering Co. [REECo], 1994).

During Phase III, the NWRPO demonstrated that drive coring methods using a solid-tube sampler (approximately 4-inch-ID by 2- or 2.5-foot-long solid tube) with a downhole air-percussion hammer produced good core recovery of alluvium from selected depth intervals in boreholes drilled with CA drilling methods (NWRPO, 2003a). In Phase IV, the NWRPO found that similar drive coring methods produced only fair core recovery of alluvium from selected depth intervals in boreholes drilled with AR-RC drilling methods (NWRPO, 2005a). The poorer core recovery obtained from AR-RC boreholes was due to borehole caving and the resulting fill that collected at the bottom of the borehole prior to coring.

In Phase IV sonic corehole 19PB, the same solid-tube core barrels were advanced by the sonic drive core methods. Regardless of the drive mechanism, a beveled, hardened-steel drive shoe was attached to the downhole end of the solid-tube core barrel, and the core barrel was lined with thin-walled brass tubes cut into 6- and 3-inch-long segments. Upon completion of each core run, samples were removed from the core barrel by a hydraulic core extruder.

Drive coring at depths exceeding several 100 ft is extremely expensive, even under the most favorable subsurface geologic conditions. Caving and/or sloughing of unstable borehole wall material in open boreholes, such as those drilled by AR-RC methods (AR-RC boreholes) in Phase IV make drive coring of undisturbed alluvium even more difficult and expensive. For these reasons, drive coring methods are generally considered unsuitable for continuous coring.

2.1.2.2 Sonic Core Methods

Sonic coring methods were used to successfully collect nearly continuous core samples with minimally disturbed PSDs (NWRPO, 2005a and 2009). Although this method disturbs the porosity and density of the alluvial samples, it maintains intact textural layering and provides representative samples suitable for detailed geologic logging and laboratory testing of selected flow and transport parameters. The method uses a dual-pipe system consisting of a core pipe (i.e., the core barrel) inside a larger diameter drill pipe (i.e., the drill casing). Both pipes are advanced using a combination of mechanically driven oscillations (i.e., vibrations), slow rotation, and hydraulic pull-down pressure. A top-mounted, hydraulically powered drill head is used to transmit the vibratory force and pull-down pressure on the core and drill pipes.

During typical sonic corehole advancement, the inner core pipe is advanced approximately 5 to 20 ft ahead of the outer drill pipe. The core pipe is then brought to the ground surface, where core is vibrated out of the pipe into polyethylene film tubing (i.e., a plastic sock) with a diameter slightly larger than the outside diameter (OD) of the core pipe. The outer drill pipe is then advanced to the bottom of the borehole and the inner core pipe is used to remove the disturbed fill material from the outer drill pipe. The above steps are then repeated to continue coring and advancing the borehole downward.

Sonic coring in Phase IV corehole 19PB and Phase V corehole 22PC was an unqualified success. This method produced nearly continuous core from the upper approximately 265.5 ft of saturated alluvium in 19PB and the upper approximately 293 ft of saturated alluvium in 22PC. It also produced continuous core from the lowest most approximately 18.5- and 10-ft intervals in the unsaturated zones of 19PB and 22PC, respectively. This core was the first continuous core to be collected from alluvium in Fortymile Wash; and was suitable for geologic, photographic, and video logging, as well as laboratory testing of several flow-related parameters.

2.2 Geologic Sampling, Logging, and Testing

2.2.1 Geologic Sampling

Drill cuttings were collected for continuous geologic logging, identification of lithologic and textural units, and laboratory testing from: all Phase III, IV, and V AR-RC boreholes, CA boreholes in Phase III, an approximately 100 ft section of alluvium drilled by DR-CA (Symmetrix Version) methods in Phase V borehole 24PA, and 460 ft of unsaturated alluvium drilled by conventional DR-CA methods in Phase V corehole 22PC.

In addition, drive core samples were collected from selected alluvial intervals in two Phase III CA boreholes (10P and 22PA), from selected depths in two Phase IV AR-RC boreholes (24P and 29P), and from several depth intervals in the Phase IV sonic corehole 19PB. These core samples were collected to: demonstrate the feasibility of the drive core method in CA, AR-RC, and sonic core boreholes; for laboratory testing of flow-and-transport-related properties on small-scale samples representative of in situ conditions; and to provide representative (i.e. minimally disturbed) samples to compare with more highly disturbed drill cuttings samples.

Finally, continuous sonic core samples were collected from the lower portion of the unsaturated zone and the upper portion of the saturated zone in Phase IV corehole 19PB and Phase V corehole 22PC as described in Section 2.1.1.2. Like drill cuttings, sonic core provided continuous samples for geologic logging, identification of lithologic and textural units, and laboratory testing. Unlike drill cuttings, sonic core (and drive core) are only minimally disturbed by the sampling process, and therefore more closely represent in situ conditions than drill cuttings from both unsaturated and saturated alluvium.

Geologic sampling and sample handling methods generally conformed to the applicable quality assurance procedures listed in NWRPO (2003a, 2005a, and 2009). Exceptions to these methods are described in geologic log form comments and/or scientific field notebooks. Sampling related processes (e.g., heat generation at the drill or core bit) that may have disturbed samples further from in situ conditions and affected geologic, photographic, or video logging descriptions and/or laboratory testing are also described in NWRPO (2003a, 2005a, and 2009).

2.2.1.1 Drill Cuttings

Continuous drill cuttings were collected at 2.5-foot intervals in unsaturated alluvium and 5-foot intervals in saturated alluvium and other rocks types. In Phase III a total of 2,824 cuttings samples were collected, including 2,474 alluvial samples and 350 non-alluvial samples. Counting splits prepared for NWRPO, YMP, and the NWRPO rock hydrologic testing laboratory, a total of approximately 7,141 cuttings samples were packaged, labeled, and handled.

In Phase IV a total of 2,176 drill cuttings samples were collected: 522 alluvial and 1,654 non-alluvial. With the addition of splits prepared for the NWRPO, DOE, and the NWRPO rock hydrologic testing laboratory, approximately 4,714 cuttings samples were packaged, labeled, and handled.

In Phase V a total of 1,234 drill cuttings samples were collected: 611 alluvial and 623 nonalluvial. With the addition of splits prepared for the NWRPO testing laboratory and DOE YMP, approximately 4,041 cuttings samples were packaged, labeled, and handled.

Laboratory tests on drill cuttings were limited to samples from alluvium. In Phase III and IV, laboratory tests on drill cuttings consisted of: gravimetric water content, soil-water extract electrical conductivity, wet sieve, and hydrometer. In Phase V these same tests were conducted on unsaturated alluvial drill cuttings samples with the addition of Atterberg limit and specific gravity tests. Numbers of samples tested are tabulated by phase, borehole, and test type in NWRPO (2003a, 2005a, and 2009).

Drill cuttings were collected at the ground surface in a cyclone separator. In the unsaturated portion of smaller diameter boreholes, the entire alluvial sample from a particular depth interval was collected in 5-gallon buckets. Buckets from each depth interval were emptied onto a tarpaulin, mixed, and subsampled by the cone and quarter method. In larger diameter boreholes where the volume of unsaturated cuttings per depth interval was very large, a Gilson dry splitter was used beneath the cyclone separator to reduce the alluvium sample size to more manageable volumes.

In the saturated portion of boreholes which produced drill cuttings samples designated for sampling, an Anaconda rotating wet splitter was attached beneath the cyclone separator to reduce the sample volume from a sample depth interval to a manageable number of 5-gallon buckets. The solid phase in the buckets was homogenized and subsampled over 5-foot depth intervals. In selected boreholes and depth intervals water was siphoned from the buckets (after the solid phase settled), the remaining wet solid sample allowed to dry, and the entire sample geologically logged in the field and tested in the laboratory.

Three split samples, each weighing approximately 5 pounds, were collected from each sample interval: two for the NWRPO and one for the DOE. A fourth split sample was collected from every second 2.5-foot interval in unsaturated alluvium for laboratory analysis.

The first NWRPO split was subsampled for field logging and the preparation of chip trays for future reference. The second NWRPO split was collected for archival at the DOE Sample Management Facility (SMF). The DOE split was collected onsite by DOE personnel. Both NWRPO and DOE splits sent to the SMF were sealed in olefin bags; splits for laboratory testing were sealed in double plastic bags. All samples were labeled with appropriate identification and shipped to their destinations under appropriate chain of custody.

2.2.1.2 Drive Core

Drive core sampling was conducted at selected depth intervals in both the unsaturated and saturated portions of alluvium in Phase III CA boreholes 10P and 22PA, the unsaturated zone

alluvium portion of Phase IV small diameter AR-RC boreholes 24P and 29P, and in the saturated alluvium portion of Phase IV sonic corehole 19PB.

As expected, caving in cased CA boreholes was not a factor and disturbed fill material was not encountered at the bottom of CA boreholes prior to coring. In contrast, removing disturbed material from the bottom of the borehole prior to coring was difficult both in uncased AR-RC boreholes and in the cased sonic corehole 19PB. As a result, disturbed fill material was found in the upper portion of the core barrel in almost every drive core run in AR-RC boreholes 24P and 29P, and in sonic corehole 19PB. In some cases the fill occupied most of the core barrel.

When possible after geologic logging of each core run, two of the least disturbed 6-inch-long core samples were labeled, sealed, and transported under chain of custody to the NWRPO testing laboratory for the following analyses: volumetric water content, saturated volumetric water content, particle and bulk density, wet sieve, hydrometer, and saturated hydraulic conductivity. Numbers of drive core samples tested are tabulated by phase, borehole, and test type in NWRPO (2003a and 2005a).

The remaining 6-inch core was labeled, sealed, and transmitted under chain of custody to the SMF for storage and possible future use by the NWRPO. All remaining samples containing representative formation material were labeled, sealed, and transmitted under chain of custody to the SMF for storage and possible future use by DOE YMP contractors and other interested parties.

2.2.1.3 *Sonic Core*

After each sonic core run was brought to the ground surface from Phase IV corehole 19PB and Phase V corehole 22PC, approximately 2-foot-long segments were vibrated from the core barrel into plastic socks with an ID slightly larger than the OD of the core. The core segments were then moved to the core logging trailer, where depth intervals were assigned. The expansion in the length of the recovered core due to the sonic vibrations was corrected to the approximate true in situ length by methods described in the applicable revision of NWRPO QA Technical Procedure TP-8.0, *Field Collection, Logging, and Processing of Borehole Geologic Samples*. Boundaries between alluvial layers with noticeably different PSDs were identified using visual-manual logging methods based on American Society for Testing and Materials (ASTM) D-2488-93 (ASTM, 1993). These layers often extended across adjacent segments and ranged in length from less than 0.25 to more than 10 ft in 19PB and from less than 0.3 to 6.8 ft in 22PC.

Grab samples from the major textural layers present in sonic core were then collected. The samples of textural layers were split for field geologic logging and NWRPO laboratory testing. The distribution of grab samples was controlled and documented with the NWRPO Transfer of Custody Form. After the removal of grab samples from core segments, digital photography, and video logging, the remaining portions of core segments were transferred from the site to the SMF under DOE chain of custody. Some of these core segments from Phase V corehole 22PC were then assigned immediately to the U.S. Geological Survey for pore water extraction and geochemical analysis. A number of core segments were later transferred from the SMF to the NWRPO Rock Hydrologic Testing Laboratory in Pahrump under Los Alamos National Laboratory (LANL) custody for a cooperative testing program. The program involved repacking sonic core samples to target dry bulk density values and determining their saturated volumetric

water content, saturated hydraulic conductivity, and bulk density values in addition to parameters also specified for grab samples as listed below.

Laboratory tests on 19PB sonic core grab samples included the same tests as drive core samples, plus soil-water extract electrical conductivity tests. The 19PB sonic core saturated volumetric water content, saturated hydraulic conductivity, and bulk density measurements were conducted on cores repacked to a range of bulk densities. Sonic core grab samples from Phase V corehole 22PC were not repacked and therefore do not include saturated volumetric water content and saturated hydraulic conductivity at different bulk densities.

The number of samples assigned to different organizations as well as the number designated for different NWRPO laboratory tests are tabulated for Phase IV corehole 19PB and Phase V corehole 22PC in NWRPO (2005a) and NWRPO (2009), respectively.

2.2.2 Geologic and Photographic Logging

Geologic logging and digital photography procedures are described in the applicable revision of NWRPO QA Technical Procedure TP-8.0. Geologic logging was conducted on all drill cuttings, drive core, and sonic samples described in the preceding section. Geologic logging data on drill cuttings were recorded on the Alluvium and Non-Alluvium Drill Cuttings Logging Forms. Examples of these forms are shown in NWRPO (2003a, 2005a, and 2009). Geologic logging data on drive core and sonic core collected from alluvium were recorded on the Alluvium Core Logging Form. An example of this form is presented in NWRPO (2005a and 2009). Digital photographs of alluvial sonic core segments from Phase III corehole 19PB and Phase IV corehole 22PC were documented on the Field Digital Photography Log.

Procedures for geologic logging of alluvial samples are based on the visual-manual logging methods described in ASTM D-2488-93 (ASTM, 1993). The alluvium logging form records soil classification parameters, many of which are related to flow and transport properties of alluvial sediments. These parameters include PSD, cementation, hydrochloric acid (HCl) reaction, color, moisture, and other soil characteristics.

The non-alluvium logging form records parameters that support the identification of lithostratigraphic units, including rock unit; color; moisture content; weathering; structure; matrix porosity; and color, size, and volume of phenocrysts and clasts. Since most rock units in the vicinity of Yucca Mountain are volcanic tuffs, additional descriptive tuff parameters include mode of deposition, degree of welding, and alteration. In addition, both alluvium and non-alluvium logging forms include rates of drilling, coring, and water production. Sample bulk-density-related measurements on these same forms have not proven useful and have been censored. A summary of these censored data and other unreliable data is included in censored data tables for Phases III, IV, and V in NWRPO (2003a), NWRPO (2005a), and NWRPO (2009), respectively.

Field estimates of PSD in alluvial samples were used to estimate gross textural variability over the sample interval. Field estimates were not used for quantitative purposes; instead, laboratory PSD measurements were used where quantitative data were required. In general, field logging observations in the saturated zone were valuable for qualitatively identifying trends in logged flow related parameters versus depth to support the location of well screens. In the unsaturated

zone field observations of trends in color, clay content, and cementation that may indicate the presence of low permeability paleosols that may in part control flow in the unsaturated zone. Also, since field estimates of PSD were determined over each 2.5 ft interval and laboratory measurements of PSD were determined over every other 2.5 ft interval, field estimates that are reasonably accurate are useful to fill in data gaps between lab measurements.

2.2.3 Laboratory and Field Results

2.2.3.1 Phase III

Findings include:

- The natural log of saturated hydraulic conductivity measurements on drive core samples correlate inversely with percent fines data and are significantly lower in magnitude than values calculated from much larger scale aquifer test measurements. Both of these trends are consistent with the findings of other workers (Todd, 1980; and Schulze-Makuch and others, 1999).
- Adjacent 3-inch and 6-inch long drive core samples show a wide variation in laboratory-measured PSD, bulk density, porosity, and saturated hydraulic conductivity values. These limited data indicate that fluvial sedimentary processes created a highly layered alluvial sequence with contrasting lithologic and hydraulic properties.
- Laboratory-measured drill cuttings PSDs from small diameter boreholes drilled primarily with AR-RC methods are reasonably representative of in situ formation conditions throughout the unsaturated zone and in the uppermost part of the saturated zone. This conclusion is based on a limited comparison of laboratory PSD data from minimally disturbed drive core samples versus drill cuttings samples collected from approximately the same depth intervals in nearby boreholes at Sites 10 and 22.
- However, once AR-RC boreholes begin to produce significant amounts of water at depths generally less than 100 ft below the water table, the laboratory-measured PSDs of drill cuttings deviated significantly from laboratory-measured PSDs of core samples and, by inference, the PSDs of in situ formation materials.
- The deviations of laboratory-measured drill cuttings PSDs from core sample PSDs below the water table are most likely due to the grinding action of the rotary drill bit on relatively soft non-welded tuffs that is greatly facilitated by the production of large quantities of water at the drill bit generally beginning within the upper 100 ft of the saturated zone.
- Inadequate drilling fluid velocities in the unsaturated zone portion of all CA boreholes and geologic sample handling errors in the saturated zone portion of these boreholes caused laboratory-measured PSDs of drill cuttings samples from these boreholes to be significantly disturbed from in situ conditions.
- As a result, it is not known if CA drilling disturbs samples below the water table to the same degree as AR-RC drilling. However, other workers have found that CA drilling can yield drill cuttings samples from the unsaturated zone with laboratory-measured PSDs that are reasonably similar to drive-core samples, and therefore to in situ conditions.

- Boreholes drilled with intermediate diameter AR-RC systems appear to produce borehole walls that are less stable than boreholes drilled with small diameter AR-RC systems. In addition, drill cuttings in the former drilling system appear more highly disturbed from in situ conditions than cuttings from the latter system.

Moisture content depth profiles in some of the AR-RC and CA boreholes provide evidence of lateral movement of lost circulation drilling fluid (primarily water) from nearby FM boreholes. 2.2.3.2 Phase IV

Results from laboratory tests on alluvial drill cuttings and drive core samples from Phase IV AR-RC boreholes include the following:

- The average fines fraction in Flat Tire Flat boreholes equals or exceeds 20% compared to 14% or less in Fortymile Wash boreholes; gravel content is generally greater in Fortymile Wash boreholes.
- A comparison of PSD depth profile data for drill cuttings vs. drive core from 24P and 29P indicates good agreement in fines content and less agreement in sand and gravel, especially for 29P.
- Significantly more gravel is found in drive core than in drill cuttings from 29P, suggesting that grinding during drilling may reduce large gravel-sized particles into smaller sand-sized ones, which is consistent with findings from Phase III boreholes.
- In general, unsaturated alluvial drill cuttings from Phase III and IV AR-RC boreholes yield percentages of coarse and fine fractions that roughly approximate those from drive core, and therefore roughly approximate to in situ conditions. This was also observed in AR-RC Phase III unsaturated alluvium drill cuttings.
- Gravimetric water contents of drill cuttings are much lower than those of drive core samples taken from adjacent depths.
- Assuming that drive core samples exhibit water contents that approximate in situ conditions, these data show that AR-RC drilling significantly dries the drill cuttings from in situ conditions. In Phase III and Phase IV it was found that AR-RC drilling reduced the gravimetric water content of alluvium drill cuttings compared to core by as much as 0.15 g/g.
- Drill cuttings water content profiles are, however, useful in identifying relative differences between AR-RC boreholes and depth intervals where excess drilling fluids were used to condition the borehole.
- As found in Phase III drive core, evidence was found in Phase IV for a linear correlation between the natural logarithm of saturated hydraulic conductivity and percentage of fines in drive core samples from 24P. Similar trends of decreasing saturated hydraulic conductivity with increasing fines percentages have been found in numerous other studies for a variety of sediments (Todd, 1980).
- The arithmetic and geometric mean values of saturated hydraulic conductivity of drive cores samples differ in 24P, suggesting that these values are log-normally distributed.

Field aquifer and laboratory test results on drive core from Phase IV corehole 19PB show the following results:

- Comparing average saturated hydraulic conductivity values from constant head field tests in 19PB with values from both smaller scale laboratory tests on drive core samples and a larger scale constant-rate 48-hour pump test in an immediately adjacent borehole (NWRPO, 2001b) suggests a direct relationship between measurement scale and saturated hydraulic conductivity value. This relation between measurement scale and saturated hydraulic conductivity in geologic materials was observed in Phase III and by numerous workers, including Schulze-Makuch and others (1999).
- However, the differences between drive core and field saturated hydraulic conductivity measurements are likely in part due to the orientation of the measurement (i.e., vertical versus horizontal) rather than due simply to scale.
- The average 19PB dry bulk density values calculated for 5 drive core runs agrees closely with the average dry bulk density values calculated for 22 sonic core runs (i.e., both 1.81 g/cm^3). This agreement in part may be coincidental, since there are numerous sources of error in both types of measurements.
- The average 19PB dry bulk density value calculated from values obtained from eight individual 6-inch long core segments is 1.89 g/cm^3 .
- Significant differences in PSD data were obtained from drive core samples collected from the same core run, especially in 19PB, which shows that on the relatively small scale of a drive core run, fluvial sedimentary processes create, in some cases, a highly layered flow system with contrasting properties.

Laboratory test results on sonic core from Phase IV corehole 19PB include the following results:

- All samples are coarse-grained and, on the average, contain approximately 14% fines, 46% sand, and 40% gravel. The Unified Soil Classification System (USCS) group name for the average PSD composition is a silty or clayey sand with gravel.
- Both hydrometer PSD and Atterberg limits data indicate that clay predominates slightly over silt in the fines fraction for most sonic core samples tested.
- Electrical conductivity of soil-water extract data from the lower part of the unsaturated zone immediately above the present water table shows several electrical conductivity spikes and valleys. It is possible that paleo-water tables may be in part responsible for these variations in electrical conductivity values.
- Repacking 7 representative sonic core segments at optimum water contents produced core samples with an average dry bulk density value of 1.90 g/cm^3 and an average porosity value of 0.25. These values are consistent with the average values of density and porosity obtained from individual 6-inch long drive core segments.
- Repacking 15 representative sonic core segments at air-dried water contents produced core samples with an average dry bulk density of 1.72 g/cm^3 and an average porosity value of 0.33 assuming a particle density of 2.56 g/cm^3 .
- Linear correlations between the natural logarithm of saturated hydraulic conductivity and percentage of fines were found for sonic core segments repacked at air-dried and

optimum water contents. A similar relationship was observed in drive core samples in Phase III and IV mentioned above.

2.2.3.3 Phase V

Results from PSD tests for alluvial drill cuttings from Phase V boreholes drilled by AR-RC and DR-CA methods include the following:

- Good agreement was found between field estimates and laboratory measurements of major particle size fractions in unsaturated alluvial drill cuttings. This agreement permitted using field estimates to fill in data gaps between laboratory measurements.
- PSD profiles of unsaturated alluvium from 13P located on the eastern edge of Crater Flat are finer grained than profiles from the other Phase V boreholes in Fortymile Wash. This is consistent with a trend in fining of PSDs identified in Phase IV boreholes as you proceed westward from Fortymile Wash.
- Very similar PSDs were measured for alluvium drill cuttings produced from approximately 60 to 150 ft bgs both in 24PA where the DR-CA Symmetrix™ method was used and in 24PB (located 37 ft from 24PA) where the AR-RC method was used.
- Since AR-RC methods have previously been shown in Phase III and Phase IV to produce drill cuttings from unsaturated alluvium with a fine fraction (silt plus clay) and coarse fraction (sand plus gravel) that approximate core samples, it is likely that the DR-CA Symmetrix™ method is also capable of producing unsaturated alluvium drill cuttings that are reasonably representative of formation conditions.
- Gravel and sand fractions in DR-CA samples from the unsaturated alluvium in 22PC are also reasonably representative of sonic core from saturated alluvium, which in turn is representative of in situ conditions. Moreover, if the loss of fines as dust from unsaturated DR-CA drill cuttings samples in 22PC could have been reduced, the fines size fraction in the DR-CA drill cuttings would also likely have been in reasonable agreement with the fines in sonic core and the formation alluvium.
- Comparison of PSDs of unsaturated alluvium from Phase V borehole 24PB and Phase IV borehole 24P (separated by approximately 150 ft) shows that the former is noticeably coarser grained than the latter. Both boreholes were drilled using similar AR-RC methods and equipment, but by different drillers. Besides some differences in drilling related factors, differences in alluvial stratigraphy between the boreholes are likely in part responsible for the differences in measured PSDs. Higher water production rates measured in 24PB are consistent with the coarser sediments penetrated in the unsaturated portion of this borehole.
- A comparison of PSD profiles of unsaturated alluvium drill cuttings between Phase V boreholes 24PB and 32P, the latter located approximately 5 miles south (downgradient) of the former, shows that 32P is slightly finer in texture than the upgradient borehole 24PB. This is not unexpected given the relative position of the boreholes in the Fortymile Wash flow system.

- As expected, AR-RC drilling methods produced similar water content depth profiles in Phase V boreholes with similar PSD depth profiles. These Phase V borehole pairs included 24PB and 32P, and 24PA and 24PB. Under drained pre-drilling conditions, water content profiles are expected to be similar in boreholes with similar PSD profiles. In addition, it is expected that drilling impacts on water contents would be similar for boreholes with similar PSDs.

Results of Phase V electrical conductivity tests on a one-to-one by weight ratio of water to alluvium drill cuttings extracts show the following:

- Close agreement is observed in electrical conductivity depth profiles of unsaturated alluvium between: Phase V corehole 22PC and Phase III borehole 22SA located approximately 60 ft apart, and in the upper 150 ft of Phase V 24PA and 24PB located 37 ft apart.
- A comparison of electrical conductivity depth profiles for Phase V 24PB and Phase IV 24P shows significant differences even though they are separated by only approximately 150 ft. This observation is consistent with the differences in alluvial stratigraphy shown in PSD depth profiles mentioned previously.
- The relatively close agreement in electrical conductivity depth profiles between Phase V 24PB and 32P, with the latter located approximately 5 miles downgradient in lower Fortymile Wash, may in part be related to similar PSD depth profiles described above.
- The magnitude of electrical conductivity peaks in 13P depth profiles exceeds all peaks in other Phase V boreholes. The high values of electrical conductivity in 13P are likely related to the basalt flow present from approximately 85 to 140 ft bgs; and more specifically, basalt weathering products, including clay minerals.

Results of Phase V field and laboratory tests on sonic core samples from corehole 22PC and some comparisons with Phase IV corehole 19PB show the following:

- The average calculated gravimetric water content for Phase V 22PC sonic core segments was 0.17, whereas for 19PB sonic core segments the average gravimetric water content was approximately 0.13. This difference of 0.04 in average water content translates into a difference of 0.04 or more in dry bulk density. That is, if the water content of 19PB was increased by 0.04, the bulk density would decrease by approximately 0.04. In summary, evaporative losses from 19PB sonic core samples in the field may in part be responsible for the higher average dry bulk densities (1.80 to 1.82 g/cm³) calculated for 19PB sonic core runs compared to average values for 22PC (1.66 to 1.71 g/cm³).
- Summary statistics for PSD data from Phase V 22PC sonic grab core samples show that all samples are coarse-grained and, on the average, contain approximately 16% fines and approximately 40% gravel and 44% sand. The USCS group name for the average PSD composition is a silty or clayey sand with gravel(SM/SC with gravel).
- A depth profile graph of major particle size fractions in 22PC sonic core determined by wet sieve analyses indicate that gravel varies more than the other major size fractions with depth. For example, the range in gravel extends from 16 to 72% and in some cases differs by more than 40 to 50% in adjacent depth intervals. This depth profile also shows

a trend of slightly increasing percentages of fines and sand with depth and a corresponding decrease in percentages of gravel with depth.

- The fines fraction is composed of nearly identical proportions of clay and silt in sonic grab core samples over the entire cored interval in Phase V 22PC based on hydrometer particle size analyses. However, there is a slight increase in fines and clay beginning at approximately 625 ft and continuing to total depth at 763 ft.
- The Atterberg limits-based classification of the fines fraction in sonic grab core samples from 22PC shows that silt (ML) predominates over clay (CL) and silty clay (CL-ML) in the upper 150 ft of the alluvial aquifer and the opposite is observed in the underlying 150 ft. The predominance of clay over silt and silty clay below approximately 625 ft corresponds to the slight trend in increasing clay mentioned previously based on hydrometer test data.
- Little difference was observed in the average values of the major size fractions between Phase V 22PC sonic core and Phase IV 19PB sonic core. The average values for the sand and gravel fractions in 22PC are only approximately 1% lower than average values in 19PB, and the average value of the fines fraction for 22PC samples is only approximately 1.5% higher than in 19PB.
- Calculated averages of PSD fractions for Phase V 22PC and Phase VI 19PB that are weighted by the variable lengths of the individual sonic core sample intervals agree even more closely than unweighted averages. A slightly greater range in sand and gravel fractions was observed in 19PB than in 22PC.
- Taken together these relatively small differences in PSDs between coreholes suggests that the approximately 3 mile separation between 22PC and 19PB in the Fortymile Wash flow system does not appear to significantly impact the PSDs in the upper portion of the alluvial aquifer in lower Fortymile Wash.
- Sonic core electrical conductivity data from the lower part of the unsaturated zone immediately above the present water table in Phase V 22PC shows only a single small spike or peak in EC that reaches 327 micromhos/cm at approximately 364 ft.
- In contrast, Phase IV sonic corehole 19PB exhibits several large spikes or peaks in electrical conductivity of approximately 1,000 micromhos/cm and valleys (i.e., low values) between 200 and 400 micromhos/cm in the interval immediately above the water table.
- It is possible that variations in paleo-water tables may be responsible in part for these greater variations in electrical conductivity values in 19PB. Numerous other factors including paleo-soils and paleo-recharge events may also play some role in the development and maintenance of these electrical conductivity peaks and valleys in 19PB.

2.3 Well Completion and Development

2.3.1 Well Completion Overview

Piezometers and monitoring wells were constructed in accordance with permit requirements and Nevada Administrative Code (NAC 534.60–534.90). In this report piezometers are defined as smaller diameter monitor wells with screened intervals generally shorter than those in multi-

screened monitor wells. Screen intervals were selected based on geologic logging, geophysical logging, and water production observations.

Tables 2.1-1, 2.1-2 and 2.1-3 summarize completion data for Phase III, IV and V, respectively. These completion data include casing sizes, screened and sand-packed intervals, and formation units adjacent to these intervals. This same information (except formation units) is presented as completion diagrams in Appendix B in Phases III, IV, and V in NWRPO (2003a), NWRPO (2005a), and NWRPO (2009), respectively. In addition, the completion diagrams show the type and depth intervals of different sand and grout seal materials used. Depth data in the above mentioned tables and appendix have not been corrected for borehole deviation.

2.3.1.1 Completion Procedures Used in the Majority of Phase III Wells and all Phase IV and V Boreholes

This section does not address the emplacement of completion materials in Phase III CA boreholes (22PA and 10P) and Phase III AR borehole 18P. These completions will be described in Section 2.3.1.2. The completion of all other Phase III, IV, and V boreholes is described in the following.

Examples of well completion diagrams applicable to this section include: Figure 2.3-1 that shows the completion of multiple screen monitor well 19IM1, Figure 2.3-2 that shows the completion of AR-RC piezometer 16P with a single screen that spans the water table, Figure 2.3-3 that shows a dual-string piezometer completion in sonic corehole 22PC, and Figure 2.3-4, that show a triple-string piezometer completion in AR-RC borehole 32P.

Depth control for the emplacement of sandpacks and grout seals was carefully monitored by estimating downhole annular volumes, tracking volumes of emplaced materials, and frequently checking depths of emplaced materials by manual tagging methods. In nearly all cases, these materials were emplaced with tremmie pipe methods. The bottom of the tremmie pipe was set approximately 10 to 30 ft above the level of completion materials to avoid plugging off the tremmie pipe. Target depths for the emplacement of sandpacks were 5 to 10 ft above and below each well screen.

Generally, grout seals in both the unsaturated and saturated zones of AR-RC boreholes consisted of intervals of high solids (i.e., more than 30% solids) bentonite grout and intervals of a mixture of 8/12-mesh silica sand and 8-mesh granular bentonite at a ratio of approximately 2 to 1 by weight. The NWRPO refers to this mixture as Bensand. The lower portion of the boreholes that required plugging back to a depth closer to the water table were sealed primarily with high solids bentonite grout, with shorter intervals of Bensand serving as solid platforms for depth measurements and to support additional quantities of high solids bentonite grout. Bensand was also used to plug zones where large amounts of high solids grout were lost to the formation. A similar grout sealing method was used in most cases in the upper portion of boreholes above the uppermost well screen and sandpack. Finally, Bensand was used to seal zones both below and above the sandpacks.

On occasion cement grout was substituted for high solids bentonite or Bensand in unstable regions of the borehole below the water table, and for high solids bentonite in the unsaturated

zone above the uppermost sandpack. Bentonite chips (3/8-inch) were also sometimes substituted for high solids bentonite in the uppermost portion of the borehole.

High solids bentonite grout was emplaced in the borehole using a diaphragm (positive displacement pump) and tremmie pipe. Similar equipment was used to emplace cement grout where required. If bentonite chips were used in the unsaturated upper portion of boreholes, they were emplaced by gravity free-fall methods.

Sandpacks and Bensand seals were emplaced using tremmie pipe and centrifugal pump methods. Pumped water was used to carry both sandpack and grout seal completion materials through the tremmie. Water was initially pumped through the tremmie followed by the addition of dry completion materials to the water stream via an open "Tee" connection on the water-intake of the centrifugal pump. Completion materials were generally emplaced in lifts approximately 5- to 10- ft thick, decreasing in thickness as target depths were approached.

In Phase V sonic corehole 22PC the drill casing was pulled back in 10 to 30 ft stages and completion materials were emplaced in these intervals. This approach minimized the adverse effects of borehole caving, related bridging, and the mixing of caving materials with the completion materials. This staged approach to completion was not strictly followed in Phase IV sonic corehole 19PB and caving occurred between 411.5 and 490 ft bgs. This resulted in the placement of the upper piezometer screen higher in the borehole than originally planned.

Wellhead protection features in all completed wells included a near surface cement grout seal, concrete pad, and locking well cap. Each well head is labeled with the well name in the cement pad. The wells were surveyed by a DOE contractor under YMP QA standards to provide location and elevation data presented in Tables 2.1-1, 2.1-2 and 2.1-3.

2.3.1.2 Completion of Phase III Boreholes 10P, 18P, and 22PA

The completion of saturated zone intervals in CA boreholes 10P and 22PA was similar to monitor wells and piezometers described in Section 2.3.1.1. However, the unsaturated zone in 10P and 22PA was instrumented with air piezometers, which required a different completion approach. Figure 2.3-5 shows the completion diagram for 22PA that includes air piezometers in the unsaturated zone and dual-string piezometers in the saturated zone. For these wells with air piezometers, the grout seals consisted of Bensand that was tremmied dry to the desired depth by gravity-feed methods. The dry Bensand was then hydrated in the annular space by conducting water down the retreating drive casings. Care was taken not to over-hydrate the grout seals directly below and above the air piezometers. The 8/12-mesh sandpack for the air piezometers was also emplaced by tremmie line and gravity feed.

As in sonic coreholes, the completion of CA boreholes 10P and 22PA was accomplished in stages. The casing was pulled back in 10- to 30-ft intervals to minimize the potential for the borehole to cave onto the well string. Following this pull-back, the bottom of the well was re-sounded to determine if there had been any caving of the borehole. Completion materials were then emplaced in the pull-back interval up to approximately 5 ft from the bottom of the casing.

Sandpacks for air piezometers were designed to be approximately 5 ft thick, extending approximately 1.5 ft above and below the 2-ft-long piezometers. However, some difficulties

were encountered with the deeper sandpacks, whereby thicker sandpacks than planned were installed. Another difficulty encountered was that in several cases water, used in installation of saturated zone well screen sandpacks and Bensand grout plugs, flooded the unsaturated annular space around deeper air piezometers. This excess moisture will be allowed to dissipate (i.e., drain and redistribute) before conducting any air-permeability-related tests with the air piezometers.

At Phase III AR borehole 18P, the saturated zone annular grout seal consists of 0.25-in. time-release bentonite pellets emplaced by gravity feed through a tremmie pipe. Above the water table, the grout seal consists of 0.375-in. bentonite chips emplaced in a similar manner. The chips were hydrated by adding water from the surface down the annular space. The surface completion for 18P as well as 10P and 22P were generally similar to the surface completions described in Section 2.3.1.1. Details of these surface and subsurface completions for 10P, 18P, and 22PA are illustrated diagrams in Appendix B of NWRPO (2003a).

2.3.1.3 *Completion of Westbay[®] Packer and Instrument Monitoring Systems in Phase III Monitor Wells*

Westbay[®] packer and instrument monitoring systems (MP55 systems with PVC casings) were installed inside the 6.625-in. OD steel casing at 10S and 22S, and inside the 7-in. OD steel casing at 19IM1. PVC was selected for chemical resistance. Inflatable packers were used to isolate discrete well-screen intervals. Within the isolated intervals, measurement ports were installed for in situ temperature/pressure sensors, and sampling ports were installed for purging, sampling, and aquifer testing. Appendix C in NWRPO (2003a) contains the diagrams of the three Phase III Westbay[®] installations. Separate reports on Westbay[®] installation operations are available in the NWRPO QARC.

2.3.2 Well Development

Phase III FM monitor wells 10S, 19IM1, and 22S were drilled using large volumes of bentonite and bentonite/polymer fluids. Large volumes of these fluids were also lost to the formation during drilling. Significant well development described in the following section was required to remove as much of these drilling fluids as reasonably possible.

Piezometers drilled with AR-RC methods in all phases and with CA methods in Phase III primarily used air as the drilling fluid in the saturated zone. As a result, in most cases these wells do not contain drilling fluids in the saturated zone that could impact well screen permeability and/or water chemistry measurements, and development of these wells to remove drilling fluids was not required.

The only exceptions were Phase III piezometer 23P and Phase IV piezometer 28P. In both boreholes significant quantities of bentonite/polymer drilling fluids were used in the saturated zone during drilling to control caving. In 23P additional large volumes of bentonite/polymer drilling fluids were added while attempting to remove the drill string that became stuck at approximately 1,340 ft bgs. Following the severing of the lower portion of the drill string with explosives, the borehole caved to approximately 712 ft. Upon completion of dual piezometers in the uncaved saturated portion of this borehole, a significant amount of suspended bentonite/polymer was observed in the lower piezometer screen. Drilling fluid was also observed in the single screen extending across the water table in 28P following completion

activities. Several development methods were required to remove drilling fluids from screened intervals in these piezometers.

2.3.2.1 Development of Multiple-Screen Monitor Wells 10S, 19IM1, and 22S

Two swabbing approaches were used to develop each Phase III monitor well. First, development was conducted using a low-flow air-lift tool (similar to that used in FM drilling) with a swab at the bottom; second, swabbing and pumping was carried out using a Grundfos® 5HP pump suspended between two swabs. In both approaches the swab system was moved up and down across well screens while removing drilling fluids and water. The rate of air-lifting water varied from 0.5 to 4 gpm, and the water pumping rate ranged from 5 to 35 gpm. The NWRPO determined that the double swab and pumping development approach was more effective than the single swab and low-volume air-lift approach.

Development of monitor wells using swabbing methods continued in most cases until the water was free of suspended matter (i.e., clear), as subjectively determined by the NWRPO. At monitor well 10S, development was terminated due to budget constraints before acceptable clarity was achieved. This well was later further developed by air-lifting methods which did not fully remove suspended drilling fluids. After this air-lifting development, the open well bore was pump tested for 48 hr, which provided the additional development required.

2.3.2.2 Development of Piezometers 23P and 28P

Limited air-lifting development was conducted in the lower piezometer screen of 23P over a period of approximately 3 hrs. During this development, care was taken not to lower the water level to a point where head differences between the inside and outside of the 2-in. Schedule 80 PVC casing could cause the casing to collapse.

Following this air-lifting development, suspended bentonite/polymer was observed in both screens in 23P and the single screen in 28P. This remaining suspended bentonite/polymer in 23P was removed by pumping the upper screen for approximately 32.5 hr and the lower screen for approximately 9.5 hr with a small piston sample pump at approximately 0.5 gpm. Pumping 28P for approximately 48 hr at a rate of approximately 0.5 gpm with the same piston sample pump cleared up most of the suspended material in the single well screen.

2.4 Borehole Lithology

2.4.1 Summary Lithologic Logs

Summary lithologic logs are found in drilling reports for Phases III, IV, and V in NWRPO (2003a), NWRPO (2005a), and NWRPO (2009), respectively.

2.4.1.1 Phase III

As presented in the NWRPO Phase III drilling report (NWRPO, 2003a), the summary lithology of boreholes drilled during Phase III is as follows:

Boreholes 10SA and 23P; Sites 19 and 22

The alluvial section in borehole 10SA becomes slightly finer-textured with depth, transitioning from a well-graded sand with silt and gravel (SW-SM) to a silty sand with gravel (SM) at approximately 350 ft bgs. The slightly finer-textured underlying SM alluvial unit in borehole 10SA extends down to the contact with Tertiary volcanic conglomerate sediments at 790 ft bgs. This similar alluvial stratigraphy is also found in Phase III boreholes located at Sites 19 and 22 along the current Fortymile Wash channel. This SM unit has been replaced by a significantly finer-textured clayey sand with gravel unit in 23P, located approximately 2 miles east of the current Fortymile Wash channel.

Borehole 18P

Tuffaceous bedrock units penetrated in 18P may potentially belong to the Paintbrush Tuff and Crater Flat groups. However, definite assignment of a specific unit name to each rock type logged is not possible because the conventional-circulation rotary-drilling method used to penetrate these units produced only very fine particle size drill cuttings. Many of the features that distinguish these units were not observable on these fine particle size drill cuttings. However, tentative preliminary assignments of formal tuff unit names have been assigned to bedrock units penetrated from top to bottom as follows: Topopah Spring Tuff, Calico Hills Formation, Prow Pass Tuff, Bullfrog Tuff, an unnamed pre-Bullfrog volcanic sandstone, and Tram Tuff. These preliminary assignments will be revised if and when additional data become available from Site 18 during future phases of the EWDP.

2.4.1.2 Phase IV

As presented in the NWRPO Phase IV drilling report (NWRPO,2005a), the summary lithology of boreholes drilled during Phase IV is as follows:

Boreholes 27P and 16P

The Miocene volcanic section stratigraphy penetrated by 27P and 16P is generally similar to other wells south of Yucca Mountain, such as WT-11 and -12.

The thickness of major pyroclastic flow deposits is consistent with like units within the main block of Yucca Mountain; the major exception is the relatively thin 150-foot section of Tiva Canyon Tuff in 27P, which suggests some restriction during deposition.

16P includes every major Miocene tuff unit from the Ammonia Tanks Tuff through the top of the Tram Tuff and penetrates nearly the entire 2,500- to 3,000-foot thickness of the upper volcanic aquifer (i.e., the top of the water table in the Rainier Mesa Tuff to the top of the Pre-Tram Tuff sedimentary rocks).

Borehole 28P

28P penetrates the upper portion of the Miocene volcanic section from the Ammonia Tanks Tuff through the Topopah Spring Tuff. However, the Crater Flat Group tuff members are missing beneath the Topopah Spring Tuff. Instead, older sedimentary (Ts) rocks are penetrated, similar to those encountered in deeper sections of Phase I and II boreholes 1DX, 3D, 2DB.

The fact that such an unconformity exists and the Crater Flat Group tuff members are missing in 28P but present in both 16P and 27P suggests that 28P is located on the footwall of a large buried syn-volcanic (i.e., growth) fault, while 16P and 27P are located on the hanging wall, with an approximate displacement of 1,500 ft or more.

The thickness of the volcanic aquifer is greatly diminished in comparison to 16P to the north. The aquifer (i.e., the top of the water table to the top of the Pre-Tram Tuff sedimentary rocks) at this location is less than 1,000 ft thick.

Borehole 24P

The first bedrock unit encountered in 24P is Bullfrog Tuff, at approximately 400 ft bgs. Several explanations for this anomalously shallow intersection are possible.

An explanation consistent with the apparent unconformity in the volcanic sequence in 28P is that 24P is also located on the footwall of a large growth fault, where lower tuff units of the Crater Flat Group were structurally uplifted and possibly eroded prior to the eruption of the Topopah Spring Tuff.

Gravity and magnetic data suggest that growth faulting could be responsible for the uplift in the Crater Flat Group-aged rocks to form a buried structural high southward from the east side of Yucca Mountain (near well UE25-p#1) to the northwest side of Busted Butte and southwestward to the west side of the Lathrop Wells cinder cone.

Borehole 29P

Borehole 29P penetrated a relatively thin 380-foot section of Paintbrush Group tuffs before being terminated at 790 ft bgs due to unstable open borehole conditions (flowing sands). The 230-foot-thick Topopah Spring Tuff, elsewhere up to 1,000 ft thick, indicates that some restriction in the basin occurs, possibly the paleotopographic high discussed in regard to 24P and 28P.

Corehole 19PB

In 19PB, intervals of gravels with clay, silt, and sand predominate between the water table and approximately 500 ft bgs. Between approximately 500 and 630 ft bgs, clayey sands with gravel predominate. The upper interval consists mainly of textural layers with less than 12% fines; the lower consists mostly of layers with 12% or more. Layers in these two intervals would be expected to exhibit different average saturated hydraulic conductivity(Ksat) values, based on laboratory tests conducted on small-scale repacked core samples. The division of the upper saturated alluvial aquifer into these two textural units may be useful in future modeling studies. However, this two-unit division may be an oversimplification, and alternative modeling approaches may be required to capture the previously described Ksat variability in the numerous textural layers.

2.4.1.3 Phase V

As presented in the NWRPO Phase V drilling report (NWRPO, 2009), the summary lithology of boreholes drilled during Phase V is as follows:

Borehole 13P

The alluvium from ground surface to a depth of 87 ft is unremarkable and similar to other near-surface alluvium in Fortymile Wash and northern Amargosa Desert. A Pliocene basalt flow (~4.1 Ma) was penetrated from 87 to 140 ft bgs; samples were not recovered from 140 to 160 ft bgs, but are thought to be alluvium based on geophysical logs. Alluvial sediments penetrated between 160 and 260 ft bgs were primarily composed of silty sand with gravel and a layer of sandy clay from approximately 180 to 200 ft bgs. The gravel component of this alluvium includes unique clasts of weakly cemented and HCl reactive sandstone and more typical welded tuff lithologies. The sandy clay unit is similar to clay-rich horizons only encountered at depths greater than 500 ft bgs in the Fortymile Wash area at boreholes 2DB, 5S, 4PB and 23P. The nature of the clay sediments suggests a playa depositional environment, probably of limited extent along a restricted drainage system prior to the eruption of the basalt flow.

Underlying the alluvium from 260 to 797 ft bgs are primarily volcaniclastic tuffaceous rocks with lacustrine-deposited tuffaceous claystone and sandstone likely deposited in a relatively lower energy environment. The water table was encountered at approximately 433 ft bgs. The interval from approximately from 797 to 1,550 ft bgs is a sequence of primarily fluvial sediments with altered tuff layers interpreted to represent preserved fault-related fan-sequences deposited in a relatively high energy environment during early post-Timber Mountain time (12.5 Ma - middle to late Miocene) during rapid extension along the Windy Wash fault. From 1,550 to 1,569 ft bgs the borehole penetrated an apparent welded tuff unit that may represent Bullfrog Tuff (member of the Crater Flat Group) or coarse clastic debris derived locally from Bullfrog Tuff (i.e. younger erosional material).

Boreholes 24PA and 24PB

Borehole 24PA was terminated at approximately 150 ft bgs as a result of downhole drilling system failure. Borehole 24PB intersected a nearly identical sequence of subsurface geological units as 24P. The alluvium-bedrock contact and groundwater was encountered at approximately 405 ft bgs, followed by Bullfrog Tuff from 405 to 900 ft bgs, pre-Bullfrog sedimentary rocks from 900 to 945 ft, and Tram tuff from 945 to 1,377 ft bgs. The borehole was terminated in Pre-Tram sedimentary rocks at 1,395 ft bgs. Volcanic units younger than Bullfrog were either eroded away or not deposited at this location.

Borehole 32P

Borehole 32P encountered alluvial units from surface to 396 ft bgs, consisting of well-graded sand with silt and gravel (SW-SM), typical of alluvial units in the upper approximately 500 ft in Fortymile Wash boreholes. The water table was encountered at approximately 260 ft bgs, with the static water level rising to approximately 245 ft bgs. Between a depth of 396 and 496 ft bgs, an approximate 4 Ma Pliocene basaltic lava flow was encountered. The basalt is underlain by a conglomeratic sandstone unit from 496 to 550 ft bgs. The sandstone grades downward into unconsolidated fluvial sediments from 550 to 940 ft bgs. Overall, the section of unconsolidated sediments shows a fining downward. Finally, underlying the unconsolidated sediments are lacustrine siltstone beds from 940 to 1,000 (TD) ft bgs.

Without the presence of a marker unit, except the Pliocene basalt, the age of the sediments below 496 ft is uncertain. It is possible that this sequence is entirely “post-volcanic”, that is younger than the last large pyroclastic eruptions of the Timber Mountain Group volcanics at approximately 11.5 Ma. An alternative interpretation is that the sedimentary sequence (below 496 ft) consists of a pre-volcanic older sedimentary units overlain by Pliocene-aged basalt. This would imply a significant unconformity or non-deposition surface at the stratigraphic top of the sedimentary sequence (496 ft bgs). Unfortunately, few direct dating methods are available to determine ages of sedimentary sequences.

Borehole 33P

Borehole 33P was drilled by DOE contractors as one of several boreholes drilled in the Yucca Mountain area for analysis of volcanic hazards. Geologic data provided by the DOE indicates that the subsurface geologic units consist of 195 ft of alluvium overlying Tertiary conglomeratic sediments from 195 to 535 ft bgs. The open borehole water level was encountered in the upper portion of this conglomeratic unit at approximately 204 ft bgs. The borehole terminated in a Tertiary volcanic unit consisting of non-welded, bedded, and reworked tuff extending from 535 to at least 657.1 ft bgs. Preliminary identification suggests that these tuffaceous rocks are a member of the Paintbrush Group volcanics. The overlying conglomeratic sediments are similar in description to rocks in 13P from 1,140 to 1,315 ft bgs, as well as 10SA and 22SA. Overall, below the alluvium, the sequence at 33P appears to represent a post-volcanic Miocene section not seen at 32P.

Corehole 22PC

This corehole was located at site 22 to collect nearly continuous sonic core samples from the lowermost unsaturated and upper saturated zone alluvial sediments (460 to 763 ft bgs). Gravel units predominate in the upper approximate 170 ft (460 to 632.1 ft), and sand units in lower approximate 130 ft (632.1 to 763.0 ft). The mainly gravelly units above 632.1 ft generally contain less than or equal to 12% fines, and below 632.1 ft the mainly sandy units generally contain more than 12% fines. That is, there is a slight fining in particle size distribution with depth.

2.4.2 Borehole Geophysics

Borehole geophysical logs conducted in Nye County boreholes are generally classified into one of three logging suites: drill string, open hole, and well completion. Tables 2.4-1, 2.4-2, and 2.4-3 contain a summary of logs run in Phase III, IV and V, respectively. Borehole geophysical logs were used for lithologic characterization and stratigraphic correlations. For the most part, only qualitative interpretations of rock properties were made from the logs.

Responses of open hole suite logs to changes in formation conditions are dampened to various degrees by drilling fluid mud and responses of drill string logs are dampened by steel drill casing. In spite of this dampening, logs in the drill-string suite clearly show the location of the water table and zones that may be producing or taking water, changes in water-filled porosity immediately above and below the water table, and where present, the contact between alluvium and tuff. The dampening effects also do not prevent open-hole suite logs from providing useful information regarding water production zones and confirmatory information on the depth of the

alluvium-tuff and the alluvium-volcanic conglomerate contacts, where present. Finally, both drill-string and open-hole logs yield valuable information regarding the impact of drilling fluids and additives on the formation fluids. Specific examples of these log responses will be described in more detail in the following sections.

Although the well-completion suite helps to confirm the location and integrity of sand packs and bentonite seals, it shows few if any trends related to formation lithology and/or water production. As a result they will not be discussed further herein. These well-completion logs may be downloaded from the Nye County website or viewed at the QARC.

Significant findings include the following:

- Increasing amounts of clay in formation materials often correlate with increasing natural gamma counts, decreasing formation resistivity log values, decreasing density values, and decreasing neutron porosity log counts (increasing water filled porosity).
- In some cases, increasing amounts of clay correlate with all of the above, except increasing natural gamma counts. In these cases, natural gamma counts may decrease (rather than increase) as a result of a decrease in the concentration of gamma emitters with depth in the formation rock.
- In alluvium, valleys in natural gamma logs and peaks in density and neutron porosity logs can correspond to clean well-graded sand and/or gravel that produces clean water. These sand and/or gravel units can serve as preferential flow paths.
- Conglomeratic arkosic sandstone generally produces increases in natural gamma, density, and neutron porosity log values.
- In volcanic units, formation resistivity logs are useful for identifying the degree of welding within ash-flow tuffs, and therefore useful for stratigraphic correlation. Higher resistivity values correlate well with welded rocks identified in the geological cuttings described at the site and low resistivity values correlate with nonwelded rocks.
- Basalt flows exhibit lower natural gamma counts and higher density values than alluvium. These correlations permitted identifying the lower basalt alluvium contact in borehole 13P where drill cuttings were not returned to the ground surface.
- In most boreholes, fluid resistivity, fluid temperature, and caliper logs could be used to identify discrete intervals where groundwater flows into or out of the wellbore. In several cases, formation resistivity, density, and neutron porosity logs supported identification of water movement into/out of the borehole.
- Optical televiewer logs, though not always of usable quality, show that in some places, these discrete flow zones are open fractures. Discrete inflow zones were identified in 16P, 27P, and 32P.
- In alluvial units in nearly every Phase V borehole, large peaks in caliper logs resulted from washout zones as well as corresponding decreases in natural gamma, density, and neutron porosity log values.
- Density and neutron porosity responses can be due to different clay contents, degree of cementation, grading of clasts, washout zones, and/or fractures.

- In the uppermost alluvial unit in boreholes located in Fortymile Wash, there is generally a slight increase in natural gamma counts and a slight decrease in density values with depth. This reflects a slight increase in finer textured fractions with depth.
- At greater depths in Fortymile Wash alluvium natural gamma, density, and neutron porosity logs generally show gradual increases with depth in response to increasing amounts of fines, overburden pressure/compaction, and possibly grading.

2.4.3 Cross Sections

New cross sections were developed and existing cross sections updated after each phase of drilling. Geologic cross sections were constructed using: 1) summary lithologic logs from EWDP boreholes; 2) borehole data from previous EWDP drilling phases; 3) geophysical data and maps from published and ongoing geophysical studies; and 4) published geologic information from the USGS and YMP. The following descriptions summarize various cross sections presented in previous drilling reports (NWRPO 2003a, 2005a, and 2009).

2.4.3.1 Phase III

The plan view of two cross-section lines prepared from summary lithology logs from EWDP boreholes in Fortymile Wash and the two alluvial cross sections are shown in the Phase III Drilling Report (NWRPO 2003a; Figure 4.5-3; Figure 4.5-4). Summary lithology logs for all boreholes shown in these cross sections are found in Appendix H of the Phase III Drilling Report (NWRPO 2003a). These include logs from boreholes 5S and 2DB that were drilled in Phases I and II, respectively.

The original summary logs for boreholes 5S and 2DB were revised to be consistent with USCS textural group terminology used in Phase III. The resulting revised summary lithology logs for these boreholes do not contain all the detail found in Phase III summary lithology logs because detailed logging forms were not used in earlier phases, the sample interval was larger, and laboratory PSD measurements were not routinely run. Moreover, all alluvium samples were washed free of fines prior to archiving, and therefore it was not possible to re-log the archive samples in a manner consistent with Phase III. Despite these difficulties, it is believed that the revised summary lithology logs for 2DB and 5S are reasonable approximations of subsurface conditions.

The Phase III cross-section A-A' that approximately parallels the primary axis of Fortymile Wash and the current channel indicates the alluvial textural units are reasonably consistent among 10SA, 22SA, and 19IM2A (NWRPO 2003a; Figure 4.5-4). However, between 19IM2A and 2DB there is a discontinuity in the alluvial units underlying the uppermost SW-SM unit. This discontinuity may be related to a subsurface fault, that may be the poorly defined Highway 95 Fault (Potter et al., 2002).

The volcanic sediments located at depth in 2DB (only the uppermost layer of these sediments is shown in Phase III cross section A-A') are commonly found in other EWDP boreholes located on the south side of the Highway 95 fault. These thick intervals of volcanic sediments differ significantly from the thick intervals of welded tuffs present closer to Yucca Mountain. Although the boreholes upgradient from 2DB along cross section A-A' do not extend deep

enough to penetrate welded tuffs, it is expected that these units or their equivalents are present at depth.

The B-B' cross section through boreholes 5S, 23P, and 22SA is almost perpendicular to the primary axis of Fortymile Wash (NWRPO 2003a; Figure 4.5-4) and shows the presence of finer-grained alluvium sediments along the eastern portion of the wash. These finer-grained sediments may be older lake deposit sediments that have been eroded away in the central region of Fortymile Wash. Alternatively, the discontinuity may be related to faulting. These finer-grained sediments may help to limit the possible migration of contaminants from Yucca Mountain to alluvial sediments located on the eastern portion of Fortymile Wash. The coarser-grained higher-permeability sediments located in the central portion of Fortymile Wash may serve as preferential conduits for groundwater flow.

Many of the interpretations presented above were reevaluated based on data from Phase IV and Phase V.

2.4.3.2 Phase IV

Phase IV geologic cross section A-A' is drawn through the Flat Tire Flat area and includes 27P, 16P, and 28P (NWRPO 2005a; Figure 6.3-1). This cross section is based on relatively close-spaced boreholes and detailed stratigraphic identifications.

Phase IV cross sections B-B' and C-C' are presented in the Phase IV Drilling Report (NWRPO 2005a; Figures 6.3-2 and 6.3-3). While all cross sections are interpretive in the projection of geologic features and correlations at depth, these cross sections, drawn at a larger scale in order to project to greater depths, are considered more interpretive, or conceptual, than Phase IV geologic cross section A-A' and are referred to herein as conceptual cross sections.

Conceptual cross section B-B' is drawn from 27P on the west side to 22SA on the east side. Conceptual cross section C-C' is drawn from 24P on the north side to 2DB on the south. The two cross sections intersect at 24P.

The Phase IV cross sections include data from boreholes drilled in EWDP Phases II and III. Lithologic logs from Phase III boreholes 2DB and 22SA are presented in NWRPO (2003a). Geologic data projected in the cross section for 19D1 is a composite of data from two closely spaced boreholes drilled from the same pad at Site 19 but to different depths. These two boreholes are 19IM2A, whose summary lithologic log is included in NWRPO (2003a), and 19D, with a less detailed lithology report that can be viewed on the NWRPO website (NWRPO, 2007a). 19IM2A was not as deep as 19D; data from 19D has been used only to extend lithologic data and interpretations below the total depth of 19IM2A.

Geologic interpretations of basins and fault structures in the cross sections were aided by a gravity-based interpretation of the thickness of Cenozoic deposits (NWRPO 2005a; Figure 1.3-3) and interpretations of aeromagnetic survey data (NWRPO 2005a; Figure 1.3-4).

Neither geologic nor conceptual cross sections identify textural groups within the alluvium. Stratigraphic units are identified by formal group name and, if practical, divided into tuff members. Contacts between groups are shown with darker lines to emphasize large-scale trends.

2.4.3.2.1 Phase IV Cross Section A–A'

Geologic cross section A–A' is constructed in two panels with a bend at 16P (NWRPO 2005a; Figure 6.3-1). The alluvial units are generalized at the scale of the cross section and labeled as Quaternary alluvium. Volcanic units are divided into the major tuff units described in the summary lithologic logs.

The water table occurs primarily within the Timber Mountain tuffs in this cross section and shows a very gentle slope.

The stratigraphy in these three closely-spaced boreholes (i.e., 27P, 16P, and 28P) shows remarkable differences. Because of these differences, other geological and geophysical data are used to infer structures between the boreholes.

Two faults are shown. The fault to the southeast, between 16P and 28P, represents a buried growth, or syn-volcanic, fault. Borehole evidence indicates that the fault was active until buried by the Topopah Springs Tuff. On the footwall of this fault, Pre-Crater Flat units are uplifted, possibly rotated and eroded, and form a paleotopographic high. The gravity and magnetic signatures of this feature (NWRPO 2005a; Figures 1.3-3 and 1.3-4) are consistent with a northeast-striking normal fault with a throw of approximately 1,640 ft. The fault to the northwest is a younger fault in comparison, offsetting all the volcanic units. This normal fault preserves the Ammonia Tanks Tuff in the hanging wall and exposes Rainier Mesa Tuff in the footwall.

2.4.3.2.2 Phase IV Conceptual Cross Section B–B'

Conceptual cross section B–B' is a west-east cross section (NWRPO 2005a; Figure 6.3-2). To help with interpretation, nearby boreholes are projected into the plane of the cross section.

The alluvial units are lumped together and labeled as Quaternary/Tertiary alluvium. The volcanic units are divided by group name; individual tuff units are not shown at this scale. A darker and wider line of color, similar to that of the individual volcanic group, represents the approximate interpreted top of that group. The top of the Paleozoic-aged rocks is based on the thickness of Cenozoic deposits (NWRPO 2005a; Figure 1.3-3).

The water table measured in wells is also drawn on this cross section. At this scale, the water table is fairly flat across several fault blocks and rock units.

The interpretation of the Paleozoic surface is based mostly on gravity data (NWRPO 2005a; Figure 1.3-3). The most prominent feature in this cross section is the structure high of Paleozoic-age units underlying the high fault block between 28P and 24P. This high block is expressed at the surface by a ridge of outcropping Paintbrush Group.

The west side of the section shows a graben-like feature of upper Tertiary volcanic units having been dropped down into the structure that defines Flat Tire Flat basin. This graben, which preserves Timber Mountain Group volcanic rocks, is expressed only in the younger Tertiary rocks. Gravity data suggests that the Paleozoic and older rocks are deep under the west end of the section toward eastern Crater Flat. If these rocks are very deep and the Paintbrush and Crater Flat

Group volcanic units are at the surface or very shallow, the Pre-Crater Flat Group (Tvo/Ts) units must thicken toward Crater Flat basin.

On the east side of conceptual cross section B–B', all units dip into Jackass Flat basin. The dip slope is broken by several normal faults, the largest of which is the Paintbrush Canyon Fault.

2.4.3.2.3 Phase IV Conceptual Cross Section C–C'

Conceptual cross section C–C' projects from south of U.S. Highway 95 near well 2DB to a location north of 24P (NWRPO 2005a; Figure 6.3-3). The water table crosses several units in this cross section due to structural relief. In 24P, the water table occurs at the alluvium/Crater Flat Group contact, in 29P it occurs in the Paintbrush Group tuffs, and in 19D1 and 2DB it occurs in the alluvium.

The interpretation of the Paleozoic surface is based mostly on gravity data (NWRPO 2005a; Figure 1.3-3). Prominent features include a fault-bounded basin north of Phase II borehole 19D1, with structural highs to the south, beneath 2DB, and to the north beneath 24P. Immediately north of 19D1 is a conceptualization of the Highway 95 Fault.

Between 2DB and 19D1, the southern edge of the basin is interpreted to step down to the north along growth faults active during deposition of the Crater Flat and Paintbrush Groups. An unidentified ash-flow tuff occurs in 19D1 but not 2DB (NWRPO 2005a; Figure 6.3-3). Positive identification of this tuff is problematic, as it is unusually yellow and does not resemble typical Paintbrush Group tuff. Whether this tuff is Paintbrush Group or possibly some younger tuff, the basin edge is thought to be the southern extent of the Paintbrush Group or an equivalent ash-flow tuff. The Paintbrush Group is exposed in outcrop between 29P and the northern end of the cross section. It has been eroded off the structural high penetrated by 24P.

An eastern splay of the Paintbrush Canyon Fault is intersected obliquely by this cross section north of 24P. It therefore has an apparent low dip angle. Along the fault, the Paintbrush Group is juxtaposed against the Crater Flat Group.

2.4.3.2.4 Phase IV Cross Section Interpretation

Cross section A–A' defines an important relationship in the evolution of the Crater Flat basin. Previous workers speculated that the thickening of Cenozoic deposits across the gravity gradient illustrated on this cross section was a result of thickening of deposits of Tvo and Ts (Potter et al., 2002). Drilling data illustrated on this cross section suggest that the thickening likely involves rocks as young as Crater Flat and Paintbrush Groups. Due to the uncertainty of the age of the units penetrated on the footwall block, the apparent throw of approximately 1,640 ft may be greater if the footwall block is deeply eroded. No well-defined stratigraphy or chronostratigraphy has been defined for the older rocks (i.e., Tvo and Ts), which limits the interpretative value of an intercept of older rocks in 16P and other EWDP boreholes.

Work by Murray and others (2003) in mapping the older sequences in the region provides a stratigraphic framework for the older rocks, but more detailed definition will be required to interpret stratigraphic location within the sequence. The scale of the total thickness of these older rocks can be misleading. Three boreholes in the Yucca Mountain region have been drilled

through the section (i.e., Felderhoff Federal 25-1, UE 25p#1 and 2DB), all at locations chosen because of a lack of thick section of these deposits. In the thickest section of the basins, such as in Crater Flat on conceptual cross section B-B' (NWRPO 2005a; Figure 6.3-2), these deposits may be more than several miles thick. The Crater Flat basin may be better described as a Late Oligocene and Early Miocene sedimentary basin capped by middle Miocene volcanic deposits.

This stratigraphic uncertainty becomes more acute where sections of the more familiar volcanic section are missing, or where the volcanic rocks interface with the older sequence along fault boundaries such as the Highway 95 area. For example, in 2DB, the volcanic stratigraphy consists of a single thin tuff unit identified as Tram Tuff by YMP workers. This thin tuff unit is overlain by a short sequence of fine-grained sedimentary and volcanoclastic units, possibly representing eruptive events to the north. The Tram Tuff in 2DB is underlain by a thick sequence of fine-grained sedimentary units without defined marker beds or detailed stratigraphy. It is therefore very difficult to understand the exact stratigraphic position of an isolated borehole or borehole intersection.

Moreover, stratigraphic correlations of similarly textured Ts can be made only at a very large scale with much uncertainty.

2.4.3.3 Phase V

Two geologic cross sections were constructed using: 1) summary lithologic logs from EWDP boreholes; 2) borehole data from previous EWDP drilling phases; 3) geophysical data and maps from published and ongoing geophysical studies; and 4) published geologic information from the USGS and YMP. The locations of the two geologic sections are shown in Figure 2.4-1. These cross sections update the Phase IV conceptual cross sections.

Phase V cross sections A-A' and B-B' are presented in Figures 2.4-2 and 2.4-3, respectively. Textural variations within the alluvium are not distinguished on the cross sections. Volcanic units are identified only to the group level. Newly recognized sedimentary units are differentiated as formations. Geologic relationships are generalized between areas of sparse borehole data where they are inferred from geophysical information.

Geologic cross section A-A' is constructed between boreholes 16P and 24P and includes extensions to the west-northwest and east-southeast that incorporate data projected from nearby boreholes 13P, 27P and 22SA. Section A-A' intersects the southernmost part of Yucca Mountain, extending eastward across Fortymile Wash in Jackass Flats. The section is approximately perpendicular to the strike of faults and potentiometric contours of the uppermost volcanic aquifers.

Geologic cross section B-B' is constructed south from borehole 24P to 19D where the section bends westward continuing to 32P. Data from nearby borehole 2DB is projected onto the southwest-trending segment. The northerly segment of the section is approximately parallel to strike of normal faults except the Highway 95 Fault. The section updates and expands on the conceptual cross section (C-C') constructed for the Phase IV Drilling Report (NWRPO, 2005a).

Information from geophysical surveys including interpretive gravity survey maps (NWRPO 2009; Figure 6.3-1), aeromagnetic surveys (Blakely et al., 2000; Perry et al, 2005; NWRPO

2009, Figure 6.3-2), a deep penetrating resistivity survey conducted by the NWRPO in conjunction with USGS Water Resources Division in 2006 (RID 7242) and a limited seismic reflection survey along a portion of the B-B' geologic section has been incorporated into the sections. Profiles of the interpretive gravity survey, "depth to Pre-Cenozoic" (Blakely and Ponce, 2001) are plotted on the cross sections.

Two types of faults are identified based primarily on previous mapping (Potter et al, 2002) and data from earlier drilling phases (NWRPO, 2005a). Early faults represent basin bounding growth faults that are buried by the thick volcanic ash-flows tuffs of the Paintbrush Group and younger tuff units. Later faults are the more familiar and well-mapped Miocene faults of Yucca Mountain. The locations of the buried older faults are based primarily on basin thickness changes identified in the gravity survey interpretations (Blakely and Ponce, 2001; NWRPO 2009, Figure 6.3-1). On the cross sections, early faults are identified as "pre-13 Ma" faults that generally provide for the depositional thickening of Pre-Crater Flat Group Sedimentary Rocks (Tvo/Ts). The younger faults are identified as "post-13 Ma" faults that offset the major ash flow tuff units of the Crater Flat and Paintbrush Group and locally the Timber Mountain Group. Several older faults are likely re-activated by younger faulting.

2.4.3.3.1 Phase V Cross Section A-A'

Section A-A' is constructed across the southeastern-most part of Yucca Mountain between eastern Crater Flat and lower Fortymile Wash (Figure 2.4-2). This is an update of the conceptual section B-B' from the Phase IV Drilling Report (NWRPO, 2005a). New Phase V information from borehole 13P at the eastern margin of Crater Flat provides data on the Windy Wash Fault in that area. This section is also close to part of the B-B' cross section by Potter, et al (2002). Depth to pre-Cenozoic rocks from the interpretive gravity map of Blakely and Ponce (2001) are plotted on both cross sections A-A' and B-B' (Figure 2.4-3).

Overall, the section presented is similar to the section published by Potter et al (2002). The relatively late closely spaced domino-style Miocene normal faulting (post-13 Ma), similar to the structural pattern observed at Yucca Mountain in the repository area, is maintained across this section. The major north-south trending faults including Windy Wash, Stagecoach Road and Paintbrush Canyon Faults are shown to have the largest throws. The cross section also illustrates structural relationships first suggested by results from Phase IV drilling (NWRPO, 2005a) including buried growth faults, paleotopographic highs, and the extent and thickness of several major ash flow tuff groups near their farthest southern extents in the Highway 95 area. In the central part of the cross section, in the area of Phase IV drill holes 27P, 16P and 28P, the cross section shows a prominent northeast trending gravity "high" where the depth to the pre-Cenozoic rocks is relatively shallow. This interpretation is supported by the intersection of Pre-Crater Flat Group Sedimentary Rocks (Tvo/Ts) underlying Paintbrush group volcanic rocks at shallow depth in borehole 28P.

The gravity feature is described by Potter, et al, (2002) as follows: "A buried northeast-striking fault is interpreted beneath southern and central Yucca Mountain and the Calico Hills from regional gravity data". Furthermore, the fault is marked by "a steep northeast-trending gravity gradient that tracks a 20-mGal northwest-side-down step in the isostatic residual gravity anomaly map" . . . and . . ." the southwest end of this trend is near Lathrop Wells Cone; it crosses

Fortymile Wash near Fran Ridge and passes to the northwest of the exposures of Paleozoic rocks in the Calico Hills”. This unnamed fault, referred to herein as the Crater Flat-Jackass Flat Basin Structure or CJS, separates the larger and deeper Miocene Crater Flat basin of Fridrich (1999) into the Crater Flat basin proper (which includes central and northern Yucca Mountain) from the smaller and shallower Miocene basin beneath much of Jackass Flat and southern Yucca Mountain. Cross section A-A’ illustrates this structure as an approximately 4 km wide zone of west-northwest-dipping buried faults defined by the steep gravity gradients. The Crater Flat basin can be characterized by thick pre-volcanic deposits (>1 km thick) overlain by a complete sequence of middle Miocene tuffs. The Jackass Flat basin is characterized by thin pre-volcanic deposits (<1 km thick) with thinner and less complete sequence of middle Miocene tuffs. The westernmost part of the footwall block of the CJS has an angular unconformity between the Topopah Springs Tuff (not differentiated) of the Paintbrush Group and lower Tvo/Ts units intersected in borehole 28P. The “fault zone” or CJS comprises a series of buried pre-13 Ma growth faults in which the hangingwall blocks preserve greater thicknesses of the depositional units of the upper section of “older volcanics and older sediments” (Tvo/Ts) and all members of the Crater Flat Group. The eastern strand of the CJS (east of 28P) is likely reactivated as the Stagecoach Road Fault presumably after the eruption of the Paintbrush tuffs.

The initial recorded Tertiary (Oligocene-early Miocene?) extension accommodated by the north-northeast trending CJS is substantial, with at least 1,600 ft of down-to-the-northwest throw between boreholes 28P and 16P and substantially more (at least 3 km) across the entire CJS. The section also illustrates the potential relationship between the growth faults inferred to be the cause of the thickness variations in Tvo/Ts units, that are inferred from Blakely and Ponce (2001), and later, more northerly-striking, middle Miocene normal faults of Yucca Mountain, specifically, the Stagecoach Road Fault, which likely developed along an older, reactivated fault among those included as part of the CJS.

The difference between “depth to Pre-Cenozoic” and the base of Tvo/Ts rocks shown for the section line A-A’ at the 28P location may be attributed to the distance, approximately 5,100 ft, across which drill hole data is projected. The line of projection of the drill hole data is nearly perpendicular within a south-southwest plunging basin based on gravity data. Unit thickness of the Crater Flat volcanics as shown on the CJS footwall thicken in the area the A-A’ section relative to the 28P location, but the 28P data is projected to demonstrate the variability of preservation of Crater Flat units in the basin, probably at the thinnest section of Crater Flat volcanic units (Figure 2.4-2).

At the location of 28P along the CJS, the top of Tvo/Ts is encountered at depths as shallow as 1,340 ft. The section includes calcareous mudstone and sandstone (Ts), locally containing pyrite, interbedded with units of “older tuffs” (Tvo). In borehole 28 P the deepest strata between 1,974 ft and TD at 2,080 ft comprise mainly mudstone and claystone locally containing green clay beds, gypsum layers and pyrite. These rocks are equivalent to the “older sedimentary rocks” discussed in the Phase IV Drilling Report.

In light of the shallow depth of the older rocks beneath units of the Paintbrush Group, a substantial unconformity exists between older sedimentary rocks (Ts) and Paintbrush tuffs along the easternmost extent of the footwall block of the CJS. It is also evident from the cuttings collected from 28P (NWRPO, 2005a, Plate 3), that these Ts rocks are deeply weathered,

indicating that the footwall block was likely uplifted, tilted and eroded prior to burial by the Paintbrush Group volcanics. Furthermore, although the exact age of the Ts units encountered in 28P is unknown (NWRPO, 2005a), the timing of the extension along this fault is assumed to be prior to the eruption of Crater Flat Group volcanic from approximately 16 to approximately 13 Ma and possibly earlier based on the thickness of older sedimentary rocks (Ts). Burial began during eruption of Paintbrush Group about 12.8 Ma.

At the western end of section A-A' data from borehole 13P provides new information about the stratigraphy in eastern Crater Flat. The borehole was drilled in the hangingwall area of the Windy Wash Fault west-northwest of 27P. Based on the geologic interpretations presented in Section B-B' of Potter et al. (2002), volcanic units of the Timber Mountain Group would be encountered at less than 100 m. During drilling no middle Miocene volcanics units (Tc, Tp, Tm) were penetrated in the 1,559-foot-deep borehole. Based on the complete sections intersected in other parts of Crater Flat and the likelihood of preservation of the middle Miocene section in the hangingwall of the Windy Wash Fault, it is interpreted that these rocks occur beneath the total depth reached in 13P.

Information from 13P indicates that the Windy Wash Fault has a larger throw and is longer lived than previously thought. Borehole 13P intersects a section of post-Timber Mountain units including volcanics (Tvy) with interbeds of volcanoclastic units and lower sedimentary units (Tsy₁ and Tsy₂). The throw and timing of the Windy Wash Fault in this area is unknown; movement along the fault is assumed to be younger than Timber Mountain tuffs (< 11.5 Ma). The preservation of a thick section of post-Timber Mountain units suggests that the fault is long-lived, possibly from middle Miocene to post-4 Ma as suggested by local offsets in the Pliocene (~4 Ma) basalt flows. If Timber Mountain Group volcanics do actually exist below the TD of 13P, the throw on the fault is approximately 3,300 ft, based on the offset of the Paintbrush Group tuffs between the hanging wall exposures east of 13P and the expected intercept below the TD in 13P.

Current models of groundwater/hydrogeology (i.e. Hydrologic Framework Model for the Saturated Zone Site-Scale Flow and Transport Model [HFM], Sandia National Laboratories [SNL], 2007.) do not address the stratigraphic and structural relations described herein. Based on the hydrogeologic definitions used in the HFM model, the footwall block of the CJS in the 28P area at A-A' is comprised of units within the Paintbrush Volcanic Aquifer (PVA) and upper Crater Flat aquifer units (CFPPA), not the fine-grained lacustrine and volcanoclastic rocks of the lower volcanic and sedimentary units (Lower VSU) intersected in 28P. In the HFM, the Lower VSU (aquitar) is located approximately 1,000 ft below the intercept of LVSU in 28P. Flow models derived from the HFM (i.e. Saturated Zone Site-Scale Flow Model, SNL, 2007) would contain a large degree of hydraulic connectivity in the volcanic aquifer units above the Lower VSU that does not exist in the area of 28P. Similarly, structural offsets and juxtaposition of tuff aquifer units against Lower VSU units at the Windy Wash, Stagecoach Road and Paintbrush Canyon Faults are not reflected in the HFM surfaces. These offsets are primary impediments to west-to-east flow. The HFM surfaces also do not model the outcrops of Paintbrush tuffs located in the footwall blocks of these faults, instead, substituting alluvial aquifers in their place.

2.4.3.3.2 Phase V Cross Section B-B'

Geologic cross section B-B' is constructed south from borehole 24P to 19D1; where the section bends westward continuing to 32P. Data from nearby borehole 2DB is projected onto the southwest-trending segment (Figure 2.4-3). The northerly segment of the section is approximately parallel to the strike of normal faults except the Highway 95 Fault. The section has been updated with data derived from the drilling of borehole 32P in northern Amargosa Valley. Deep-penetrating resistivity surveys (RID 7242) provide control on the extent of large-scale subsurface units, centered primarily near the Highway 95 fault. The survey resolved the depth and extent of contrasting resistivity units (interpreted as gross geologic units) along the section line to depths of 3,000 to 5,000 ft.

The new borehole data, deep-penetrating resistivity survey data, and gravity data are used to improve earlier interpretations of the structural relationships first presented in the Phase IV Drilling Report (NWRPO, 2005a), add to geologic information from earlier phases (NWRPO, 2001a; NWRPO, 2003a), to interpret the discontinuous geology between wells and identify major bounding faults, and to resolve the depth of the post-volcanic basin-fill to help resolve the complex nature of the Highway 95 Fault. The cross section replaces the conceptual cross section C-C' from the Phase IV Drilling Report (NWRPO, 2005a).

The southern margin of the Yucca Mountain area coincides with the northeastern boundary of Amargosa Valley that is the locus of paleospring deposits. This discontinuity also coincides with the Highway 95 Fault which may have accommodated right-lateral movement during opening of the Crater Flat basin (Fridrich, 1999). Potter et al., 2002 depict the Highway 95 Fault as a nearly east-west right-lateral oblique fault with a down-to-the-north dip-slip component. The Highway 95 Fault (NWRPO, 2005a, Conceptual Cross Section C-C') is shown as a north-dipping growth fault bounding a volcanic basin to the north, cut by a younger right lateral oblique fault (slightly to the north).

In this updated interpretation, the Highway 95 Fault is a complex series of faults (i.e., fault zone) that form a roughly symmetrical graben-like feature (or sag) (Figure 2.4-3). This feature is bounded by an older master fault as the southern north-dipping right lateral oblique structure acting as a growth fault, a similar smaller parallel fault to the north (~2,500 ft), and younger and steeper graben faults again to the north that down-drop and preserve the thin volcanic units and produce a basin in which younger sedimentary rocks were deposited. The younger graben features preserve post-Paintbrush sedimentary basin-fill units and the unique younger tuff encountered in borehole 19D.

The Highway 95 Fault is a steep right-lateral strike-slip fault zone that may have been modified during subsequent deformation. The graben-like feature (or sag) shown on section B-B' may reflect uplift of the Paintbrush tuff on the north side of the Highway 95 Fault caused by contraction orthogonal to the strike of Miocene normal faults. The sag is bounded on the south by the main strike-slip fault.

Within the fault zone, post-volcanic sedimentary basin-fill rock units identified based on drilling data are designated as Tsy₁, Tsy₂, and Tsy₃, based primarily on stratigraphic relationships in borehole 2DB, the most complete section drilled, and less complete sections in nearby boreholes 19D1, 22SA and 10SA in western Fortymile Wash.

Unit Tsy₁ is comprised primarily of fine-grained interbedded poorly to well-sorted sandstone, laminated siltstone and claystone, and locally containing gravel or conglomeratic beds of fluvial and shallow lacustrine origin. These rocks are penetrated by borehole 2DB (see Summary Lithologic Log [RID 7196], and Cuttings Sample Logs [RID 4466]) where Tsy₁ occurs from 1,010 to 1,155 ft bgs. In 2DB Tsy₁ consists of interbedded poorly sorted sandstone with beds of clay/claystone and siltstone. The rocks are weakly cemented and have limited reaction to HCl, indicating little carbonate component. Locally conglomeratic beds are present with clasts exclusively of volcanic origin. In borehole 19D (see Summary Lithologic Log [RID 2569], and logs [RID 2565]), Tsy₁ occurs from 1,245 to 1,438 ft bgs (TD) and consists of interbedded gravelly sands, sand, clay, and silt.

Overlying the fine-grained volcanoclastic Tsy₁ unit are coarser-grained volcanoclastic conglomeratic sandstone and conglomerates designated as Tsy₂, intersected in boreholes 2DB from 925 to 1,010 ft, 22SA (see Summary Lithologic Log, RID 5472 [22SA]) from 1,110 to 1,200 ft (TD), and 10SA (see Summary Lithologic Log, RID 5471 [10SA]) from 790 to 1,200 (TD). The unit is comprised primarily of cobble to boulder volcanic conglomerate. Clasts are composed primarily of Paintbrush welded tuff in a matrix of clayey sand containing volcanic crystals. This unit is more than 400 ft thick in Fortymile Wash at site 10S.

The highest unit in the sequence, Tsy₃, identified in 2DB from 670 to 925 ft, consists of light colored sandy and silty clay with gravel, lean clay/claystone and silt/siltstone with a significant carbonate component. This unit is interpreted to represent shallow lacustrine deposits possibly with spring deposits developed over the Highway 95 Fault(s). Tsy₃ underlies alluvium in lower Fortymile Wash. Previous interpretations (Phase III Drilling Report, A-A', NWRPO, 2003a or RID 5613) had included the Tsy₂ and Tsy₃ units as part of the alluvial section. However, the sedimentary units did correlate northward with alluvial units in borehole 19IM2A. In the new interpretation, the Tsy₃ unit is shown as being deposited in a small, structurally controlled basin. Tsy₃ overlies older sediments (Ts) south of the southern strand of the Highway 95 Fault and younger sediments (Tsy₁ and Tsy₂) to the north. These fine-grained sediments were not intersected in the wells to the north (19D1, 22SA and 10SA) or southwest in 32P. Additionally, the Tsy₃ depositional units are relatively elevated with respect to the underlying depositional surface (~60m, see Phase III Drilling Report, A-A', NWRPO, 2003a), indicating the possibility that the Tsy₃ forms a constructional landform. This observation may suggest that either the unit is a deeply eroded remnant of larger or more widespread depositional unit, or that the deposits formed a constructional feature such as spring mounds. Further work including sediment mesh analysis and paleobotany of select samples is on-going to better understand the Tsy₃ sediments.

Gravity survey data (and the interpreted "depth to pre-Cenozoic") support the general sag-like form of the Highway 95 Fault zone at this location, but appears to be offset to the north approximately 3,300 ft, compared with the resistivity data. Nye County has proposed the collection of higher density gravity and seismic reflection data to resolve this discrepancy.

Borehole 32P is near the end of the section in northern Amargosa Valley. At this location, unsaturated and saturated alluvial layers are underlain by Pliocene-age basalt flows that were apparently extruded on to the land surface. Sediments below the basalt are strongly cemented and grade downward in to uncemented sediments of primarily volcanically derived detritus. These volcanoclastic sediments are correlated with post-volcanic sediments (Tsy₁) in boreholes

2DB and 19D. Below 940 ft, the volcanoclastic sediments are underlain by homogeneous siltstone units correlated with pre-volcanic sedimentary rocks (Ts). A northwest-striking growth fault between wells 2DB and 32P is interpreted to exist where the gravity-based “depth to pre-Cenozoic” increases toward the southwest.

2.4.3.3.3 *Phase V Cross Section Interpretations*

New subsurface data provides the opportunity to reinterpret stratigraphic and structural relationships to depths of 1,600 to 3,300 ft with additional geologic constraints. The interpretations benefit from drilling information supplemented with targeted geophysical surveys. The new geologic insights are also useful for developing models of groundwater flow. The new interpretations provide a substantially different interpretation of the two largest features in the flow system south of the Yucca Mountain, namely the CJS and the Highway 95 Fault. There is evidence that both of these features impact or possibly control groundwater movement in the general area. Large upward hydraulic gradients are observed in wells in close proximity to the Highway 95 Fault (wells 19D, 2DB, 33P and 3D), presumably as a result of upward leakage along faults from the higher head zone in the underlying Paleozoic carbonate rock aquifers.

In the eastern section of the Highway 95 Fault (intersected by B-B'), east of Windy Wash, uncertainty exists where the thick ash-flow tuff sheets of the Southwest Nevada Volcanic Field (SWNVF) and Yucca Mountain terminate at or near this feature. The area is obscured by thick alluvial cover, and without the benefit of drill data and/or targeted deep-penetrating geophysical methods, the nature of this feature is speculative. Magnetic surveys (Perry et al, 2005) indicate that the magnetic volcanic rocks terminate rather abruptly at approximately the latitude of 19D, either as an abrupt pinch out, or as a southward-dipping package below younger basin-fill, in an apparent basin that should preserve these units. This would suggest that the Highway 95 Fault forms a growth fault (as in NWRPO, 2005a Conceptual Cross Section C-C') with a deeper basin to the north of the fault, as suggested by the gravity surveys (NWRPO 2009; Figure 6.3.3), and that by Paintbrush age (~12.8 Ma), forms a buttress feature that restricts the extent of welded ash-flow tuffs.

Drilling at 2DB, south of the Highway 95 Fault, confirms that volcanic units are not present in the subsurface south of the fault. If these tuffs were deposited, they were eroded prior to deposition of alluvium (Figure 2.4-3). In post-volcanic time (after ~11.5 Ma), the region south of the fault, was structurally elevated, leading to a nonconformity between pre-volcanic rocks and deposition of the first alluvial cover. The alluvial cover thickness is relatively uniform in the area near 2DB (compared with other boreholes in western Fortymile Wash [19D, 22S, and 10S]), also suggesting that the area south of the fault was structurally stable during alluvial deposition (presumably after ~10 Ma). Based on this new data and interpretation, the Highway 95 Fault can be described as a complex fault zone (approximately 2 miles wide) with progressively younger structures toward the north (Figure 2.4-3). These younger faults form grabens (or, on a large scale, a sag) that through time are filled with progressively younger sedimentary basin-fill units toward the center. The oldest volcanic units terminated against the oldest and southernmost fault (a growth fault) and subsequent younger grabens formed north of this, which allow the thickening and preservation of post-volcanic sedimentary units (Tsy), younger volcanic (Tmt) and alluvium. The magnetic ash flow tuff units (primarily the Paintbrush Tuffs) are preserved at depth and magnetically muted by the younger cover.

Based on the new data and interpretation, the extent of the Highway 95 Fault can be extrapolated along strike to the east and west from the B-B' section. It would appear that previous interpretations of the location and strike (Potter et al., 2002) were based primarily on the newer magnetic data available at the time (Blakely et al., 2000). Using the gravity maps (and interpretive Depth to Pre-Cenozoic Map, Figure 6.1-1, Blakeley and Ponce, 2001), the Highway 95 Fault would be better traced by a "line" following the northern side of the gravity "high" in northernmost Amargosa Valley, north of Highway 95. This line, or fault trace, trends west-northwest (not east-west) and terminates against the northeast-trending fault(s) depicted on Section A-A' (CJS; NWRPO 2009; Figure 6.3-4), near the Stagecoach Road Fault (a younger feature), northeast of the Lathrop Wells Cone. This interpretation suggests left-lateral movement along the CJS Fault and related structures. The movement may have offset the Highway 95 Fault.

Evidence from the resistivity geophysical surveys indicates that the Highway 95 Fault has two sub-parallel strands, an older master fault to the south, and a slightly younger sympathetic hangingwall fault to the north (approximately 2,620 ft). Using the same criteria to extend the fault westward, it would appear that the fault is offset southwestward (approximately 2 miles) along the CJS and reappears to the southwest of the Lathrop Wells Cone near well 3D, and continues with a similar west-northwest strike to terminate against the Bare Mountain Fault. Distribution of paleosprings and abrupt changes in the potentiometric surface also provide objective indications of a possible fault at depth. Based on this interpretation, the Highway 95 location and strike is significantly different than in previous publications, but is consistent with the updated geophysical data sets. These strands of the Highway 95 Fault are shown on the aeromagnetic survey map which shows boreholes that will be discussed in connection with the fault strands (NWRPO 2009; Figure 6.3-2).

The western portion of the fault also has a similar structural character, whereby the extent and thickness of Miocene-aged tuffs are abruptly terminated southward at this fault. However, along this western section of the Highway 95 Fault, the termination of tuff units are relatively elevated, end more abruptly than similar units in the eastern section, and dip northward at approximately 10°, in contrast to the eastern section where the tuff units terminate more gradually and are buried by younger sedimentary and alluvial materials. Also, some magnetic volcanic units (probably Paintbrush group) extend southward "over" the Highway 95 Fault, mostly in the far western section in the area of wells 9SX and 12PA (NWRPO 2009; Figure 6.3-2). This relationship would suggest that the timing of displacement along the western portion of the fault is different than the eastern portion. Using this new interpretation, the western Highway 95 Fault would be better characterized as a fault system oriented similarly to the eastern Highway 95 Fault, but displaced left laterally by the CJS bounding fault. These two separate faults systems, an eastern and western fault (zone) could be described as "West Highway 95 Fault" and "East Highway 95 Fault" (NWRPO 2009; Figure 6.3-1).

Studying the depth to pre-Cenozoic and magnetic maps, three dominant features (East and West Highway 95 Faults and the CJS) are evident at the southern extent of the SWNVF south of Yucca Mountain. Collectively, these features are similar, as they represent concealed growth faults, which roughly define the terminus of the voluminous ash flow tuff sheets (carapaces from the calderas to the north), and control the thickness of Tertiary basin-fill and/or greatly modify the nature of deposition, either sedimentary or volcanic in nature. These faults (or fault zones)

define the boundaries of structural domains in which the “style, timing and magnitude of extension change abruptly,” as discussed by Fridrich (1999). Therefore, these faults are similar to and can be compared with, the other bounding faults of the Crater Flat basin, namely, the Bare Mountain Fault, Yucca Wash Fault, and the Gravity Fault (Fridrich, 1999).

3.0 REGIONAL GEOLOGIC CHARACTERIZATION

3.1 Surface Geophysics

Square-array direct-current resistivity (SAR) measurements and a dipole-dipole direct-current resistivity survey were conducted by the USGS in cooperation with Nye County. The SAR measurements were collected near borehole 29P in the spring of 2005 and the dipole-dipole direct-current resistivity survey was conducted from December 2006 to January 2007.

The SAR measurements were collected in efforts to determine whether this method would help identify the subsurface fractures in thick alluvial deposits (RID 6833). It was determined that without prior knowledge of depth to bedrock through the aid of lithologic logs from previously drilled boreholes, anisotropic conditions present in the alluvium may incorrectly be identified as subsurface fractures in the target bedrock units (Hoffman, 2006).

The dipole-dipole direct-current resistivity survey was conducted from December 2006 to January 2007 with the objective of better characterizing the Paintbrush Canyon Fault system in lower Fortymile Wash. The survey line ran from north of site 24 to south of SH 95 for 10 kilometers with station spacing of 300 meters. Data were processed to remove the effects of topography, and used to calculate an apparent resistivity pseudosection, an inverse resistivity model, and a resistivity response profile (RID 7242).

3.2 Structural Investigation of Western Rock Valley, Specter Range Region, and Northern Spring Mountains

3.2.1 Introduction and Overview of Results

This section summarizes the products of geologic field investigations that were produced by Nye County contractors with expertise in structural geology from the University of Pittsburgh. These individuals included Danielle Deemer and Damian Piaschik under the direction of Thomas Anderson. The section includes field investigations, interpretations, and conclusions having to do with the character of the Las Vegas Valley shear zone (LVVSZ) and its effects upon groundwater. The field studies were conducted as part of the overarching objective to assess the nature of faults and associated fractures in the vicinity of the Yucca Mountain repository and to gauge their role in providing pathways along which groundwater may move south away from the Yucca Mountain repository and the adjacent NTS toward the Town of Amargosa Valley (Amargosa Valley) and other populated areas (Figure 3.2-1). A major step in achieving this objective has been to characterize the nature of the Highway 95 fault, determine its tectonic setting and age, and establish its relationship, if any, to the LVVSZ. The work was initiated as a study complementary to the Nye County EWDP that aimed to assess the significance of a linear array of paleosprings along the boundary between Amargosa Valley and Crater Flat, and that coincide with the trace of the inferred Highway 95 fault (Figure 3.2-2).

Nye County work suggests that the discontinuity called the Highway 95 fault, which is marked by the paleosprings south of Yucca Mountain, is linked to the LVVSZ along a fault segment extending between Amargosa Valley and Mercury (Figure 3.2-1). The Highway 95 fault separates mainly Miocene volcanic rocks to the north from slightly older Miocene strata, mainly sedimentary, and probably underlying Oligocene beds to the south. The LVVSZ is a major, regional, right-lateral strike slip fault that extends northwestward about 100 km from Las Vegas to Mercury, Nevada. Estimates of offset along the shear zone range from 40 to 74 km. Barnes and others (1982) report 40-64 km offset based on Ross and Longwell's (1964) study of Ordovician stratigraphy. Fleck (1970) estimated 72 km of displacement based upon offset of isopach data for the Precambrian Stirling Quartzite; 30 km of offset is attributed to strike-slip movement and the remaining offset is from oroflexural bending (Barnes and others, 1982). Previous mapping and structural studies suggest that the LVVSZ ends or stops at Mercury or even Indian Springs, which seems unlikely along a shear zone with an estimated 48 ± 7 kilometers of displacement (Burchfiel, 1965; Wernicke and others, 1988). Although the trace of the LVVSZ has not been delineated north of Mercury (Barnes and others, 1982, Burchfiel 1965) shows an inferred extension of the LVVSZ that bends to the west beneath the southern flank of the Specter Range in the direction of the Highway 95 fault, a major fault that forms the southern boundary of the volcanic rocks of the Yucca mountain repository site. The Highway 95 fault is an important structure as indicated by; 1) field studies of ancient spring deposits near its trace and, 2) the juxtaposition of different lithologies across the fault as indicated by data from Nye County EWDP wells. Field investigations conducted by Nye County support the interpretation of a connection between the LVVSZ and the Highway 95 fault.

The LVVSZ influences the regional flow of groundwater as shown by Winograd and Thordarson (1975) (Figure 3.2-3). Winograd (1962) had also suggested that faulting and folding within this region controls groundwater flow and contaminate transport between basins and within the bedrock aquifers. Where the LVVSZ juxtaposes an aquitard and an aquifer a barrier to flow is created. Winograd and Thordarson (1975) noted a zone of high transmissibility southwest of Mercury although they did not attribute the transmissibility of this zone to the presence of the LVVSZ.

The zone of high transmissibility recognized by Winograd and Thordarson (1975) crosses the inferred transpressional segment of the LVVSZ, extending between Amargosa Valley and Mercury Valley, southwest of Mercury in the vicinity of the southern Specter Range and northern Spring Mountains (Figure 3.2-3). Current structural models of the Specter Range and northern Spring Mountains do not adequately explore the diverse structures that may accommodate the movement of groundwater in this region.

Field studies show that Mesozoic and Tertiary structures not only juxtapose clastic aquitards and carbonate aquifers, but also create flow paths and secondary porosity that increases transmissibility (Figure 3.2-4 and 3.2-5). Stratigraphic units shown in Figure 3.2-4 are defined in Figure 3.2-6. Detachments, which dip north-northeast under the Specter Range, distinguish a zone that correlates with the domain of high transmissibility noted by Winograd and Thordarson (1975) (Figure 3.2-3). The detachments are associated with thick layers of breccia, which affect the porosity and permeability of the rocks (Figure 3.2-5). Interconnected fractures and secondary porosity are common within breccia exposed near the surface (Figure 3.2-7).

Detachments appear to have a stronger effect on transmissibility than previous research estimated (e.g. Winograd and Thordarson, 1975; McKee and others 1998).

Among the detached rocks, the Specter Range thrust is interpreted as a major contractional feature co-genetic with transpression along the LVVSZ (Figure 3.2-1). The Specter Range thrust may be the principal structural expression of the restraining bend of the LVVSZ that strongly influences the flow of groundwater. The thrust may influence the movement of groundwater southwest from Mercury. In this region the hanging wall on the north side of the fault is composed of the lower aquitard that may deflect southward flow from the NTS towards the west. South of the thrust, intense fracturing, faulting, and brecciation that occur in the footwall are compatible with the extremely high transmissibility through rocks of the southern Specter Range and northern Spring Mountains.

3.2.2 Field Mapping and Reconnaissance

Near the end of 2001, mapping along Jackass flats Road between Skull Mountain and the Specter Range (Figure 3.2-8) revealed previously unrecognized folds in Miocene strata of Pavits Spring and underlying, older, Early Miocene beds (Figure 3.2-9). Field work during 2002 continued within the same region but was aimed at: 1) gathering structural data from rocks along the contact between Early Miocene (?) beds (Horse Spring equivalents) and underlying Cambrian strata; 2) gaining familiarity with Paleozoic formations and structures that they contain within the Specter Range; and 3) establishing structural relationships between the Striped hills and correlative units south of Little Skull Mountain and within the Specter Range.

Subsequently during 2006 and 2007 field study focused on the area between the Specter Range and northern Spring Mountains covering approximately 90 square kilometers between Amargosa Valley and Mercury Valley (Figure 3.2-1). A principal objective of this work was to conduct structural mapping in order to: 1) characterize fault zones, 2) document and measure extensional and contractional structures, and 3) determine direction and timing of fault motions based on structural relationships. The collection of field data and observations in southern Nevada spanned more than 10 weeks during three trips (Spring 2006, Winter 2006, and Spring 2007). Fieldwork focused upon three domains in the northern Spring Mountains and Specter Range: 1) the Point of Rocks quadrangle, 2) the hanging wall of the Specter Range thrust, and 3) the area surrounding the Stirling Mine. The areas encompassed approximately 80 km², 5 km², and 8 km² respectively. Geologic maps were produced from both field observation and structural measurements.

Nye County map analyses and field data interpretation resulted in: 1) recognition and characterization of structures related to activity along the LVVSZ, and 2) delineation of fault zones within which rocks may be especially porous and permeable. These results will be discussed in the following sections.

3.2.3 Results and Discussion from Field Studies and Analyses

Folded Tertiary strata, which crop out in Jackass Flats (Figures 3.2-8 and 3.2-9) record contraction interpreted as evidence for a transpressional structure. Geologic mapping southwest of Mercury shows that Neoproterozoic and Early Paleozoic carbonate and clastic strata comprise a thick section of rocks deformed by multiple gently dipping faults, commonly parallel to

bedding planes (Figure 3.2-5). The strata comprising footwalls and hanging walls adjacent to the fault surfaces have been detached as generally indicated by pebbly cataclastic breccia or less commonly by foliation in fine-grained rocks. The fault surfaces, or detachments, which commonly crop out in the northernmost Spring Mountains, dip gently north toward the Specter Range.

Within the mapped areas gently dipping faults cut Stirling Quartzite, Wood Canyon Formation, Zabriskie Quartzite, Cararra Formation, Bonanza King Formation, Dunderburg Shale, and Nopah Formation (Figure 3.2-6). The principal bedding-parallel fault in the northern Spring Mountains is the Point of Rocks detachment that separates the Dunderburg Shale and the overlying Goodwin Limestone. The fault is marked by a horizon comprising tens of meters of cataclastic breccia derived from Nopah Formation (Figure 3.2-10). The breccia sheet is locally folded about northeast plunging hinges. The footwall of the Point of Rocks detachment also contains older Cambrian and Precambrian units with north plunging folds formed during Mesozoic contraction (Burchfiel, 1965; Burchfiel and others, 1974; Abolins, 1999; and Cole and Cashman, 1999). Most of the map units comprising the footwall beneath the detachment are thinner than normal because of processes along the detachment faults have the tendency to grind away much of the rock.

A transect from the southeast to the northwest corners of the mapped domain shows 3,070 meters of section missing between the footwall and hanging wall of the Point of Rocks detachment (Figures 3.2-5 and 3.2-6). Although some loss by erosion cannot be precluded, the minimum section cut out due to detachment faulting is approximately 1,000 meters.

Rare slickenline lineations along detachment faults show two trends, east-west or southeast. East-west slickenlines record bedding parallel slip, compatible with Mesozoic folding (Burchfiel, 1965; Burchfiel and others, 1974; Abolins, 1999; and Cole and Cashman, 1999). Southeast trending slickenlines suggest south directed transport of the hanging wall, compatible with Tertiary transpression along the LVSZ (Deemer and Anderson, 2002).

In summary, rocks within the region between Skull Mountain and Highway 95, along the southern margin of the Specter Range, record ductile and brittle structures that Nye County attributes to contraction along a constraining bend of the LVVSZ during Miocene time. Structures were recognized such as folds, stratigraphic detachments, brecciation, thrust faults, left-lateral strike-slip faults and normal faults, most of which record the effects of contraction that may be attributed to transpression along the LVVSZ. These structures are described in more detail in the following. In addition, older Mesozoic structural features will be described as well as structural events creating several basins in the region.

3.2.3.1 Folds

Folds, recorded in Jackass Flats by rocks of Pavits Spring, are shown in Figure 3.2-9. The folds trend east and verge northward. Figure 3.2-11 is a working cross-section of this region and shows the general northward vergence of folding. Sargent and Stewart (1971) and Maldonado (1985) mapped some folds in Tertiary strata in the region but did not attribute them to transpressional contraction that inverted strata (Pavits Spring and Horse Spring equivalents) that had accumulated in the Late Oligocene-early Miocene Hamel Wash basin. Tertiary beds overlie Cambrian strata with a gentle angular unconformity as revealed in exposures north of Mercury.

Northeast of the Striped Hills steep dips are recorded locally by carbonate beds that generally occur low in sections of Horse Spring and equivalent strata. The steeply upturned Tertiary strata against comparably dipping Cambrian beds that characterize the Striped Hills indicate that tilting of the Tertiary and Paleozoic sections is co-genetic. Nye County speculates that the rocks of the Striped Hills were emplaced as a hanging wall onto mid-Paleozoic strata, as inferred by the map of Sargent and Stewart (1971) in Mesozoic time. During Tertiary contraction they were detached, peeled off the older thrust and folded along with the overlying Tertiary beds.

Abolins (1999) and Burchfiel (1965) noted north-plunging hinges in the northern Spring Mountains. Burchfiel also noted northeast plunging folds. Carr and others (1996) and Abolins (1999) did not recognize northeast plunging folds during later mapping, probably because they both mapped the Dunderberg Shale as a unit of the Nopah Formation.

Detail geological mapping by Nye County within the northern Spring Mountains and southern Specter Range delineated folds with two general orientations: north plunging and northeast plunging. Two types of north plunging folds are preserved: large synclines and anticlines and second order parasitic or M-folds. The large open upright synclines and anticlines involve the Johnnie Formation through the Guilmette Formation.

The hanging wall of the Nopah Detachment in the northern Spring Mountains also contains open plunging folds (Figure 3.2-12). The Nopah breccia sheet is locally folded about northeast plunging hinges. The current orientation of the Nopah Formation in the hanging wall and the bedding in the Dunderberg shale define the fold hinges.

3.2.3.2 *Stratigraphic Detachments*

Detachment is a nongenetic term which means a low-angle normal fault with younger units in the hanging wall and older units in the footwall (Axen, 2007). Low-angle normal faults or detachments in the past were typically interpreted to be odd thrust faults, mega-landslide faults, or unconformities (Axen, 2007). Detachments have recently been recognized in both extensional and contractional settings (Axen, 2007). Detachments are recognized via either stratigraphic discontinuities or by breccia and deformation that indicates a fault zone. Detachments along layering in Cambrian carbonate strata have been mapped in the eastern Specter Range and northern Spring Mountains (Burchfiel, 1965; Burchfiel and others, 1974; Sargent and Stewart, 1971). Stratigraphic discontinuities in the northern Spring Mountains between the Johnnie Formation and Stirling Quartzite, Stirling Quartzite and Wood Canyon Formation, and at the base of the Nopah Formation were mapped by Abolins (1999), who was the first to interpret these structures as detachments. Both Burchfiel (1965) and Abolins (1999) noted that section is missing along these detachments: 750 m along the Johnnie-Stirling detachment, 300 m along the Stirling-Wood Canyon detachment, and 3,000 m along the Nopah-Stirling detachment (Figure 3.2-12). Abolins (1999) interpreted the Stirling-Johnnie detachment to be older and folded during Mesozoic east-west contraction. The small “klippen” of Nopah Formation were first noted by Burchfiel (1965) and Burchfiel and others (1974) who interpreted it as landslide deposits related to the complex structural relationships. Later the “klippen” were grouped into a regional structure by Abolins (1999).

Nye County mapping within the northern Spring Mountains and southern Specter Range corroborates common detachments among miogeoclinal units (Figure 3.2-6). Interformational

and intraformational detachments affect the: Johnnie, Stirling Quartzite, Wood Canyon, Zabriskie Quartzite, Cararra, Bonanza King, Dunderberg Shale, and Nopah Formations. Pebbly cataclastic breccia and gouge are commonly preserved between the hanging wall and footwall of the detachment faults (Figure 3.2-10). The most brecciated unit is the Nopah Formation, with tens of meters of breccia located, stratigraphically and structurally between the Dunderberg Shale and Pogonip group (Figure 3.2-5). Three separate detachments were mapped at different structural levels within the Nopah Formation. Detachments commonly coincide with silty and shaly beds, although strong layers are also detached and intensely brecciated. The detachments generally dip north-northwest towards the Specter Range. Most units beneath detachments are thinner than the regional equivalent. The Nopah Formation is 100-325 meters thick in the northern Spring Mountains, 220 meters thinner than Nopah sections measured in the Nopah Range to the south.

3.2.3.3 *Brecciation*

Extensive brecciation characterizes Cambrian and some overlying rocks in the Specter Range and northern Spring Mountains throughout an area of hundreds of km² (Figures 3.2-5 and 3.2-7). A major detachment in the northern Spring Mountains separates the Nopah Formation from underlying Wood Canyon Formation and Stirling Quartzite. About 3,000 meters of section is missing. The hanging wall of the detachment contains Nopah Formation, composed of crudely massive layers of breccia with angular fragments ranging from boulders to gouge (Figure 3.2-10). Hand sample and thin section analysis of fault rocks show shear fractures, secondary porosity between breccia fragments, gouge zones with survivor grains, highly rotated clasts, and high density fractures along cleavage planes within dolomite and calcite (Figure 3.2-7).

Nye County attributes most of the intense cataclastic deformation in Paleozoic carbonate strata to mid-Miocene deformation rather than landslides or the development of karst features in mid-Paleozoic or later times.

3.2.3.4 *Thrust Faults*

A major thrust occurs in the Specter Range (Figure 3.2-1). The Specter Range thrust strikes east-northeast and places Cambrian strata onto Siluro-Devonian formations. According to Sargent and Stewart (1971) the Specter Range thrust has a minimum heave of ~1.5 km. Steeply dipping Cambrian beds record folding in a klippe of the hanging wall. It is postulated that thrusts, similarly oriented, in the northern Spring Mountains record Tertiary contraction.

3.2.3.5 *Left-Lateral Strike-Slip Faults*

Left-lateral faults that strike northeasterly are present within the Specter Range (Figure 3.2-13). These faults cut the shallow detachments and some steeper faults in the hanging wall of the Specter Range thrust. Based upon the crosscutting relations, these left-lateral faults may be among the latest fault structures associated with simple shear deformation along the LVVSZ. Nye County interprets the left-lateral strike slip faults as structures that accommodate the effects of late contraction during which detached beds in both walls of the Specter Range thrust began to splinter and extrude or escape southwestward. Displacements based on interpreted piercing points along these faults are estimated to be between ~100 m to ~750 m.

3.2.3.6 *Rock Valley Fault and Associated Normal Faults*

The northeast-striking Rock Valley fault (Figure 3.2-14) which cuts thrusts, stratigraphic detachments and brecciated carbonate Paleozoic strata, is among the youngest faults in the study area. The Rock Valley fault is postulated to accommodate ~ 4 km of left-lateral displacement (O'Leary, 2000). This fault may cut and displace the LVVSZ constraining bend. Development of the Rock Valley fault indicates the transition to pure shear strain from simple shear strain among rocks within the region.

3.2.3.7 *Mount Shader Basin*

The Mt. Shader Basin (Figure 3.2-3) is a Miocene basin that extends from the Gravity fault (thick green line in Figure 3.2-3) to the edge of the northern Spring Mountains (Brocher and others, 1993). Paleozoic bedrock horsts separate the Mt. Shader basin into a series of subbasins (Brocher and others, 1993). Holocene, Pleistocene, and Pliocene alluvium unconformably cover the Miocene deposits within the basin (Brocher and others, 1993 and Workman and others, 2002).

In the southwest corner of the mapped area a few exposures of Miocene basin deposits crop out. These exposures represent the easternmost subbasin of the larger Mt. Shader basin. The Miocene deposits dip to the northeast indicating rotation due to faulting either post or contemporaneous with deposition. The basin-bounding faults are not exposed but are inferred to be parallel to the dip of the Tertiary units. The lowest exposed units in this mapped area crop out along the principal arroyo that cuts across a north-south normal fault and into the Miocene basin deposits comprising the footwall. The downthrown block is composed of younger Miocene tuffaceous deposits. This suggests that there have been two separate extensional events within the Tertiary, (1) northwest trending normal faults creating the Mt. Shader basins and (2) younger north-south normal faulting cutting the Miocene deposits. The relationships observed at the surface of eastern sub-basin of the Mt. Shader basin can also be observed in subsurface along an east-west seismic reflection profile conducted by the USGS (Figure 3.2-15)

The exposed Miocene basin deposits within the eastern subbasin of the Mt. Shader Basin comprise two mappable units, masses of breccia and beds of Tertiary basin fill conglomerate (Figure 3.2-16). The thicknesses of units are correct for dip. The breccia is composed of angular carbonate fragments in finer-grained matrix. The base of the unit commonly contains vertical sedimentary dikes composed of underlying Tertiary basin fill. The Tertiary basin fill is poorly lithified, crudely bedded, epiclastic breccia (conglomerate) composed of angular to sub-angular pebbles, cobbles, and boulders of carbonate and rarely quartzite. The matrix is composed of silt and sand sized particles (Figure 3.2-17).

3.2.3.8 *Mesozoic Features*

Few Mesozoic features are recognized within the region of study. A Mesozoic thrust is inferred (Sargent and Stewart, 1971) to coincide with the trace of the southern part of the Rock Valley fault. The basis for this thrust is the presence of duplicated Cambro-Ordovician carbonate strata that form a hanging wall, which is exposed in the Striped Hills. The easternmost extent of the hanging wall may be marked by outcrops of steeply dipping Cambro-Ordovician carbonate strata

that correlate with those in the Striped Hills. The hanging wall section may be different from the footwall section in that the Nopah formation is not exposed in the Striped Hills.

Abolins (1999) documents folds south of Highway 95 with northerly trending fold hinges, which suggests eastward-directed transport of the Mesozoic thrust. Since the thrust inferred by Sargent and Stewart (1971) is not north-south trending, it is speculated that this trace records the effects of Tertiary deformation rather than Mesozoic deformation.

3.2.3.9 Development of the Yucca Mountain Pull-Apart

Near Forty Mile Wash, the LVVSZ is interpreted to bend sharply north; that is, to the right (a transtensional step) (Figure 3.2-14). The right step resulted in the formation of a pull-apart basin that is now Yucca Mountain (Carr, 1984). The bounding faults of the basin are the Gravity fault in the east, Highway 95 fault in the south, and Bare Mountain fault in the west.

3.2.3.10 Sequence of Deformation

Based on the above described structural data, the following sequence (youngest to oldest) of deformation in western Rock Valley, the southern Specter Range, and the northern Spring Mountain region it is proposed:

- Left-lateral displacement along Rock Valley fault and normal faults at releasing steps.
- LVVSZV (simple shear strain) transpressional structures including left-lateral strike-slip faults, and bedding parallel detachments, folds, and thrusts.
- Mesozoic thrust with north-trending fold hinges in the footwall south of the region of study.

3.2.4 Summary and Conclusions

Locally, fracturing and brecciation along the LVVSZ provide significant pathways for groundwater flow. Structures related to faulting, folding, and other deformation within southern Nevada strongly influence groundwater flow and contaminant transport between basins and among bedrock aquifers. Faulting and strong brittle deformation in carbonate rocks along the restraining bend of the LVVSZ between Mercury and Lathrop Wells coupled with subsequent strike-slip faulting along the Rock Valley that transects the restraining bend have created an unusually porous and permeable body of rock that may contribute importantly to the transmission of groundwater from Yucca and Frenchman Flats via the Mount Shader Basin to Amargosa Valley.

On the basis of Nye County field work and map analyses it is concluded that:

- The LVVSZ bends west near Mercury and is thereby linked to the Route 95 fault by means of a left (restraining) step between Mercury and Lathrop Wells.
- Right-lateral displacement along this segment of the LVVSZ, possibly tens of kilometers, occurred between about 16 and 10 Ma; and was accommodated by transpression marked by

rocks that record contractional structures within a wide zone extending tens of km north and south of the of the principal fault trace.

- Eruption of the volcanic rocks that form Yucca Mountain and the subsequent development of calderas composing the Southwest Nevada Volcanic Field occurred contemporaneously with transpression along the LVVSZ to the east.
- This eruption occurred within a releasing bend of the LVVSZ, west of, but adjacent to, the constraining step, when magma pushed through thinned crust between 16 and 10 Ma.
- The Highway 95 fault is part of a regional structure that was probably active during Early Miocene and possibly before.
- The segment of the fault between Bare Mountain and Lathrop wells, that forms the southern margin of the Yucca Mountain pull-apart basin, was active between about 16 and 10 Ma.

4.0 WATER LEVEL MONITORING

4.1 Introduction and Background

Nye County, as part of its on-going ISIP has been monitoring water levels in the Amargosa Desert and Pahrump Valley since 1999 (Table 4.1-1). These efforts have been aimed at addressing the lack of data on hydrogeologic conditions in key areas of concern. Major areas of uncertainty include the lack of detailed characterization of groundwater flow paths and travel times, the magnitude and probability of adverse impacts on the water resources of the region, and the likely effects of future development on the performance of the proposed nuclear waste repository at Yucca Mountain.

During the period FY02 through FY06 Nye County has conducted its own investigations to evaluate the reasonableness of the DOE's groundwater flow models of the Yucca Mountain Region. Nye County's research has been focused on two key areas: 1) evaluating the impacts of population growth and climate change on groundwater levels in the region, and 2) evaluating the hydrogeologic assumptions in the DOE's Total System Performance Assessment (TSPA). This section summarizes the investigative efforts by Nye County to evaluate these important issues.

4.2 Devils Hole Workshops

Local resource managers and science teams in the region have taken the opportunity to coordinate their organizational missions by participating in the special sessions of the Devils Hole Workshop hosted by the Nye County ISIP, and other organizations. Nye County presenters have generally focused on water resource issues and most of the presentations focused on either resource management issues, or the scientific investigations that Nye County has conducted in this field. In the period spanning FY02 – FY06 Nye County has made numerous technical presentations at the Devils Hole Workshops detailing the results of their scientific investigations and studies. Professional papers and posters have been presented at the special sessions and field trips have been conducted in areas of local interest.

Topics discussed within these presentations and reports have included general Nye County groundwater evaluations, low altitude recharge in arid environments, spatial and temporal variations in groundwater levels in southern Nye County and adjacent areas, testing of alternative conceptualizations of the shallow hydrologic units in northern Amargosa Desert, a description of the mission of Nye County's ISIP, and a field trip for the participants of the 2004 Workshop focusing on the hydrogeology along the flow path from the Spring Mountains to Devils Hole.

4.3 Data Collection

Presentations by many of the stakeholders at the Devils Hole Workshop have cited scientific uncertainty as a major hindrance in managing water resources and growth. Nye County's scientific investigations and water level monitoring program are focused on providing data and information that will help fill significant data gaps down gradient of Yucca Mountain, including Amargosa Valley, Pahrump Valley, and other affected communities. In the future, Nye County would like to perform a large-scale aquifer pump test in the Yucca Mountain – Amargosa Valley area. This test would provide needed hydraulic information and estimates of important vertical

and horizontal aquifer parameters, and will provide investigators with valuable data for calibrating numerical flow models.

Local groups in the various affected communities have an extensive list of concerns regarding water issues and future impacts of population growth. To address these issues and to aid the County in implementing effective water resource management, Nye County's NWRPO has compiled historic water level data from the Nevada Division of Water Resources Well Log database, the USGS National Water Information System (NWIS) database, DOE Underground Test Area (UGTA) Project potentiometric database, and supplemented those databases with recent water level measurements made by Nye County field personnel spanning the period from 1999 to the present. These data collected by Nye County are contained in a database that is available to interested parties from the QARC located at the Nye County NWRPO.

In the Ash Meadows area there is still not enough data to accurately define the depth to groundwater, and discharge and perennial yield estimates rely on this knowledge. In Amargosa Valley, additional monitoring wells are needed between the pumping centers in the farms area and the wildlife refuge, and there is an on-going effort by Nye County to improve the depth-to-water resolution in the Ash Meadows area. The issues facing managers and decision makers in Pahrump Valley center around large potential impacts resulting from urban growth and development, including subsidence, degradation of water quality, and increased pumping costs.

Throughout the period FY02 - FY06, Nye County continued its implementation of its water level monitoring program in an effort to refine the depth-to-water distribution. To date, the monitoring and associated evaluations have provided better definition of the groundwater conditions and have helped to answer questions regarding the directions and rates of groundwater flow, spatial and temporal variations in water levels in the region, the impacts of existing and future groundwater withdrawals, the significance of the contour interval selected in the preparation of potentiometric maps, and the use of composite hydrographs (available in the Nye County regional water level database) to better understand long-term water level trends in areas of insufficient data. The basic data collected by Nye County, and the associated data analyses and evaluations, have led to a better understanding of the hydrogeologic conditions at both the regional and local scales.

4.4 Growth and Decay of Groundwater Mounds

There is evidence of groundwater mounding in the Yucca Mountain region. D'Agnese and others (1998) presented a potentiometric map of the region and noted a number of mounds. The most prominent mound in the region is under the Spring Mountains, where water levels are more than 1500 m above those in Las Vegas Valley and Pahrump Valley, but many other lesser mounds were also noted. Dudley and Larson (1976) present a potentiometric map that shows the presence of a groundwater mound over the Devils Hole Hills. The observed mounds by these investigators were identified on the basis of recent water level data but the mounds present height, extent, and decay rate may reflect a combination of both Pleistocene and Holocene recharge rates.

Subsequently, D'Agnese and others (1999) evaluated the effects of climate change on water levels in the region. These workers simulated full-glacial, modern, and transitional climates. Their simulations suggested that large differences may exist between present day water levels in

the region, and those of only 20,000 years ago. Simulated water levels under glacial conditions were more than 1,000 m higher than today in some areas, and were 50 m to 500 m over most of the model domain. D'Agnese et al (1999) did not, however, link the simulations to determine the effects of paleoclimates on modern water levels. In Nye County's investigation, Buqo and Brooks (2006) evaluated this linkage to determine the likely effect of past climate on modern water levels.

The growth and decay of groundwater mounds under recharge areas has a well established mathematical foundation. Nye County performed evaluations to determine the suitability of groundwater flow modeling as a tool in evaluating the growth and decay of groundwater mounds. The numerical code used was MODFLOW Version 3.2, a block-centered finite difference code that can simulate aquifer conditions. The first series of evaluations were developed to simulate a field experiment conducted by Haskell and Bianchi (1965) in which the growth and decay of a mound were measured. The results of the simulations were similar to those from the Haskell and Bianchi field test in terms of the total height of the mound, but with some differences in the rate of growth and decay and the configuration of the mound.

Next, a series of two-layer numerical models were developed to evaluate the effects of various recharge configurations on the growth and decay of a groundwater mound over a long time frame for specific mountain ranges in the Yucca Mountain region. Multiple three-dimensional numerical models were developed for each of the areas. First, recharge was applied to simulate the wetter Pleistocene climate, then recharge was simulated at the modern rate, and finally, a simulation was run combining the Pleistocene and modern climate. Contour maps, cross-sections, and mass balance charts were prepared for each simulation. Each of the models resulted in simulated water levels that were higher during the Pleistocene than during the Holocene. This finding is consistent with the results of D'Agnese and others (1999). In four of the five models, the simulations representing the wetter Pleistocene climate followed by reduced precipitation and recharge during the Holocene resulted in groundwater mounds that were significantly higher than the mounds simulated on the basis of modern climate only.

Based upon the results of these simulations, it was concluded that the current regional and site-scale models of Yucca Mountain would more accurately simulate the flow regime if they simulated past-climate conditions that existed during the late Pleistocene. Further, it was concluded that the existing Yucca Mountain models tend to overestimate groundwater travel times and underestimate groundwater fluxes. This finding conflicts with Belcher and others (2004) who stated an expectation that simulating heads still affected by elevated water levels during glacial periods would only result in a small bias in the regional model and that any effects on transient simulations would also be small.

4.5 Regional Potentiometric Map

A key model that has been developed by DOE as part of the TSPA is the Death Valley Regional Groundwater Flow System model (DVRGFS) (D'Agnese and others 1998). The DVRGFS has a number of applications but, within the context of TSPA, it is primarily the source for the boundary fluxes used in the Yucca Mountain Site Scale model. This model is underlain by a number of assumptions and estimates of hydrologic parameters and continues to be updated as new information becomes available.

As part of the ISIP, Nye County has assessed the appropriateness of assumptions used in the DVRGFS at both the regional and site scales. Investigators have found that the published regional potentiometric map by D'Agnese and others (1998) with 100 meter contour intervals (Figure 4.5-1), is adequate for representing generalized regional flow directions and gradients but the large contour interval is poorly suited for presenting single basin or sub-basin water table configurations. The blue contours help outline the major valleys and subbasins; whereas, the thinner gray contours help to locate upland and mountainous areas as well as Death Valley.

Nye County attempted to fill in data gaps in Figure 4.5-1 by using a larger and more up-to-date (2004) data set and applying hand-drawn adjustments to computer generated contours developed using the minimum curvature method for gridding of irregularly spaced water level data. The hand-drawn adjustments honor individual data values to the extent possible as shown in Figure 4.5-2. This adjustment approach attempts to overcome shortcomings of the minimum curvature method used as a starting point by Nye County and as a final product by D'Agnese and others (1998). However, although Figure 4.5-2 shows more detail and is likely more accurate in some areas than in Figure 4.5-1, the approximately 328 ft (100 m) contour interval still does not provide water-level detail around known agricultural pumping centers in the Amargosa Desert and municipal water supply wells in the Pahrump Valley.

Figure 4.5-3 shows results in the Pahrump Valley using the hand-drawn adjustment approach for computer generated 300 ft and 25 ft contour intervals, respectively. The 25 ft contour interval map clearly provides better definition of drawdown in the vicinity of pumping centers associated with municipal water supplies in the Pahrump Valley. The comparison of the maps in Figure 4.5-3 clearly demonstrates that flow directions and gradients can be accurately represented only with local water level data and a contour interval that is small enough to allow the identification of localized pumping centers. The DVRGFS regional potentiometric map (Figure 4.5-1) has too large of a contour interval to accurately portray the extreme variability in the configuration of the water table in developed areas with numerous pumping wells.

4.6 Groundwater Discharge in Amargosa Desert

A series of evapotranspiration studies by the USGS were conducted in support of the DVRGFS model. The methods, approach, and results have been published in a series of reports by Czarnecki (1997), Lacznia and others (1999, 2001), Reiner and others (2002) and DeMeo and others (2003). A review of the methodologies presented in these reports by Nye County found that the depth to groundwater was not used in the estimates of discharge, and that the method used in the classification of evapotranspiration units may have been in error, resulting in serious underestimates of the total groundwater discharge.

Preliminary depth to groundwater maps prepared by the Nye County Natural Resources Office for southern Amargosa Desert found that the areas of shallow groundwater (less than ten ft) were far larger than the areas evaluated in the USGS estimates. Further evaluations found that the published estimates did not fully account for evaporative losses from bare soil, especially in areas where the depth to groundwater is less than ten ft below land surface. Significant discrepancies were also identified between the methods used by the USGS studies in the Yucca Mountain region with other published evapotranspiration studies in Nevada, particularly with respect to how the satellite imagery was classified, and the treatment of losses from bare soils. A

formal evaluation of the USGS methods and results in determining evapotranspiration and discharge in the Amargosa Desert will be presented in the future.

5.0 GROUNDWATER CHEMISTRY

An analysis of groundwater chemistry is one way to better understand actual flow paths, methods and location of recharge, and the evolution of water chemistry. This section summarizes a variety of methods used to examine groundwater chemistry trends.

5.1 Groundwater Sampling and Analysis

Nye County ISIP groundwater sampling and analysis of wells and boreholes since calendar year 1994 is summarized in Table 5.1-1. Nye County sampling has been performed in a manner to maximize the opportunity of DOE, NRC, the State of Nevada, USGS, LANL, University of Nevada Las Vegas Harry Reid Center, and any other interested parties to collect samples from Nye County Wells. Groundwater samples are collected according to established quality assurance technical procedures and shipped to qualified testing laboratories for analysis.

Nye County reviews quality assurance analyses conducted by testing laboratories and conducts their own quality assurance analyses of laboratory testing results. This information is included in quality assurance metadata produced by the NWRPO for all laboratory analyses of groundwater samples. Metadata is on file together with the original laboratory test data and QA procedures at the Nye County QARC.

In addition, quality assurance analyses have included a comparison of charge balance and direct measurements on split samples determined by NWRPO and the USGS testing laboratories (NWRPO, 2003c). USGS data displayed significantly higher variations in charge balance (average 7%) than the NWRPO data, suggesting lower analytical error for NWRPO major ion data. The direct comparison of analytical data for split samples generally indicated good agreement between NWRPO and USGS results.

Results of groundwater chemistry analyses are continually added to the Nye County NWRPO web site (www.nyecounty.com) and made available for download by any interested party. The open sampling and data sharing policy best serves the Nye County mission of promoting knowledge and safety.

5.2 Results and Trend Analyses

Major ions collected from most of the EWDP wells listed in Table 5.1-1 from 1994 to April 2003 were subjected to 3 types of trend analyses (statistical factor analysis, tertiary diagrams, and enrichment graphs) in an annual groundwater chemistry report for 2002 (NWRPO, 2003c). Each analysis resulted in 3 similar groups of wells separated in space: those near paleosprings along Hwy 95, those located in Fortymile Wash, and those possibly separated from the above groups by the Hwy 95 fault. In addition, each group is distinguished by different water chemistry.

Tertiary diagram analysis, a traditional method of evaluating major groundwater chemistry, will be repeated herein for the expanded EWDP data set of major ions from 1994 to April 2007.

More in-depth statistical analyses of a much larger data set covering most of the Amargosa Desert region will be presented in Sections 5.2.2 and 5.2.3. This data set was obtained from the NWRPO website (NWRPO, 2007a) and a database compiled by Los Alamos National Laboratory (LANL, 2003). In addition, the results of these statistical analyses will be compared to supporting data including chloride (Cl⁻) and total dissolved solid (TDS) concentration contours, radio-carbon isotope age date contours, and stable isotopes of water data plotted as contours and against each other in Section 5.2-4.

5.2.1 Tertiary Diagram Trends in EWDP Data

Tertiary (Piper) diagrams have been used historically to evaluate hydrochemical facies and evolution of water chemistry along flow paths. Figure 5.2-1 plots the results for Nye County wells in the Piper Diagram format. The well groupings shown were determined by the statistical methods described below using a larger regional water chemistry database. The plots indicate that, with the exception of the group titled “High Ca & Mg”, the Nye County wells are dominated by sodium bicarbonate. The “High Ca and Mg” well grouping is only high in calcium and magnesium in comparison to other regional wells.

5.2.2 Principle Component Factor Analysis Method

The Principle Component Factor Analysis Method (PCFA), a multivariate statistical analysis method summarized in this report, is described in detail in NWRPO (2005b) and Woocay and Walton (2008). Another similar method (Correspondence Analysis [CA]) is also described in NWRPO (2005b), but will not be addressed herein because the results from both PCFA and CA are similar in NWRPO (2005b). Both of these multivariate statistical factor analysis methods calculate new descriptive variables from the original variables in an attempt to detect structure or similarities among the original variables (Mellinger, 1987). Factor analysis allows for a reduction in the number of variables that describe the behavior of a system and helps identify new parameters that describe data and may provide new insight into the behavior of the data.

PCFA was performed on the major ion chemistry from 211 wells in the Amargosa Desert region. These data are contained in the NWRPO (2007a) and LANL (2003) data sets with the addition of data from Nye County wells up to April, 2007. The 210 sampling locations are shown on a digital elevation model (DEM) of the region (Figure 5.2-2). Sampling locations are mostly wells, some of which have multiple screened depths, while the remaining are fresh water springs. This figure also includes contours of regional groundwater Cl⁻ concentrations, which will be discussed in Section 5.2-4.

Statistica™ (StatSoft, 2007) was used to perform the PCFA of the major ion data from 211 sampling locations. The first four factors were extracted to reduce the number of variables from seven to four and to find relationships among the original variables. All together, the first four factors represent 96% of the system’s variation. Unrotated Factor 1 encompasses 66% of the data variation, and is interpreted as a size factor as it is highly loaded in all the major ions and is therefore an analog for TDS. A normalized varimax rotation of these factors is performed to distribute the amount of variation between these factors (Mellinger, 1987). Following rotation, the rotated factor loadings for the major ion chemistry and rotated factor scores for each of the 210 sampling locations were generated.

The first four rotated PCFA factor scores for the sampling locations were subjected to a k-Means Cluster Analysis (KMCA), also in Statistica™, to group observations with a similar genesis into separate hydrochemical facies. Both empirically and from previous analysis, it was decided to use seven groups for the KMCA (Figure 5.2-3). The names selected for the derived hydrochemical facies are intended to be descriptive of either their general sample locations and/or dominant ions. Although the seven hydrochemical facies are derived independently of lithological data, they are found to be in good agreement with their respective lithology thus validating these groups as hydrochemical facies. The first two rotated factor loadings for major ions and factor scores for sampling location, grouped into hydrochemical facies, are presented in the biplot on Figure 5.2-3. Sampling locations are shown as symbols and ions are shown as vectors with their tips located at the factor loading values. Each factor, with a certain chemical composition, implies a dominating hydrochemical process, and a clustered group implies a hydrochemical facies with similar genesis, evolution and/or composition indicated by the underlying factors.

In this analysis, a contour plot of a factor would be equivalent to a contour plot of a hydrochemical process indicating its direction of evolution and delineating areas influenced by that process. Contour plots of each of the resulting factors were overlaid on a DEM of the region to reveal ground water signatures and potential flow paths. In this summary report, only Rotated Factor 1 contours are presented in a figure format (Figure 5.2-4).

5.2.3 PCFA Statistical Results

Rotated Factor 1, dominated by Mg^{2+} and Ca^{2+} ions (Figure 5.2-4), is interpreted as an indication of the degree of influence of, or mixing with, the carbonate aquifer. High values are found at Crater Flat, Amargosa Flat and Ash Meadows, which are down gradient of outcrops of the underlying carbonate aquifer located at Bare Mountain, Specter Range, Striped Hills, and Skeleton Hills. The Striped Hills and Skeleton Hills are located west of the Specter Range. Rotated Factor 1 contours also exhibit a trough of low concentrations of Mg^{2+} and Ca^{2+} along Fortymile Wash to a point where it joins the Amargosa River as well as the presence of “noise” in the contours along the Highway 95 Fault. Similar evidence of a trough of low value contours along Fortymile Wash as well as contour noise along the Highway 95 Fault is also observed in contour plots of Rotated Factors 2, 3, and 4 (not shown herein). Third, a gradual increase in Ca^{2+} , Mg^{2+} and Cl^- occurs along the pathway of the Amargosa River coming out of the Oasis Valley.

Rotated Factor 2, primarily composed of Cl^- , Na^+ , and SO_4^{2-} , is perceived as a measure of the degree of evolution through evaporation, and is very similar to Cl^- contours.

Rotated Factor 3, dominated by alkalinity and Na^+ , is related to weathering of silicate minerals with release of alkalinity and concomitant release Na^+ . These values present a clear separation between groundwater west and east of Yucca Mountain. Finally, Rotated Factor 4, mostly composed of K^+ , suggests that silicate weathering is significant in this system. Factor four suggests a faint pathway originating in the Oasis Valley and following the Amargosa River, however the density of wells in this area is not sufficient to clearly delineate the trend.

The Yucca Mountain West Face group has the lowest Ca^{2+} , Mg^{2+} , K^+ , SO_4^{2-} and Cl^- concentrations of the groups. The Fortymile Wash group has the lowest concentration of Na^+ and

alkalinity of all the groups. Both of these groups have similar low concentration of SO_4^{2-} and Cl^- , and therefore are believed to represent the groups with the least amount of groundwater evolution through evaporation, thus supporting the hypothesis of groundwater beneath Fortymile Wash originating from the infiltration and recharge of surface water runoff. The High Ca and Mg group is named for its high concentration of these ions, and is mostly seen in Crater Flat, east of Bare Mountain (outcrop of the underlying carbonate aquifer). This group appears to be the one with the greatest amount of carbonate aquifer influence or mixing. The Amargosa Desert East group has high concentrations of Mg^{2+} , which are associated with the underlying carbonate aquifer that outcrops at the Specter Range, Striped Hills and Skeleton Hills, all of which contain dolomite ($\text{CaMg}(\text{CO}_3)_2$).

Together, these contour plots of rotated factors and locations of wells grouped by hydrochemical facies suggest five potential flow paths in the Amargosa Desert region (Figure 5.2-4). Evidence for the Fortymile Wash flow path is the strongest. There is some uncertainty regarding the pathway along the Amargosa River in the northwestern portion of the Amargosa Desert due to the scarcity of wells in this region. The chemistry of waters taken from the west and east sides of Yucca Mountain area are distinctly different, suggesting separate flow paths. In the southern portion of the Amargosa Desert, the chemical signatures on either side of the Funeral Mountains suggest a flow path extending underneath the Funeral Mountains into Death Valley.

5.2.4 Supporting Data and Analyses

Data and analyses supporting the PCFA major ion results described above are briefly described below. These data were also obtained from the NWRPO (2007a) and LANL (2003) data sets and include: Cl^- and TDS, oxygen-18 (^{18}O), hydrogen-2 (^2H), carbon-13 (^{13}C), and radio-carbon (carbon-14 or ^{14}C). Cl^- and TDS were available from 210 sampling locations and the isotope data were available from 107, 107, 135, and 111 of 210 locations in the Amargosa Desert region, respectively.

Chloride and TDS

As noted previously, Figure 5.2-2 includes contours of regional groundwater Cl^- concentrations. Concentrations along Fortymile Wash are notably lower than adjacent areas to the wash and are consistent with total dissolved solid contours (not shown). This indicates that a large trough of more dilute water closely follows the path of Fortymile Wash, which supports the hypothesis that groundwater beneath Fortymile Wash results mainly from infiltration and recharge of surface runoff in the wash.

Carbon-14

Figure 5.2-5 shows ^{14}C age date contours for groundwater that have been adjusted using ^{13}C data (NWRPO, 2005b). These contours show that groundwater is younger beneath Fortymile Wash than on adjacent highlands. A similar trend was observed for uncorrected ^{14}C age date contours (NWRPO, 2005b). This indicates that water below the wash has a different source than adjacent highlands and is consistent with Cl^- and TDS data, which suggest that groundwater underlying the wash is derived from focused infiltration of runoff and not migration of groundwater from adjacent highlands.

Oxygen-18 and Hydrogen-2

Stable isotopes of ^{18}O and ^2H in soil water and groundwater partially reflect the isotopic composition of precipitation, which is correlated with mean annual temperature and may thus provide paleoclimate information (Liu and others, 1995). When plotted against each other, ^{18}O and ^2H data in precipitation usually fall along a single line due to the process of fractionation that occurs at the moment of condensation; this line is referred to as the global meteoric water line (GMWL). The location of precipitation along the GMWL depends primarily on the average temperature during precipitation, with lighter (depleted) waters associated with cold temperatures/climate and heavier waters with warmer temperature/climate.

The ^{18}O and ^2H contour data presents a spatial signature along Fortymile Wash similar to the one found by the PCFA results and ^{14}C data. Following Fortymile Wash southward to the Amargosa Desert, ^{18}O values become more depleted (Figure 5.2-6). Furthermore, ^{18}O values of groundwater in the highlands to the east and west of the lower portion of the wash exhibit the most depletion. ^2H data (not presented herein) show the same trends in depletion. The more depleted the values of these stable isotopes, the colder the climate at the time of precipitation. Less depletion in ^{18}O and ^2H data in samples located near the upper portion of Fortymile indicate that the precipitation fell during a warmer, but still colder than present day, climate. This warmer climate occurred more recently than the colder climate, therefore the water is younger in the upper part of Fortymile Wash. The colder climate occurred longer ago and the water is therefore older in the lower reaches of Fortymile Wash, and especially in the highlands to the east and west of lower Fortymile Wash. These age related data from groundwater stable isotopes agree with ^{14}C data presented above.

Figure 5.2-7 presents ^{18}O and ^2H groundwater values from samples beneath the Amargosa River, beneath Fortymile Wash, and beneath the intersection of these ephemeral water drainages, compared to the GMWL. In this figure the orange arrow is a linear regression line for ^2H and ^{18}O data pairs from samples collected along the Amargosa River, where the tip of the arrow identifies the approximate furthest down-river sample and the opposite end of the arrow identifies the approximate furthest up-river sample. The ^2H and ^{18}O data pairs located beneath the Amargosa River (orange crosses) from the Oasis Valley until it merges with the fan of Fortymile Wash show a linear regression slope of 5.4.

The data in the mixing section (green crosses) correspond to sampling locations in the fan of Fortymile Wash, the junction of the Amargosa River with the fan, and slightly beyond the fan of Fortymile Wash near Ash Meadows. These data are associated with groundwater mixing beneath the river and wash, and a clear difference can be noted from the unmixed groundwater beneath the wash.

The blue arrow is a regression line for ^2H and ^{18}O data pairs from samples collected along Fortymile Wash where the arrow tip corresponds to samples in the lower reaches of the wash. The stable isotope values beneath the wash fall (are plotted) nearly parallel (slope = 7.8) to the GMWL, with successive depletion of ^2H and ^{18}O values suggesting not an evaporation curve, but evidence of climate change.

5.2.5 Conclusions from Analysis of Groundwater Chemistry

Three common trends are observed from contours of the rotated factors in the multivariate statistical PCFA. First, a large trough of more dilute waters follows along the path of Fortymile Wash and turns to the southeast, where the wash joins the Amargosa River. Second, the presence of “noise” in the contours, apparent along the Highway 95 Fault. Third, a gradual increase in Ca^{2+} , Mg^{2+} and Cl^- along the pathway of the Amargosa River coming out of the Oasis Valley. The geochemical data presented herein suggests that groundwater beneath Fortymile Wash follows the surface of the wash until it appears to merge and mix with groundwater beneath the Amargosa River.

Groundwater samples from beneath Fortymile Wash are younger (^{14}C values) and fresher (lower Cl^- and TDS) than those on adjacent highlands, indicating that the highlands are not their source. The ^2H and ^{18}O contour signatures are similar to ^{14}C and PCFA contour signatures and are evidence of changes to the groundwater system as the climate became warmer and dryer. Beginning at the source of Fortymile Wash in the north and following south along the wash, groundwater becomes sequentially older, suggesting that the average reach of runoff events and recharge have diminished over time. Regional ^2H versus ^{18}O values suggest a humid-climate precipitation, with little surface evaporation before infiltration. The stable isotope values beneath the wash fall parallel to the GMWL, with successive depletion of ^2H and ^{18}O values suggesting not an evaporation curve but evidence of climate change from cold to warm, although still colder than the present. The signature from Fortymile Wash is believed to represent the relic of focused infiltration of surface runoff along the course of the wash during past pluvial periods, when the climate was colder and wetter than the present and the amount of runoff in the wash was significantly greater.

5.3 Engineered Barrier System Groundwater Chemistry Modeling

Nye County examined separation of individual anions from an initially mixed aqueous solution in the near field environment. Details of this work have been described previously (NWRPO, 2003c; Hall and Walton, 2006). The concept is based upon sequential precipitation of differentially soluble salts from a solution, which is subject to evaporation while it flows within the rock or on any of the many surfaces present in the Engineered Barrier System (EBS). Differential solubility of specific salts dictates that sometimes this will result in different anions being preferentially precipitated at separate locations. As relative humidity rises over time in the repository, deliquescence of the now separated salts can result in solutions dominated by one anion.

Evidence indicates that NO_3^- and to a lesser extent SO_4^{2-} anions inhibit the corrosive effects of Cl^- on metals (Payer, 2005). A general rule of thumb is that if the ratio of Cl^- to NO_3^- is less than 5 to 1, metal corrosion will be significantly inhibited. It was generally thought by DOE investigators that NO_3^- was present in all Yucca Mountain waters and Cl^- to NO_3^- ratios were always less than 5:1. The following presents evidence that the flow separation of anions can occur in the EBS environment and the potential for Cl^- corrosion may be greater than previously thought under certain restricted conditions described in Hall and Walton (2006).

Figure 5.3-1 presents two mathematical models for describing potential mineral deposition: a single cell mixing tank, in which all minerals precipitate and dissolve at the same physical

location; and a multiple cell mixing tank, in which minerals may precipitate and dissolve at different locations based on differential solubility. Multiple cell mixing tank models can be run with different numbers of cells, with the limit of infinite cells giving the maximum degree of separation anticipated by this process.

In the multiple cell model, the source water enters the first cell as a dilute solution with a full suite of dissolved constituents. The separation occurs during a period of net evaporation, as water moves from cell to cell. Each mixing cell in the series is physically separated from the previous cell, separating each suite of minerals precipitating in each cell from those in the previous cell. Less soluble minerals are deposited preferentially near the water source and highly soluble minerals are precipitated from the more concentrated solution further from the source. Flow separation processes do not cause complete separation during mineral formation; in most situations several minerals will precipitate simultaneously from solution. Simultaneous precipitation of different minerals is visible on logarithmically scaled graphs but tends to rapidly disappear from linearly scaled graphs.

An example of flow separation (i.e. precipitation sequence) in a multiple cell model for Paintbrush non-welded tuff (PTn) pore water is graphically shown in Figure 5.3-1b. This figure shows that CO_3^{2-} is the first anion to precipitate. It precipitates as calcite (CaCO_3), due in part to the large concentration of Ca^{2+} present in the initial source water. The middle portion of the precipitation sequence is dominated by the precipitation of SO_4^{2-} as gypsum (CaSO_4); and Cl^- precipitates as primarily as halite (NaCl) at the end of the precipitation sequence. NO_3^- precipitates as niter (KNO_3) and soda niter (NaNO_3) in relative small quantities relative to halite prior to the end of the precipitation sequence. The resulting precipitates form an area at the end of the evaporation/precipitation sequence that is very high in Cl^- . After rehydration, this area in particular, potentially presents an increased corrosion risk because of the absence NO_3^- and SO_4^{2-} to mitigate the effects of the large mass of Cl^- .

6.0 AQUIFER TESTING

The Nye County NWRPO conducted aquifer testing at three sites (Sites 10, 19, and 22) located in lower Fortymile Wash along potential flow paths from Yucca Mountain to Amargosa Valley from May 2001 through May 2006 as part of the EWDP. The location of these sites is shown in Figure 6.0-1. Test wells included four pump and spinner logging wells (19IM1, 19IM2, 22S, and 10S) and four interference (observation) wells (19D, 22PA, 22PB, and 10P). All wells were completed with multiple screened/sandpacked depth intervals (test zones or zones), which are listed in Table 6.0-1.

Details of well completions, aquifer test methods, and test results of wells listed above are presented in Nye County aquifer test technical reports NWRPO (2002, 2003b, 2004, and 2006). Detailed subsurface geologic information for these wells is presented in an NWRPO drilling, logging, and lab testing related report for EWDP Phase III boreholes (NWRPO, 2003b).

Well screens/sandpacks zones were located in thick alluvial deposits and the upper portion of either Tertiary volcanic conglomerate or Tertiary volcanic ash-flow tuffs (Table 6.0-1). Saturated alluvium consisted primary of layers of silty sand with gravel (NWRPO, 2003b) that becomes slightly finer with depth.

The depth intervals of test zones in pumping and spinner logging wells generally corresponded closely with test zones in nearby observation wells within a particular site (Table 6.0-1). Test zones were located to the extent possible in higher permeable zones based on drilling data and field geologic and geophysical logging. In some wells, water level and aquifer test data indicated that one or more of the intervals between different test zones acted as partially confining layers.

Several tests and associated results were also summarized at the 2002, 2003, and 2004 meetings of the Devils Hole Workshop. The tests demonstrated generally high permeability in the screened zones of valley-fill sediments and the volcanics, but with notable differences between wells. Vertical-flow barriers were inferred from the head response of several of the tests. More details concerning these and other significant results are presented in Section 6.2.

6.1 Methods and Procedures

When reasonably possible, Nye County uses a comprehensive aquifer testing approach to determine and analyze the hydraulic properties of wells drilled in the EWDP program. Comprehensive testing incorporates the use of pressure/temperature probes and data loggers, spinner logs, open-wellbore constant-rate pump tests, and individual isolated screen/sandpack zone pumping tests.

Aquifer pump tests were conducted in accordance with NWRPO quality assurance plans and procedures, including the following:

- Technical Procedure TP-9.0: Pump-Spinner in Unscreened Open Boreholes and Screened Boreholes
- Technical Procedure TP-10.0: Pumping/Injection Tests of Packed-Off Zones in Unscreened Open Boreholes or in Multiple Screen Boreholes with or without Observation Wells
- Test Plan TPN-9.1: Pump Test of Individual Screens in NC-EWDP-22S
- Work Plan WP-4: Aquifer Testing Plan for Nye County's Independent Scientific Investigation Program

6.1.1 Monitoring Instrumentation and Pump Spinner Logging Methods

All test zones were instrumented with calibrated pressure/temperature probes connected to data loggers at the ground surface. Pumping flow rates were determined by flow meters and/or a stopwatch and a 55-gallon drum.

Pump spinner logs were generally run at 2 different logging speeds (30 ft/min and 45 ft/min) to calibrate for the effects of changes in logging rates. A two-pass method involving both up and down logging runs at the same speed was employed to reduce potential errors caused by borehole size changes, tool idiosyncrasies, and other factors. Stationary readings were also taken in the blank pipe above each screen as a quality control check.

6.1.2 Data Analysis Methods

The well test data were analyzed using standard techniques, sophisticated software packages, and custom-programmed analysis tools as appropriate. Over the past decade, advances in well test interpretation techniques in the petroleum industry have allowed researchers to obtain more information from tests using computer-assisted software analysis packages. The analyses of constant-rate open-wellbore pump tests reported herein for Sites 19 and 10 were conducted using SAPHIR™ computer-assisted well testing program (Kappa Engineering, 1999). For the same tests at Site 22 the FAST WELLTEST™ computer-assisted well test analysis program was used (Fekete Associates, 2002). The data from constant-rate pump tests in isolated test zones in 22S was analyzed using a standard leaky aquifer model (Hantush, 1959) to calculate transmissivity, storativity, and leakance; and the method of Cox and Onsager (2002) to calculate skin factor and well efficiency. With these tools and using additional analysis methods developed on an as-needed basis, it was possible to account for variable flow rates, multiple layers, flow barriers, changing wellbore storage, and many other factors not addressed by common analysis techniques.

6.1.3 Site 22 Test Wells and Approach

Well completion, aquifer test, and data analysis methods for Site 22 tests are described in detail in NWRPO (2003b and 2004) and briefly summarized in the following. Aquifer testing performed at Site 22 exemplifies the comprehensive test methodology used by Nye County for multi-screened wells. The Site 22 complex consisted of three wells during the test period: 22S, a multiple-screen monitoring well that served as the spinner-logging and pumping well; and 22PA and 22PB, both smaller-diameter, nested, dual-completion piezometers that served as observation wells. These wells are located in a triangular array separated from each other by less than 70 ft as shown in Figure 6.1-1.

Four test zones were screened, sandpacked, and isolated with grout seals in 22S (Table 6.0-1). The upper three zones in 22S are completed in alluvium consisting primarily of silty sand with gravel layers becoming slightly finer in texture with increasing depth, and the lower screen is in a Tertiary volcanic conglomerate.

Piezometers 22PA and 22PB were each completed with 2 screen/sandpack zones. The zones in 22PA are located at depths corresponding to the upper two zones in 22S; those in 22PB correspond to the lower two zones in 22S.

Spinner logs were run in 22S to quantify flow rates between screens (crossflow) under static (nonpumping) and pumping conditions. Following spinner logging, an approximately 24-hour constant-rate pump test was conducted in 22S with all screened/sandpacked zones open to the wellbore to permit calculation of aquifer properties such as transmissivity and well efficiency for the total open interval footage. The pump-spinner logs permit allocating these aquifer properties to the individual zones. In addition, pressure heads were monitored in Zones 1 and 2 in 22PA and Zones 3 and 4 in 22PB to permit calculating interwell transmissivity and well efficiency in each of the 4 zones between these observation wells and pumping well 22S. Finally, separately pumping each individual isolated zone in 22S for 11 hours and monitoring drawdown and recovery responses in all isolated zones in 22S, 22PA, and 22PB permitted a more accurate determination of the aquifer properties for each zone.

A single layer model with cylindrical flow was used with the well test analysis program FAST WELLTEST™ (Fekete Associates, 2002) to analyze open wellbore pump data from Site 22 wells. Larsen (1981) showed that multilayered flow systems could be modeled as equivalent single layered systems as long as aquifer properties do not vary significantly between zones.

Pump test results from isolated zones in 22S were analyzed using a standard leaky aquifer model (Hantush, 1959). More complex analysis methods (e.g. FAST WELLTEST™ or SAPHIR™) were not used in the isolated zone testing analysis at Site 22 because the 10-second data recording frequency used in testing was inadequate to obtain the necessary data required for the computer- assisted data analysis packages.

6.1.4 Site 19 Test Wells and Approach

Well completion, aquifer test, and data analysis methods for pump wells 19IM1 and 19IM2, and observation wells 19D and 19P are described in NWRPO (2002). The following will briefly summarize this information.

The location of these wells at Site 19 with respect to each other is shown in Figure 6.1-2. No discernable response to pumping was observed in observation well 19P, and it will not be discussed further herein. The maximum distance between wells is approximately 90 ft. 19IM1 and 19IM2 were completed with five screened/sandpacked zones from approximately 410 to 950 ft bgs (Table 6.0-1). The upper four zones in each well were completed in alluvium, and the bottom zone in each well was completed in an ash flow tuff unit.

Well 19D, which served as an observation well during pump testing of wells 19IM1 and 19IM2, was completed with seven screened intervals (NWRPO, 2002). The upper five intervals in well 19D are equivalent to the five screened/sandpacked zones in the 19IM1 and 19IM2 wells. In addition, well 19D has two deeper screened intervals in ash flow tuffs. Pump tests were conducted in 19D in 2000 (Questa Engineering Corporation, 2000) and summarized in the previous five year ISIP report (NWRPO, 2001a). A NWRPO revised version of the Questa report (NWRPO, 2001b) is substantially the same as the Questa report and will not be discussed further herein.

Static-spinner and pump-spinner logging was also conducted in the five screened/sandpacked zones in 19IM1 and 19IM2. Pump-spinner logs were successfully conducted in 19IM2 prior to the 48-hour constant-rate test; and in 19IM1 shortly after the start and immediately before shutting down the 49.5-hour constant-rate pump test. During the 49.5 hour test in 19IM1, 19IM2 and 19D served as observation wells; and during the 48 hour test in 19IM2, 19IM1 and 19D served as observation wells. Unlike 22S, pump tests of isolated individual well zones were not conducted in 19IM1 and 19IM2.

A single layer model without flow boundaries was used with the well test analysis program SAPHIR™ (Kappa Engineering, 1999) to analyze aquifer test data from open wellbore pumping in 19IM1 and 19IM2. As in the case of 22S, a single layer model can represent a multilayered system as long as aquifer properties do not vary significantly between zones (Larsen, 1981).

6.1.5 Site 10 Test Wells and Approach

Well completion, aquifer test, and data analysis methods for dual-screen/sandpack pump well 10S and dual-completion observation well 10P are described in NWRPO (2006). The screen/sandpack zones in 10P are at depths corresponding to those in 10S (Table 6.0-1). The location and separation of these wells at Site 10 are shown in Figure 6.1-3.

The testing approach at Site 10 was similar to the approach taken at Site 19 and included static- and pump-spinner logging and a constant-rate open-wellbore pump test. The latter pump test was modeled with SAPHIR™ (Kappa Engineering, 1999) as 2 non-communicating layers with a constant head boundary located approximately 150 ft from 10S. The source, strength, and direction of the boundary could not be determined.

6.2 Test Results

A detailed description of test results is given in NWRPO (2002) for Site 19 tests, NWRPO (2003b and 2004) for Site 22 tests, and NWRPO (2006) for Site 10 tests. The following briefly summarizes some of major results from these tests.

6.2.1 Static Spinner Logging

In 19IM1, approximately 3 gpm was observed entering the wellbore from Zone 5 and exiting the wellbore in Zones 1, 2, and 3 during static-spinner logging. In 19IM2, approximately 4 gpm was observed entering the wellbore from Zone 5 and exiting the wellbore in Zones 1, 2, and 4. These results are consistent with water levels measured in individual zones in 19IM1 after they were isolated with Westbay® packer systems. Zone 5 contained the highest non-pumping water level, Zones 3 and 4 were approximately 7.3 ft lower than Zone 5, and Zones 1 and 2 were 14.1 ft lower than Zone 5.

Analysis of the static-spinner surveys in 22S indicates there was no significant cross flow (either up or down) or a vertical pressure gradient in this well. Any fluid movement in the well prior to pumping was at rates below the observable threshold of the spinner logging tools used. A detailed review of the piezometric levels in each observation zone and the composite level measured in the 22S pump well indicated that the levels were within 0.1 ft of each other, with the highest level in the shallowest zone (Zone 1). The absence of significant head differences among the four screens suggests there is sufficient vertical permeability in the sediments between the various layers for water levels to rapidly equilibrate to a common piezometric level.

Static spinner results in 10S showed no evidence of flow between screen/sandpack zones, even after further well development to remove the residual drilling mud in Zone 2 of the borehole. As observed in 22S, piezometric water level data show virtually no difference between zones.

6.2.2 Pump Spinner Logging

Table 6.2-1 displays the results of the pump-spinner logging together with constant-rate pump test results in open-wellbore tests in 19IM1, 19IM2, and 22S. Reliable pump-spinner logging data were not obtained from 10S and therefore are not included in Table 6.2-1.

As mentioned previously, the primary purpose of the pump-spinner logs is to allocate flow rates (and by inference, transmissivity and permeability) from the open-wellbore pump test to individual zones. This allocation of reservoir flow characteristics is valid if the head differentials and wellbore efficiencies are similar for the various zones (Daltaban and Wall, 1998). Results from open-wellbore tests will be discussed further in the following section which focuses on constant-rate pump test results.

Pump-spinner results combined with open-borehole constant-rate pump test results for 19IM1 and 19IM2 indicate that Zone 3 is the most productive and exhibits the highest hydraulic conductivity. Zone 4 in both wells exhibits the lowest hydraulic conductivity of the alluvial zones and is approximately equal to the conductivity of the underlying Tertiary ash flow tuff unit (Zone 5). Zones 1 and 2 are the least conductive.

The hydraulic conductivity of each zone in 19IM2 is at least twice as large as the conductivity of the corresponding zone in 19IM1. This is somewhat surprising considering the proximity of the two wells and the fact that the wells were drilled with the same method by the same driller (NWRPO, 2003b). Moreover, more drilling fluid (MAX GEL®) was used in 19IM2 than in 19IM1 (NWRPO, 2003b) and the 19IM2 well efficiency was far less than that of 19IM1 (16 vs. 48%).

In 22S the upper two zones exhibit hydraulic conductivities 2 to 3 time larger than the lower two zones. Moreover, 22S exhibits an average hydraulic conductivity 2 to 5 times larger than the 19IM1 and 19IM2 averages. This difference between sites may be due to the fact that Site 19 is located approximately 3 miles downstream of Site 22 in the Fortymile Wash flow system.

6.2.3 Constant Discharge Rate Pump Tests

Constant-rate pump test measurements and aquifer property calculated results are presented in Table 6.2-2. This table shows that the highest transmissivity and permeability values were calculated for 22S and the lowest values were calculated for 10S. The lowest skin factor and highest well efficiency were calculated for Zone 1 in 10S while the highest skin factor and lowest well efficiency were determined for Zone 2 in 10S. Drilling mud in Zone 2 of 10S is likely mainly responsible for the calculated skin and well efficiency values.

Relatively high skin values and low well efficiency values in isolated zone 11 hour pump tests in 22S are likely a combination of factors including formation and sandpack damage during drilling and completion activities; flow factors such as inertia, turbulence, and convergence effects; and head loss due to friction in the relatively small diameter Westbay® casing system. The latter effect may be the most important because the Westbay® system was not designed for pumping at the relatively high rates used in the 11 hour constant discharge tests.

Table 6.2-2 also shows that transmissivity and storage coefficient values determined for the 11 hour tests in isolated zones were significantly lower in value than those calculated from the earlier 24 hour pump test and pump spinner logging in the open wellbore. For example, the calculated transmissivity in Zone 1 from the isolated zone pump test is 24% lower than the value calculated previously in the open-wellbore tests, while the calculated storativity is 28% lower. These results are likely due to lower leakance between layers in the open wellbore tests because all zones were producing water.

7.0 TRACER TESTING

The primary objectives of the Nye County tracer tests at Site 22 are to evaluate and refine the conceptual transport models in alluvium used in the site-scale saturated-zone model for dissolved radionuclides and colloids and to obtain field-scale parameters for use in transport model simulations. The primary tools for achieving these objectives are single-well tracer tests, cross-hole tracer tests, and natural gradient tests. Nye County tracer test methods, results, analyses, and interpretation have been recently described in detail for completed single-well and cross-hole testing at Site 22 (NWRPO, 2007b). These completed tests as well as ongoing natural gradient testing by Nye County are briefly described herein.

The suite of single-well, cross-hole, and natural gradient tests run by Nye County at Site 22 augments the testing previously carried out in the C-Wells Complex (BSC, 2004), which examined transport through the fractured volcanic tuffs, and the three single-well tracer tests performed in the alluvium at the ATC in well 19D at Site 19 (BSC, 2004). DOE contractors (USGS and LANL) took the lead in designing and implementing both the C-Well and 19D tests. Nye County's role in these previous tests involved supplying equipment and field technician support for the 19D tests. Nye County's role in the Site 22 tests described in this present report involved taking the lead in permitting, designing, and conducting all testing.

Single-well tracer tests generally involve injecting a tracer solution into the formation through a selected well screen/sandpack (zone), pushing the tracer out into the formation with chase water previously obtained from the formation, permitting the tracer to drift with the natural gradient for a time period ranging from zero to tens or hundreds of hours, then pumping (pulling) the solution back from the formation into the selected screen/sandpack zone, and finally analyzing produced water samples for tracer concentrations.

Cross-hole tracer tests involve injecting tracer solution into the formation through a selected screen/sandpack zone in an injection well offset (e.g. upgradient or crossgradient) from a pumping well. The pumping well is generally screened/sandpacked over the same depth interval(s) as the injection well. Following addition of tracer solution in each injection well, the tracer is pushed into the aquifer with a measured volume of chase water. The tracer is then recovered from the offset pumping well by continuous pumping through the same or an adjacent screen/sandpack zone and produced water samples are analyzed for tracer concentrations. These tests continue until the rate of tracer recovery at the pumping well becomes insignificant for the tracers tested or until the expiration of the discharge permit.

Natural gradient cross-hole tests are similar to forced (i.e. pumping induced) gradient cross-hole tests described above, except pumping is not included. Major disadvantages of natural gradient tests are the long test times required and the possibility that no tracer will be observed at the downgradient wells in the allotted time, or possibly ever. However, if detected, the tracer recovery data can be used to determine field-scale transport parameters as well as directly measure the natural groundwater velocity.

7.1 Overview of Tracer Test Methods and Procedures

All tests were conducted at Site 22, located in Fortymile Wash approximately 5 miles north of Lathrop Wells. Figure 6.0-1 displays the location of Site 22 in relation to other nearby EWDP

wells and the proposed Yucca Mountain repository site. The site as shown in Figure 7.1-1 consists of one larger-diameter well and three smaller-diameter piezometers as follows:

- 22S is a four-screen well that served as both the injection and pumping well in single well tests, and the spinner logging and pumping well in cross-hole tests.
- 22PA, 22PB, and 22PC are nested, dual-completion piezometers that served as pressure monitoring wells and tracer injection points.

Well screen/sandpack depth intervals (test zones) in these wells are summarized in Table 6.0-1. These zones are numbered from shallowest to deepest in each well. Zones 1 and 2 in 22S correspond to Zones 1 and 2 in 22PA and 22PC. Zones 3 and 4 in 22S correspond to the same zones in 22PB.

The tracer tests described in this report were conducted in accordance with detailed procedures included in the following NWRPO quality assurance test plans:

- Test Plan TPN-9.2: Single-Well Push/Pull Tracer Test at Well NC-EWDP-22S
- Test Plan TPN-9.3: Cross-Hole, Multiple-Well Tracer Test at Site 22
- Test Plan TPN-9.4: Site 22 Cross-Hole Tracer Test Using Perrhenate and Iodide
- Test Plan TPN-9.5: Natural Gradient Cross-Hole Tracer Test at Site 22

Each of these plans describes pertinent pumping well and piezometer completion information, equipment and instrument installation, pipe and container plumbing required for tracer injection/chasing and pumpback, procedures for injection/chasing and pumpback, and procedures for groundwater/tracer sample collection and analysis.

Table 7.1-1 summarizes tracer injection, chase water, and pumping well information presented in these plans as well as data related to injection, chasing, and pumping collected during each of the tracer tests. An overview of these tests is given in the following two sections.

7.1.1 Single-Well Tests

Two single-well push/pull tracer tests were conducted in 22S between mid-December 2004 and mid-March 2005 (Table 7.1-1). Both tests involved injecting approximately 1,000 gallons of tracer solution into Zone 2 of 22S, pushing these tracers into the formation by chasing them with approximately 20,000 gallons of previously collected formation water, allowing the tracers to “drift” slightly down-gradient with the natural movement of formation water, and then pulling them back to 22S by pumping 22S Zone 2 at approximately 48 gpm. The following tracers and “drift” (i.e. non-pumping rest periods) were used in these tests:

- Pentafluorobenzoic acid (PFBA) and iodide with a 70-hr rest period
- 2,3,4,5-tetrafluorobenzoic acid (2,3,4,5-TeFBA) and iodide with a 716-hr rest period

The two push/pull tests differed primarily by length of rest period (i.e. time the tracers were allowed to “drift”). The two tracers used in each test had different diffusion coefficients, and the response curves provided information on the importance of diffusion into stagnant zones in the

formation. The tracer response curves also provided information on the effective porosity, the natural gradient, and hydrodynamic dispersion.

7.1.2 Cross-Hole Well Tests

Five cross-hole tests were conducted at Site 22 primarily in Zone 2 beginning in mid-January 2005 and ending in October 2005. Four of the five tests were initiated in mid-January 2005 (Phase I tests), and the fifth test (Phase II test) in late August 2005 (Table 7.1-1). These tests involved injecting approximately 250 to 275 gallons of different tracers into piezometer strings 22PA Deep, 22PA Shallow, and 22PC Deep and then monitoring the tracer response (i.e., concentrations) in pumping well 22S, located approximately 60 ft from the injection piezometers. Approximately 100 gallons of previously collected formation water was then injected into the same piezometer strings to help chase the tracer solutions out of the piezometer screen and into the sand pack and formation. The tracers were then pulled toward and into 22S by pumping at approximately 48 gpm over a time period of approximately four months. Groundwater samples were collected from pumping well 22S and analyzed for tracer concentrations throughout the term of the cross-hole tests.

These cross-hole tracer tests used the following conservative tracers: iodide, bromide, and several fluorobenzoates; microsphere colloids; and an oxidation/reduction (redox) sensitive anion (perrhenate), which mimics the behavior of a radioactive contaminant (pertechnetate) that could potentially be released from waste stored at Yucca Mountain. Perrhenate acts as a conservative tracer under oxidizing conditions and a nonconservative reactive tracer under reducing conditions.

The use of perrhenate as a tracer required a major modification to Nye County's Underground Injection Control (UIC) permit, since perrhenate was not approved as a tracer in the original permit. During the time required to obtain this modification (from March 18 to August 25, 2005), pumping of cross-hole Phase I tracers into 22S was suspended in order to minimize the amount of water produced and to limit overall testing costs.

The tracer response curves from the cross-hole tests provided a larger-scale estimate than a single-well push/pull test of effective flow porosity, longitudinal dispersion, and stagnant zones. In addition, a cross-hole test between Zone 1 in 22PA and Zone 2 in 22S provided qualitative information regarding communication between hydrostratigraphic layers or zones. Finally, these tracer response data provided information regarding preferential flow paths present between injection piezometers and the pumping well, the importance of colloid transport in the alluvium, and the effect of redox conditions in the alluvium of Fortymile Wash on a redox-sensitive tracer.

Note that pumping 22S from mid-January to mid-March 2005 served to move the majority of tracers into 22S, both from the first four cross-hole tests and the second single-well push/pull test. Pumping of 22S then resumed in late August 2005, continued into October 2005, and served to complete the recovery of tracers from the above mentioned tests as well as the recovery of most of the tracers injected as part of the fifth cross-hole test.

7.2 Tracer Testing Results

A visual examination of normalized tracer recovery curves for different tracer tests can provide valuable information regarding relative tracer velocities, possible related flow pathways, and the existence of stagnant flow layers. These curves are plots of normalized tracer mass versus volume of water pumped.

Several quantitative analytical and numerical methods are also available for analyzing tracer test data. These methodologies include individual well analysis of tracer response, well pair analysis of tracer response, and coupled response analysis using numerical simulation (Leap and Kaplan 1988; Reimus et al. 2006). Since the observed tracer responses in Zone 2 of 22S from the two injection wells (22PA Deep and 22PC Deep) were so different (NWRPO, 2007b), finite-element numerical simulation was used to perform a coupled analysis. The simulation package used consisted of Visual MODFLOW® v. 3.1.0.86 from Waterloo Hydrogeologic (WH) coupled with the Modular 3-D Transport model, Multi-Species (MT3DMS). MT3DMS was used to solve the tracer transport, while MODFLOW was used to solve the fluid flow.

It was determined that the development of a conceptual geologic model and the calibration of this model could be accomplished efficiently and in a technically sound manner by first focusing on cross-hole conservative tracer tests. The resulting cross-hole calibration parameters determined from matching simulated with measured tracer recoveries could then be used as starting points to simulate single-well recovery curves.

7.2.1 Cross-Hole Well Test Results

A geologically realistic model was developed based on preliminary tracer response and related hydraulic data capable of accounting for fast pathways between 22PA and 22S and slower pathways between 22PC and 22S. The observed rapid breakthrough of tracer material from 22PA Zone 2 to 22S Zone 2 in the first cross-hole test (Figure 7.2-1) suggests a low effective porosity pathway in Zone 2 between these two wells. Figure 7.2-2 shows a significantly slower pathway in Zone 2 between 22PC and 22S in the second cross-hole test, suggesting a higher effective porosity.

Prior to these tracer tests, hydraulic testing (NWRPO, 2004) indicated high permeability for Zone 2 between 22PA and 22S. This combination of low effective porosity and high permeability is typically associated with the fractured volcanic aquifer at Yucca Mountain, and not the alluvial valley fill geologic setting at Site 22.

The channel system observed in nearby Fortymile Wash (Figure 7.2-3) provides a possible template for the presence of one or more geologically supported sinuous-shaped paleochannels at depth beneath Site 22. Qualitative and quantitative analyses of the hydraulic and tracer responses suggest that 22S lies on the edge of a low effective-porosity paleochannel.

One conceptual model of adjacent sinuous-shaped paleochannels that would account for the location of 22S and both the fast 22PA-22S pathway and slower 22PC-22S pathway is shown as a horizontal plane through Zone 2 at Site 22 in Figure 7.2-4. The width of these channels is expected to be at least 10 m based on the width of present-day Fortymile Wash. This conceptual horizontal plane through Zone 2 shows that 22PA Zone 2 is located in the center of a very low

effective-porosity channel; 22PC Zone 2 is located in the center of an adjacent channel with an intermediate effective porosity; and 22S Zone 2 is located at the edge of this same intermediate effective-porosity channel, which abuts the channel that has very low effective porosity.

Once the above conceptual geologic model was developed, the following calibration procedures were implemented:

- The model was populated with hydraulic and transport parameters obtained from previous testing and from published or public data sources.
- The geologically reasonable model was calibrated to conservative tracer responses observed among the three wells (22S, 22PA Deep, and 22PC Deep). The hydraulic and transport parameters were adjusted in a defensible manner to obtain a reasonable match between observed and simulated tracer response data.
- Sensitivity analysis was used to study how the hydraulic gradient magnitude and azimuth affected the response of curves following pump downtime.
- Hydraulic properties were adjusted to refine the calibration of observed and simulated hydraulic head data.
- The single-well push/pull tracer test was modeled using hydraulic properties from calibrated cross-hole tracer tests; changes to relevant transport properties were made as needed for calibration.

Although multiple cross-hole tracers were injected in upgradient piezometers, only two unique conservative tracer responses were noted in well 22S during the cross-hole testing. These unique responses in 22S were for bromide injection into 22PA Zone 2 (cross-hole test 1) and 2,6-DFBA injection at 22PC Zone 2 (cross-hole test 2). Further, these unique responses allowed the model calibration of the cross-hole tests to be addressed by modeling only two conservative tracer responses. Calibration parameters for these tests are listed in Table 7.2-1. Figure 7.2-5 compares the measured and simulated recovery curves (i.e. calibration match) using the fitted parameters listed in Table 7.2-1 for cross-hole test 2. A similar good match was obtained between the measured and simulated recovery curves for the first cross-hole test.

Tracers with different diffusion coefficients were injected in both the cross-hole and single-well tests in the anticipation that potential diffusion into stagnant layers could be identified. No conclusive evidence of diffusion was determined in any of the tests given the uncertainty in laboratory analysis. A review of the fundamental equations governing dispersion provides insight into the observed results. As shown in the equation below for dispersion in one direction (x tensor; S.S. Papadopoulos & Associates, Inc., 1990):

$$D_{xx} = \alpha_L \frac{v_x^2}{|v|} + \alpha_{TH} \frac{v_y^2}{|v|} + \alpha_{TV} \frac{v_z^2}{|v|} + D^*$$

Where

D_{xx} = principal component of the dispersion tensor, ft²/day

α_L = Longitudinal dispersivity, ft

α_{TH} = Transverse dispersivity, ft

α_{TV} = Vertical dispersivity, ft

v = velocity in x, y, or z direction, ft/day

D^* = effective molecular diffusion coefficient, ft²/day

$|v| = \sqrt{v_x^2 + v_y^2 + v_z^2}$ = magnitude of the velocity vector, ft/day

A quick review of the calibration parameters used in the analysis (as shown in Table 7.2-1) illustrates the insignificance of diffusion in the tracer dispersion. In the cross-hole tests diffusion was expected to account for much less than one tenth of 1% of the dispersion. Diffusion becomes more important in extremely low velocity tests, such as natural gradient testing, and to a lesser extent, the single-well push/pull tests. However, in each of these low velocity tests, placement of the tracer into the formation is accomplished at a relatively high velocity, which can then dominate the tracer dispersion and subsequent analysis.

Perrhenate and iodide were injected into 22PA Zone 2 (cross-hole test 4). Perrhenate and iodide tracer response curves (Figure 7.2-6) show the same fast response for first arrival and peak. The small differences between perrhenate and iodide responses fall within expected laboratory analysis error; therefore, oxidizing conditions appear to exist. Perrhenate injection at 22PA Zone 2 was not used in model calibrations because it did not contain a natural drift component in its response curve.

The response of lithium, a reactive tracer, and microsphere colloids were not used in model calibration. Both of these tracers displayed complex recovery curve behavior with rapid breakthroughs, followed by rapid initial declines, followed by very slow declines. This behavior was considered too complicated to calibrate, given time and budgetary constraints.

The pump downtime period, which was a consequence of adding the approval of perrhenate as a tracer to the original UIC permit, presented an unanticipated opportunity to observe the tracer mass response to the natural gradient. The perpendicular locations of the tracer injection points (22PA and 22PC) compared to the producing well (22S) also maximized the potential to observe both the azimuth and the magnitude of the natural gradient acting on the in situ tracer masses.

This response indicated the natural gradient has a north-south azimuth and a magnitude of 0.00014 ft/ft.

Finally, the cross-hole test between 22PA Zone 1 and 22S Zone 2 (cross-hole test 3) showed no evidence of communication between zones.

It is important to note that no modeling effort is unique. Multiple models can be calibrated to match the observed tracer response. The goal of the analysis is to match the observed responses with a reasonable geologic model, which can then be used to gain an understanding of the modeled flow system.

7.2.2 Single-Well Tests Results

The first single-well test, which used iodide and PFBA and a 70-hr. rest period, exhibited high (greater than 90%) cumulative tracer recovery for both tracers. The nearly identical measured mass normalized tracer recovery curves are presented in Figure 7.2-7. The lack of differentiation between the tracer recovery curves indicates that mechanical dispersion was the dominant factor affecting the shape of the recovery curves and that diffusion into a stagnant layer was nonexistent or very limited. Mechanical dispersion coefficients for the two tracers should be identical in value, and they should therefore affect the shape of the recovery curve similarly. Also, these coefficients are typically several orders of magnitude larger than diffusion coefficients, at the minimum. The specific diffusion coefficients for the tracers used in this test only differ by a factor of two, approximately. Mechanical dispersion is many orders of magnitude larger than diffusion at the higher fluid velocities induced by long-term pumping in these cross-hole tests. Thus, mechanical dispersion effects on recovery curves should mask any effects of diffusion. The second single-well test, which used iodide and 2,3,4,5-TeFBA and a 716-hr. rest period also exhibited nearly identical recovery curves after a mass balance problem was corrected by UNLV.

The results from numerical simulation analysis of the single-well push/pull tests 1 and 2 can be found in Table 7.2-1. Figure 7.2-8 compares the measured and simulated recovery curves (i.e. calibration match) using the calibration parameters listed in Table 7.2-1 for the first single-well test. A similar good match was obtained between the measured and simulated recovery curves for the second single-well test.

8.0 VENTILATION RELATED MODELING STUDIES

Since the mid-1990s, the NWRPO has conducted independent modeling studies to analyze the feasibility and potential benefit of long-term ventilation at the proposed U.S. DOE high-level radioactive waste repository at Yucca Mountain, Nevada. From FY02 through FY06, the NWRPO contracted the University of Nevada, Reno, to conduct coupled hydrothermal-ventilation modeling to support the evaluation of the design and performance of the repository. One major NWRPO interest is the use of ventilation in the repository design to enhance performance and thereby minimize long-term health and environmental impacts to southern Nye County. The NWRPO is specifically interested in the potential use of ventilation to keep repository temperatures below the water boiling limit and relative humidity below 100% in most parts of the emplacement area. Reduction in temperature by ventilation allows for using the safest, smallest portion of the mountain for long-term isolation of the nuclear waste.

The NWRPO, other stakeholders, and numerous independent reviewers believe that keeping repository temperatures and relative humidities below these levels can reduce uncertainties in performance assessment models, improve safety, and ultimately benefit citizens living downgradient of Yucca Mountain. Many of these entities believe that minimizing the total storage area by ventilation for a given waste load will help ensure the emplacement of waste in the most stable, and therefore safest, area available.

The main purpose of Nye County ventilation studies is to understand the complex heat and moisture transport processes during both pre-closure and post-closure repository operations. During the past five years (FY02 through FY06) 12 ventilation related tasks were performed and reported. Tasks 1 through 3 were conducted in FY02 and reported in the FY02 annual report to Nye County (NWRPO, 2003d) and the proceedings of a technical conference (Danko and Bahrami, 2003a and 2003b). Tasks 4 through 8 were conducted in FY03 and FY04 and reported in a final letter report to Nye County for FY03 (Danko, 2004a) and in the FY04 annual report for Nye County (NWRPO, 2005c). The results of these tasks were also published in five technical papers (Danko, 2004a and 2004b; Danko and Bahrami, 2004a and 2004b; and Danko and others, 2004). Tasks 9 through 12 were performed in FY05 and FY06 and included as part of this summary report. The results of Tasks 9 through 12 have also been presented at one technical meeting (Bahrami and others 2006) and published in six technical papers (Bahrami and Danko, 2006; Danko, 2006; Danko and Bahrami, 2006a and 2006b; Danko and others, 2007; and Walton and others, 2006). The results were also reported in the form of monthly progress reports.

The following sections summarize the purpose, procedures, results, and conclusions of the ventilation modeling tasks conducted during the period of FY02 through FY06. Recommendations for future studies are also presented.

8.1 Task 1: A Numerical Verification Test of the Correctness of MULTIFLUX (FY02)

MULTIFLUX is a coupled hydrothermal-ventilation model and software (MULTIFLUX, 2003). It couples a non-equilibrium, saturated and unsaturated, flow and transport model for the rock domain, such as Nonisothermal Unsaturated-saturated Flow and Transport (NUFT), (NUFT, 2000) with a computational fluid dynamics (CDF) model for the airway domain, including waste

packages. NUFT was developed, calibrated, and verified by Lawrence Livermore National Laboratory for simulating heat and moisture flows in the rock domain.

8.1.1 Task 1 Purpose and Procedures

The purpose of Task 1 was to compare (i.e. calibrate) MULTIFLUX results with known analytical solutions to a quasi-three-dimensional convection-conduction ventilation problem. Four different solutions were compared as follows:

- Solution 1: MULTIFLUX calculation, applying the embedded NUFT model (NUFT, 2000) for the rock, using 137 time divisions;
- Solution 2: MULTIFLUX calculation with a rock model applying an analytical-based, Carslaw & Jaeger (1986) reference solution with first-kind boundary condition with 35, 69, and 137 time divisions;
- Solution 3: Approximate, analytical calculation using a Carslaw & Jaeger (1959) solution with third-kind (convective) boundary condition, superposition, and numerical integration with 500 time divisions;
- Solution 4: Reference calculation generated by John Walton, Professor, University of Texas, El Paso, using the same Carslaw and Jaeger (1959) analytical solution without numerical integration. This analytical solution is assumed to be the most accurate solution.

8.1.2 Task 1 Results and Conclusions

Predicted drift wall temperature histories for Solutions 1 through 4 are presented for differences along the drift airway in Figure 8.1-1.

- MULTIFLUX with the Carslaw and Jaeger rock model (Solution 2) closely approximates the Carslaw and Jaeger reference analytical solution (Solution 4).
- MULTIFLUX with the NUFT rock model (Solution 1) also closely matches the reference solution (Solution 4). This agreement was significant because it implicitly validated the NUFT model configuration against a textbook result.
- The approximate Carslaw and Jaeger analytical solution with superposition (Solution 3) agrees very well with the reference analytical solution (Solution 4). The difference may be caused by the difference in the number of time divisions.
- In summary, comparison of the four different solutions (Figure 8.1-1) showed excellent agreement. It was, therefore concluded that the MULTIFLUX software was capable of modeling the time-dependent, coupled convection-conduction problem without moisture transport correctly.

8.2 Task 2: A Preliminary MULTIFLUX Study of Temperature and Relative Humidity Variations in a Conceptual Yucca Mountain Repository Design (FY02)

8.2.1 Task 2 Purpose and Procedures

The purpose of Task 2 was to analyze temperature and relative humidity variations in a conceptual, ventilated nuclear waste repository at Yucca Mountain. Figure 8.2-1 shows the model geometry, with all length units in meters, following the conceptual design developed by DOE. The MULTIFLUX model applied a series of un-connected, chimney-type NUFT rock model-elements similar to what is used in DOE's Multi-Scale Thermal Hydrologic Model (DOE, 2004b) for the Line-averaged-heat-source Drift-scale Thermal-Hydrological LDTH model component. This model selection rendered the study approximate and conservative, ignoring edge-cooling and mountain-scale effects. The drifts were assumed to be mechanically ventilated for 25 years with a forced, constant air flow rate of 15m³/s for 25 years, then ventilated from year 25 until year 300 under natural buoyancy pressure driving force through an open system and, finally, naturally ventilated by air infiltration through backfilled intake and exhaust shafts and tunnels from year 300 until year 5,000. MULTIFLUX provided balanced results for air, heat, and moisture flows. A balanced solution between the pressure loss and pressure gain due to buoyancy was achieved in 15 total system iterations.

Figure 8.2-2 shows the pre- and post-closure wall temperature and relative humidity distributions in time and space. As shown, even in this early version, the MULTIFLUX model was capable of simulating pre- and post-closure time-periods as one, continuous, integrated task.

8.2.2 Task 2 Results and Conclusions

- Natural ventilation was found adequate for keeping rock wall temperatures below boiling for the 25 to 300 years time period.
- The air flow rate decreased only moderately when the fans were removed in year 25.
- The backfill of the access shafts and tunnels at year 300 decreased, but did not eliminate natural ventilation that is beneficial to controlling temperatures and relative humidities.
- Although wall temperatures in the drift slightly exceeded the boiling limit near the air exhaust shaft for the period of 700 to 4,000 years, the temperature rise in the drift was greatly delayed and reduced in magnitude by the infiltrating airflow during post-closure, relative to the un-ventilated, sealed off base case (DOE, 2004b).
- The trend of the post-closure natural air flow rate variation with time indicated that natural ventilation may continue for much longer time periods.
- The temperature results for the long, post-closure time period from this model must be considered conservatively high, due to lack of the un-heated rock mass and its edge cooling effect.

- The relative humidity levels were found consistently lower than those predicted in some of the current corrosion related performance assessment studies at Yucca Mountain.

8.3 Task 3: Preliminary MULTIFLUX Sensitivity Studies (FY02)

8.3.1 Task 3 Purpose and Procedures

The purpose of Task 3 was to study the sensitivity of temperatures and relative humidities to the variation of selected input properties and ventilation parameters at Yucca Mountain. The perturbed site input properties were: rock heat conductivity, thermal diffusivity, and heat transfer coefficient on the drift surface. The ventilation air flow rate, input air temperature, areal thermal heat load, and the average water percolation rate due to precipitation were also varied as input parameters.

8.3.2 Task 3 Results and Conclusions

- The temperatures and heat removal rates by ventilation were found to be most sensitive to the thermal conductivity, exceeding 100% at low ventilation rate. This finding underlines the importance of the thermal conductivity values for Yucca Mountain, since any input percentage error in conductivity may affect the predicted temperature fields by a higher percentage error.
- High sensitivities to intake air temperatures were also observed, underlining the importance of studying seasonal temperature and possible future climate changes in the repository design.

8.4 Task 4: Model Update and Baseline Case Simulation (FY03 - FY04)

8.4.1 Task 4 Purpose and Procedures

All model elements were revised to reflect the most recent repository design configuration known in 2004 (DOE, 2004b) and used by DOE during the preparation for license application. The rockmass domain was updated in the MULTIFLUX model by adding the unheated edges. The new mountain-scale rockmass domain around an emplacement drift is shown in Figure 8.4-1. Barometric pressure in this task as well as in Task 5 was assumed to remain constant as in all DOE modeling work. A base case simulation of temperature, humidity, and condensation was conducted in emplacement drifts, with forced ventilation for a 50-year pre-closure period, followed by a 5,000-year post-closure period of natural ventilation as described in NWRPO (2005c). Figure 8.4-2 shows the CFD model configuration in the airway showing repeated sequence of eight waste packages in an emplacement drift; a schematic transport diagram of pre-closure powered ventilation; and a schematic transport diagram of post-closure natural air movement with axial dispersion.

8.4.2 Task 4 Results and Conclusions

An example of representative results of drift wall temperature and relative humidity from the MULTIFLUX calculations for the baseline case are shown in Figure 8.4-3. Related

condensation rates along the drift wall are presented in Figure 8.4-4. Note that condensation shown in this figure begins after temperatures fall below boiling near both ends of the emplacement drift. As temperatures decrease, condensation rates also decrease, but condensation appears to continue well beyond the end of the simulation period (5000 years). In addition, dispersion coefficients were varied to cover a reasonable range in values ($0.1 \text{ m}^2/\text{s}$ and $0.004 \text{ m}^2/\text{s}$) and their effect on drift temperature, humidity, and condensation were determined.

- Temperature, relative humidity, and condensation distribution in the emplacement drift can be established relatively quickly and easily if barometric pressure variation with time is disregarded, as done in DOE reports.
- Maximum relative humidity and condensation occurs near the unheated edge areas of drifts.
- It is difficult to compare the results of Task 4 (and Task 5) to those in DOE reports because of the differences in model conditions, assumptions, and simplifications (DOE, 2004a). Clearly, a thorough comparison and evaluation of differences between Nye County and DOE models will be needed in the future, especially regarding condensation distribution.
- Another example of model differences is the DOE assumption that the dispersion coefficient is a constant. Task 4 modeling showed that the dispersion coefficient cannot be regarded as a universal constant and reasonable variations in its magnitude can have a significant influence on condensation distribution along an emplacement drift.

8.5 Task 5: Pre-Closure Time Study (FY03 - FY04)

8.5.1 Task 5 Purpose and Procedures

The Task 4 simulation was repeated using pre-closure forced ventilation periods of 100, 200, and 300 years to simulate a cooler repository; the changes in temperature, humidity, and condensation in the emplacement drifts as a function of the forced ventilation time period were studied.

8.5.2 Task 5 Results and Conclusions

The results of the MULTIFLUX calculations of drift wall temperature and relative humidity for pre- and post-closure time periods with 300-year ventilation period are shown in Figure 8.5-1. Related condensation rates (and temperatures) along the drift wall are presented in Figure 8.5-2. Note that condensation shown in this figure begins after temperatures fall below boiling near both ends of the emplacement drift and appears to continue well beyond the end of the simulation period (5,000 years). Maximum condensation rates occur near year 750 at the very ends of the drift and correspond to maximum temperatures in the central portion of the drift. As temperatures decrease, condensation rates decrease, but occur over a greater length of drift near each end.

- Based on a perhaps oversimplified study model (e.g. assuming a constant barometric pressure), an extended pre-closure ventilation period carries some hydrothermal advantages as well as disadvantages.
- Lower temperatures with longer pre-closure ventilation result in diminished condensation at focused locations; however, relative humidity may actually increase due to lower temperatures.
- Long time periods are found for the development of the maximum temperature during post-closure. The evolution time for peak temperature of 750 years, with 300 years of pre-closure ventilation, may be disadvantageous regarding monitoring and performance confirmation.

8.6 Task 6: Barometric Pressure Pumping Study (FY03 - FY04)

8.6.1 Task 6 Purpose and Procedures

The effects of barometric pressure pumping on the temperature and moisture histories were simulated for the arrangement modeled in Tasks 4 and 5. It was expected that the effects would increase relative humidity and condensation rates as the result of more moisture inflow in to the emplacement drift. Barometric pressure data from various locations close to Yucca Mountain were combined to simulate daily barometric pressure variations. Fourier analysis was used to describe the cyclic nature of the data. The dominant component was characterized by a 10.66 day frequency period and an amplitude of 1160.5 Pa. The data were simplified into a square wave with the same frequency and amplitude, equal to the RMS (root-mean-square) value of the variation around the mean values. The RMS variation of pressure may be referred to as the standard deviation, $\sigma(P_{\text{bar}})$, of the barometric pressure variation. The barometric pressure was applied only to drift level and not to the ground surface. As a further model simplification, the drift wall vapor pressure and temperature were assumed to remain constant. These simplifying assumptions, affecting condensation and relative humidity along the drift, were later re-examined and refined in the FY05 - FY06 modeling studies, described in Section 8.10.

8.6.2 Task 6 Results and Conclusions

Figure 8.6-1 shows the results of moisture inflow, drift condensation rate, and temperature as a function of time. In addition, moisture inflow and condensation were determined for the base case (constant pressure used in Tasks 4 and 5) and the low barometric pressure case, $P_{\text{bar}_{\text{av}}} - \sigma(P_{\text{bar}})$, where $P_{\text{bar}_{\text{av}}}$ is the average barometric pressure and $-\sigma(P_{\text{bar}})$ is one standard deviation below the average. Between 50 and 500 years the entire drift is above boiling and the moisture inflow is approximately 16 times higher than that of the base case. Starting from approximately Year 750, the minimum drift wall temperature drops below boiling near the edges and elevated condensation (approximately 12 times higher than for the base case) is seen along the below boiling drift section. When minimum drift wall temperature drop below boiling (somewhere between Year 2000 and 3000), drift wall moisture flux and condensation rate agree with the base case, as there is no moisture inflow deviation resulting from barometric pressure cycling.

- The always-present barometric pressure variation appears to have a significant effect on relative humidity and condensation distribution in the emplacement

drifts during the few thousands of years when at least part of the emplacement drift is above boiling.

- It should be noted that the average barometric pressure used in DOE modeling to date as well as in Task 4 of this study is hypothetical as opposed to actual barometric pressure, which is variable.
- The model has many simplification assumptions and a refined model configuration was recommended. This task was indeed re-visited later in Task 10.

8.7 Task 7: Fate of Condensation Study (FY03 - FY04)

8.7.1 Task 7 Purpose and Procedures

The amount of condensation shown in previous tasks to develop on rock surfaces in the emplacement drifts was applied as a water source on the drift surface. Water saturations and flux in the rock around the drift, including on the drift floor where it may have the greatest influence on radionuclide transport, were evaluated.

8.7.2 Task 7 Results and Conclusions

Figure 8.7-1 shows the effect of applying the condensation to the roof nodes resulting in the return of the moisture into the drift airspace. This case demonstrates the potential of drippage. Applying the condensate to the invert causes no significant change in the moisture flux as shown in Figure 8.7-1.

- It is critical to know the distribution of condensate around the drift perimeter. Condensation on the roof may not be able to be imbibed and may cause drippage. More studies are needed with the numerical model to understand condensation distribution and the amount of condensation at a specific location that may cause drippage.
- This phenomenon has not been well understood or reported in the literature, and more studies would be needed in the future.

8.8 Task 8: Laboratory Test Preparation (FY03 - FY04)

Progress was made in preparing a numerical simulation of a future laboratory condensation experiment in a large welded tuff boulder. The simulation would help design the laboratory experiment, including the selection of measurement parameters and procedures, to physically verify condensation processes shown in modeling results from Tasks 4 through 7. Careful planning of the laboratory experiments on condensation imbibition would be necessary before conducting laboratory measurements. Ambient air-dry condition of rock in the laboratory would be altered by the measurement; it would be difficult to repeat the experiment without a lengthy initialization.

Although simulation preparation for the laboratory test for condensation model calibration was made, the test was postponed for a future, and more convenient time.

8.9 Task 9: Examine the Potential Significance of Water Vapor Migration Between the Network of Drifts for the Baseline Repository Design (FY05 - FY06)

8.9.1 Model update

Model update included the following main changes:

- Detailed in-drift model configuration with under and above drip shield regions.
- Unheated 80-m drift sections at both ends.
- 600-m heated section versus 714-m heated drift in the 2005, FY 04 study report.
- Recent addition of air flow CFD solver.
- Inclusion of latent heat of condensation at the unheated drift sections.

8.9.2 One-directional air flow studies

A small, post-closure, buoyancy-driven air infiltration through the drift bulkhead to neighboring drifts was assumed. The air flow variation with time is shown in Figure 8.9-1, selected based on a previous, natural ventilation model (NWRPO, 2005c). The temperature and relative humidity variations at year 500 are shown in Figure 8.9-2 for two different air flow directions (from left to right, and from right to left) in the emplacement drift.

The effect of one-directional flow is estimated to be about 15°C in temperature in the cold section and no significant change in the heated section. An overall effect of about 10% RH reduction is also seen from the model results. The explanation of this phenomenon is that the cold, condensing drift section dries out some of the moisture content of the air, increasing its capacity to absorb humidity during the flow across the drift, irrespective of the flow direction.

8.9.3 Recirculation air flow studies

New model calculations were performed using a new natural air flow model element in the CFD model of one emplacement drift. The MULTIFLUX code modification and verification was supported by the SNT Project (Danko and others, 2007a.). The modeling work of a more complex configuration was performed for Nye County reported in this report. The same model configuration, except with the line averaged heat load was used for MF testing. The new element of the model configuration was that the heat and mass transport within the drift air space included the effects of carrying air velocities. The velocity field was autonomously calculated in MULTIFLUX, solving for natural airflow, driven by temperature and humidity differences, resulting in natural buoyancy effects. The simulation provided a fully balanced solution between the heat and mass transport processes in the drift air space and in the surrounding rock mass.

In order to depict the three-dimensional velocity field from the numerical solution in simple, two-dimensional figures, lumped air nodes are used as follows. The air1, air2, air3, and air4 designate air nodes inside the drip shield air space at a given cross section along the drift, shown in Figure 8.9-3. The air5, air 6, air7, and air8 identify air nodes outside the drip shield in the air space at a given cross section along the drift, shown in Figure 8.9-4. Note that the average of all four air velocities weighted with their corresponding flow cross sections either above or below the drip shield would give approximately zero average since the net average axial air mass flow rate is zero. It is only the circulation which is non-zero in a closed air space. All four vertical air flow velocity components are averaged into one circulation velocity either above, or below the drip shield. Positive velocity in the horizontal direction means airflow from drift entrance toward the exit, from left to right. Positive velocity in the vertical direction loop means counter-clockwise circulation, shown in Figure 8.9-5. The two-dimensional, simplified representation of the large-scale airflows in the horizontal circulation direction is shown in Figures 8.9-6a and 8.9-6b for the airspace inside and outside the drip shield at year 1,000. The vertical air velocities in each drift cross section and with the variation along the drift length at year 1,000 are shown in Figures 8.9-7a and -7b for the air space inside and outside the drip shield, respectively.

The results show that well-defined, large-scale axial airflow re-circulation loops form in the drift. It can be seen in Figure 8.9-6 that in each half-drift section, air velocity at one or two air lines move toward the drift center and others move away toward the drift ends. The air circulation is maintained by the natural buoyancy pressure difference even in the case of a perfectly horizontal drift. The height difference within the 5.5m diameter drift and the axial temperature difference between the cold ends and the hot middle section along the drift length provide apparently enough driving force for natural re-circulation. Two main axial loops form, one above, and one below the drip shield. In either air space, the average air velocity is around 0.05 m/s over half of the drift cross section in either direction. This gives a travel time of about two hours for convective exchange between the center and the ends of the drift at year 1,000 during post closure. Note that the axial velocity at the drift center is zero, due to symmetry between the left and right side of the drift. Air circulation in the vertical plane is somewhat weaker than the recirculation in the horizontal direction. This is explained by the smaller temperature difference between hot and cold surfaces in the radial than in the horizontal direction within the emplacement drift. Apparently, it is not the temperature gradient, but rather the total, integrated temperature difference over the circulation loop length that matters in the buoyancy driving potential. The vertical and the horizontal re-circulation air loops are inter-connected in the above drip shield and the below drip shield air spaces but the two air spaces are separated except for their connection at the drift ends. The intercommunications allow slight variations in the magnitude of the axial velocities. The new model results represent a significant success in modeling turbulent flow with a lumped-parameter CFD model, and coupling it with the rock model for mountain scale temperature distribution calculation with the MULTIFLUX software.

For comparison and model validation purposes, the equivalent, effective dispersion coefficient along the drift length was inverse-calculated from the convective moisture transport due to the velocity field. Figure 8.9-8 shows the equivalent dispersion coefficient for three different post-closure time periods. As shown, the equivalent dispersion coefficient varies with both time, and location. The range in peak values (approximately 0.07 to 0.13 m²/s) for all time periods agrees well with the maximum value of 0.1 m²/s from the Yucca Mountain literature for the air space outside the drip shield. The equivalent dispersion coefficient range for the air space inside the

drip shield is approximately 0.05 to 0.08 m²/s, a factor of 10 higher than the 0.006 m²/s value published for a comparable arrangement for an emplacement drift. The good agreement for the equivalent dispersion coefficient in the above-drip shield domain is taken as a successful comparison for model calibration against published data. The poor agreement in the below-drip shield domain is worrisome, and warrants further investigation. The working hypothesis is that the calculated dispersion coefficient in the below drip shield domain in the literature did not capture the axial transport processes accurately.

Temperature, relative humidity, and rate of condensation distributions along the drift length are shown for selected post-closure time periods in Figures 8.9-9, 8.9-10 and 8.9-11 at three different segments of the drift wall: the roof; the sidewalls; and the floor over the invert. Significant differences are seen in the relative humidity and condensation rates over the segments of the drift circumference, while the temperatures remain nearly constant. It is interesting to notice that the relative humidity and condensation rate are both higher on the floor than over the rest of the drift wall. This fact may be significant for two reasons. Firstly, the floor segment is under the drip shield and it constitutes the area which is in direct contact with the waste packages. The appearance of liquid water from condensation on the floor (and already under the drip shields) may provide aqueous transport of particles from this area towards the water table, in spite of having drip shields over the waste packages. Secondly, the floor segment and the drip shields form a relatively separated micro-tunnel from the rest of the drift air space, and the air in this micro-tunnel constitutes the primary storage environment for the waste packages. While this micro-tunnel is shielded from direct drippage to the floor, vapor is supplied at an elevated rate from the floor relative to the sidewalls and the roof, giving ample moisture source. On the other hand, the transport cross-section of the micro-tunnel is only a fraction of that of the main air space in the drift, impeding the axial transport of heat and moisture. For these reasons, modeling of the storage environment in the micro-tunnel appears to be an important task, especially considering that no project data are available for this region since other baseline models for Yucca Mountain (e.g., DOE, 2004b, Birkholzer et al., 2006) treat the volume of the micro-tunnel as solid material with average properties, attached to the waste packages.

Figures 8.9-12 a and b compares the new, convective model results based on an explicit, three-dimensional, natural air flow field in the drift (both under, and over the drip shields) with the results from a previous, simplified model, using the equivalent dispersion coefficient. The results for temperature, relative humidity, and rate of condensation distributions along the drift length are shown in Figure 8.9-12 only for the floor segment of the drift wall and for two post-closure time periods: year 1,000 (a); and year 5000 (b).

Finally, the results of a brief sensitivity study are shown in Figures 8.9-13 and 8.9-14. The equivalent dispersion coefficient, as an easy-to-understand parameter and comparable to published data, are divided for the air space outside and inside the drip shield in Figure 8.9-13a and -13b, respectively, as a function of the air flow friction loss parameter. This figure shows that the equivalent dispersion coefficient is not very sensitive to the air flow friction loss parameter. Similar results are obtained showing the effect of large-eddy, turbulent kinetic shock loss factor on the equivalent dispersion coefficient in Figures 8.9-14a and 8.9-14b for inside and outside the drip shield airspaces, respectively.

8.9.4 Task 9 Conclusions

- A one-directional, small air flow caused by air movement through bulkheads to neighboring drifts may cause only moderate changes in temperature. Slight asymmetry may develop between the two drift ends; the magnitude of the asymmetry is quite insignificant.
- Humidity is also only slightly affected by one-directional air migration in the drift.
- The equivalent dispersion coefficient ($0.1 \text{ m}^2/\text{s}$) for over the drip shield domain used to date in modeling is a reasonable approximation and shows a low sensitivity to the vertical friction loss coefficient and to the kinetic shock loss factor.
- Large-scale, natural, buoyancy-driven air recirculation loops will form both above and below the drip shields during post-closure. The three-dimensional velocity field is strongly coupled to the temperature and the humidity distribution requiring a fully-coupled numerical model. To date, MULTIFLUX is the only model available for solving this task.
- Large effects on lowering temperature, increasing humidity, and related increased condensation zones are seen due to natural air re-circulation in the drift. The large-scale, axial, in-drift natural air circulation is a new phenomenon that has not been seen before in publications.
- The new results obtained using the MULTIFLUX thermal-hydrologic-air flow model represents a breakthrough in coupling a porous-media model for the rockmass with a CFD model for the airspace with turbulent flow.

8.10 Task 10: Barometric Pressure Fluctuation Studies with a Refined Model (FY05 – FY06)

The effect of barometric pressure variation with time was re-examined during the past year with an improved numerical model, refined specifications and assumptions, and the newest conceptual waste arrangement in the emplacement drift. See details in Section 8.9.1 for model update information.

8.10.1 The Effect of Revised Model Assumptions on Moisture Influx and Condensation

The new conceptual design for Yucca Mountain includes 80 m long unheated sections at drift ends which were not included in the previous FY03 – FY04 annual report's model assumptions (NWRPO, 2005c). This modification significantly alters the moisture transport within the drift.

The effect of the unheated drift section has been studied before and found to be significant (Danko et al, 2006). The unheated section at low temperature creates a low vapor pressure point (or vapor concentration) which causes the enhanced moisture transport from the heated section toward the unheated section.

Also previously, the pressure variation was applied only at the drift level while the barometric pressure was kept constant at the surface. In FY05 and 06 modeling, this assumption was revised with the pressure variation applied both at drift level and at the ground surface simultaneously. The application of pressure only at drift level caused and enhanced moisture inflow, which resulted in more humid, and more time-variable conditions inside the heated emplacement drift.

In addition, the previous annual report (NWRPO, 2005c) did not include the effect of latent heat of condensation on the temperature field. The current analysis, using a more sophisticated MULTIFLUX model, incorporates this effect. This modification alone has caused a significant effect on the results reducing the rate of condensation in the cold sections by increasing temperatures.

Taken together, the revised model assumptions result in an enhancement factor of moisture inflow in the hot (over boiling) drift section of 4 and 0.5 times the case of average pressure ($P_{bar_{av}}$) for low ($P_{bar_{av}} - \sigma(P_{bar})$) and high ($P_{bar_{av}} + \sigma(P_{bar})$) barometric pressure, respectively. Previously (NWRPO, 2005c) the moisture flux enhancement at $P_{bar_{av}} - \sigma(P_{bar})$ was 6 to 8 times the flux at $P_{bar_{av}}$.

The previous modeling results for the upper and lower relative humidity bounds on the drift surface are shown in Figure 8.10-1 and the updated modeling results are shown in Figures 8.10-2, 8.10-3, and 8.10-4 for three different segments on the drift wall circumference: the roof, the sidewall, and the floor over the invert. The 714m heated drift did not include any unheated section, while the current model is 600m with two 80m unheated sections for a total of 760m model. The lower pressure bound in Figure 8.10-1 is the base case pressure and the upper bound is $P_{bar_{av}} - \sigma(P_{bar})$; whereas the lower bound in Figures 8.10-2 through 8.10-4 is $P_{bar_{av}} + \sigma(P_{bar})$ and the upper bound is the same as in Figure 8.10-1.

Note that the shaded areas in Figures 8.10-1 through 8.10-4 represent the variation between upper and lower pressure bounds. The relative humidity will swing between the upper and lower bounding curves with a 10.66-day period time as a statistical average. The primary importance of the variations in relative humidity is that some of the accumulated salts resulting from evaporation into the drifts are hygroscopic and will deliquesce. Deliquescence can lead to dripping of concentrated salt solutions from the roof of the drifts and periodic wetting and drying cycles on a time scale measured in days.

8.10.2 Task 10 Conclusions

- The current model uses more realistic and less conservative assumptions, resulting in significant changes in the results relative to the results of the previous study NWRPO (2005c).
- The overall effect of the barometric pressure variation is not as significant as it was reported in NWRPO (2005c).
- One reason for the difference between the new and old results is the presence of 80-m unheated drift sections. These cold sections create a low vapor pressure area, which attracts moisture during the above boiling period.

- Another reason for the reduced enhancement of the drift moisture inflow is due to the fact that the pressure variation is simultaneously applied in the present study to both the drift level and to the ground surface. At year 1000 some condensation occurs in the heated section as a result of cold trap process caused by the variable temperature profile along the drift due to waste package heat load variations.
- Still another reason for reduced enhancement of moisture inflow is the incorporation of latent heat of condensation into the model and its effect on the temperature field.
- The pressure variation effect disappears after year 1000 when the entire emplacement drift goes below boiling. During the above boiling period of years 50-1000, the effect of pressure variation is mainly seen in the unheated sections with a few locations in the heated section showing condensation until around year 600. Variation in relative humidity is seen until around year 1000 at various parts of the hot drift section.

8.11 Task 11: Long-Term, Forced Ventilation Studies (FY05 – FY06)

The non-linear processes associated with the above-boiling temperature design can be mitigated by reducing temperatures. Relative humidity variation with time reduces to insignificant levels at below-boiling temperatures. Repository performance at below-boiling temperatures can be predicted with greater confidence. A series of modeling studies with open-system repository ventilation were conducted to support a conceptual solution to temperature reduction. The possibility of increasing the storage capacity, and lowering the maximum temperatures below-boiling at the same time, was also studied.

8.11.1 Task 11 Modeling Procedures and Results

Figure 8.11-1 shows the temperature and relative humidity variations along the drift length for 300 years of pre-closure and 5000 years of post-closure time periods for the previous baseline design without heated sections. As shown, the maximum temperatures are about the same, and close to boiling limit during (1) the 300 years pre-closure time period with cross-ventilation and (2) during the post-closure time period with no powered ventilations. These results indicate that 300 years ventilation may bring the current baseline design to below-boiling.

A doubled storage capacity with 600 years pre-closure ventilation time period was also studied as a hypothetical exercise. Figure 8.11-2 shows the temperature and relative humidity variations along the drift length for a 600 year pre-closure ventilation period and 5000 years of post-closure time periods for the current baseline design dimensions, but containing double the amount of waste assuming no waste aging. Note that temperatures are significantly below boiling for all time periods. With waste re-processing, the necessary pre-closure ventilation cooling time period may be greatly reduced, or even eliminated.

8.11.2 Task 11 Conclusions

- A below-boiling temperature design with doubled storage capacity may be achieved with 600 years pre-closure ventilation, assuming no waste re-processing.

With waste re-processing, the necessary pre-closure ventilation cooling time period may be greatly reduced, or even eliminated.

- Change to a below boiling repository would reduce the potential for localized corrosion during the thermal period since (a) Alloy-22 is more resistant to localized corrosion at lower temperatures; (b) at below boiling temperatures the accumulation of salts will be less; and (c) at below boiling temperatures, the barometric pressure changes will no longer lead to cycles of variations in relative humidity and condensation.

8.12 Task 12: In-rock Vapor Flow Studies (FY05 – FY06)

Examination of modeled liquid water and vapor flow directions in the rockmass around the emplacement drift provides evidence for total evaporation in this region of rock, and reinforces the salt accumulation hypothesis and deliquescence briefly mentioned in Section 8.10.

8.12.1 Task 12 Description of Modeling and Results

The revised rockmass model described in Sections 8.9 and 8.10 was used for the rockmass surrounding the emplacement drift. It was a post-closure study of 5000 years time period, preceding with 50-year pre-closure cooling by forced ventilation. No barometric pressure variation or air infiltration in the drift was assumed during post-closure.

Results for the above-boiling temperature, baseline design from the new model are shown in Figures 8.12-1a and 8.12-1b for temperature and relative humidity distributions on the drift wall with time and along the length. Slight variations in the results with the drift length are caused by the heat dissipation variations between individual WPs.

Figure 8.12-2a shows spatial and temporal variations of condensation. The vapor inflow into the drift air space is depicted in Figure 8.12-2b in the form of the water attraction ratio, a non-dimensional ratio between the spatial and temporal vapor flux into the drift and the percolation water flux calculated over the springline width, D , of the drift. The W in the W/D water attraction ratio may be pictured as an imaginary width over which the natural ambient water percolation flux is collected, and transported into the drift by evaporation or seepage. The $W/D=1$ isoline is marked in Figure 8.12-2b. In the domain where $W/D>1$, the drift is effectively a water attractor. This domain approximately coincides with the spatial and temporal domain where the temperature is above-boiling.

Evaporation in the rockmass around the drift naturally means that dissolved ions from the source water will precipitate and accumulate as solids. Total evaporation of the percolation water flow as well as the pore water initially present in the rock matrix represents a source of solid species that must precipitate according to mass conservation. It is possible to estimate the accumulation over the drift crown numerically using the percolation flux towards the drift footprint for the time period over which the evaporation is complete, evidenced by dead-end percolation flow patterns. Figure 8.12-2c is an upper estimate of chloride ion (Cl^-) accumulation, associated with the total evaporation of water over the drift width, D , as a function of the axial position along drift length and time. The chloride accumulation at this point is a hypothesis based on the assumption that the concentration of chloride in pore water is 117 mg/L at Yucca Mountain

(DOE, 2000), and that the total amount of chloride is deposited in the rock wall during complete evaporation. The numerical model results are used only within the boundaries of total evaporation with no dissolution due to lack of percolating liquid water leaving a control volume of the rockmass. Further trends are indicated in Figure 8.12-2c as possible continuations with and without salt discharge. Two processes are in competition in the rockmass at the front of evaporation: (1) salt thickening (by liquid water evaporation) and (2) discharge (by water flow transport). The rate of deposition or dissolution is a complex phenomenon that can be modeled with TOUGHREACT (Xu and Pruess, 2001). However, during total evaporation and no liquid water discharge from a rockmass volume, a simple estimation of salt accumulation is possible without using a kinetic model.

Figure 8.12-3a through -3f are liquid water and vapor flow patterns from the NUFT model-element in the fractured and porous rockmass surrounding the emplacement drift in its middle section at three different time instants. Until year 1500, at which time the drift is already slightly below-boiling, all percolating water disappears and turns into vapor form. The liquid water flow above the drift will dead-end in the rockmass, and become a vapor source, as shown in the diverging vapor flow fields in Figure 8.12-3b and -3d. A very small diversion of the percolation water flow at the drift crown is seen at year 2000 in Figure 8.12-3e, indicating the onset of potential solute discharge and the effect of drift shadow. Vapor flow is still active all around the perimeter including the drift crown and the floor, as depicted in Figure 8.12-3f, showing that vapor accumulation above the drift and vapor discharge into the floor of the drift may coexist for some time.

8.12.2 Task 12 Conclusions

- One consequence of the high temperature operation mode is that the vapor flow into the drift must give rise to salt accumulation in the rock wall, especially in the crown of the drift, during the above-boiling time period, when evaporation of the water percolation is complete. This conclusion is supported by the analysis of total evaporation, and water mass balance in the rock above and around the emplacement drift, evidenced by vapor and water flow fields calculated by NUFT, shown in Figures 8.12-3a to -3d.
- Another consequence of the high temperature operation mode is that the variable vapor flow, as a modulation due to barometric pressure variation, creates fluctuating relative humidity in the emplacement drift. The drift wall at certain locations may vary between dry and wet conditions periodically over time.
- Salt accumulations in conditions conducive to flow separation of anions, combined with relative humidity cycling may create a potentially more aggressive corrosion environment than currently being considered for the above-boiling design.

The main conclusion of the studies is that the convective heat and moisture transports have a major influence upon the temperature and humidity conditions and resulting condensation in and around the drifts both during the pre- as well as post-closure time periods. Consequently, any thermal-hydrologic model that is designed to predict the likely operating environment at Yucca Mountain with a reasonable degree of certainty must have the capabilities of incorporating the

heat and mass transport represented by laminar or turbulent air flow during both pre- and post-closure operation.

This finding is diagonally opposite to what has been used as a working hypothesis in the Multi-Scale Thermal Hydrologic (MSTH) modeling concept, applied to the YMP for analysis and design. According to the MSTH model results, the axial flow of heat and moisture is insignificant and has no impact on the thermal-hydrologic storage environment. The effects of this contention may be far-reaching.

The presence of axial transport is expected to affect the operating environment during the first few thousand years. The higher the temperature regime, the larger impact is expected and so is the uncertainty created by the absence of axial transport in DOE's process models. On the other hand, at below-boiling operating temperature, the axial transport is indeed insignificant, reducing with other factors, modeling complexity and uncertainty.

Long-term ventilation is seen as a viable technology for reducing operating temperature even if the storage capacity is increased at the same time, relative to the waste load density in the baseline design.

MULTIFLUX has grown into a fully capable numerical model that has proven to solve the coupled in-drift and in-rock transport processes with full drift simulations with turbulent flows during both pre- and post-closure operations.

Such a modeling capability will be needed for explaining performance confirmation measurements at Yucca Mountain from the onset of operations. Nye County has a vested interest in monitoring the relevant processes at play at Yucca Mountain that includes air discharges into the accessible environment. Through the coupled in-rock and in-air transport processes, the exhaust air parameters from the emplacement drifts and the air shafts have an important and intricate confirmatory value to understanding the entire thermal-hydrologic-air process evolution at Yucca Mountain.

9.0 SUMMARY OF MAJOR FINDINGS AND RECOMMENDATIONS

9.1 Drilling, Sampling, Logging, Well Construction, and Testing

9.1.1 Major Findings

9.1.1.1 Drilling

AR-RC (open-hole) drilling methods used to drill and sample the vast majority of footage proved to be relatively rapid and inexpensive, produced drill cuttings from unsaturated alluvium and from both unsaturated and saturated valley-fill and bedrock units that were reasonably representative of in situ formation rock, minimized the disturbance of the formation rock and groundwater chemistry, and produced boreholes suitable for completing piezometer screens across and beneath the water table. In most cases, very little development work was required in AR-RC-drilled piezometers due to a lack of drilling fluids used in the monitored intervals. The

development of piezometer screens, primarily by low-flow-rate pumping of at least several hundred gallons of water, removed most suspended sediment from the produced water.

Larger diameter multi-screen wells drilled with FM methods (Phase III wells) provided stable boreholes for completion of well screens and construction of sandpacks and seals without problems. Using polymer-free bentonite mud products during drilling eliminated the need for prolonged well development.

Piezometer wells drilled with CA method in Phase III were successful for constructing multiple string piezometers with sandpacks and grout seals. Additionally, unsaturated zone air piezometers were installed in 10P.

Sonic coring of alluvial materials in 19PB and 22PC was a success and produced nearly continuous core from the upper approximately 260 ft and 293 ft of saturated alluvium, respectively, suitable for logging (e.g., geologic, digital photographic, and video logs) and laboratory testing of parameters independent of porosity, and produced coring-related data to permit calculation of in situ dry bulk density and porosity values.

The sonic coring process resulted in some disturbance of the core samples from in situ conditions. Core expansion of unconsolidated alluvial sediments occurs resulting in higher core porosity and lower density values, although textural layers remained intact. Migration of silt and clay from the interior of the core to the outside surface of the core also occurs, however, there was no evidence of migration of fines along the length of the core. Finally, some migration of water from core in the lower region of the core barrel migrates to core in the upper region, due to heat produced primarily at the core bit.

Drive core samples were successfully collected from both unsaturated and saturated alluvium in CA boreholes using drive-core methods with 2.0- and 2.5-ft-long by approximately 4-in. ID solid-tube core barrels. Drive-core methods were less successful in uncased AR-RC boreholes due to an inability to completely clean out rotary cuttings prior to drive coring.

DR-RC methods used to drill larger diameter portions of several Phase V boreholes primarily in unsaturated alluvium produced drill cuttings with PSDs similar to AR-RC methods for most size fractions.

Borehole conditioning methods using small amounts of bentonite-based drilling mud in RC boreholes drilled with AR-RC methods successfully stabilized borehole walls both above and below the water table. Exceptions included: 23P, where conditioning methods failed to prevent caving of the borehole leading to sticking the BHA in the lower portion of the borehole; 13P, where these methods failed to prevent caving, to re-establish circulation, and to advance the borehole beyond a depth of 1,569 ft bgs; and 29P, where these methods, as well as the use of cement grout, failed to prevent caving of the borehole below approximately 700 ft bgs and prevented advancing the borehole below approximately 790 ft bgs.

Well drilling, installation, and development approaches used produced monitor wells and piezometers that showed little evidence of residual drilling fluids and additives. The exceptions were 10S, 23P, 13P and 32P which required additional development work.

U-tube sampling and tracer injection lines were successfully installed at target depths in 24PB to support future single well tracer tests planned by Office of Scientific and Technical Information (OSTI). Aggressive development of the lower piezometer in 19PB, using swabbing and air-lifting, caused the collapse of this screen. This well was recompleted as part of Phase V.

9.1.1.2 Geologic and Borehole Logging

Comparisons of field estimates of the PSDs of the sand and fines fractions of drill cuttings samples (and the related USCS group symbols) differ significantly from lab measurements in Phase III and IV samples. The field estimates and classifications made should only be used as an approximation of the general alluvial lithologies and are not suitable for quantitative analyses. In contrast to Phase III and IV, field logging estimates and laboratory measurement of the PSDs in Phase V (i.e., major size fractions of gravel, sand, and fines) of both alluvium drill cuttings and core agree remarkably well; as a result, field estimates of PSDs were not censored in Phase V.

Geologic logs indicate that alluvium penetrated contains clasts solely of volcanic origin; non-alluvium was composed primarily of volcanic rocks or sediment derived from these rocks.

The observed water contents of drill cuttings from the vast majority of 2.5 ft sample intervals from the unsaturated zone were significantly decreased by the drilling process; that is, they were observed as dry. Most narrow wet peaks in water content were due to drilling fluids used to condition the borehole walls and/or from cement grouting of the surface casing. Some broader peaks of moderate and wet cuttings were observed in 22PC near the capillary fringe of the water table and where lateral flow resulted from lost circulation of liquid drilling fluids in a previously drilled Phase III borehole (22S) located nearby. Finally, drill cuttings collected from 32P from immediately below the water table (245 ft bgs) showed evidence of drying 15 ft into the saturated zone. Drill cuttings collected below the water table show evidence of drying for distances ranging from 5 to 50 ft into the saturated zone.

Little or no cementation was observed in unsaturated zone alluvial drill cuttings from boreholes in Flat Tire Flat (28P, 16P, 27P); however, more intervals of weak and moderate cementation were noted in similar samples from boreholes in Fortymile Wash (10SA, 22SA, 19IM1A, 19IM2A). The fact that little or no strong cementation was observed in unsaturated alluvial drill cuttings from all RC boreholes suggests that little soil development is present in unsaturated alluvium in both Flat Tire Flat and western lower Fortymile Wash. Cementation was not observed in drill cuttings of unsaturated alluvium in Phase V boreholes (32P, 33P). However, older and deeper saturated fluvial sediments exhibited strong cementation from 500 to 540 ft bgs in 32P. In addition, several weakly cemented thin intervals were observed in this borehole between 700 and 900 ft bgs in the same fluvial sediments. Evidence of cementation was consistently observed in saturated zone drill cuttings samples from boreholes at Sites 22 and 23.

Numerous weakly cemented zones were observed in the upper approximately 260 ft of the saturated zone in 19PB. These zones were not observed in alluvial drill cuttings collected in Phase III boreholes drilled at the same location. The differences are due to the difficulty of detecting cementation in drill cuttings samples significantly disturbed by drilling. No evidence of strong cementation was observed in sonic core samples from saturated alluvium in 19PB.

Geologic logs of sonic core in 22PC indicate some variation in cementation with depth. However, the cemented core intervals observed in 22PC did not correlate with drill cuttings intervals observed to be cemented Phase III borehole 22SA, which was located approximately 60 ft from 22PC. These differences do not indicate spatial variation in cementation between boreholes located at Site 22. Rather, as pointed out previously, these differences illustrate the difficulty in identifying degrees of cementation in drill cuttings.

Due to the difficulty in observing evidence of cementation in drill cuttings and the likely disturbing effects of drilling on cementation evidence, consideration will be given to eliminating cementation from geologic logs of alluvium drill cuttings in future EWDP Phases.

Drilling rates were generally highest in exploratory AR-RC boreholes, followed by CA boreholes, followed by larger diameter AR-RC piezometer boreholes. This trend is related to borehole diameter as well as drilling system design and operating factors. The highest drilling rates (i.e., 1 foot per minute or greater) were recorded in alluvium, clastic sedimentary rocks (e.g., siltstone or claystone), volcanoclastic sedimentary rocks, and nonwelded intervals in volcanic tuffs. The lowest drilling rates (i.e., less than 1 foot per minute) were recorded in the welded portions of most tuff units. The inverse relationship between drilling rate and degree of welding in tuffs is most clearly illustrated in 27P and 29P.

Typically, water production increased with depth, especially in zones of moderately or densely welded tuff that are presumably highly fractured. Moreover, nonwelded tuff generally appeared to slow water production to a nearly constant rate as it was penetrated. The use of bentonite mud containing polymer to condition and stabilize the walls of several of the AR-RC boreholes below the water table likely reduced water production rates in the conditioned intervals.

HCl reaction on drill cuttings shows no apparent trend with depth, nor does there appear to be a correlation between HCl reaction and observed cementation in alluvium. HCl reaction was more easily observed than cementation and the reaction for different sample intervals ranged from none to strong in Phase V boreholes. Since alluvium penetrated in Phase V boreholes does not contain carbonate rocks, HCl reaction indicates the presence of calcite, a potential cementing agent. However, because of the lack of visual evidence of cementation, it is likely that calcite does not play a significant role in cementation. A similar conclusion regarding calcite as a cementing agent was reached in Phase IV boreholes (NWRPO, 2005a).

HCl reaction was not observed in 22PC sonic core samples over the total coring interval from 460 to 763 ft bgs. Drill cuttings samples from 22SA over the same depth interval also showed no evidence of HCL reaction. These findings indicate that significant calcic horizons are not present in the capillary fringe above the water table and to depths of several hundred ft below the water table at Site 22. Moreover, the mechanism for precipitation of calcite at the water table in arid settings suggested by some workers, including Walvoord and others (2005), is not operative to a significant degree at 22PC.

Examination of a limited number of drive core samples indicates that clasts of relatively soft non-welded tuffs that are easily disturbed by drilling are present in significant percentages in gravel and various sand fractions in all depths sampled.

In 19PB, 24P, and 29P, drive core drying occurred in the downhole end of core barrels, due to heat generated at the core bit.

The colors of sonic core from 19PB and 22PC in the upper intervals of saturated alluvium penetrated indicated oxidizing conditions throughout this depth interval.

Geologic logs of alluvial core from 22PC from 460 to 763 ft bgs show that the alluvium is composed of 100% volcanic rocks. This observation is consistent with observations based on geologic logs from Phase III and IV boreholes previously drilled and logged at Site 22.

9.1.1.3 Laboratory Measurements on Geologic Samples and Drilling and Sampling Impacts

9.1.1.3.1 Laboratory Tests on Alluvial Core Samples: PSD's, Hydrometer and Atterberg Limit Data

A depth profile graph of major particle size fractions in 19PB sonic core determined by wet sieve analyses indicate that samples are coarse-grained and, on the average, contain approximately 14% fines, 46% sand, and 40% gravel. The USCS group name for the average PSD composition is a silty or clayey sand with gravel. Both hydrometer PSD and Atterberg limits data indicate that clay predominates slightly over silt in the fines fraction for most sonic core samples tested.

A depth profile graph of major particle size fractions in 22PC sonic core determined by wet sieve analyses indicate that gravel varies more than the other fraction sizes with depth. For example, the range in gravel extends from 16 to 72% and in some cases differs by more than 40 to 50% in adjacent depth intervals. This depth profile also shows a trend of slightly increasing percentages of fines and sand with depth and a corresponding decrease in percentages of gravel with depth. Summary statistics for PSD data from 22PC sonic grab core samples show that all samples are coarse-grained and, on the average, contain approximately 16% fines and approximately 40% gravel and 44% sand. The USCS group name for the average PSD composition is a silty or clayey sand with gravel.

The Atterberg limits-based classification of the fines fraction in sonic grab core samples from 22PC shows that silt (ML) predominates over clay (CL) and silty clay (CL-ML) in the upper 150 ft of the alluvial aquifer and the opposite is observed in the underlying 150 ft. The predominance of clay over silt and silty clay below approximately 625 ft bgs corresponds to the slight trend in increasing clay mentioned previously based on hydrometer test data.

The fines fraction is composed of nearly identical proportions of clay and silt in sonic grab core samples over the entire cored interval in 22PC based on hydrometer particle size analyses. There is a slight increase in fines and clay beginning at approximately at approximately 625 ft bgs and continuing to total depth at 763 ft bgs.

Little difference was observed in the average values of the major size fractions between 22PC sonic core and Phase IV 19PB sonic core. The average values for the sand and gravel fractions in 22PC are only approximately 1% lower than average values in 19PB, and the average value of the fines fraction for 22PC samples is only approximately 1.5% higher than in 19PB. Calculated averages of PSD fractions for 22PC and 19PB that are weighted by the variable lengths of the

individual sonic core sample intervals agree even more closely than unweighted averages. However, a slightly greater range in sand and gravel fractions was observed in 19PB than in 22PC. Taken together these relatively small differences in PSDs between coreholes suggests that the approximately 3 mile separation between 22PC and 19PB in the Fortymile Wash flow system does not appear to significantly impact the PSDs in the upper portion of the alluvial aquifer in lower Fortymile Wash.

Significant differences between these coreholes are however found in major particle size fractions when the weighted averages over depth intervals corresponding to sandpack and bentonite seal intervals are calculated, rather than taking the average over the entire cored interval. For example, the lower sandpack interval in 22PC averages 17.9% fines, while the lower sandpack interval in Phase IV corehole 19PB averages only 13.8% fines. If it is assumed that saturated hydraulic conductivity is inversely related to fines content as proposed by Todd (1980), the lower screen in 22PC would be expected to exhibit a lower conductivity value than the lower screen in 19PB. This hypothesis will be tested when tracer test activities are completed at 22PC.

Close agreement was found between field estimates and lab PSD measurements made on alluvium sonic core segments from 22PC. Summary statistic averages (NWRPO 2009; Table 5.3-1) for field estimates and lab measurements of major size fractions are as follows: fines content, 13% estimated versus 16% measured; gravel content, 39% estimated versus 40% measured; and sand content, 48% estimated versus 44% measured. Even closer agreement was found between field estimates and lab measurements for unsaturated alluvium drill cuttings from both 24PB and 32P (NWRPO 2009; Tables 5.3-2 and 5-3.3 respectively).

PSD data from a limited number of drive core segments from 10P, 22PA, 24P and 29P indicate that alluvial sediments consist of coarse-grained sands and gravels, with fines ranging from approximately 5 to 25% by weight. Adjacent 3-in. and 6-in. long drive core samples show a wide variation in laboratory-measured PSD, bulk density, porosity, and saturated hydraulic conductivity values. These limited data indicate that fluvial sedimentary processes created a highly layered alluvial sequence with contrasting lithologic and hydraulic properties.

9.1.1.3.2 Laboratory Tests on Drill Cuttings: PSD's, Hydrometer and Atterberg Limit Data

Laboratory-measured drill cuttings PSDs from Phase III AR-RC boreholes drilled primarily with compressed air are reasonably representative of in situ formation conditions throughout the unsaturated zone and in the uppermost part of the saturated zone. This conclusion is based on a limited comparison of laboratory PSD data from minimally disturbed drive core samples versus drill cuttings samples collected from approximately the same depth intervals in nearby boreholes at Sites 10 and 22, as well as the similarity in PSD depth profiles between boreholes at these sites and at Sites 19 and 23.

In general, unsaturated alluvial drill cuttings from Phase III and IV AR-RC boreholes yield PSD roughly approximate to those from drive core, and therefore roughly approximate to in situ conditions. In contrast, data from Phase III boreholes demonstrated that AR-RC drilling significantly disturbs the PSD of drill cuttings from saturated alluvium and that these cuttings are representative of neither drive core nor in situ conditions.

Once AR-RC boreholes begin to produce significant amounts of water at depths generally less than 100 ft below the water table, the laboratory-measured PSDs of drill cuttings deviated significantly from laboratory-measured PSDs of core samples and, by inference, the PSDs of in situ formation materials. As a result, laboratory-measured PSDs of drill cuttings beginning approximately 100 ft below the water table were censored in 10SA, 19IM1A, 19IM2A, 22SA, and 23P.

PSD depth profiles are similar for Flat Tire Flat boreholes (i.e., 16P, 27P, and 28P), which differ significantly from those of Fortymile Wash. The average fines fraction in Flat Tire Flat boreholes equals or exceeds 20% compared to 14% or less in Fortymile Wash; gravel content is generally greater in Fortymile Wash boreholes. The significant differences in PSD between Flat Tire Flat and Fortymile Wash may be due to differences in source rock and/or drainage basin size.

A comparison of PSD depth profile data for drill cuttings and drive core from 24P and 29P indicates good agreement in fines content and less agreement in sand and gravel, especially for 29P. Significantly more gravel is found in drive core than in drill cuttings from 29P, suggesting that grinding during drilling may reduce large gravel-sized particles into smaller sand-sized ones, which is consistent with findings from Phase III boreholes.

The deviations of laboratory-measured drill cuttings PSDs from core sample PSDs below the water table are most likely due to the grinding action of the rotary drill bit on relatively soft non-welded tuffs that is greatly facilitated by the production of large quantities of water at the drill bit generally beginning within the upper 100 ft of the saturated zone.

Inadequate drilling fluid velocities in the unsaturated zone portion of Phase III CA boreholes (10P, 22PA) and sample handling errors in the saturated zone portion of these boreholes caused laboratory-measured PSDs of drill cuttings samples from these boreholes to be significantly disturbed from in situ conditions.

Unsaturated zone alluvial drill cuttings from smaller-diameter AR-RC boreholes appear to be slightly less disturbed from in situ conditions than similar drill cuttings from intermediate-diameter AR-RC piezometer boreholes.

Comparison of PSDs of unsaturated alluvium from 24PB and 24P (separated by approximately 150 ft) shows that the former is noticeably coarser grained than the latter. Both boreholes were drilled using similar AR-RC methods and equipment, but by different drillers. Besides some differences in drilling related factors, differences in alluvial stratigraphy between the boreholes are likely in part responsible for the differences in measured PSDs.

A comparison of PSD profiles of unsaturated alluvium drill cuttings between Phase V boreholes 24PB and 32P, the latter located approximately 5 miles south (downgradient) of the former, shows that 32P is slightly finer in texture than the 24PB. This is not unexpected given the relative position of the boreholes in the Fortymile Wash flow system.

The excellent agreement between field estimates and laboratory measurements of PSDs for drill cuttings permit using field estimates determined for every 2.5 ft sample interval to fill in data gaps between lab measurements made on every other 2.5 ft depth interval. A comparison of

these data shows that the variations in PSDs observed in every 2.5 ft interval was at least as great as that determined by laboratory measurements on every second 2.5 ft depth interval. These drill cuttings data show that alluvial sediments contain even more textural layers than previously observed using lab data alone. Moreover, these data are consistent with the high frequency of textural layering observed in sonic coreholes 22PC and 19PB.

9.1.1.3.3 Gravimetric Water Content Data

In Phase III and Phase IV it was found that AR-RC drilling reduced the gravimetric water content of alluvium drill cuttings compared to core by as much as 0.15 g/g. Similar reductions are expected in Phase V AR-RC samples, although core was not collected to verify the magnitude of drying of drill cuttings by AR-RC and DR-CA methods.

As expected, AR-RC drilling methods produced similar water content depth profiles in Phase V boreholes with similar PSD depth profiles. These borehole pairs included 24PB and 32P, and 24PA and 24PB. Under drained pre-drilling conditions, water content profiles are expected to be similar in boreholes with similar PSD profiles. In addition, it is expected that drilling impacts on water contents would be similar for boreholes with similar PSDs.

Water contents of drill cuttings are much lower than those of drive core samples taken from adjacent depths. Assuming that drive core samples exhibit water contents that approximate in situ conditions, these data show that AR-RC drilling significantly dries the drill cuttings from in situ conditions.

Although not representative of in situ conditions, drill cuttings water content profiles are useful in identifying relative water content differences between boreholes, and depth intervals where excess drilling fluids were used to condition the borehole.

Gravimetric water contents, ECs of soil-water extracts, and PSDs of unsaturated drill cuttings appear to be disturbed from in situ conditions less by faster drilling rates than by slower drilling rates.

9.1.1.3.4 Electrical Conductivity Data

Sonic core EC data from the lower part of the unsaturated zone immediately above the present water table in 22PC shows only a single small spike or peak in EC that reaches 327 micromhos/cm at approximately 464 ft bgs. In contrast, Phase IV sonic corehole 19PB exhibits several large spikes or peaks of approximately 1,000 micromhos/cm and valleys (i.e., low values) between 200 and 400 micromhos/cm in the interval immediately above the water table. It is possible that variations in paleo-water tables may be responsible in part for these great variations in EC values in 19PB. Numerous other factors including paleo-soils and paleo-recharge events may also play some role in the development and maintenance of these EC peaks and valleys in 19PB.

Regarding paleo-recharge events, wetting fronts may have reached the water table more frequently at 22PC located further upstream and less frequently at the downstream location in 19PB. This could result in flushing of salts from the unsaturated zone more often in 22PC compared to 19PB. Alternatively, the fact that 22PC is presently located on a terrace

approximately 800 ft from the incised main Fortymile Wash channel may preclude wetting fronts from impacting the subsurface at 22PC. In contrast 19PB is presently located on the edge of the braided channel network in lower Fortymile Wash that periodically transmits flows that result in infiltration/percolation wetting fronts, where the spikes in EC may correspond to the terminus of these different wetting fronts.

A comparison of EC depth profiles for 24PB and Phase IV 24P shows significant differences even though they are separated by only approximately 150 ft. This observation is consistent with the differences in alluvial stratigraphy shown in PSD depth profiles mentioned previously.

The relatively close agreement in EC depth profiles between 24PB and 32P, with the latter located approximately 5 miles downgradient in lower Fortymile Wash, may in part be related to similar PSD depth profiles described above.

- The magnitude of EC peaks in 13P depth profiles exceeds all peaks in other Phase V boreholes. The high values of EC in 13P are likely related to the basalt flow present from approximately 85 to 140 ft bgs and basalt weathering products, including clay minerals.

EC depth profiles for all AR-RC boreholes show peaks in EC values in the upper 15 ft of each borehole, indicating salt accumulation in the near surface. However, at depths below the near-surface peaks, the EC profiles differ noticeably between Fortymile Wash and Flat Tire Flat boreholes. These differences in EC profiles may be in part due to differences in source rock and the size of the drainage basins.

Close agreement is observed in EC depth profiles of unsaturated alluvium between: 22PC and Phase III 22SA located approximately 60 ft apart, and in the upper 150 ft of 24PA and 24PB located 37 ft apart.

19PB sonic core sample EC data from the lower part of the unsaturated zone immediately above the present water table shows several EC peaks and valleys. It is possible that paleo-water tables may be in part responsible for these variations in EC values.

The magnitude and the number of narrow, well-defined peaks in the EC of soil-water extracts of drill cuttings from boreholes located along the primary axis of Fortymile Wash appear to decrease in the upstream direction. This may be related to increases in the duration of ephemeral surface water flows and associated increases in downward infiltration and percolation flux in the upstream direction.

9.1.1.3.5 Dry Bulk Density and Porosity Tests on Core Runs

Field measurements were made to determine the mass and volume of each sonic and drive core run. These measurements, together with laboratory measurements of gravimetric water content, were used to determine the dry bulk density of each core run based on depth-weighted averages of core segment lengths making up each core run.

Dry bulk density values calculated for drive-core runs in 24P (e.g., 1.92 g/cm³) and 29P (e.g., 1.97 g/cm³) are slightly greater than for those in 19PB (e.g., 1.81 g/cm³), which may be due to

the method of advancing the core barrel and/or the fact that core runs in 24P and 29P were in unsaturated alluvium and those in 19PB in saturated alluvium.

The average 19PB dry bulk density values calculated for 5 drive core runs agrees closely with the average dry bulk density values calculated for 22 sonic core runs (i.e., both 1.81 g/cm^3). This agreement may be coincidental, since there are numerous sources of error in both types of measurements.

Saturated hydraulic conductivity measurements on core samples correlate inversely with percent fines data and are significantly lower in magnitude than values calculated from much larger scale aquifer test measurements. Both of these trends are consistent with the findings of other workers.

Repacking of 15 representative sonic core segments in 12-inch-long by 6-inch-diameter PVC tubes at air-dried water contents produced core samples with an average dry bulk density value of 1.72 g/cm^3 and an average porosity value of 0.33. Repacking 7 of the original 15 representative sonic core segments at optimum water contents produced core samples with an average dry bulk density value of 1.90 g/cm^3 and an average porosity value of 0.25. Drive core and geophysical logging data indicate that an average dry bulk density value of 1.90 g/cm^3 and an average porosity value of 0.25 are more representative of in situ conditions than values of 1.72 g/cm^3 and 0.33, respectively.

Evidence was found for a linear correlation between the natural logarithm of Ksat and percentage of fines in drive core samples from 24P. Similar trends of decreasing Ksat with increasing fines percentages have been found in numerous other studies for a variety of sediments (Todd, 1980). The smaller sample population size for drive core samples from 29P and 19PB may in part be responsible for this lack of linear correlation in samples from these boreholes. The arithmetic and geometric mean values of Ksat differ in 24P, suggesting that these values are log-normally distributed.

Linear correlations between the natural logarithm of Ksat and percentage of fines were found for sonic core segments repacked at air-dried and optimum water contents. As expected, the geometric and arithmetic mean Ksat values for sonic core samples repacked at optimum water contents are significantly lower than those of the same core material repacked at air-dried water contents. Also as expected, mean Ksat values for sonic core samples repacked at optimum water contents were significantly higher than those for drive core samples. Numerous workers have found that, on the average, the smaller the volume of the sample being tested, the lower the resulting Ksat value. Presumably, smaller samples are expected to contain fewer porosity-related heterogeneities and preferential flowpaths.

Sonic core collected with the smaller diameter core barrel (i.e., 4.5-inch-OD) yields dry bulk density values that are slightly higher on the average (1.71 g/cm^3 vs. 1.66 g/cm^3) than those on core collected with the larger diameter core barrel (i.e., 6.16-inch-OD). No other trends with depth are apparent. These average density values translate into average porosity values of 0.32 and 0.34 using an average laboratory determined particle density of 2.53 g/cm^3 .

These slightly differing bulk density and porosity values may be due in part to the greater difficulty in determining the amount of lost core when using the smaller diameter core barrel.

Other possible sources of error in these bulk density calculations include the estimated corehole diameter as well as the measured gravimetric water content. Regarding the latter, it was recognized during analysis of density data from Phase IV corehole 19PB that significant evaporative loss of water occurred during sample handling and logging in the field. As a result steps were taken to minimize this water loss when logging and handling 22PC sonic core. The average calculated gravimetric water content for 19PB core segments was approximately 0.13, whereas the average value for 22PC core segments was 0.17. This difference of 0.04 in average water content translates into a difference of 0.04 or more in dry bulk density. Evaporative losses from 19PB core samples in the field may in part be responsible for the higher average dry bulk densities (1.80 to 1.82 g/cm³) calculated for 19PB core runs.

9.1.1.3.6 Field Saturated Hydraulic Conductivity Tests at Site 19

Constant head injection tests conducted in 19PB produced Ksat values more than 10 times lower for the shallow piezometer screen than for the deep one. This difference was not expected and may be related to the preferential accumulation of fines or smearing of fines on corehole walls of the shallow piezometer by a yet-to-be-defined mechanism. An attempt to remove fines from the corehole walls in the vicinity of the piezometer screens by aggressively swabbing and air lifting damaged the blank casing of the deep piezometer in the vicinity of the upper piezometer screen and created direct hydraulic communication between piezometers.

Comparing average Ksat values from constant head tests in 19PB with values from both smaller scale laboratory tests on core samples and a larger scale constant-rate 48-hour pump test in an immediately adjacent borehole suggests a direct relationship between measurement scale and Ksat value. However, the differences between drive core and field Ksat measurements are likely in part due to the orientation of the measurement (i.e., vertical versus horizontal) rather than due simply to scale.

9.1.1.4 Trends in Lithostratigraphy

9.1.1.4.1 *Summary Lithology Logs – Phase III*

Depth profiles of laboratory-measured PSDs in drill cuttings from Phase III boreholes located along the primary axis of Fortymile Wash (19IM2A, 22SA, and 10SA) are nearly identical throughout the unsaturated zone and the upper approximately 100 ft of the saturated zone.

In all boreholes along the primary axis of Fortymile Wash, the alluvial section becomes slightly finer-textured with depth, transitioning from a well-graded sand with silt and gravel (SW-SM) to a silty sand with gravel (SM) at depths ranging from approximately 300 to 450 ft bgs. The slightly finer-textured underlying SM alluvial unit extends down to various underlying volcanic rocks with contacts ranging from approximately 800 to 1,100 ft bgs. The texture classification for the lower part of this SM unit was extrapolated from laboratory-measured PSDs from drill cuttings and core samples from the upper portion of the unit. PSD data from drill cuttings from the lower part of this unit were highly disturbed from in situ conditions by drilling.

Discontinuities in the alluvial and underlying bedrock sections between 19IM2A and Phase II borehole 2DB, located approximately 1 mile to the southwest, may be related to the presence of the Highway 95 Fault located between these boreholes.

A cross section perpendicular to the primary axis of Fortymile Wash through Phase III boreholes 22SA and 23P, and Phase I borehole 5S shows the presence of finer-grained alluvial sediments along the eastern portion of the wash. These finer-grained sediments may limit the eastward migration of possible future contaminants from Yucca Mountain and focus their transport in coarser-grained sediments along the central portion of Fortymile Wash.

9.1.1.4.2 Summary Lithology Logs – Phase IV

Borehole 27P

27P penetrated the Miocene volcanic section from the base of the Rainier Mesa Tuff to the Bullfrog Tuff. The water table occurs within the upper lithophysal zone of the Topopah Spring Tuff.

Borehole 16P

16P penetrated the Miocene volcanic section from the bottom of the Ammonia Tanks Tuff through the top of the Tram Tuff. Every major tuff interval is represented. The water table occurs within the Rainier Mesa Tuff. The thickness of the volcanic aquifer, although not fully penetrated, likely approaches 2,500 to 3,000 ft from the top of the water table to the top of the Pre-Tram sedimentary rocks.

Borehole 28P

28P penetrated the upper portion of the Miocene volcanic section from the Ammonia Tanks through the Topopah Spring Tuff. Below the Topopah Spring Tuff, at 1,145 ft bgs, an unconformity with Pre-Tram sedimentary rocks was discovered. The water table occurs near the base of the Ammonia Tanks Tuff. The approximately 1,000 foot thickness of the volcanic aquifer in 28P is greatly diminished in comparison to 16P to the north.

Borehole 24P

24P penetrated the lower portion of the Miocene volcanic section from the Bullfrog Tuff to the Pre-Lithic Ridge sedimentary rocks (i.e., claystone, siltstone, and sandstone). The water table occurs near the contact of the alluvium and underlying Bullfrog Tuff.

Borehole 29P

29P penetrated a relatively thin section of Paintbrush Group from the base of the Tiva Canyon Tuff through a relatively thin section of Topopah Spring and Pre-Topopah Spring Tuffs, before termination at 790 ft bgs due to flowing sands. The water table occurs within the Tiva Canyon Tuff.

Corehole 19PB

19PB penetrated the upper 260 ft of the saturated alluvial aquifer. The upper 130 ft of the saturated zone portion of the aquifer are composed primarily of numerous relatively thin alternating intervals of gravels with clay and clayey gravels that contain generally less than 12%

finer. Below 500 ft, relatively thick intervals of clayey sands predominate, and are divided primarily by thinner intervals of clayey gravels and contain generally 12% or more fines. This division into two major USCS groups suggests that the upper saturated zone in 19PB could be divided into two hydrogeologic units expected to exhibit very different average Ksat values based on laboratory tests.

9.1.1.4.3 Summary Lithology Log – Phase V

Borehole 13P

Borehole 13P penetrated thin alluvium underlain by Pliocene basalt and older alluvium to a depth of 202 ft. The remainder of the borehole penetrated post-volcanic valley-fill units consisting of an upper section of reworked younger volcanic sediments and a lower section of primarily fan deposited sediments. The borehole was terminated at 1,569 ft in possible welded units of the Bullfrog Tuff.

Boreholes 24PA and 24PB

Borehole 24PB intersected a nearly identical sequence of subsurface geological units as 24P. The alluvium-bedrock contact and groundwater was encountered at approximately 405 ft bgs, followed by Bullfrog Tuff, pre-Bullfrog sedimentary rocks, and Tram Tuff. The borehole was terminated in Pre-Tram sedimentary rocks at 1,395 ft bgs. Volcanic units younger than Bullfrog were either eroded away or not deposited at this location.

Borehole 32P

Borehole 32P penetrated alluvial units from surface to 396 ft bgs, consisting of well-graded sand with silt and gravel (SW-SM). The water table was encountered at approximately 260 ft bgs, with the static water level rising to approximately 245 ft bgs. Between a depth of 396 and 496 ft bgs a basaltic lava flow was encountered. The basalt is underlain by a conglomeratic sandstone unit with mixed clast lithologies that fine downward into unconsolidated fluvial sediments from 550 to 940 ft bgs. The unconsolidated sediments are underlain by pre-Tram lacustrine siltstone beds from 940 to 1,000 (TD) ft bgs.

Borehole 33P

Borehole 33P was drilled by DOE contractors as one of several boreholes drilled in the Yucca Mountain area for analysis of volcanic hazards. Geologic data provided by the DOE indicates that the subsurface geologic units consist of 195 ft of alluvium overlying Tertiary conglomeratic sediments from 195 to 535 ft bgs. The borehole terminated in a Tertiary volcanic unit consisting of non-welded, bedded, and reworked tuff extending from 535 to at least 657.1 ft bgs. Overall, below the alluvium, the sequence at 33P appears to represent a post-volcanic Miocene section not seen at 32P.

Corehole 22PC

22PC penetrated the lowermost unsaturated and upper saturated zone alluvial sediments from 460 to 763 ft bgs. The summary log shows that gravel units predominate in the upper

approximate 170 ft (460 to 632.1 ft bgs), and sand units in lower approximate 130 ft (632.1 to 763.0 ft bgs). The cored mainly gravelly units above 632.1 ft bgs generally contain less than or equal to 12% fines, and below 632.1 ft bgs the mainly sandy units generally contain greater than 12% fines.

Sonic corehole 19PB, located approximately 3 miles downstream from 22PC in the Fortymile Wash flow system, shows similar trends in gravel and sand units (NWRPO, 2009) as described above for 22PC.

9.1.1.5 Borehole Geophysical Logging

Borehole geophysical logs were used for lithologic characterization and stratigraphic correlations. For the most part, only qualitative interpretations of rock properties were made from the logs.

In Tertiary volcanic units, formation resistivity logs are useful for identifying the degree of welding within ash-flow tuffs, and therefore useful for stratigraphic correlation. Higher resistivity values correlate well with welded rocks identified in the geological cuttings described at the site and low resistivity values correlate with nonwelded rocks. In some boreholes, fluid resistivity and fluid temperature logs could be used to identify discrete intervals where groundwater flows into the wellbore. Optical televiewer logs, though not always of usable quality, show that, in some places, these discrete flow zones are open fractures. Discrete inflow zones were identified in 16P and 27P.

In alluvial units, valleys in natural gamma logs and peaks in density and neutron porosity logs can correspond to clean well-graded sand and/or gravel that produces clean water. These sand and/or gravel units can serve as preferential flow paths. Increasing amounts of clay in formation materials often correlate with increasing natural gamma counts, decreasing formation resistivity log values, decreasing density values, and decreasing neutron porosity log counts (increasing water filled porosity). In some cases increasing amounts clay correlate with all of the above, except increasing natural gamma counts. In these cases, natural gamma counts may decrease (rather than increase) as a result of a decrease in the concentration of gamma emitters with depth in the formation rock. In nearly every Phase V borehole, large peaks in caliper logs resulted from washout zones with corresponding decreases in natural gamma, density, and neutron porosity log values.

In most Phase V boreholes, fluid resistivity, fluid temperature, and caliper logs could be used to identify discrete intervals where groundwater flows into or out of the wellbore. In several cases, formation resistivity, density, and neutron porosity logs supported identification of water movement into/out of the borehole. Optical televiewer logs, though not always of usable quality, show that, in some places, these discrete flow zones are open fractures. Discrete inflow zones were identified in 32P.

In conglomeratic arkosic sandstone valley-fill units, logs show increases in natural gamma, density, and neutron porosity log values.

In basalt flows, logs exhibit lower natural gamma counts and higher density values than alluvium. These correlations permitted identifying the lower basalt/alluvium contact in borehole 13P where drill cuttings were not returned to the ground surface.

In the uppermost alluvial unit in boreholes located in Fortymile Wash, there is generally a slight increase in natural gamma counts and a slight decrease in density values with depth. This reflects a slight increase in finer textured fractions with depth. At greater depths in Fortymile Wash alluvium natural gamma, density, and neutron porosity logs generally show gradual increases with depth in response to increasing amounts of fines, overburden pressure/compaction, and possibly grading.

9.1.1.5.1 Gravity and Magnetic Features – Phase IV

Previous surface-based gravity and aeromagnetic studies identified the following linear features that were helpful in locating boreholes and interpreting drilling results. A large east-west-trending magnetic gradient coincides roughly with the path of Stagecoach Road as it passes from Fortymile Wash, across Flat Tire Flat, and into Crater Flat. Borehole 27P was drilled on the south side of this feature and future plans include drilling borehole 26P on the north side of this feature. A large gravity gradient trends northeast from west of the Lathrop Wells Cone to south of Busted Butte on the western boundary of the NTS and runs between 27P and 16P. This gravity feature played a role in locating 28P, 16P, and 27P. A northeast-trending magnetic feature between 28P and 16P helped to locate these boreholes. Drilling data indicate that this feature likely results from a buried fault.

These linear geophysical gradients, whether they represent a fault or some other type of steep contact between the basin fill and Paleozoic rocks, could have significant control on groundwater flowpaths in this area south of Yucca Mountain.

9.1.1.6 Geologic Interpretations from Drilling and Geophysical Data Phase IV

Three cross sections were constructed to help interpret the stratigraphy penetrated by Phase IV boreholes. The cross sections were based on drilling data and geophysical information. The cross sections differ significantly from recent USGS map interpretations.

Cenozoic deposits thicken across an interpreted growth fault between 28P and 16P. Displacement on the fault likely involves rocks as young as those of the Crater Flat and Paintbrush Groups, but probably older than Tiva Canyon Tuff. The age of the interpreted faulting between 28P and 16P is pre-Basin and Range. The stratigraphic offset across the fault is, conservatively, approximately 1,500 ft. The maximum extent of the offset may be larger; however, the stratigraphy and/or ages of the older rocks penetrated in the footwall block have not been determined.

Boreholes 24P, 28P and 29P are located on a structurally high block where Paleozoic rocks are relatively shallow. Pre-Crater Flat Group stratigraphic units are interpreted to thicken markedly into the Crater Flat structural basin under 16P and 27P.

The Highway 95 Fault is interpreted to mark the southern depositional boundary of the Tertiary volcanic aquifers as characterized within Yucca Mountain. Juxtaposition of volcanic aquifers

north of the fault against less permeable Pre-Tram fine-grained sedimentary rocks on the south side of the fault probably forces southward groundwater flow up into the alluvial aquifer system in lower Fortymile Wash and into Amargosa Valley.

9.1.1.7 Geologic Interpretations from Drilling and Geophysical Data Phase V

New drilling data, deep-penetrating resistivity survey data, and gravity data were used to construct two geologic cross sections (Figures 2.4-2 and 2.4-3). These new cross sections replace conceptual cross sections presented in the Phase IV Drilling Report (NWRPO, 2005a).

New interpretations provide different interpretations of the two largest features in the flow system south of Yucca Mountain, namely the Crater Flat-Jackass Flat Basin Structure (CJS) and Highway 95 Fault. There is evidence that both the CJS and Highway 95 Fault impact or possibly control groundwater movement in the area, including upward hydraulic gradients observed in wells in close proximity to the Highway 95 Fault.

The Highway 95 Fault location and strike is significantly different than in previous publications. The Highway 95 Fault has two sub-parallel strands, an older master fault to the south, and a slightly younger sympathetic hanging wall fault to the north. The fault is offset southwestward (approximately 3 km) along the CJS and reappears to the southwest of the Lathrop Wells Cone near well 3D, and continues with a similar west-northwest strike to terminate against the Bare Mountain Fault. The timing of displacement along the western portion of the Highway 95 Fault is different than the eastern portion.

At sites 1, 7 and 9, the alternative conceptual model proposes that deep-seated faulting has breached the lowermost (and higher head) aquifers, and provided natural “piezometers” to the lower carbonate heads. This structurally controlled lower carbonate-sourced higher-head water discharges in the near subsurface environment (as leakance between normally isolated flow systems) above the regional (primarily volcanic) aquifer system, probably over very limited geographic extents at locations where deep-seated structures provide open pathways. These zones of upward leakance are now recognized along both the eastern and western strands of the buried Highway 95 Fault, and possibly along other similar structures.

9.1.2 Recommendations

9.1.2.1 Phase III

- As a result of drilling-related disturbances to drill cuttings in Phase III RC boreholes (and possibly in CA boreholes), the collection of saturated alluvium geologic samples in future EWDP boreholes should be modified as follows: Drive-core samples should be collected at regular depth intervals (e.g., 20 to 40 ft) beginning approximately 100 ft below the water table. This will ensure the production of geologic samples from saturated alluvium with flow-and-transport-related parameters that are (to the extent possible) representative of in situ conditions.
- The possibility that the PSDs of drill cuttings collected below the water table in Phase I and II RC boreholes were also significantly disturbed should be considered. For example, the analysis and interpretation of laboratory tests of flow-and-transport-related

parameters conducted by the NWRPO and DOE contractors on drill cuttings samples from 19D should take into account the possibility that these samples contain elevated percentages of fines and reduced amounts of gravel compared to in situ conditions.

- To facilitate field and laboratory measurements, and to ensure core samples are as representative of in situ conditions as possible, core samples should be driven a sufficient distance to completely fill and tightly pack each core barrel. Core samples collected in this manner are more likely to approximate in situ conditions than core samples collected from partially full core barrels.
- To obtain a realistic small-scale picture of layering in alluvial sediments and the variability in hydraulic parameters measured on these layers, a number of adjacent core segments from each 2.0- to 2.5-ft core run must be subjected to laboratory tests.
- To facilitate developing future FM monitor wells, more aggressive double swab and pumping development methods, rather than single swab methods, should be used.
- To support bulk density calculations from drilling-related data in the unsaturated zone in future EWDP phases, drill cuttings should be collected and weighed both during drilling and hole cleaning operations to ensure the total drill cuttings sample from each drilled interval is available for total weight and water content measurements.

9.1.2.2 Phase IV

- The recommendations in this section focus primarily on future drilling, sampling, and well construction activities.
- It is recommended that air-percussion hammer reverse circulation (APH-RC) methods not be used to drill unconsolidated sediments in future small-diameter exploratory RC boreholes, as problems with plugging of various airways and hole conditioning will likely be encountered.
- Collecting drive core from unsaturated alluvium in uncased RC boreholes is not recommended. It is very difficult, if not impossible, to completely remove fill material from the borehole before coring, which results in collecting a significant amount of fill together with in situ formation material in the core barrel.
- It is recommended that the realistic Phase IV sonic core density data be used to help assign accurate depths to future sonic core that has expanded during coring.
- To avoid preferentially sampling the fines-rich outer surface or the fines-poor center of sonic core when collecting the grab samples in the field, it is recommended to split the core horizontally in half or collect pie-shaped samples with their apex terminating in the center of the core.
- To minimize the effects of caving during well-completion activities in sonic coreholes, it is recommended that the drill casing be pulled back and completion material emplaced in short intervals (i.e., 20 to 40 ft), rather than longer ones.

- To facilitate more aggressive development of small-diameter piezometer strings, the use of stainless steel blank casing and screen rather than PVC is recommended.
- It is recommended that another exploratory borehole be drilled at the location of 29P, using casing-advance methods to penetrate and seal off flowing sands between approximately 700 and 790 ft bgs. Penetrating and characterizing the stratigraphy beneath the Paintbrush Group will help assess the structural orientation and possible erosional level of the footwall block in the area of 29P and 24P.
- It is recommended that the optical televiewer or another borehole imaging tool be included in conjunction with temperature and fluid resistivity logs to help identify fracture flow zones.
- Modeling approaches that capture the variability of Ksat and PSD parameters in the highly layered alluvial sediments described in this study should be considered in addition to approaches that rely on average parameter values for thick intervals.
- Finally, it is recommended that additional drilling and coring investigations be conducted in Fortymile Wash alluvium in conjunction with crosshole tracer tests to better characterize the continuity or extent of coarse-grained textural layers with high Ksat values that could potentially act as preferential pathways for water and solutes.

9.1.2.3 Phase V

- Do not use the DR-CA Symmetrix™ drilling system in future EWDP boreholes until the system is proven to be more robust.
- If conventional DR-CA systems are used in future EWDP boreholes, use a dust control system to capture dust and allow it to be sampled. In addition, use large enough air compressors to efficiently move drill cuttings to the surface.
- Evaluate the pros and cons of using 1.25-inch pipe in future EWDP boreholes requiring multiple-string nested piezometers in ≤ 6.5 -inch diameter boreholes.
- Eliminate the recording of density related weights in alluvium geologic logging forms for drill cuttings.
- Continue recording field estimates of major particle size fractions in alluvium drill cuttings logging forms. These data are proving very useful in characterizing the textural layering in the alluvium downgradient from Yucca Mountain.
- Continue running natural gamma, caliper, formation resistivity, density, neutron porosity, sonic, fluid temperature, and fluid resistivity geophysical logs.
-

9.2 Regional Geologic Characterization Major Findings and Recommendations

Locally, fracturing and brecciation along the LVVSZ provide significant pathways for groundwater flow. Structures related to faulting, folding, and other deformation within southern Nevada strongly influence groundwater flow and contaminant transport between basins and among bedrock aquifers. Faulting and strong brittle deformation in carbonate rocks along the restraining bend of the LVVSZ between Mercury and Lathrop Wells coupled with subsequent strike-slip faulting along the Rock Valley that transects the restraining bend have created an unusually porous and permeable body of rock that may contribute importantly to the transmission of groundwater from Yucca and Frenchman Flats via the Mount Shader Basin to Amargosa Valley.

On the basis of Nye County field work and map analyses it is concluded that:

- The LVVSZ bends west near Mercury and is thereby linked to the Highway 95 Fault by means of a left (restraining) step between Mercury and Lathrop Wells.
- Right-lateral displacement along this segment of the LVVSZ, possibly tens of kilometers, occurred between about 16 and 10 Ma; and was accommodated by transpression marked by rocks that record contractional structures within a wide zone extending tens of kilometers north and south of the of the principal fault trace.
- Eruption of the volcanic rocks that form Yucca Mountain and the subsequent development of calderas composing the Southwest Nevada Volcanic Field occurred contemporaneously with transpression along the LVVSZ to the east.
- These eruptions occurred within a releasing bend of the LVVSZ, west of, but adjacent to, the constraining step, when magma pushed through thinned crust between 16 and 10 Ma.
- The Highway 95 Fault is part of a regional structure that was probably active during Early Miocene and possibly before.
- The segment of the fault between Lathrop Wells and Bare Mountain, that forms the southern margin of the Yucca Mountain pull-apart basin, was active between about 16 and 10 Ma.

9.3 Water Level Monitoring Major Findings and Recommendations

Throughout the period FY02 - FY06, Nye County continued implementation of its water level monitoring program in an effort to refine the depth-to-water distribution. To date, the monitoring and associated evaluations have provided better definition of the groundwater conditions and have helped to answer questions regarding the directions and rates of groundwater flow, spatial and temporal variations in water levels in the region, the impacts of existing and future groundwater withdrawals, the significance of the contour interval selected in the preparation of potentiometric maps, and the use of composite hydrographs (available in the Nye County regional water level database) to better understand long-term water level trends in areas of insufficient data. The basic data collected by Nye County, and the associated data analyses and evaluations, have led to a better understanding of the hydrogeologic conditions at both the regional and local scales.

Based upon the results of these groundwater mound decay simulations, it was concluded that the current regional and site-scale models of Yucca Mountain would more accurately simulate the flow regime if the models simulated past-climate conditions that existed during the late Pleistocene. Further, it was concluded that the existing Yucca Mountain models tend to overestimate groundwater travel times and under estimate groundwater fluxes.

Results are shown from re-contouring of potentiometric maps in the Pahrump Valley using the hand-drawn adjustment approach for computer generated 300 ft and 25 ft contour intervals, respectively. The 25 ft contour interval map clearly provides better definition of drawdown in the vicinity of pumping centers associated with municipal water supplies in the Pahrump Valley (Figure 4.5-3). The comparison of the maps demonstrates that flow directions and gradients can be accurately represented only with local water level data and a contour interval that is small enough to allow the identification of localized pumping centers. The DVRGFS regional potentiometric map has too large of a contour interval to accurately portray the extreme variability in the configuration of the water table in developed areas with numerous pumping wells.

Preliminary depth to groundwater maps prepared by the Nye County Natural Resources Office for southern Amargosa Desert found that the areas of shallow groundwater (less than ten ft) were far larger than the areas evaluated in the USGS estimates. Further evaluations found that the published estimates did not fully account for evaporative losses from bare soil, especially in areas where the depth to groundwater is less than ten ft below land surface. Significant discrepancies were also identified between the methods used by the USGS studies in the Yucca Mountain region with other published evapotranspiration studies in Nevada, particularly with respect to how the satellite imagery was classified, and the treatment of losses from bare soils. A formal evaluation of the USGS methods and results in determining evapotranspiration and discharge in the Amargosa Desert will be presented in a Nye County Natural Resources Office report scheduled to be completed in the future.

9.4 Water Chemistry

9.4.1 Major Findings

- The Nye County EWDP has had tremendous success in providing DOE, NRC, and the public with a source of high quality groundwater chemistry and flow information.
- Tertiary diagrams that have been updated with major ion data from EWDP wells constructed and sampled from 1994 through April 2007 continue to support the concepts of Winograd and Thordarson (1975) groundwater flow in the Amargosa Desert region.
- The use of multivariate methods of statistical analyses of groundwater chemistry coupled with simple contour plots of major ions and isotopes in groundwater provide further understanding of ground water flow and evolution in the Amargosa Desert region.
- These analyses of major ion and isotope data in groundwater indicate that Fortymile Wash has been a high source of localized recharge over the past 10,000+ years.

- Flow separation modeling indicates that NO_3^- will not always be present in micro environments on the waste packages. In these cases localized corrosion could initiate and/or propagate. Prior to the NWRPO work, NO_3^- was assumed to be universally present in aqueous solutions.
- Following the publication of NWRPO (2003c), Nye County recommended that flow separation be included into DOE performance assessment calculations. As a result, this process has been incorporated into DOE's TSPA Model and represents an example of the Nye County ISIP contributing to improved safety.

9.4.2 Recommendations

- Continue to fill data gaps in the NWRPO groundwater chemistry database by sampling and analyzing newly constructed EWDP wells.
- Continue to update multivariate statistical analyses of groundwater chemistry data with newly acquired major ion data from new EWDP wells.
- Design and emplace a series of low cost samplers to measure the water chemistry of water infiltrating along Arroyos subsequent to runoff generating storms.
- Estimate the effects of more realistic simplifying assumptions concerning movement of moisture through the Engineered Barrier System on release rate and dose at the accessible environment.

9.5 Aquifer Testing

9.5.1 Major Findings

Results from aquifer testing indicate that with computer-assisted aquifer test analysis programs and additional analysis methods developed on an as-needed basis, it was possible to account for variable flow rates, multiple layers, flow barriers, changing wellbore storage, and many other factors not addressed by common analysis techniques. Accurate high frequency data are required to utilize computer-assisted analysis tools.

Comprehensive testing as implemented at well 22S incorporated the use of pressure/temperature probes, spinner logs, constant-rate pump tests, and individual isolated zone pumping tests; and provided high-quality data for hydraulic property analysis. Alluvial test zones at Site 22 exhibit transmissivity and hydraulic conductivity values that are 2 to 5 times larger than zones at Site 19 located approximately 3 miles downstream from Site 22.

These differences in aquifer properties may be a result of the different location of the sites in the Fortymile Wash flow system. Comparable alluvial test zones in closely spaced wells 19IM1 and 19IM2 exhibit significant and consistent differences (i.e.; differ at least by a factor of 2) in transmissivity and hydraulic conductivity.

Vertical-flow barriers confirmed by head differences exist between the ash flow tuff (Zone 5) and the uphole alluvium in wells 19IM1 and 19IM2.

Nearly equivalent water levels in all zones in 22S isolated by Westbay® packers indicate good vertical communication exists between Tertiary volcanic conglomerate and the uphole alluvium. Similarly, good vertical communication was also observed between Tertiary volcanic conglomerate and uphole alluvium in 10S despite the presence of drilling mud in the conglomerate zone.

The magnitude of storativity values suggests that most zones are confined or semi-confined.

Since the aquifer compressibility is not known, it is not feasible to compute the effective porosity.

9.5.2 Recommendations

- Construct and test additional wells and conduct additional surface geophysical surveys between Yucca Mountain and potentially affected areas of Nye County to fill gaps in data about these complex geologic and hydrologic systems.
- In addition to providing adequate spatial coverage, locate wells (where possible) to characterize aquifer properties within compartments and boundaries between compartments, such as the vertical barriers observed between the alluvium and volcanic tuffs at Site 19.
- Continue to conduct aquifer tests (on the largest scale possible) to better define aquifer properties within compartments and, if possible, incorporate cross-well tracer testing during the aquifer test.

9.6 Tracer Testing

9.6.1 Major Findings

The results from tracer testing at sites 22 and 19 indicate that the aquifer was in an oxidizing state and that little to no diffusion occurs into stagnant layers.

At site 22, a fast pathway, best modeled as a low effective-porosity system, exists in Zone 2 between 22PA and 22S. The natural gradient is best modeled (as determined during sensitivity analysis) with a north-to-south azimuth and a magnitude of approximately 0.00014 ft/ft (value published in BSC, 2004).

Tracer testing indicates that microspheres and lithium tracers displayed complex behavior with rapid breakthroughs along with rapid initial declines, then very slow declines. Single-well push/pull tests provide near-wellbore hydraulic information, but cannot replace cross-hole tests for aquifer characterization. Cross-hole tracer testing using multiple wells provides a better estimation of distributed hydraulic parameters than single-well testing due to the greater amount of aquifer tested. Use of tracers with diffusion coefficients less than two orders of magnitude different in the alluvium during forced-gradient cross-hole tracer testing leads to ambiguous results and is not cost-effective.

9.6.2 Recommendations

- Confirm the magnitude and azimuth of the natural gradient by conducting a natural-gradient tracer test.
- Consider effects of pumping interruptions during tracer tails for future tracer testing.
- Incorporate numerical modeling into analyses of multiple-well cross-hole tracer tests.
- Incorporate numerical modeling sensitivity analyses during the design of future tracer tests.
- Revised distributions of both effective porosity and longitudinal dispersivity for the alluvial aquifer system should be considered for the Site Scale Flow Model based upon the model calibration results discussed in this report.

9.7 Ventilation Studies

9.7.1 Major Findings

The main conclusion of Nye County's ventilation studies is that the convective heat and moisture transport have a major influence upon the temperature and humidity conditions and resulting condensation in and around the drifts both during the pre- and post-closure time periods. Consequently, any thermal-hydrologic model that is designed to predict the likely operating environment at Yucca Mountain with a reasonable degree of certainty must have the capability to incorporate the heat and mass transport represented by laminar or turbulent air flow during both pre- and post-closure operation.

This finding is opposite to what has been used as a working hypothesis in the Multi-Scale Thermal Hydrologic (MSTH) modeling concept, applied to the YMP for analysis and design. According to the MSTH model results, the axial flow of heat and moisture is insignificant and has no impact on the thermal-hydrologic storage environment. The effects of this contention may be far-reaching.

The presence of axial transport is expected to affect the operating environment during the first few thousand years. The higher the temperature regime, the larger the expected impact and the uncertainty created by the absence of axial transport in DOE's process models. On the other hand, at below-boiling operating temperature, the axial transport is indeed insignificant, reducing modeling complexity and uncertainty, along with other factors,

Long-term ventilation is seen as a viable technology for reducing operating temperature even if the storage capacity is increased at the same time, relative to the waste load density in the baseline design.

9.7.2 Recommendations

MULTIFLUX has grown into a fully capable numerical model that has been proven to solve the coupled in-drift and in-rock transport processes with full drift simulations and turbulent flows during both pre- and post-closure operations.

Such modeling capability will be needed for explaining performance confirmation measurements at Yucca Mountain from the onset of operations. Nye County has a vested interest in monitoring the relevant processes at play at Yucca Mountain that includes air discharges into the accessible environment. Through the coupled in-rock and in-air transport processes, the exhaust air parameters from the emplacement drifts and the air shafts have an important and intricate confirmatory value to understanding the entire thermal-hydrologic-air process evolution at Yucca Mountain.

10.0 REFERENCES

- Abolins, M.J. 1999. *The Kwichup Spring Thrust in the Northwestern Spring Mountains, Nevada: Implications for Large-Magnitude Extension and the Structure of the Cordilleran Thrust Belt*. Pasadena, California: California Institute of Technology. 143 p.
- ASTM (American Society for Testing and Materials). 1993. ASTM D-2488-93. Standard Practice for the Description and Identification of Soils (Visual-Manual Procedure). Philadelphia, Pennsylvania: American Society for Testing Materials. Readily available.
- Axen, G.J., 2007, Research focus; significance of large-displacement, low-angle normal faults: *Geology* (Boulder), v. 35, no. 3, pp. 287-288.
- Bahrami, D. and G. Danko. 2006. *Thermal-Hydrologic Model of an Alternative Waste Package Design for Yucca Mountain Repository*. *Journal of Nuclear Technology*, Vol. 154, pp. 247-264.
- Bahrami, D., G. Danko. and J. Walton. 2006. *Water, Vapor, and Salt Dynamics in a Hot Repository*. Material Research Society, 2006 Fall meeting.
- Barnes, H., E.B Ekren, R.L Cleaves, and D.C. Hedlund. 1982. *Geologic and Tectonic Maps of the Mercury Quadrangle, Nye and Clark Counties, Nevada*: U.S. Geologic Survey I-1197 1:24,000.
- Belcher, W.R., ed, 2004. *Death Valley Regional Ground-Water Flow System, Nevada and California – Hydrogeologic Framework and Transient Ground-Water Flow Model*. U.S. Geological Survey Water-Resources Investigations Report 2004-5205.
- Birkholzer, J., N. Halecky, S.W. Webb, P.F. Peterson, G.S. Bodvarsson, 2006. *The Impact of Natural Convection on Near-Field TH Processes at Yucca Mountain*. Proceedings, 11th International High-Level Nuclear Waste Conference, April, Las Vegas, NV.
- Blakely, R.J.; V.E. Langenheim, D.A. Ponce; and G.L. Dixon. 2000. *Aeromagnetic Survey of the Amargosa Desert, Nevada and California: A Tool for Understanding Near-Surface Geology and Hydrology*. Open-File Report 00-188. Denver, Colorado: U.S. Geological Survey. 25 p.
- Blakely, R.J. and D.A. Ponce. 2001. Map Showing Depth to Pre-Cenozoic Basement in the Death Valley Ground-Water Model Area, Nevada and California: U.S. Geological Survey Miscellaneous Field Studies Map MF-2381-E. Denver, Colorado. U.S. Geological Survey.
- Brocher, T.M., M.D. Carr, K.F Fox, and P.E Hart, 1993. *Seismic Reflection Profiling Across Tertiary Extensional Structures in the Eastern Amargosa Desert, Southern Nevada Basin and Range Province*: Geological Society of America Bulletin, v. 105, pp. 30-46.
- BSC (Bechtel SAIC Company). 2002. *Ventilation Model*. ANL-EBS-MD-000030 REV 01D draft. Las Vegas, Nevada: Bechtel SAIC Company, ACC.

- BSC. 2004. Saturated Zone In-Situ Testing. ANL-NBS-HS-000039 REV 00, 01. Las Vegas, Nevada: Bechtel SAIC Company.[www.osti.gov/energycitations]
- Buqo, T S and C. Brooks, 2006. *The Growth, Decay, and Hydrologic Significance of Groundwater Mounds in the Yucca Mountain Region*, NWRPO-2006-09, June 2006. Nye County Nuclear Waste Repository Project Office.
- Burchfiel, B.C. 1965. *Structural Geology of the Specter Range Quadrangle, Nevada, and its Regional Significance*: Geological Society of America Bulletin, 76, pp. 175-191.
- Burchfiel, B.C., R.J. Fleck, D.T. Secor, R.R. Vincelette, and G.A. Davis, 1974. *Geology of the Spring Mountains, Nevada*: Geological Society of America Bulletin, v. 85, pp. 1013-1023.
- Carr, W.J., 1984. *Regional Structural Setting of Yucca Mountain, Southwestern Nevada, and Late Cenozoic Rates of Tectonic Activity in Part of the Southwestern Great Basin, Nevada and California*: U. S. Geological Survey, Open-File Report 84-0854, 114 p.
- Carr, M.D., Sawyer, D.A., Nimz, K., Maldonado, F., and Swadley, W.C., 1996. Digital bedrock geologic map database of the Beatty 30 X 60-minute quadrangle, Nevada and California: U.S. Geological Survey Open-File Report 96-261, scale 1:100,000, 41 p.
- Carslaw, H.S. and J.C. Jaeger. 1959. *Conduction of Heat in Solids*. 1st Edition, Oxford: Clarendon Press. pp. 73-75.
- Carslaw, H.S. and J.C. Jaeger. 1986. *Conduction of Heat in Solids*. 2nd Edition, Oxford: Clarendon Press. pp. 58-71.
- Cole, J.C., and Cashman, P.H., 1999. *Structural Relationships of Pre-Tertiary Rocks in the Nevada Test Site Region, Southern Nevada*: U.S. Geological Survey Professional Paper 1607, 39 p.
- Cox, D.O. and P.R. Onsager. 2002. *Application of Leaky Aquifer Type Curves for Coalbed Methane Characterization*. Paper SPE 77333, Presented at the Society of Petroleum Engineers Annual Technical Conference and Exhibition, San Antonio, Texas, Sept. 29 – Oct. 2, 2002.
- Czarnecki, J.B. 1997. *Geohydrology and Evapotranspiration at Franklin Lake Playa, Inyo County, California*. U.S. Geological Survey Water-Supply Paper 2377, 75 p.
- D'Agnese, F.A., C.C. Faunt, and A.K. Turner. 1998. *An Estimated Potentiometric Surface of the Death Valley Region, Nevada and California*, Developed Using Geographic Information System and Automated Interpolation Techniques. U.S. Geological Survey, Water-Resources Investigations Report 97-4052, Denver, Colorado.
- D'Agnese, F.A., G.M. O'Brien, C.C. Faunt, and C.A. San Juan. 1999. *Simulated Effects of Climate Change on the Death Valley Regional Ground-Water Flow System, Nevada and California*. U.S. Geological Survey, Water-Resources Investigations Report 98-4041, Denver, Colorado.

- Daltaban, T.S. and C.G.Wall. 1998. *Fundamental and Applied Pressure Analysis*. pp. 539–541. London, England: Imperial College Press.
- Danko, G. 2004a. *Final Letter Report for Nye County Ventilation Modeling (4/1/03 - 3/31/04)*. Includes two papers for the July 2004 American Society of Mechanical Engineers (ASME) and presentation for the Nuclear Waste Technical Review Board (NWTRB), January 2004.
- Danko, G. 2004b. *Numerical Transport Code Functionalization Procedure and Software Functions*. Proceedings of ASME, Heat Transfer/Fluid Engineering, July 11-15, 2004, Charlotte, North Carolina, USA. 10 p.
- Danko, G. 2006. *Functional or Operator Representation of Numerical Heat and Mass Transport Models*. ASME J. of Heat Transfer, Vol. 128, pp. 162-175.
- Danko, G. and D. Bahrami. 2003a. *Sensitivity Analysis of Ventilation Parameters and Site Input Properties*. Proceedings, 10th Int. High-Level Radioactive Waste Management Conference. 8 p.
- Danko, G. and D. Bahrami. 2003b. *Powered, and Natural, Passive Ventilation at Yucca Mountain*. Proceedings, 10th Int. High-Level Radioactive Waste Management Conference. 8 p.
- Danko, G. and D. Bahrami. 2004a. *Coupled, Multi-Scale Thermohydrologic-Ventilation Modeling with MULTIFLUX*. Preprint 04-144, SME Annual Meeting and Exhibit, Denver, CO, February 23-25. 15 p.
- Danko, G. and D. Bahrami. 2004b. *Heat and Moisture Flow Simulation with MULTIFLUX*. Proceedings of ASME, Heat Transfer/Fluid Engineering, July 11-15, 2004, Charlotte, North Carolina, USA.
- Danko, G. and D. Bahrami. 2006a. *The Effect of Pre-Closure Ventilation on the Environmental Conditions at Yucca Mountain*. Proceedings, Int. High-Level Radioactive Waste Management Conference. Las Vegas, 2006.
- Danko, G. and D. Bahrami. 2006b. *Barometric Pressure Variation Effects on Emplacement Drift Environmental Conditions at Yucca Mountain*. Proceedings, Int. High-Level Radioactive Waste Management Conference. Las Vegas, 2006.
- Danko, G., Bahrami, D., Birkholzer, J.T., (2006). *The Effect of Unheated Sections on Moisture Transport in the Emplacement Drift*. Proceedings, Int. High-Level Radioactive Waste Management Conference. Las Vegas, 2006.
- Danko, G., D. Bahrami, and J. Walton. 2004. *Status of Nye County Ventilation Studies*. Invited presentation to: Nuclear Waste Technical Review Board, January 19, 2004, Las Vegas.
- Danko, G., J. Walton, and D. Bahrami. 2007. *Increased Storage Capacity at Yucca Mountain Favors Thermal Management for a Cold Repository*. (Approved for publication in the Journal of Nuclear Technology, 2007).

- Danko G., J. Birkholzer and D. Bahrami, 2007a. *Thermal-Hydrological Near-Field Model Studies and Impact of Natural Convection of Seepage*, 2nd Quarterly report for Office of Science and Technology and International.
- Deemer, Danielle L. and Thomas H. Anderson. 2002. *Transpressional structures in Northern Specter Range and Striped Hills, Nevada*: Strong contraction within an extensional orogen, [abs.]: Abstracts with Programs, Geological Society of America Annual Meeting, 34, 6,
- DeMeo, G.A., R.J. Laczniaik, R.A. Boyd, J.L Smith, and W.E. Nyland. 2003. *Estimated Ground-Water Discharge by Evapotranspiration from Death Valley, California, 1997 – 2001*. U.S. Geological Survey, Water-Resources Investigations Report 2003-4254.
- DOE (U.S. Department of Energy). 2000. Yucca Mountain Project Technical Database [TDR-NBS-MD-000001, 2000].
- DOE. 2004a. *In-Drift Natural Convection and Condensation*. Prepared by Bechtel SAIC Company, LLC. MDL-EBS-MD-000001 REV 00. Yucca Mountain Project. Las Vegas, Nevada.
- DOE. 2004b. *Multiscale Thermohydrologic Model*. Prepared by Bechtel SAIC Company, LLC. ANL-EBS-MD-000049 REV 01. Yucca Mountain Project. Las Vegas, Nevada.
- Dudley, W.W. and J.D. Larson. 1976. *Effects of Irrigation Pumping on Desert Pupfish Habitats in Ash Meadows, Nye County, Nevada*. U.S. Geological Survey, Professional Paper 927.
- Fekete Associates Inc. July 2, 2002. *WELLTEST Well Interpretation Software, Version 3.1 Release Notes*. Calgary, Alberta, Canada: Fekete.
- Fleck, R.J. 1970. *Age and Possible Origin of the Las Vegas Valley Shear Zone, Clark and Nye Counties, Nevada*, [abs.]: Geological Society of America Abstract with Programs, v. 2, no. 5, p. 333.
- Fridrich, C.J., 1999, *Tectonic Evolution of the Crater Flat Basin, Yucca Mountain Region, Nevada*, in Wright, L.A., and Troxel, B.W., eds., *Cenozoic Basins of the Death Valley Region*: Boulder, Colorado, Geological Society of America Special Paper 333, pp. 169-195.
- Hall, D and J.C. Walton. 2006. *Conceptual Model for Flow Separation Processes Affecting Waste Package Chemical Environment, Yucca Mountain, Nevada*. Applied Geochemistry, Volume 21, Issue 6, pp 859-869.
- Hammermeister, D. P., D. O. Blout, and J.C. McDaniel. 1986. *Drilling and Coring Methods that Minimize the Disturbance of Cuttings, Core, and Rock Formations in the Unsaturated Zone, Yucca Mountain, Nevada*. In Proceedings of the NWWA Conference on Characterization and Monitoring of the Vadose (Unsaturated) Zone, Denver, Colorado, 507-541. Worthington, Ohio: National Water Well Association.
- Hantush, M.S. 1959. *Non-steady Flow to Flowing Wells in Leaky Aquifers*. Trans., AGU. Vol. 27, pp. 702–714.

- Haskell Jr., E.E., and W.C. Bianchi. 1965. *Development and Dissipation of Ground Water Mounds Beneath Square Recharge Basins*. Journal of the American Water Works Association, March, 1965, pp. 349-353.
- Hoffman, J. 2006. *Square Array Direct Current Resistivity Measurements Conducted at Nye County near Borehole NC-EWDP-29P*. Tucson, Arizona. U.S. Geological Survey letter report.
- Kappa Engineering. 1999. *SAPHIR v. 3.10, Document V3.10.00*. Paris, France: Kappa Engineering.
- Laczniak, R.J., Cole, J.C., Sawyer, D.A., and Trudeau, D.A. 1996. *Summary of Hydrogeologic Controls on Ground-Water Flow at the Nevada Test Site, Nye County, Nevada*. U.S. Geological Survey Water-Resources Investigations Report 96-4109, 59 p.
- Laczniak, R.J., G.A. DeMeo, S.R. Reiner, J.L. Smith, and W.E. Nylund. 1999. *Estimates of Ground-Water Discharge as Determined from Measurements of Evapotranspiration, Ash Meadows Area, Nye County, Nevada*. U.S. Geological Survey Water Resources Investigation Report 99-4079, 70 p.
- Laczniak, R.J., J.L. Smith, P.E. Elliott, G.A. DeMeo, M.A. Chatigny, and G.J. Roemer. 2001. *Ground-Water Discharge as Determined from Estimates of Evapotranspiration, Death Valley Regional Flow System, Nevada and California*. U.S. Geological Survey Water Resources Investigation Report 01-4195, 51 p.
- LANL (Los Alamos National Laboratory). 2003. Regional ground water hydrochemical data in the Yucca Mountain are used as direct input to ANL-NBS-00021, Revision 01. LA0309RR831233.001 May, 2003.
- Larsen, L. 1981. *Wells Producing Commingled Zones with Unequal Initial Pressures and Reservoir Properties*. SPE 10325. Presented at the Annual Fall Technical Conference in San Antonio, Texas, Oct. 5–7, 1981. Society of Petroleum Engineers: Dallas, Texas.
- Leap, D.L. and P.G. Kaplan. 1988. *A Single-Well Tracing Method for Estimating Regional Advective Velocity in a Confined Aquifer: Theory and Preliminary Laboratory Verification*. Water Resources Research, vol. 24, no. 7, pp. 993–998.
- Liu, B., F. Philips, S. Hoines, A.R. Campbell, and P.Sharma. 1995. *Water Movement in Desert Soil Traced by Hydrogen and Oxygen Isotopes, Chloride, and Chlorine-36, Southern Arizona*. Journal of Hydrology, 168. pp. 91-110.
- Maldonado, F. 1985. *Geologic Map of the Jackass Flats Area*. U.S. Geologic Survey I-1519 1:48,000.
- McKee E.H., T.A. Wickham, and K.L. Wheeler, 1998. *Evaluation of Faults and Their Effect on Ground-Water Flow Southwest of Frenchman Flat, Nye and Clark Counties, Nevada*. U.S. Geological Survey Open File Report 98-580, 17 p.

- Mellinger, M. 1987. *Multivariate Data Analysis: Its methods*. Chemometrics and Intelligent Laboratory Systems, 2. pp. 29-36.
- Murray, D.A., K.D. Ridgway, and J.A. Stamatakis. 2003. *Stratigraphy of Oligocene and Lower Miocene Strata - Yucca Mountain Region*: Proceedings of the 10th International High-Level Radioactive Waste Management Conference, La Grange Park, IL, American Nuclear Society (CD-ROM publication)
- MULTIFLUX. 2003. *Draft Software Qualification Documents*. Prepared for Bechtel SAIC Company, LLC (BSC) by George Danko, University of Nevada, Reno.
- NUFT. 2000. *Flow and Transport Code Version 3.0s*. Software Configuration Management, Yucca Mountain Project – STN: 10088-3.0S-00. Prepared by Lawrence Livermore National Laboratory.
- NWRPO. 2001a. *Nye County Nuclear Waste Project Office Independent Scientific Investigations Program Final Report, Fiscal Years 1996–2001*. NWRPO-2001-04, Pahrump, Nevada: Nuclear Waste Repository Project Office. 148 p.
- NWRPO. 2001b. *Analysis of Pump-Spinner Tests and 48-Hour Pump Tests in Well NC-EWDP-19D, Near Yucca Mountain, Nevada*. NWRPO-2001-03, Pahrump, Nevada: Nuclear Waste Repository Project Office. 43 p.
- NWRPO. 2002. *Preliminary Analysis of Pump-Spinner Tests and 48-Hour Pump Tests in Wells NC-EWDP-19IM1 and -19IM2, Near Yucca Mountain, Nevada*. NWRPO-2002-05, Pahrump, Nevada: Nuclear Waste Repository Project Office. 40 p.
- NWRPO. 2003a. *Nye County Drilling, Geologic Sampling and Testing, Logging, and Well Completion Report for the Early Warning Drilling Program Phase III Boreholes*. Technical Report No. NWRPO-2002-04. Pahrump, Nevada: Nye County Nuclear Waste Repository Project Office.
- NWRPO. 2003b. *Preliminary Analysis of Pump-Spinner Tests and Pump Tests in Wells NC-EWDP-22S, Near Yucca Mountain, Nevada*. NWRPO-2002-06, Pahrump, Nevada: Nuclear Waste Repository Project Office. 39 p.
- NWRPO. 2003c. *Groundwater Chemistry Monitoring, Sampling, and Analysis Annual Report for Fiscal Year 2002*. Technical Report No. NWRPO-2003-04. Pahrump, Nevada: Nuclear Waste Repository Project Office. December 2003. 65 p.
- NWRPO. 2003d. *Coupled Hydrothermal-Ventilation Studies for Yucca Mountain Annual Report for April 2002-March 2003*. Technical Report No. NWRPO-2003-05. Pahrump, Nevada: Nuclear Waste Repository Project Office. December 2003.
- NWRPO. 2003e. NWRPO Quality Assurance Program Plan. Pahrump, Nevada: Nye County NWRPO. 40 p.

- NWRPO. 2004. *Analysis Aquifer Pump Tests in Individual Well Zones at Site 22, Near Yucca Mountain, Nevada*. NWRPO-2004-02, Pahrump, Nevada: Nuclear Waste Repository Project Office. 45 p.
- NWRPO. 2005a. *Nye County Early Warning Drilling Program, Phase IV Drilling Report*. Technical Report No. NWRPO-2004-04. Pahrump, Nevada: Nuclear Waste Repository Project Office.
- NWRPO. 2005b. *Groundwater Chemistry Analysis Annual Report for April 2004 through March 2005*. Technical Report No. NWRPO-2005-01. Pahrump, Nevada: Nuclear Waste Repository Project Office. July 2005. 42 p.
- NWRPO. 2005c. *Coupled Hydrothermal-Ventilation Studies for Yucca Mountain Annual Report For April 2004-March 2005.*, Technical Report No. NWRPO-2005-02. Pahrump, Nevada: Nuclear Waste Repository Project Office. September 2005. 176 p.
- NWRPO. 2006. *Analysis of 48-Hour Pump Test at Site 10, Near Yucca Mountain, Nevada*. NWRPO-2006-01, Pahrump, Nevada: Nuclear Waste Repository Project Office. 31 p.
- NWRPO 2007a. *Data files. Nye County, Nevada NWRPO website.* (<http://www.nyecounty.com>)
- NWRPO. 2007b. *Nye County Tracer Tests at Site 22, Near Yucca Mountain, Nevada*. NWRPO-2007-07, Pahrump, Nevada: Nuclear Waste Repository Project Office.
- NWRPO. 2009. *Nye County Early Warning Drilling Program, Phase V Drilling Report*. Technical Report No. NWRPO-2009-02. Pahrump, Nevada: Nuclear Waste Repository Project Office.
- O'Leary, D.W. 2000. Tectonic Significance of the Rock Valley Fault Zone, Nevada Test Site. U.S. Geologic Survey Digital Data Series. 13 p.
- Payer, Joe, 2005. *The Proposed Yucca Mountain Repository from a Corrosion Perspective, in Scientific Basis for Nuclear Waste Management XXIX*, edited by P. Van Isheghem (Mater. Res. Soc. Symp. Proc. 932, Warrendale, PA, 2006), Paper Number 32.
- Perry, F.V. et al., 2005. *Uncovering Buried Volcanoes at Yucca Mountain*: EOS, V. 86, No. 47, pp 485, 488.
- Potter J, D.S. Sweetkind, R.P. Dickerson, and M.L. Killgore. 2002. *Hydrostructural maps of the Death Valley region flow system, Nevada and California*: U. S. Geological Survey, Miscellaneous Field Studies Map, MF-2372, scale 1:350,000.
- Questa Engineering Corporation. 2000. *Analysis of Pump/Spinner Test in Borehole NC-EWDP-19D, Yucca Mountain, Nevada*. Draft. Golden, Colorado: Questa. 25 p.
- Raines, G.L., D.L. Sawatsky, and K.A. Connors, 1996. Great Basin geoscience data base: U. S. Geological Survey Digital Data Series 0041, scale 1:500,000.

- Reamer, C.W. 1999. *Review of Nye County Quality Assurance Program for the Early Warning Drilling Program*. Letter from C.W. Reamer (NRC) to L. Bradshaw (NWRPO), April 12, 1999, with enclosures, *Acceptance Evaluation of NWRPO Quality Assurance Program Plan*.
- Reimus, Paul W., Robert Jones, Ezra Wasson, John Kelly, Alexander Sanchez, Walter Slack, and Jeanette Daniels. 2006. Results of Tracer Testing in the Saturated Alluvium South of Yucca Mountain, *Proceedings of the 2006 International High-Level Radioactive Waste Management Conference*, April 30–May 4, 2006, Las Vegas, Nevada. LaGrange Park, Illinois: American Nuclear Society.
- Reiner, S.R., R.J. Laczniaik, G.A. DeMeo, J.L. Smith, P.E. Elliott, W.E. Nylund, and C.J. Fridrich. 2002. *Ground-Water Discharge Determined from Measurements of Evapotranspiration, Other Available Hydrologic Components, and Shallow Water Level Changes, Oasis Valley, Nye County, Nevada*. U.S. Geological Survey Water Resources Investigation Report 01-4239, 66 p.
- REEC Co. (Reynolds Electrical and Engineering Co., Inc.) 1994. *Site Characterization and Monitoring Data from Area 5 Pilot Wells, Nevada Test Site*, Nye County Nevada. Special Projects Section, Environmental Management Division, Las Vegas, NV. DOE/NV/11432-74.
- Ross, R.J. and C.R. Longwell, 1964. *Paleotectonic Significance of Ordovician Sections South of the Las Vegas Shear Zone*, p. C-88-C-93 in Ross, R. J., Jr., Middle and Lower Ordovician Formations in southernmost Nevada and adjacent California: U.S. Geological Survey Bulletin 1180-C, 101 pp.
- SNL (Sandia National Laboratory). 2007. Hydrologic Framework Model for the Saturated Zone Site-Scale Flow and Transport Model
- Sargent, K.A. and J.H. Stewart. 1971. Geologic Map of the Specter Range NW Quadrangle Nye County, Nevada: U.S. Geologic Survey GQ-884 1:24,000.
- Schulze-Makuch, D., D. A. Carlson, D. S. Cherkauer, and P. Malik. 1999. *Scale Dependence of Hydraulic Conductivity in Heterogeneous Media*. Ground Water, Vol. 37, No. 6, pp. 904-919.
- S.S. Papadopoulos and Associates, Inc. 1990. MT3D A Modular Three-Dimensional Transport Model for Simulation of Advection, Dispersion and Chemical Reactions of Contaminants in Groundwater Systems, eq. 2.9a, Rockville, Maryland: S.S. Papadopoulos and Associates, Inc.
- StatSoft, Inc. 2007. *STATISTICA Version 7.1*. Tulsa, OK. www.statsoft.com.
- Stewart, J.H., and J.E. Carlson. 1974. Preliminary geologic map of Nevada: U. S. Geological Survey Open-File Report 74-0068.
- Surfer Version 8. 2002. Contour and 3D Surface Mapping Software Program.
- Todd, D. K. 1980. *Groundwater Hydrology*. New York: Wiley. pp. 69–71.

- Walton, J. G. Danko, and D. Bahrami, 2006. *Effect of Cyclic, Sporadic, or Episodic Processes on Evolution of Environments in a Repository in Yucca Mountain*. Invited Presentation at the Nuclear Waste Technical Review Board Corrosion Workshop, Las Vegas, NV, September 2006.
- Walvoord and others, 2005. *Fluxes and isotopic speciation in a deep unsaturated zone*. Water Resources Research, Vol. 41, Issue 2.
- Waterloo Hydrogeologic (WH). Visual MODFLOW® v. 3.1.0.86. Modular 3-D transport model with Multi-Species (MT3DMS). www.waterloohydrogeologic.com. Waterloo, Ontario, Canada: WH.
- Wernicke, B., P.L. Guth, and G.J. Axe. 1988. *Tertiary Extensional Tectonics in the Sevier Thrust Belt of Southern Nevada*, in Weide, D.L., and Faber, M.L., eds., *This Extended Land; Geological journeys in the southern Basin and Range*; Geological Society of America Cordilleran Section Field Trip Guidebook: University of Nevada at Las Vegas Geoscience Department Special Publication, no. 2, p. 473-499.
- Winograd, I.J., 1962. *Interbasin Movement of Ground-Water at the Nevada Test Site*: U.S. Geological Survey Technical Report, TEI-807, 12 p.
- Winograd, I.J. and W. Thordarson. 1975. *Hydrogeologic and Hydrochemical Framework, South-Central Great Basin, Nevada-California, with Special Reference to the Nevada Test Site*. Professional Paper 712-C. Washington D.C.: U.S. Geological Survey.
- Woocay, A and J.C. Walton. 2006. Climate Change Effects on Yucca Mountain Region Groundwater Recharge. IHLRWM 2006, Las Vegas, NV, April 30-May 4, 2006, pp. 191-198.
- Woocay A. and J. C. Walton, 2008, *Multivariate Analyses of Water Chemistry: Surface and Ground Water Interactions*. Journal of Ground Water, Vol.46, May-June, pp.437-449.
- Workman, J.B., C.M. Menges, W. R. Page, E.M. Taylor, E.B. Ekron, P.D. Rowley, G.L. Dixon, R.A. Thompson, and L.A. Wright. 2002. Geologic map of the Death Valley ground-water model area, Nevada and California: Miscellaneous Field Studies Map MF-2381-A, scale 1:250,000.
- Xu, T. and K. Pruess. 2001. *Modeling Multiphase Non-Isothermal Fluid Flow and Reactive Geochemical Transport in Variably Saturated Fractured Rocks: 1. Methodology*. American Journal of Science, Vol. 301, January, pp. 16-33.

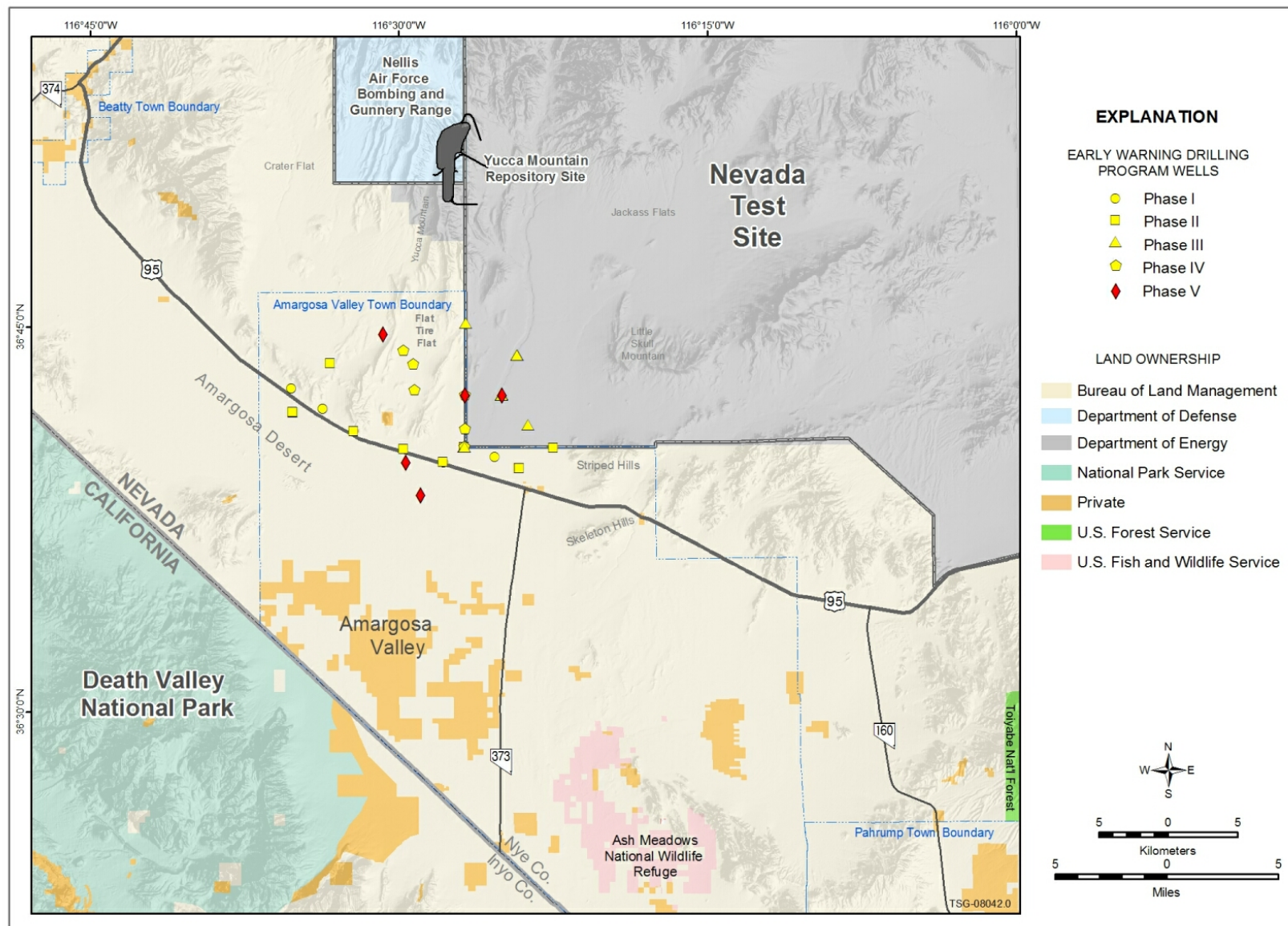


Figure 1.1-1
Early Warning Drilling Program Region

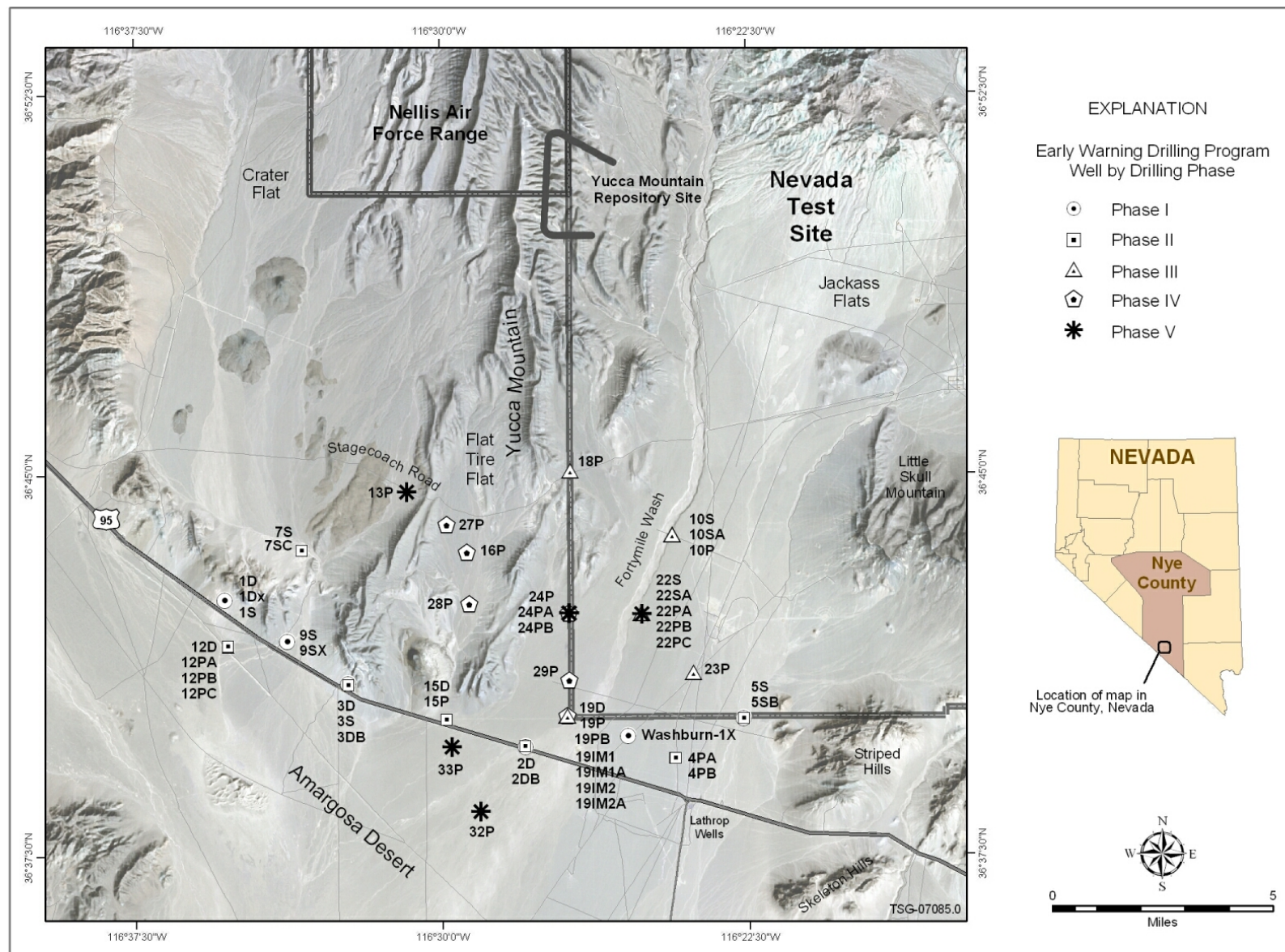


Figure 2.0-1
Early Warning Drilling Program Well Locations by Phase

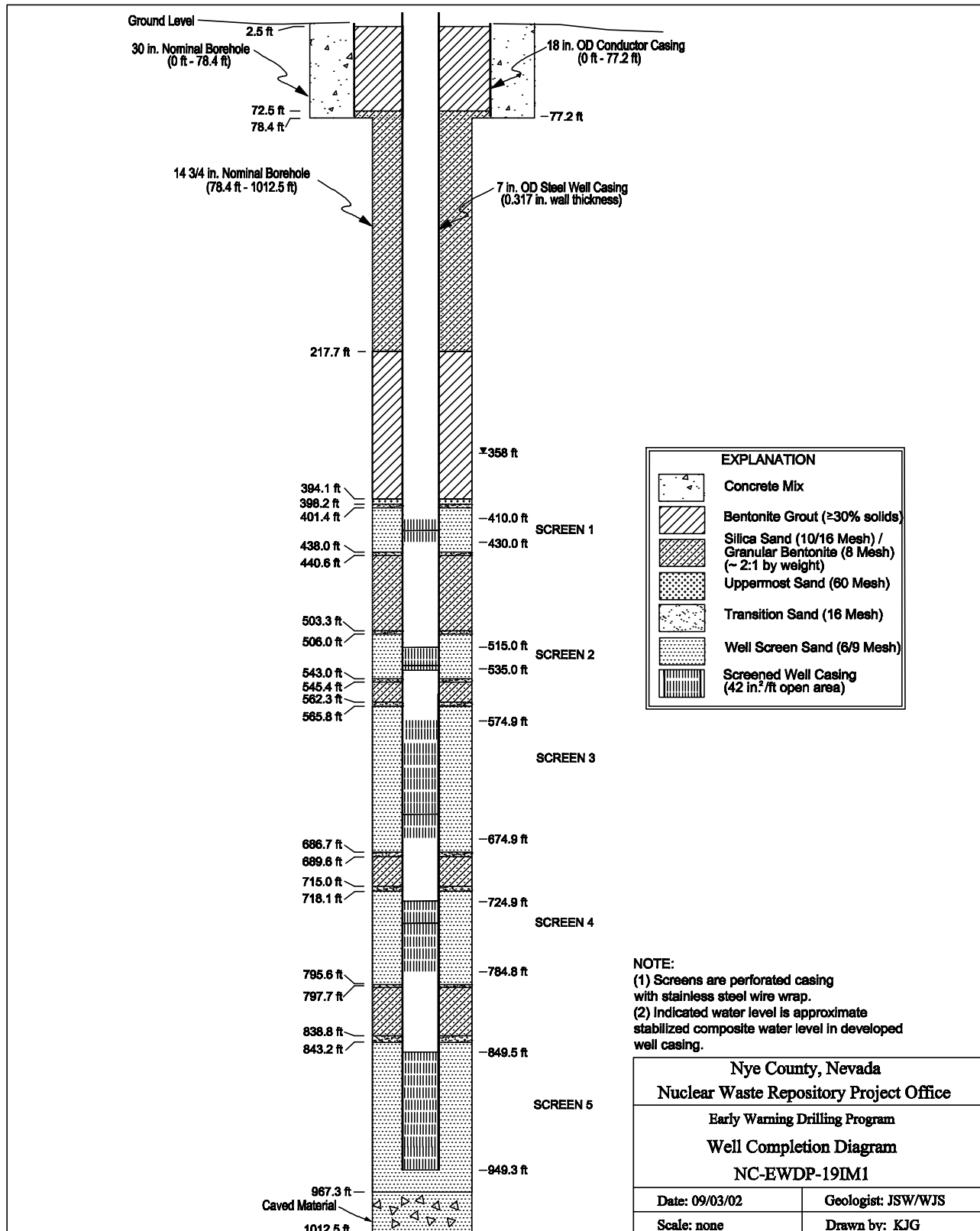


Figure 2.3-1
Typical Monitor Well Completion Diagram

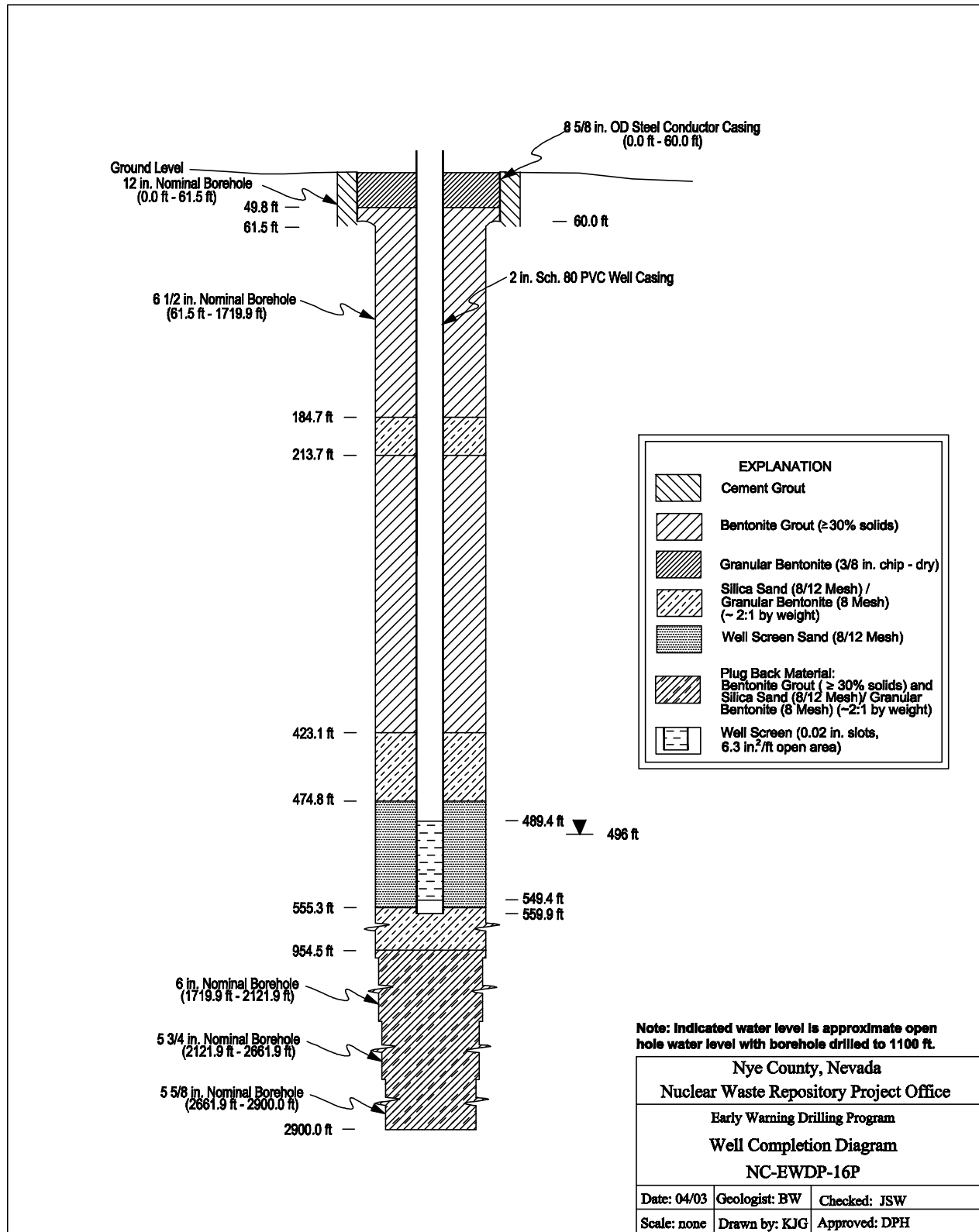


Figure 2.3-2
Schematic Single-String Piezometer Completion Diagram for 16P

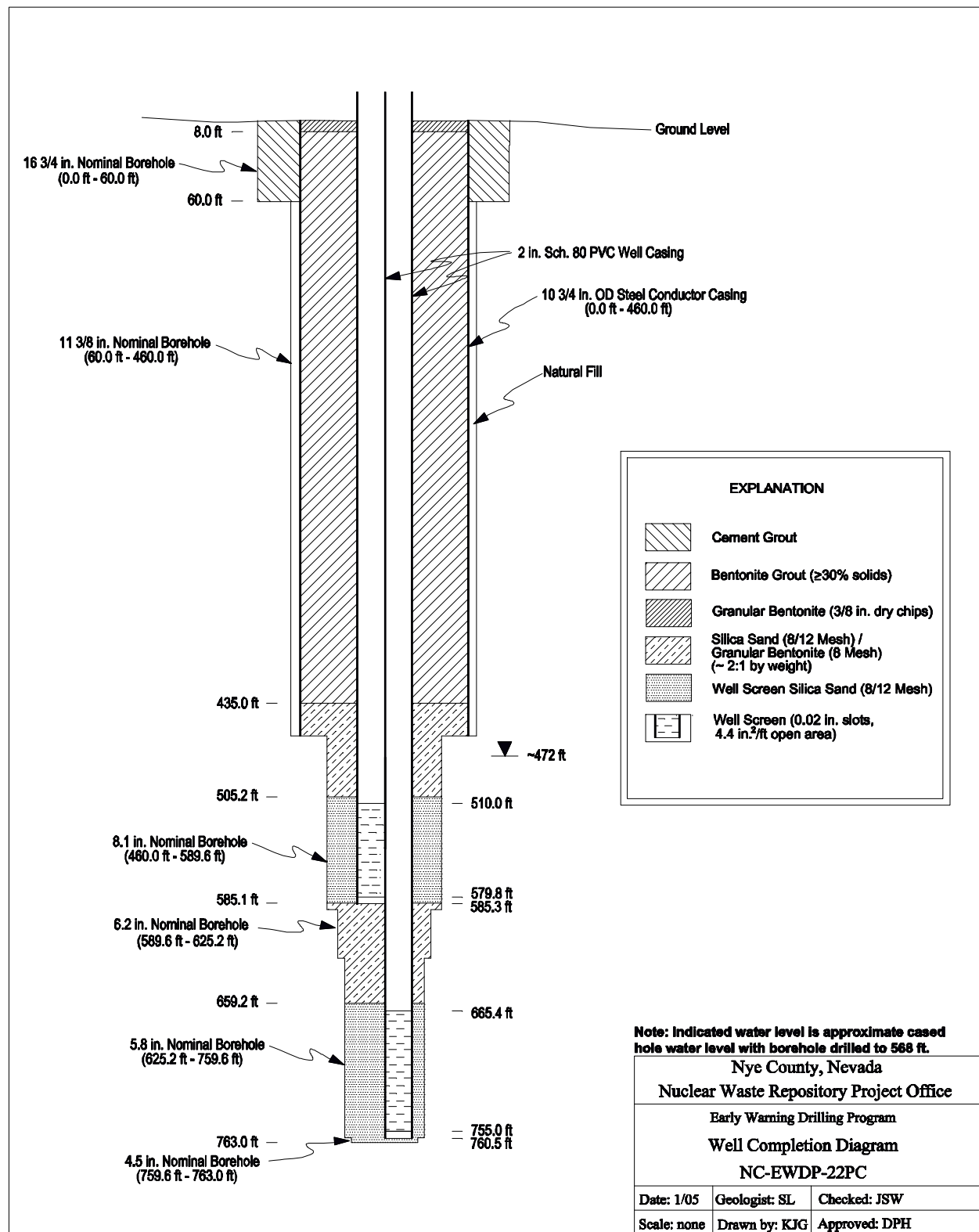


Figure 2.3-3
Dual-String Piezometer Completion Diagram for 22PC

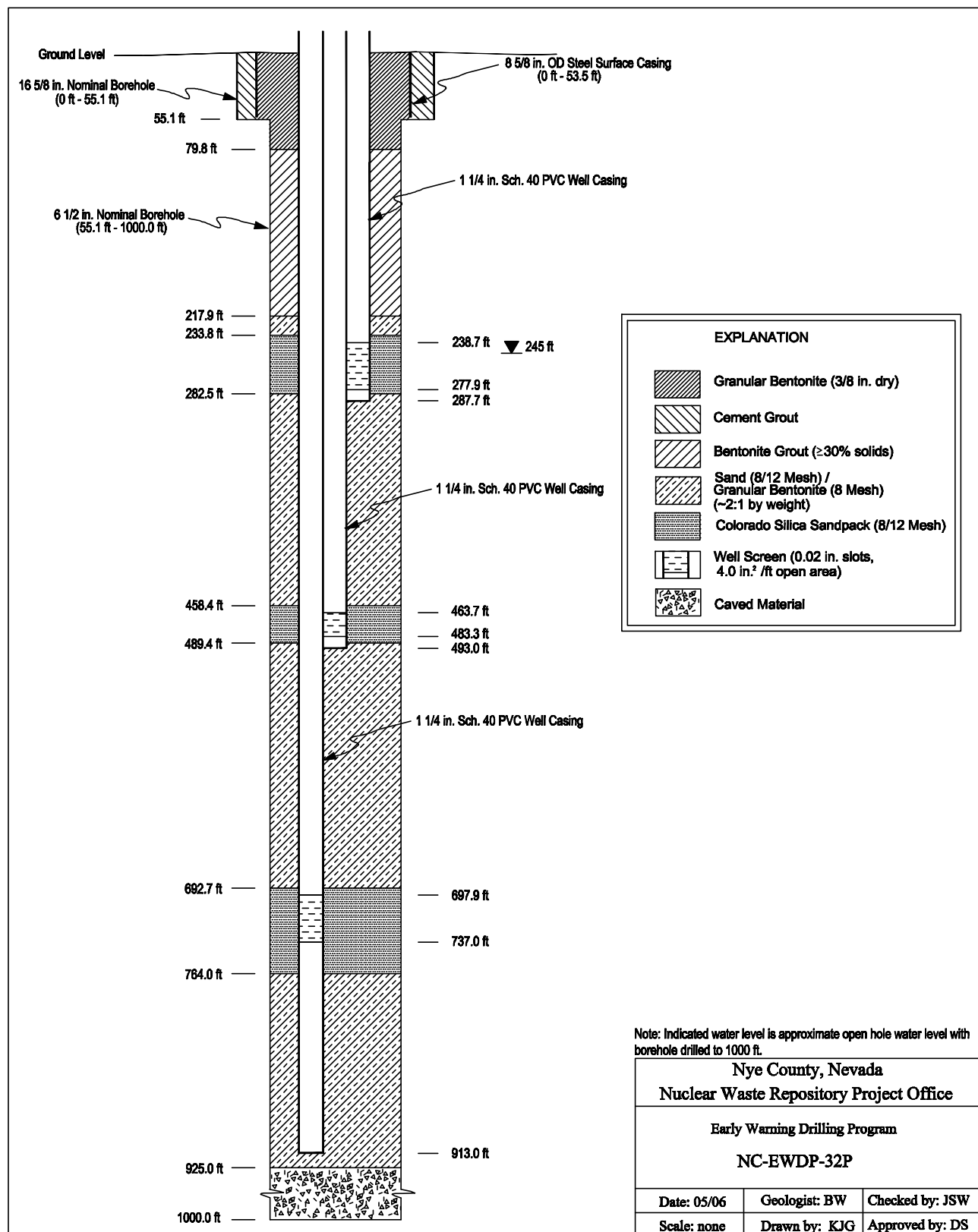


Figure 2.3-4
Triple-String Piezometer Completion Diagram for 32P

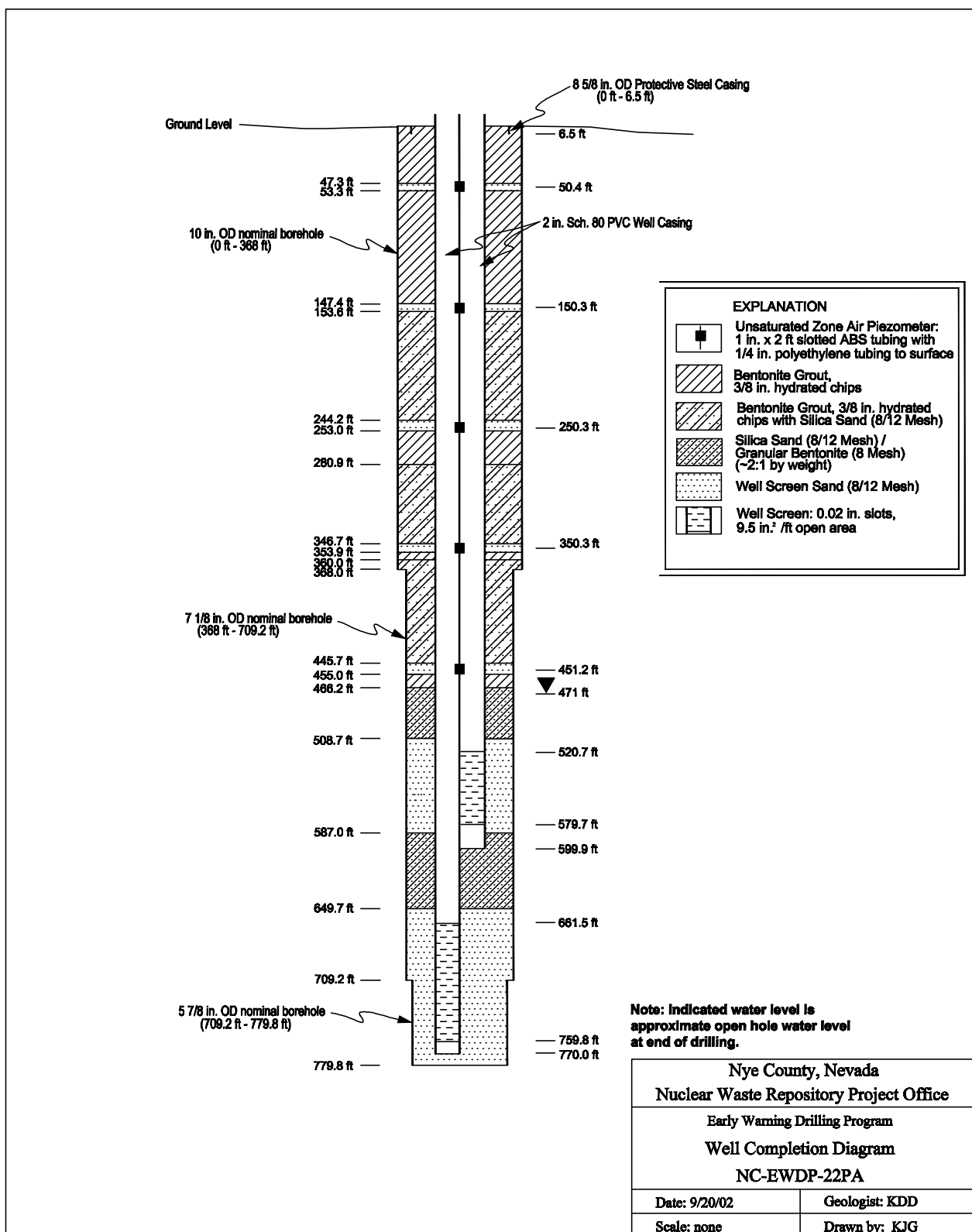


Figure 2.3-5
Typical Piezometer Well Completion Diagram

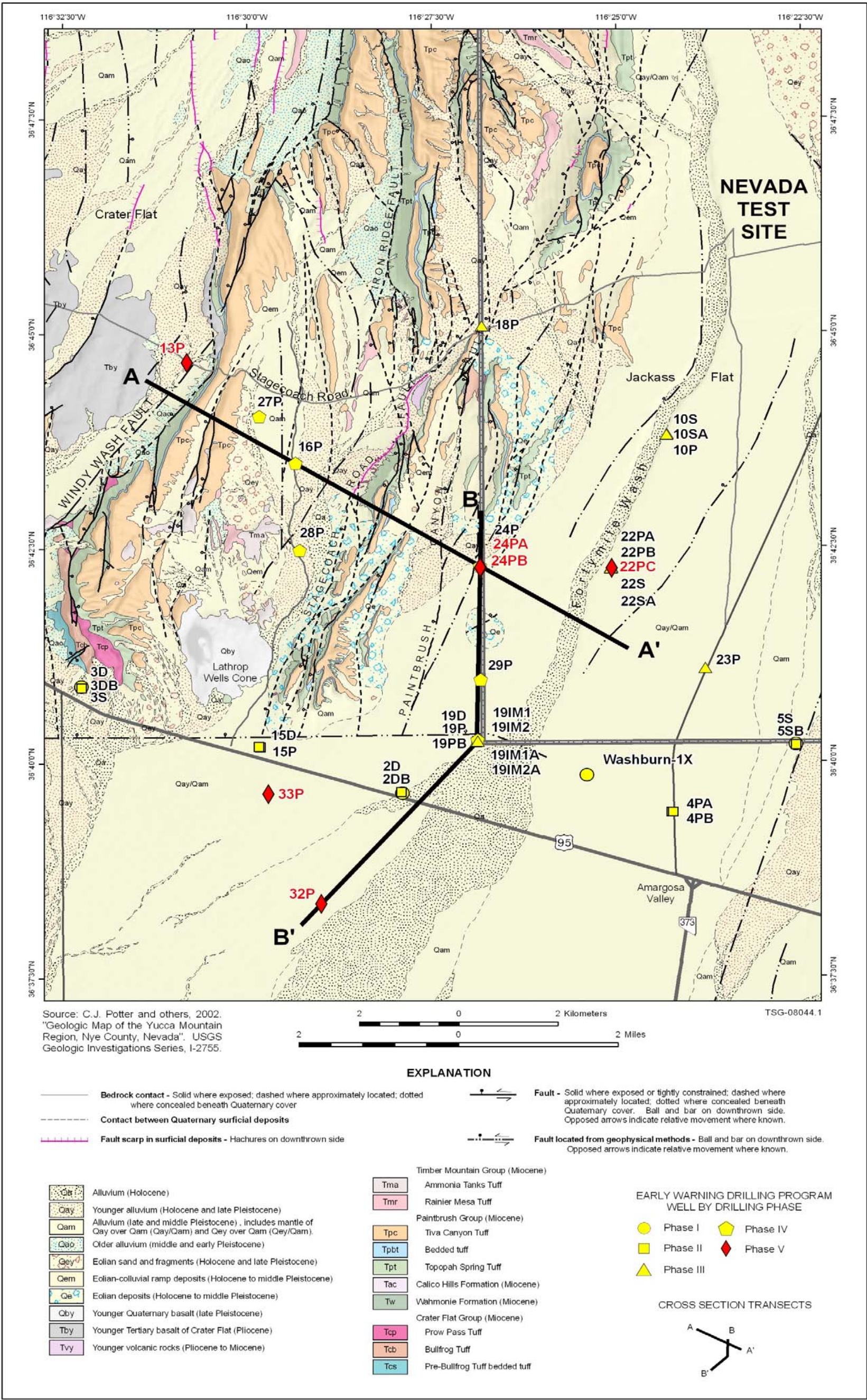


Figure 2.4-1
Geologic Map of the Yucca Mountain Area

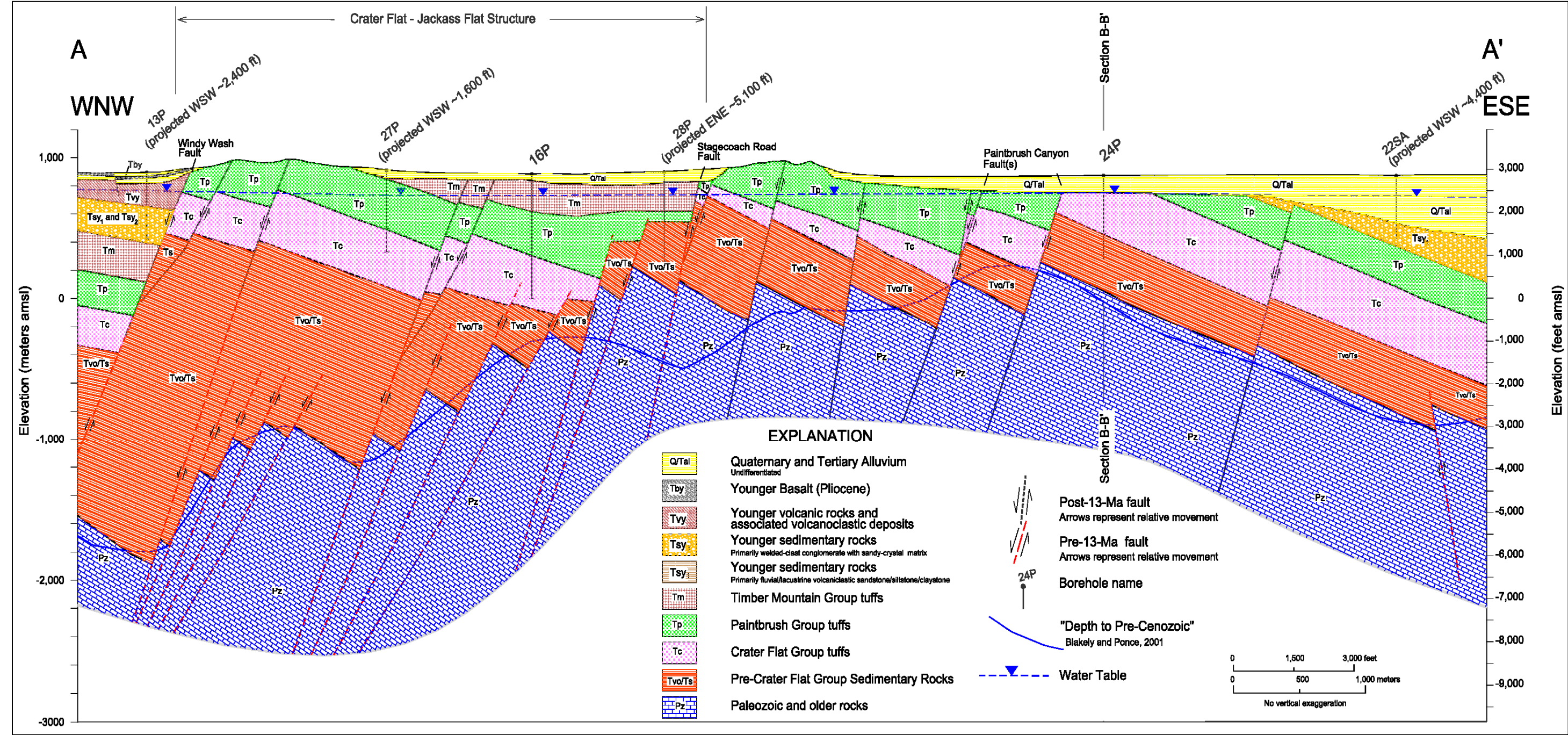


Figure 2.4-2
Phase V Geologic Cross Section A-A'



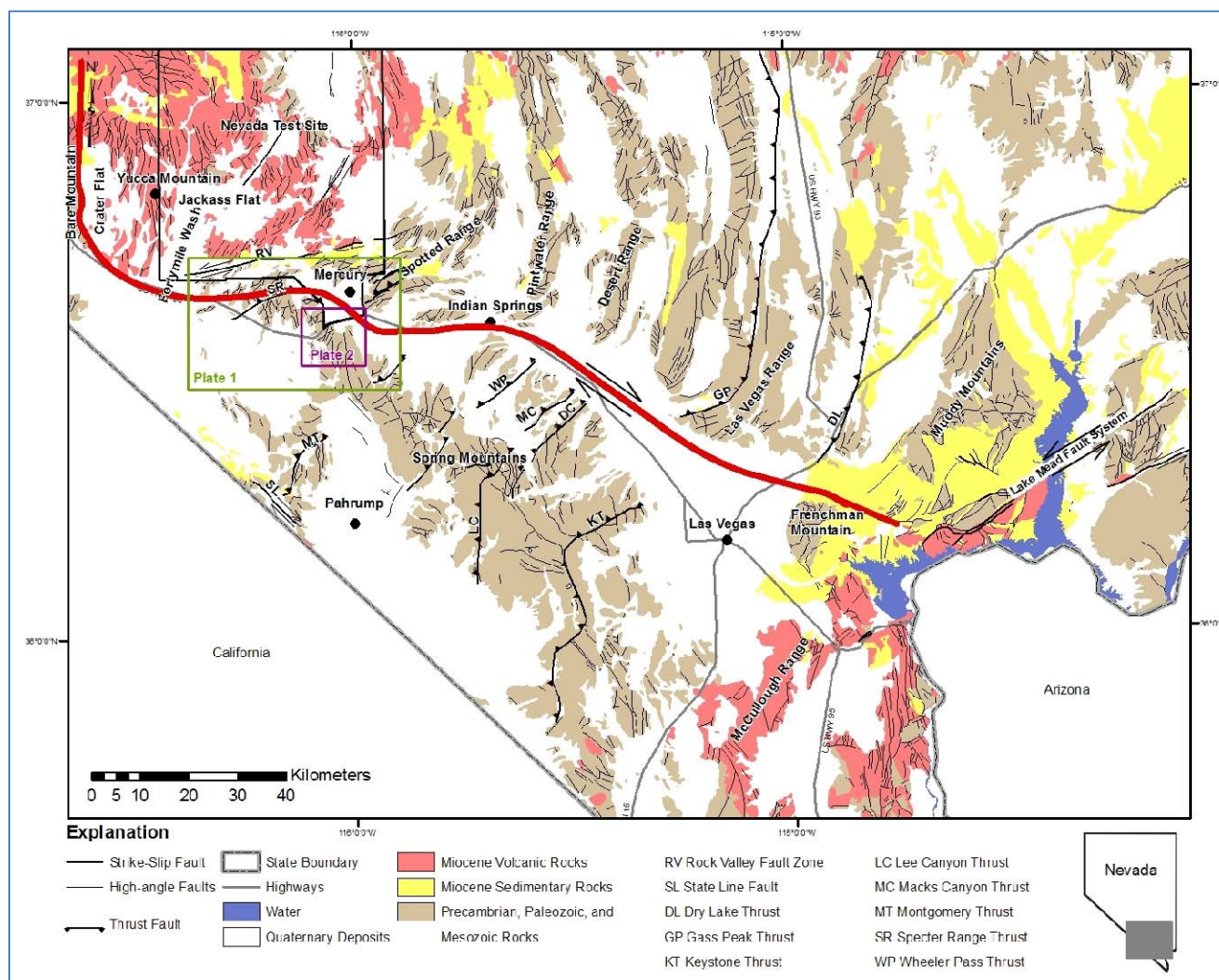


Figure 3.2-1

Generalized regional geologic map of southern Nevada data modified from Raines and others, (1996) geology modified from Stewart and Carlson, (1974). The red line represents the inferred trace of the Las Vegas Valley shear zone.

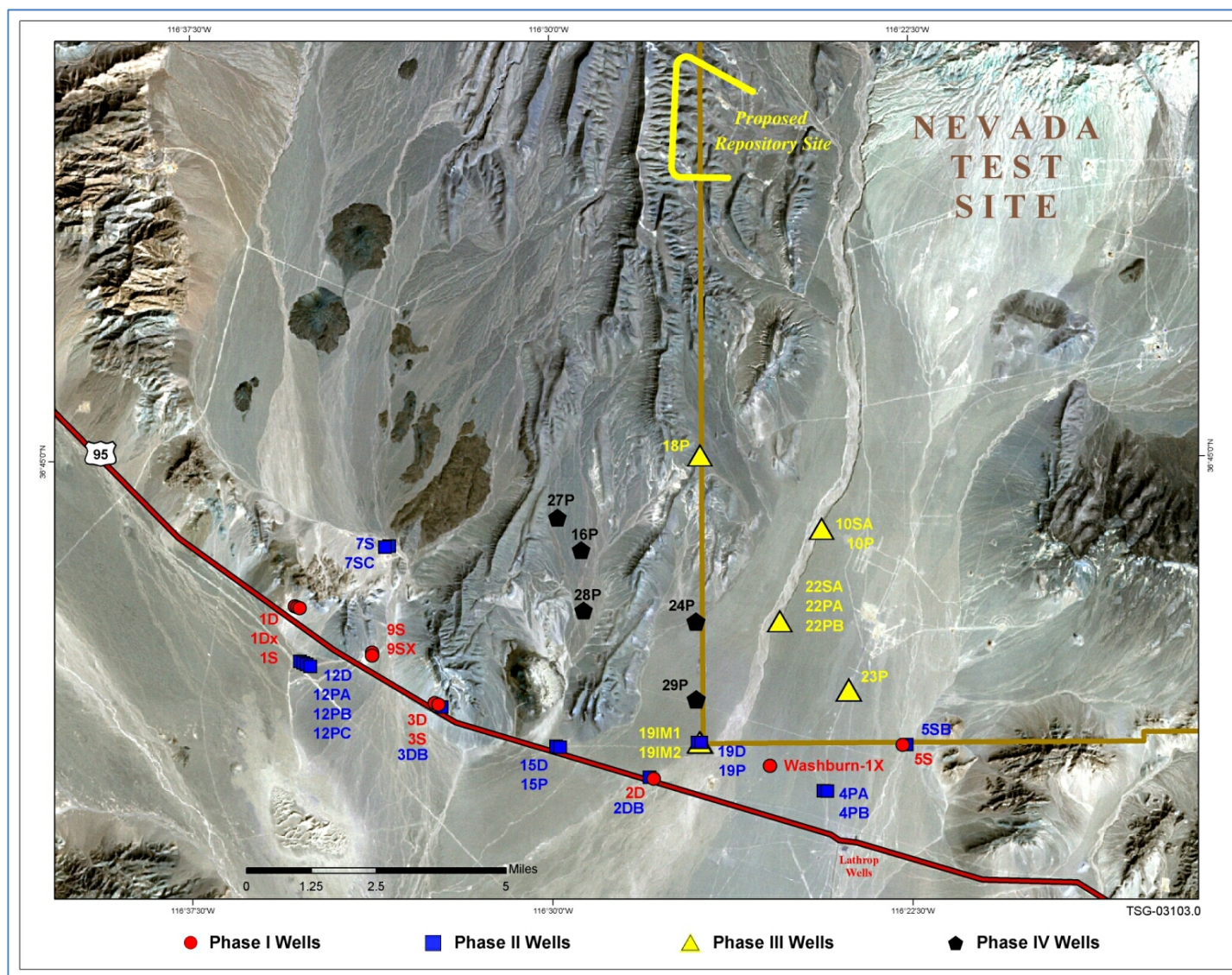


Figure 3.2-2
 Photograph of Crater Flat region that shows Early Warning Drilling Program well sites.
 Phase 1 wells along Highway 95 are very close to paleospring deposits that are interpreted to indicate the trace of the inferred Highway 95 fault.

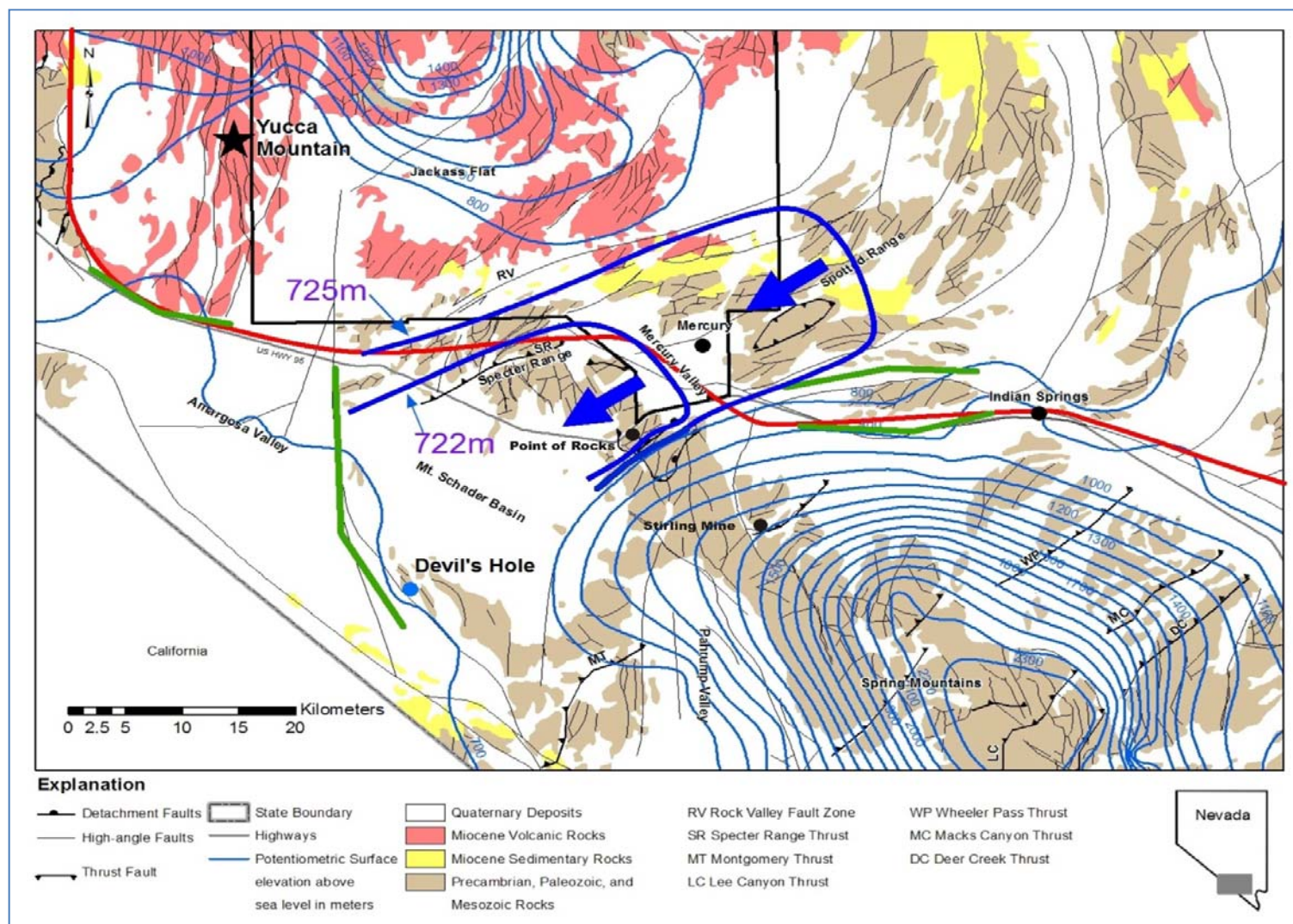


Figure 3.2-3

Hydrogeologic map of the bedrock aquifer in southern Nevada.

The thick green lines represent barriers to groundwater flow, thick blue lines represent local potentiometric surface, and blue arrows indicate the direction of groundwater from Winograd and Thordarson (1975). Regional potentiometric surface and faults modified from Potter and others, (2002). The red line represents the interpreted trace of the Las Vegas Valley shear zone.

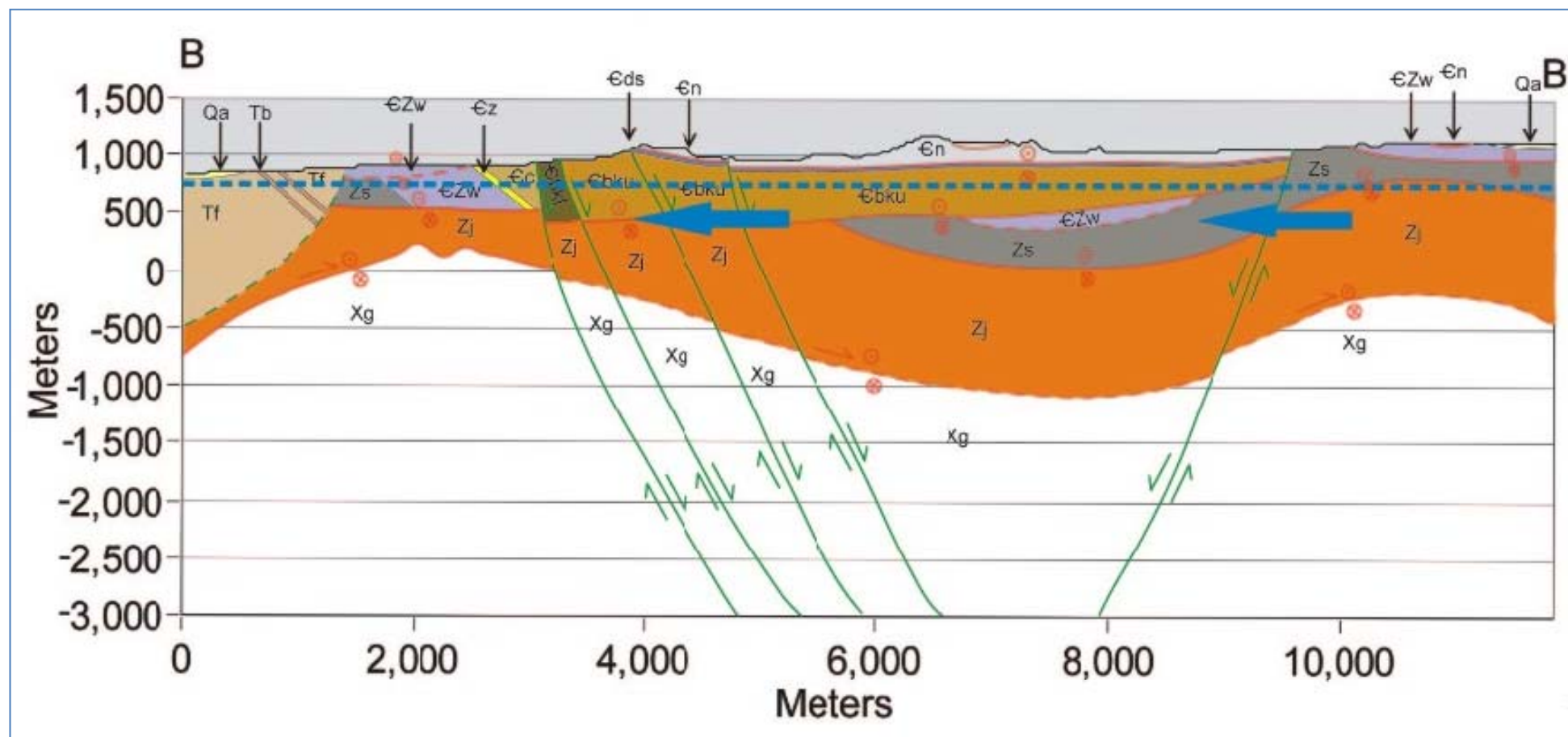


Figure 3.2-4

Hydrogeologic cross-section across the northern Spring Mountains, the dashed blue line represents the potentiometric surface and the blue arrows indicate the direction of groundwater flow according to Winograd and Thordarson (1975).

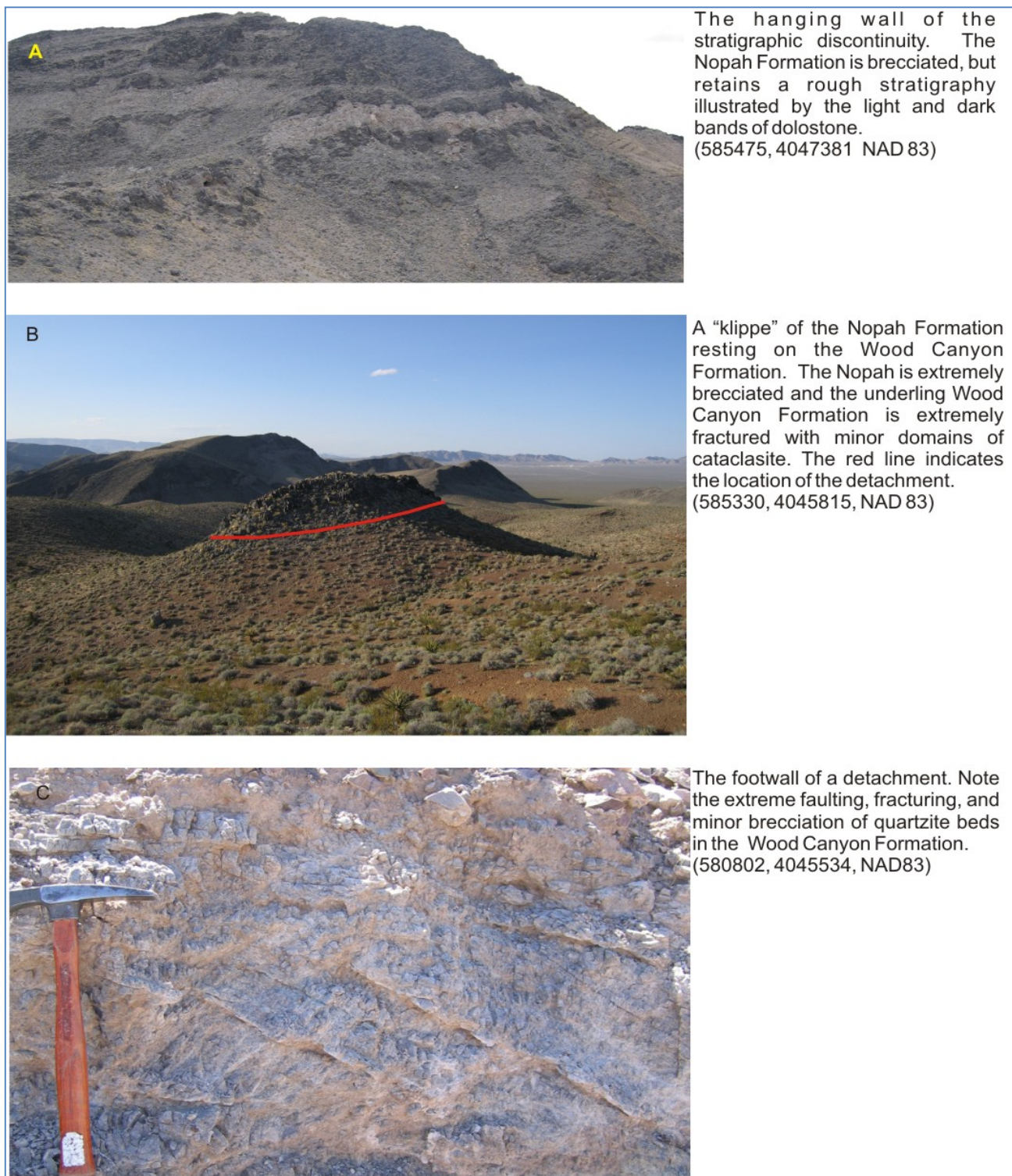


Figure 3.2-5
Field photos of the major detachment in the northern Spring Mountains: (A) hanging wall, (B) fault contact, and (C) footwall.

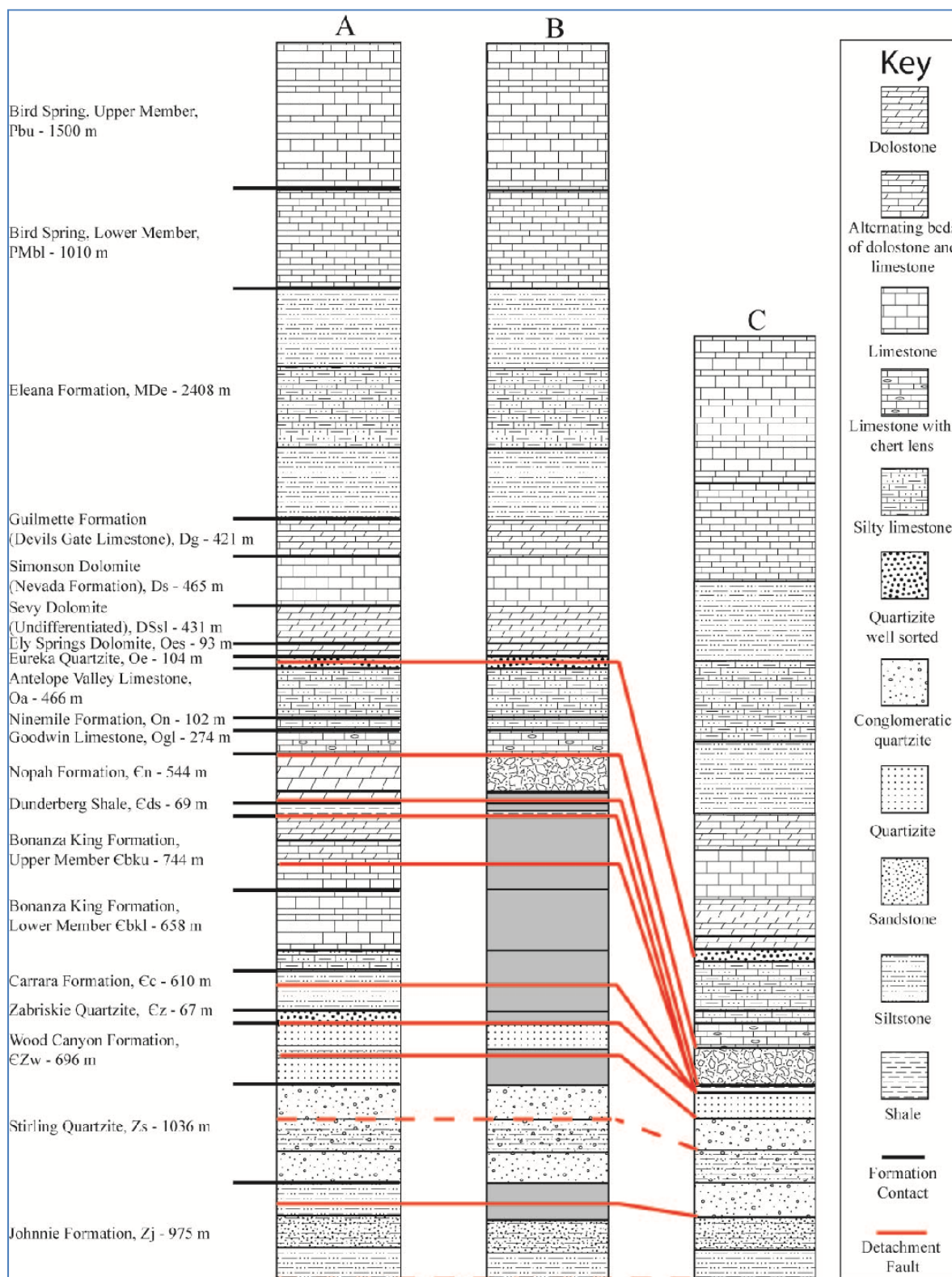
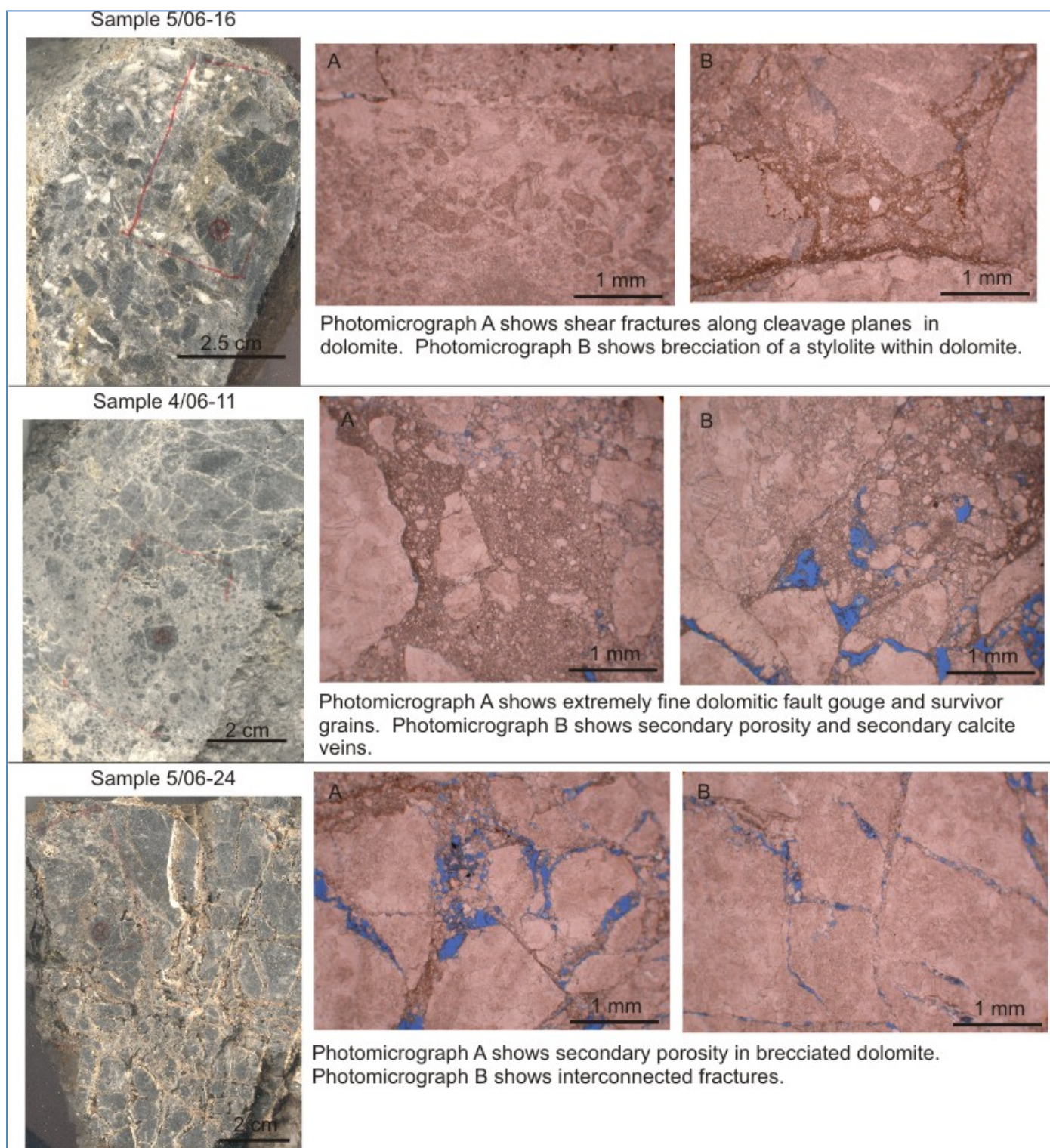


Figure 3.2-6

Stratigraphic columns that show: a) stratigraphic units, lithologies, and thicknesses of Paleozoic and Neoproterozoic strata in the Northern Spring Mountains and the Specter Range b) the thicknesses of units missing (shown in gray) among detachments c) stratigraphic column showing the detachments within the study area.

**Figure 3.2-7**

Nopah breccia samples from the hanging wall of the major detachment in the Spring Mountains. Blue domains in photomicrographs represent pore space.



Figure 3.2-8

Index map of 2001 structural investigations east of Yucca Mountain along Jackass Flats Road. Mountainous terrain south of Jackass Flats Road composes Spector Range. Little Skull Mountain and Skull Mountain form the northern margin of Jackass Flats.

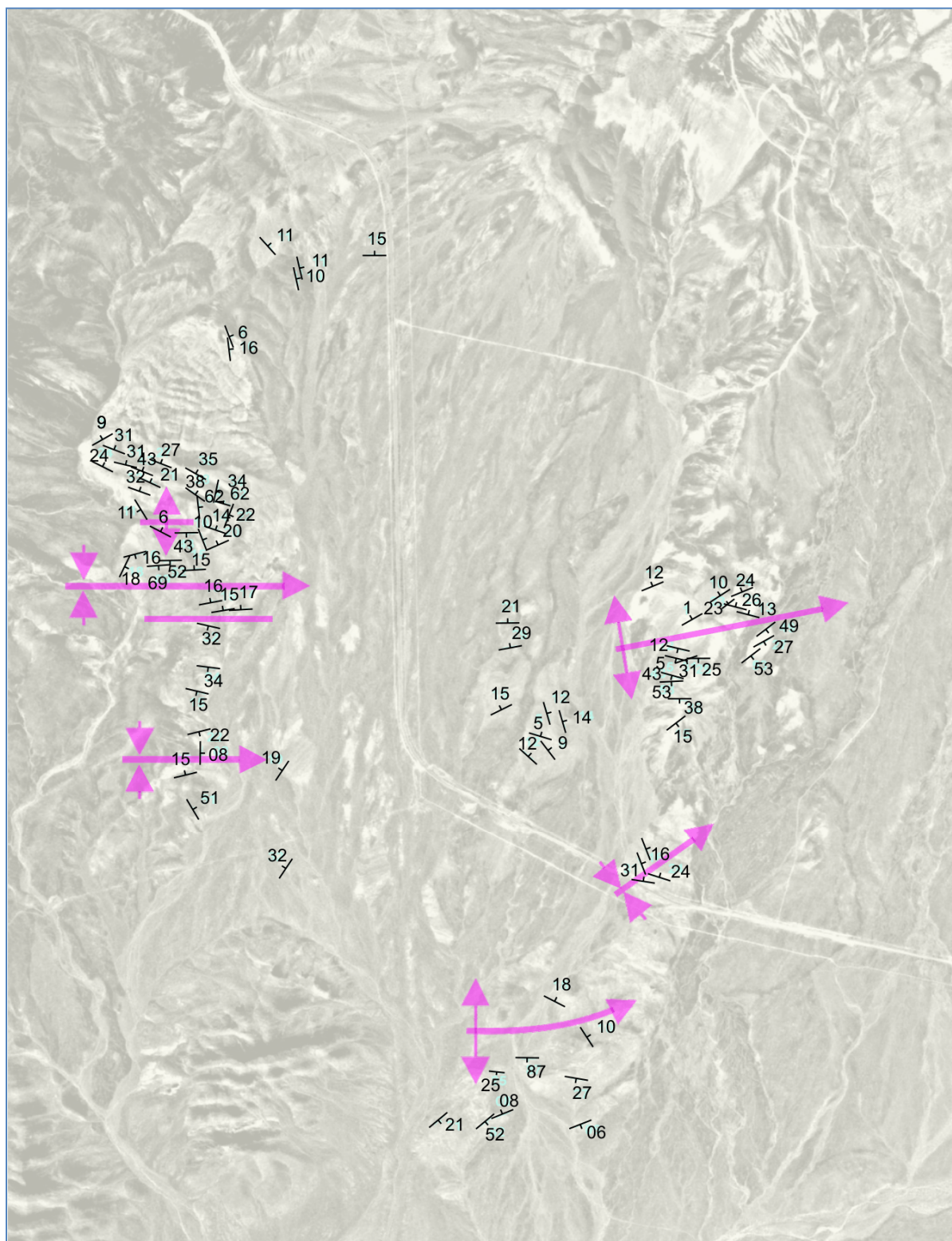


Figure 3.2-9
Aerial photo depicting folds in Tertiary strata of Pavits Spring east of Yucca Mountain along Jackass Flats Road.



Figure 3.2-10

Photo showing brecciated Nopah Formation along the Point of Rocks detachment. Clasts range in size from 1-20 cm, rock hammer for scale.

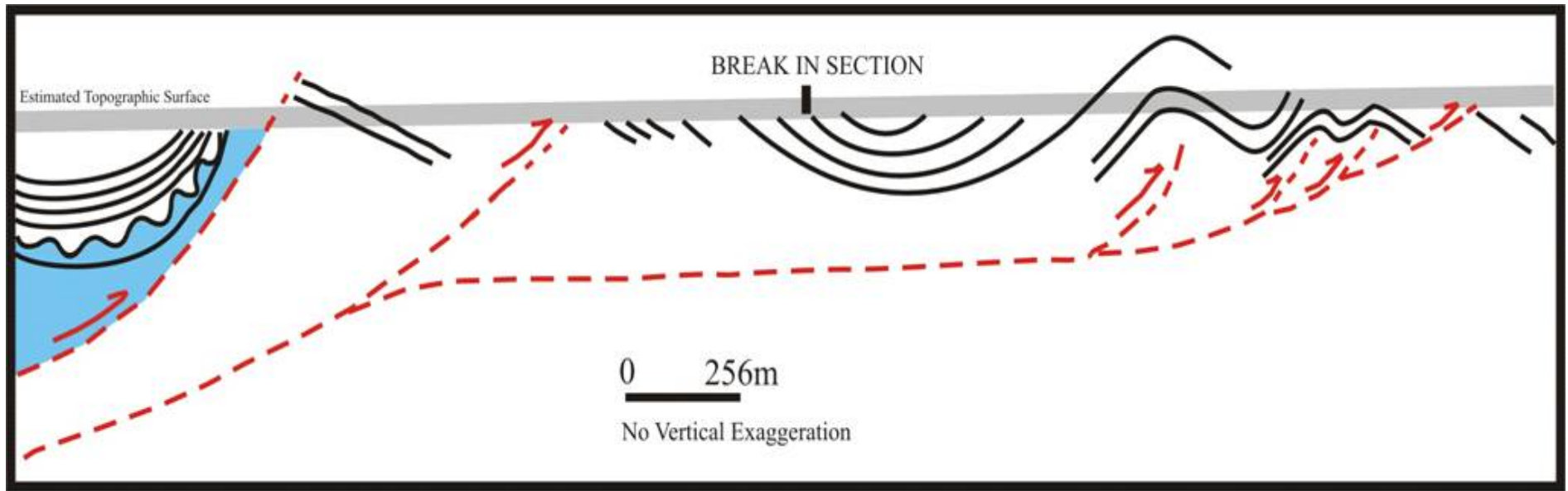


Figure 3.2-11
Working cross-section of folds in Tertiary strata of Pavits Spring east of Yucca Mountain from south to north.

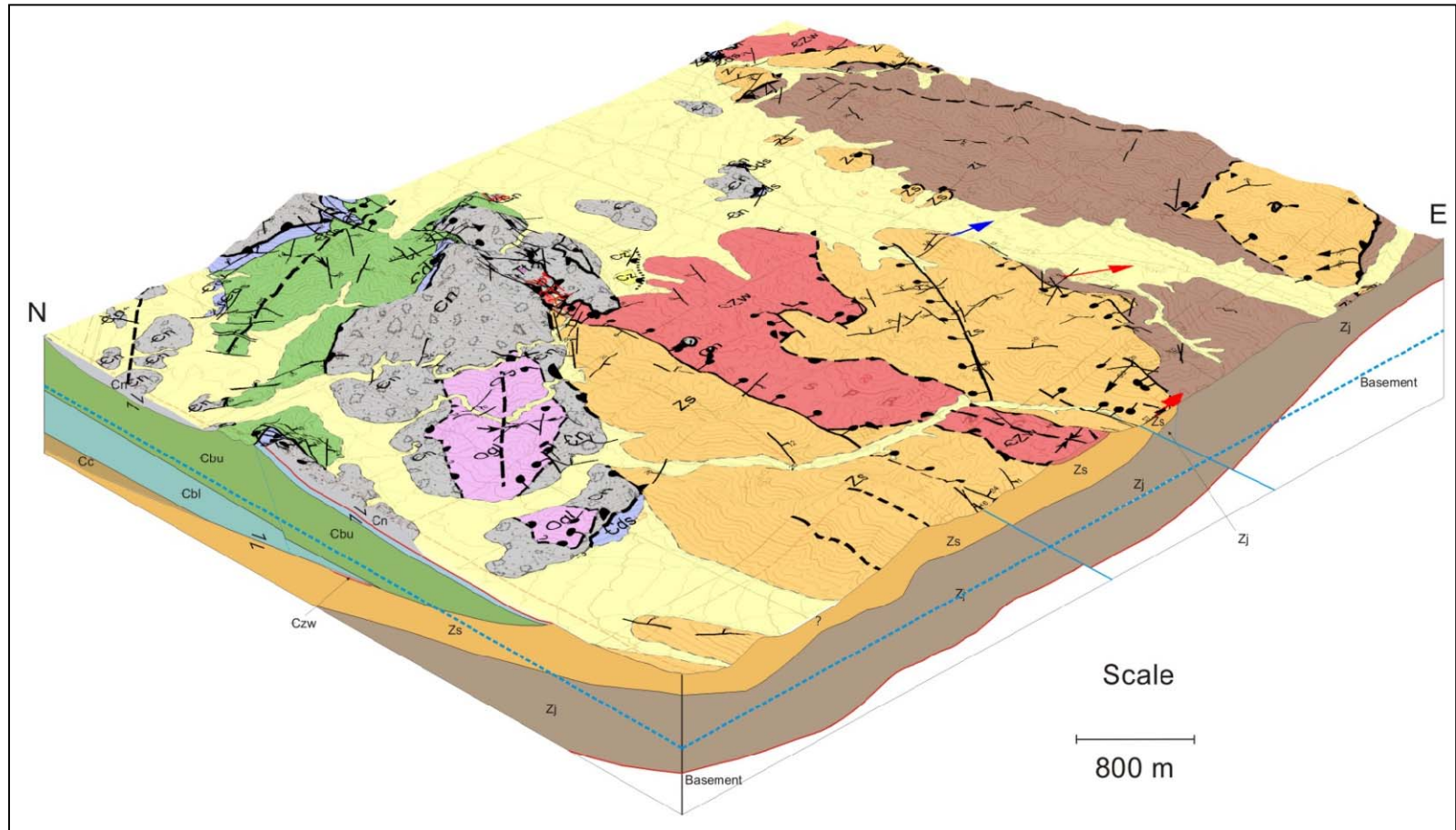


Figure 3.2-12

Schematic block diagram of part of study area. Red lines represent detachment faults; red arrows show trend and plunge of lineations; blue lines represent normal faults; dashed blue lines represent the potentiometric surface and black lines represent formation contacts.

Note north plunging folds in the Stirling Quartzite, Wood Canyon, and Johnnie Formations on the south half of the diagram.

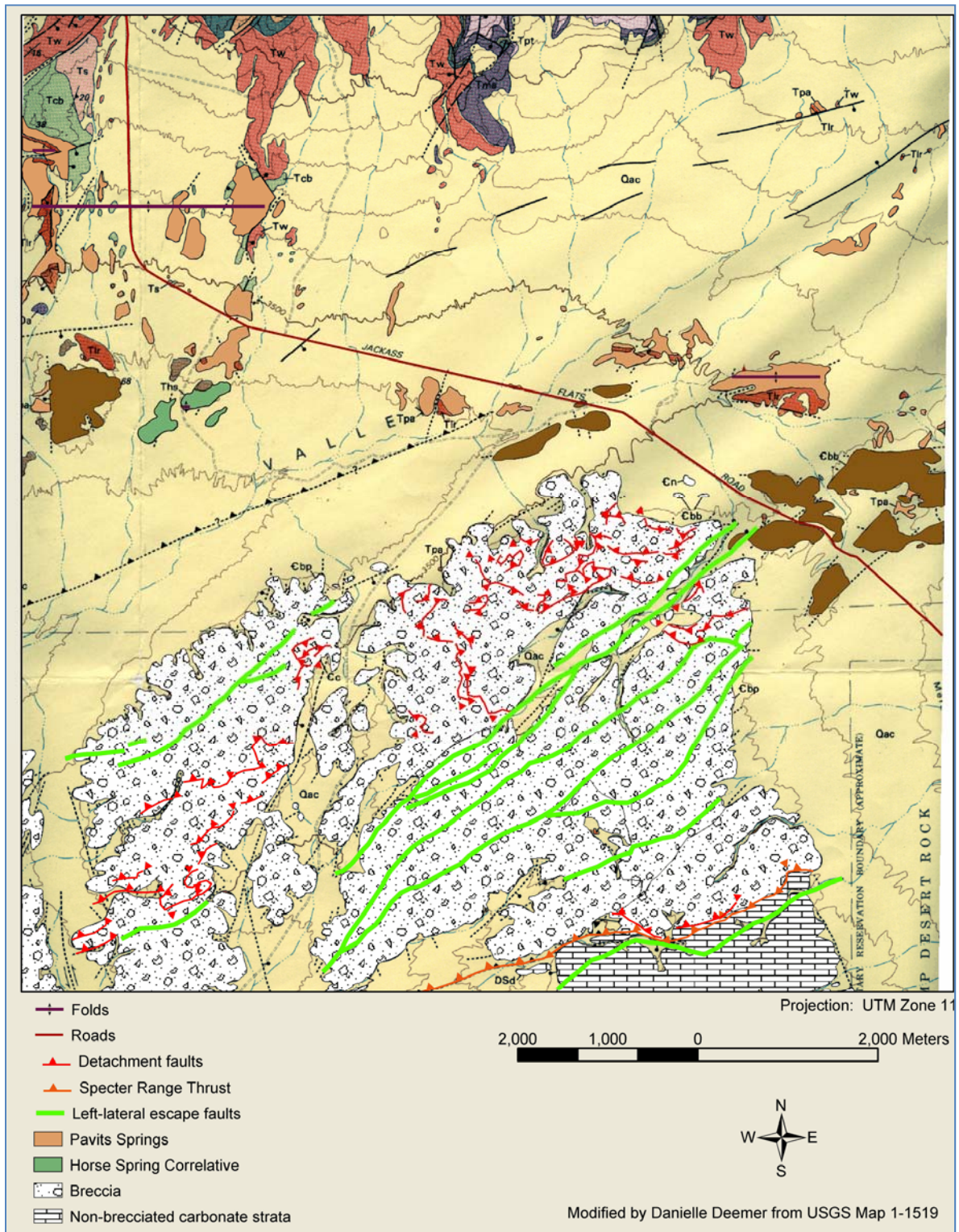


Figure 3.2-13
Structure map of northeastern Specter Range

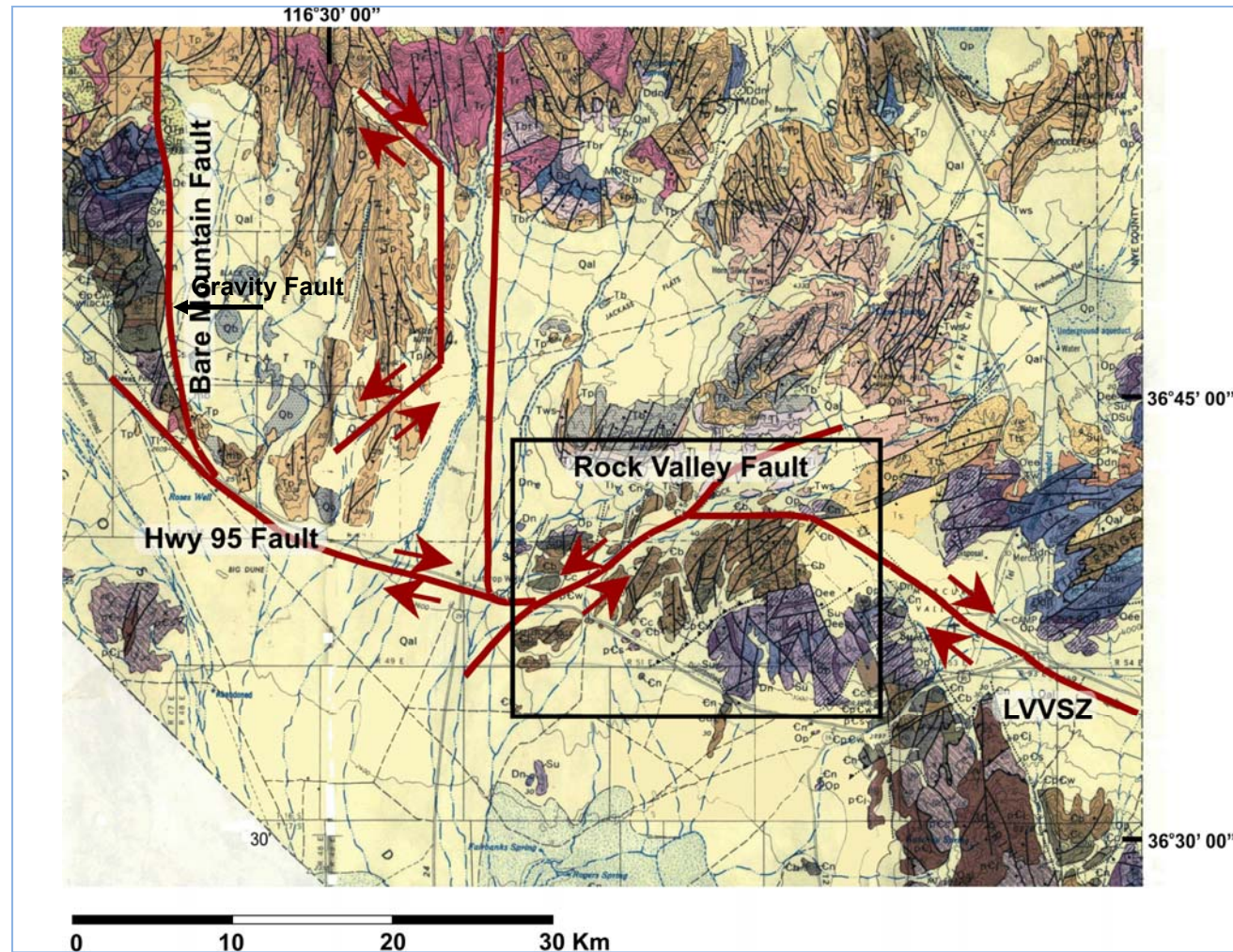
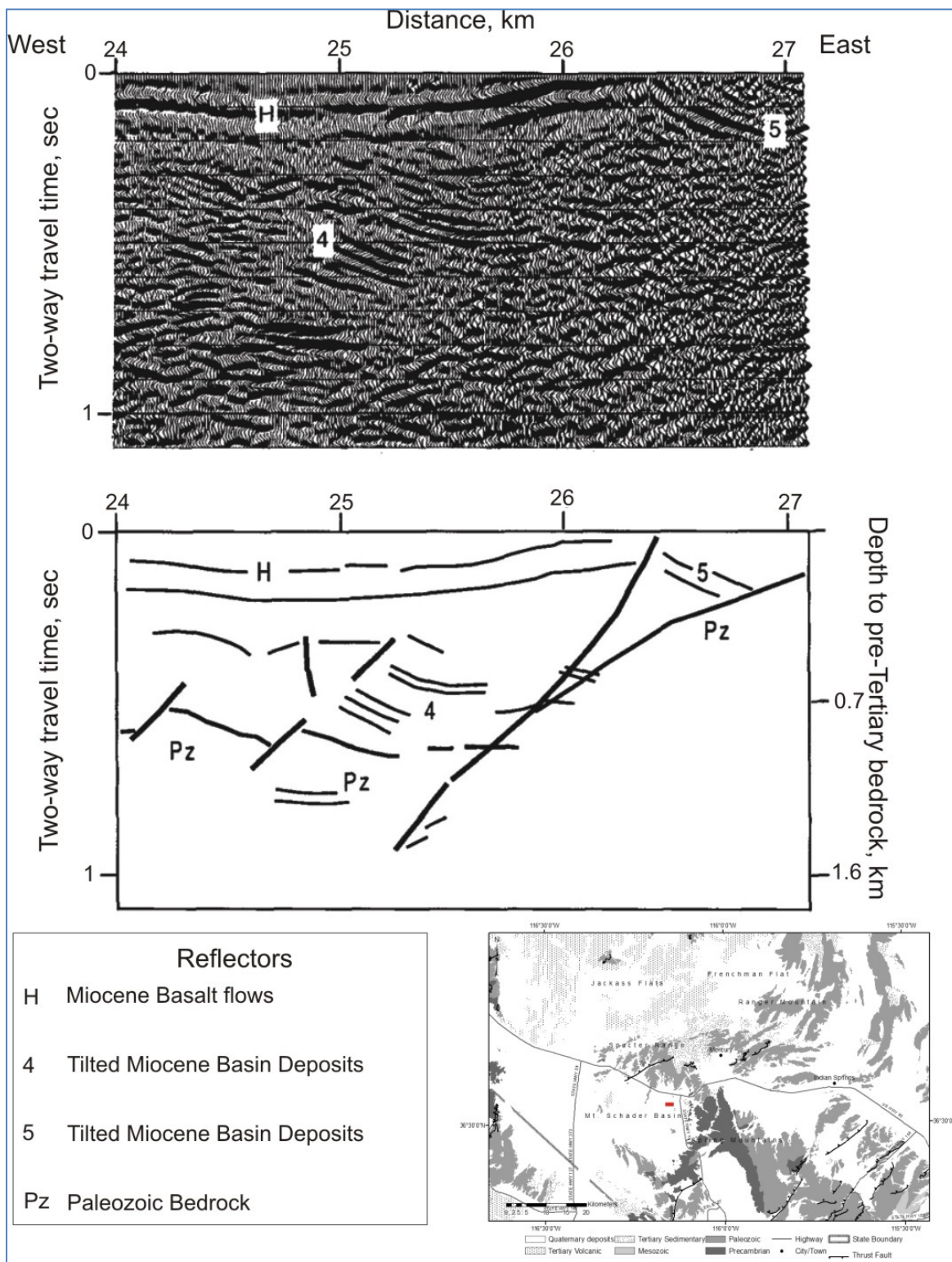


Figure 3.2-14

Geologic Map with major faults of the southwestern part of the Nevada Test Site: Northern Spring Mountains, Jackass Flats, Crater Flat, Bare Mountain and southeastern Amargosa Valley. LVVSZ and Highway 95 fault were active between ~16 and 10 Ma. and Rock Valley Fault and faults affecting strata in Crater Flat, active mainly after 10 Ma.

**Figure 3.2-15**

Diagrams showing the uninterpreted (top) and interpreted (middle) detail of the most easterly segment of the USGS seismic line AV-1. The red line segment on the regional map (lower right) shows the location of USGS seismic line AV-1 Modified from Brocher and others, (1993).

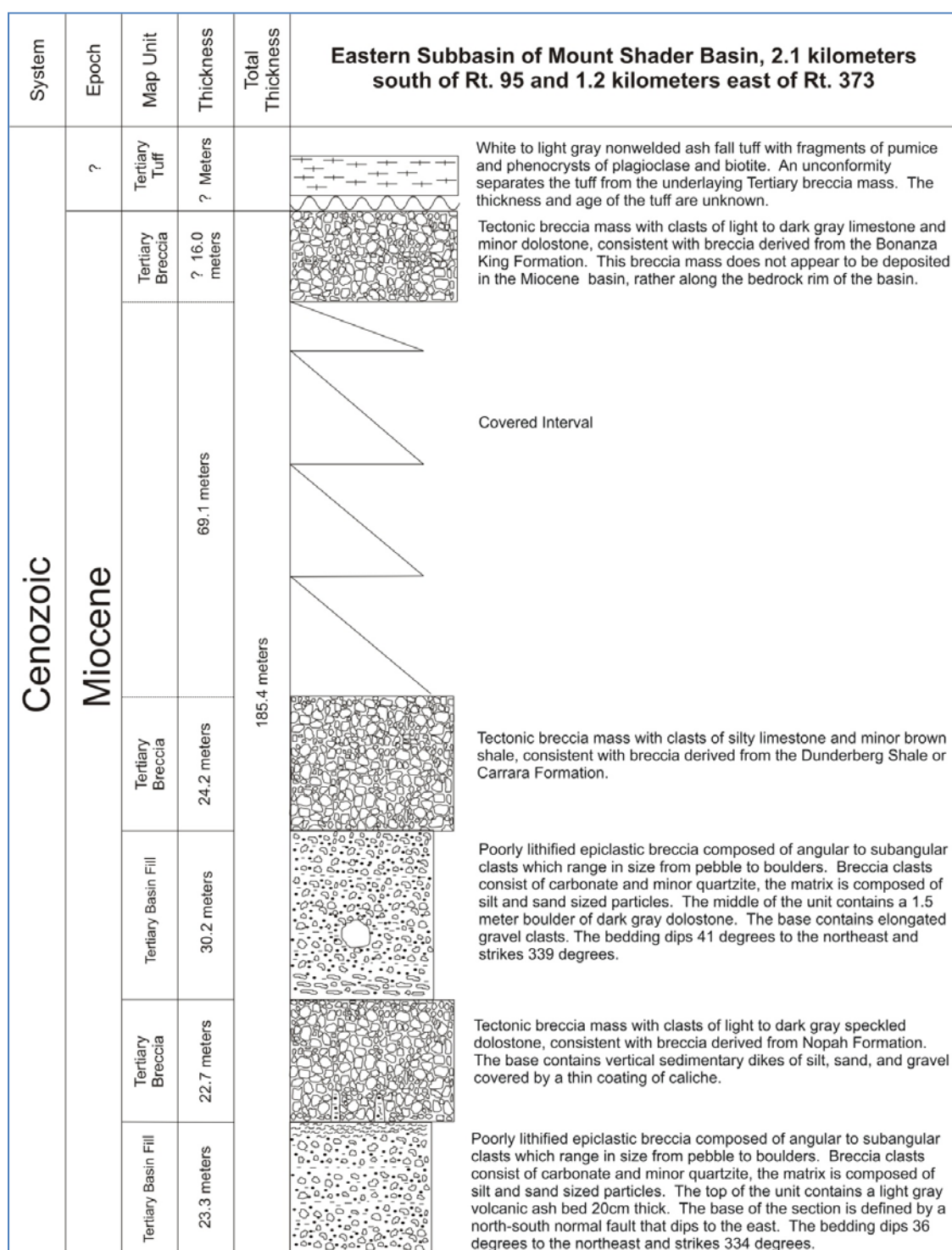


Figure 3.2-16

Stratigraphic column showing a measured section of exposed Miocene deposits within the eastern subbasin of the Mt. Shader basin. The thicknesses of units are corrected for dip.

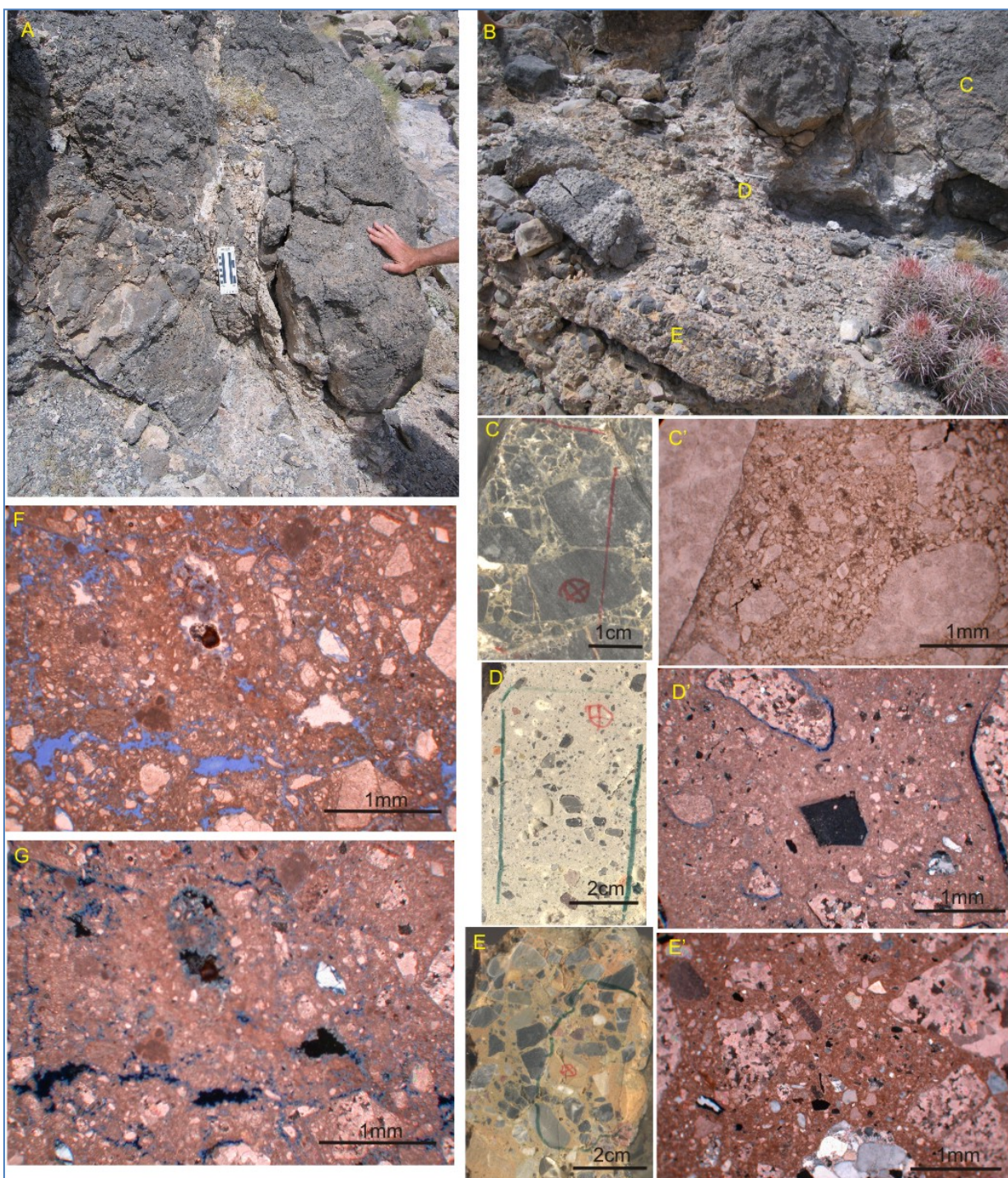


Figure 3.2-17

Photographs that show outcrops of Miocene basin deposits (A and B); and rocks sampled from Miocene basin units (C, D and E). Locations are shown in Photograph B. Photomicrographs show: cataclastic texture in a breccia mass (C', plane light); volcaniclastic ash bed with angular fragments of glass (D', crossed polars); epiclastic breccia with clasts of quartzite, dolomite, limestone, and volcanic fragments (E', crossed polars); and sedimentary dike (F, G) from location A showing clasts of glass, dolomite, and calcite, note similarity to D'.

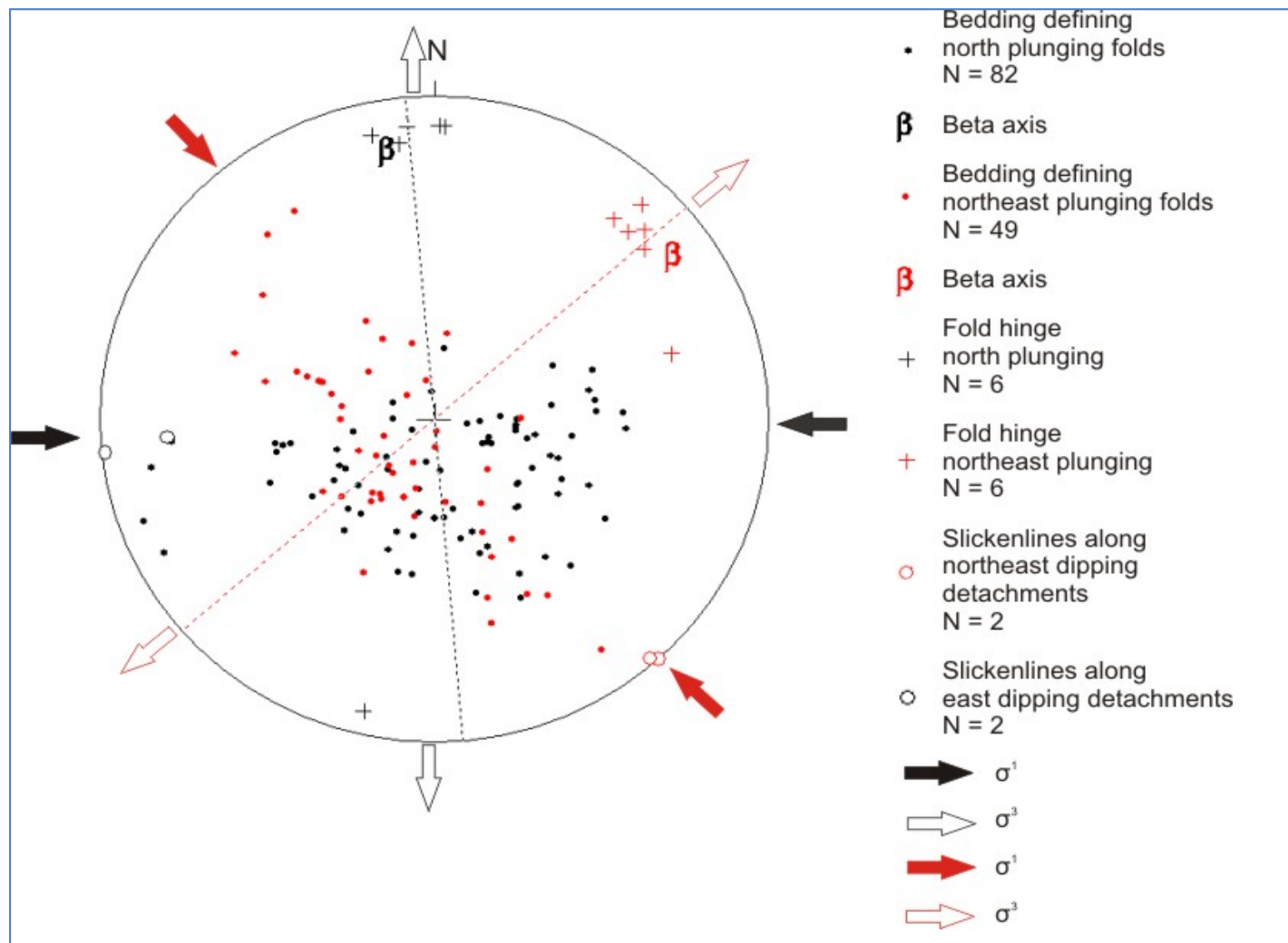


Figure 3.2-18

Equal area lower hemisphere stereogram of poles to bedding, folds, and slickenlines from the northern Spring Mountains. Dashed lines represent orthogonal lines to slickenlines, note the association with fold hinges. North-plunging folds are the oldest structures as they are cut by all other faults and folds. Northeast-southwest normal faults are cut by detachment faults and north-south normal faults. The detachments are next in age, as they are cut by north-south normal faults and detachment breccias are folded about northeast plunging hinges. Northeast plunging folds are cut by north-south normal faults indicating that north-south normal faults are the youngest structures in the northern Spring Mountains.

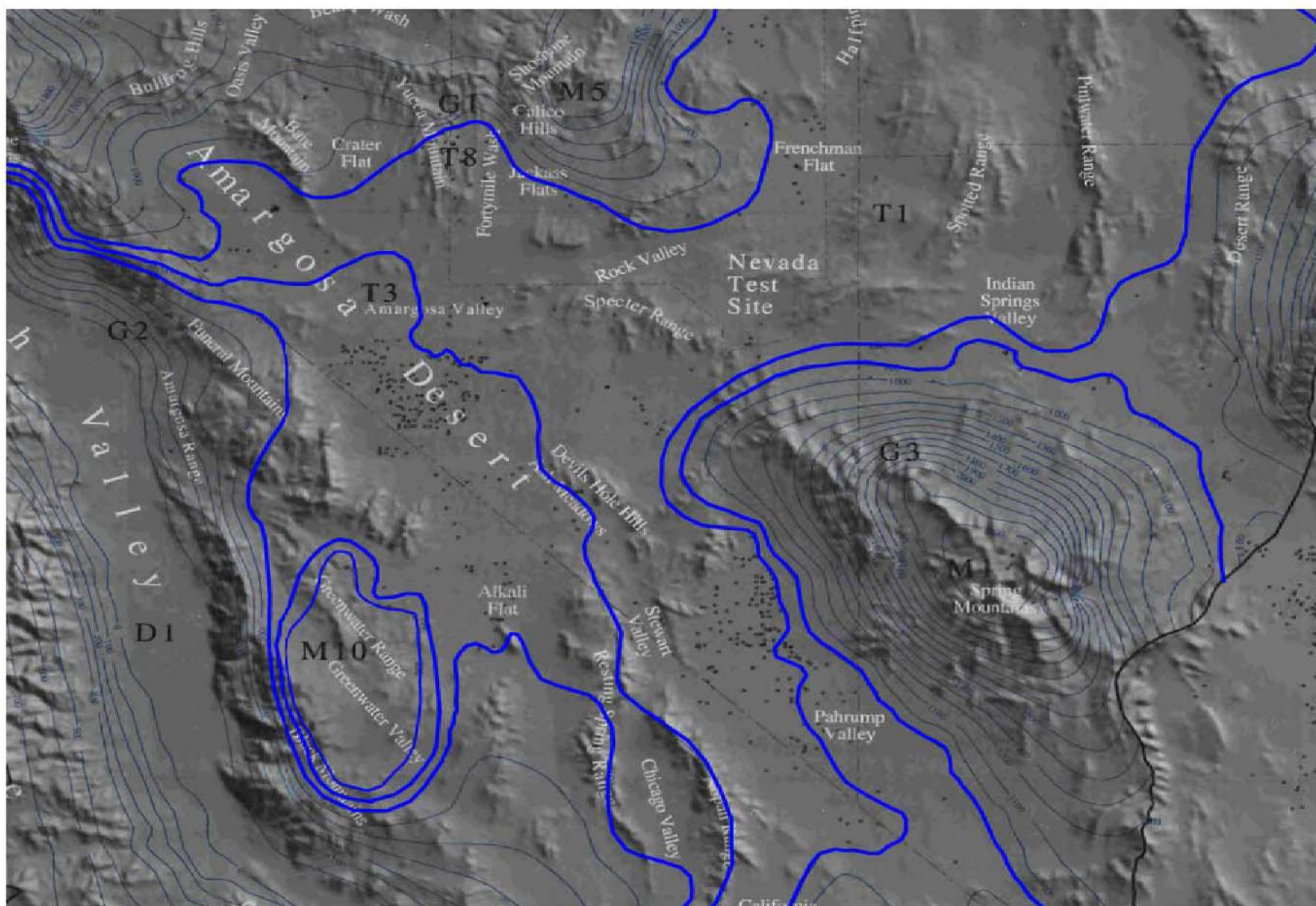
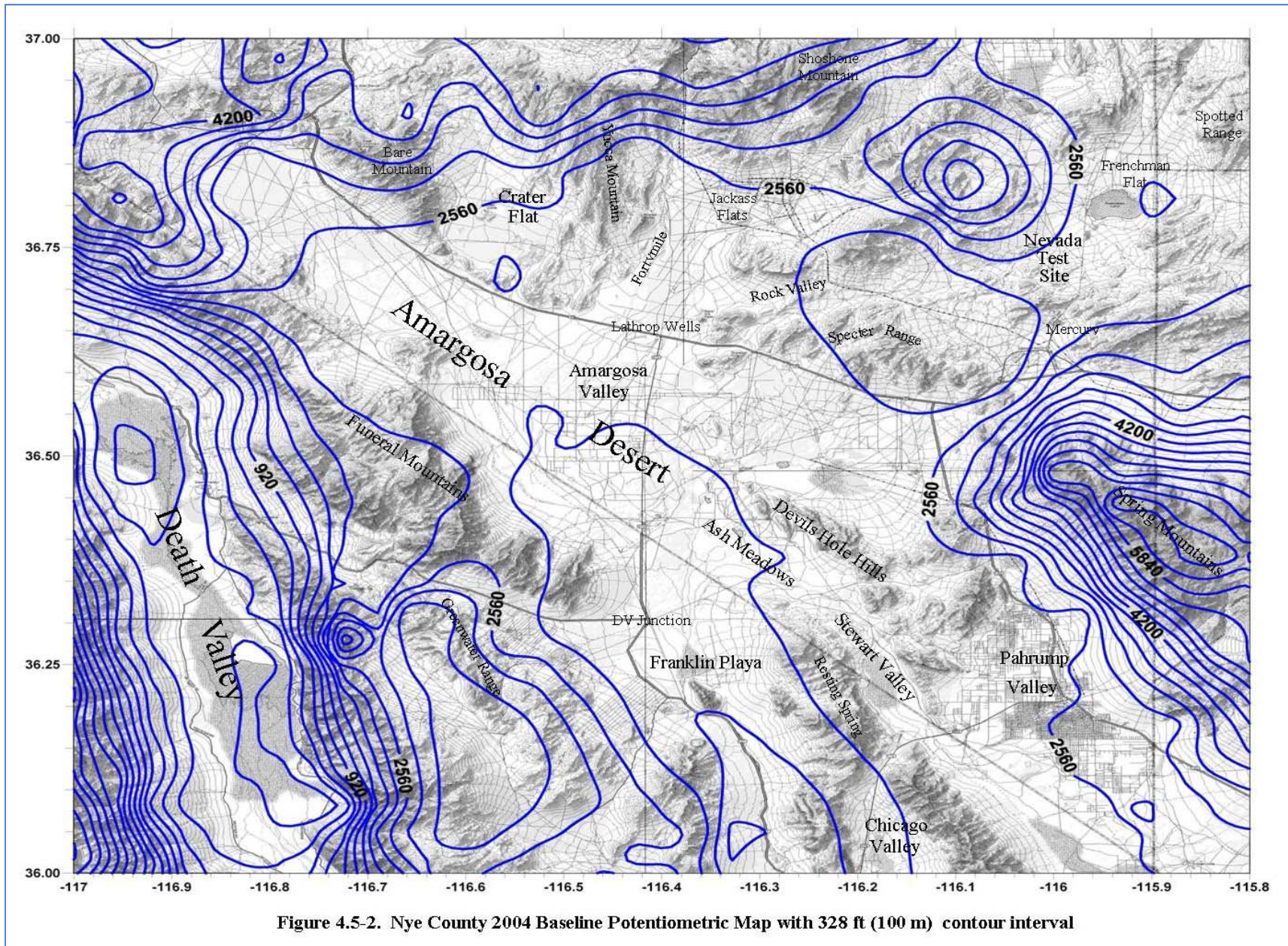


Figure 4.5-1. Regional Potentiometric Map with 100 meter contour interval



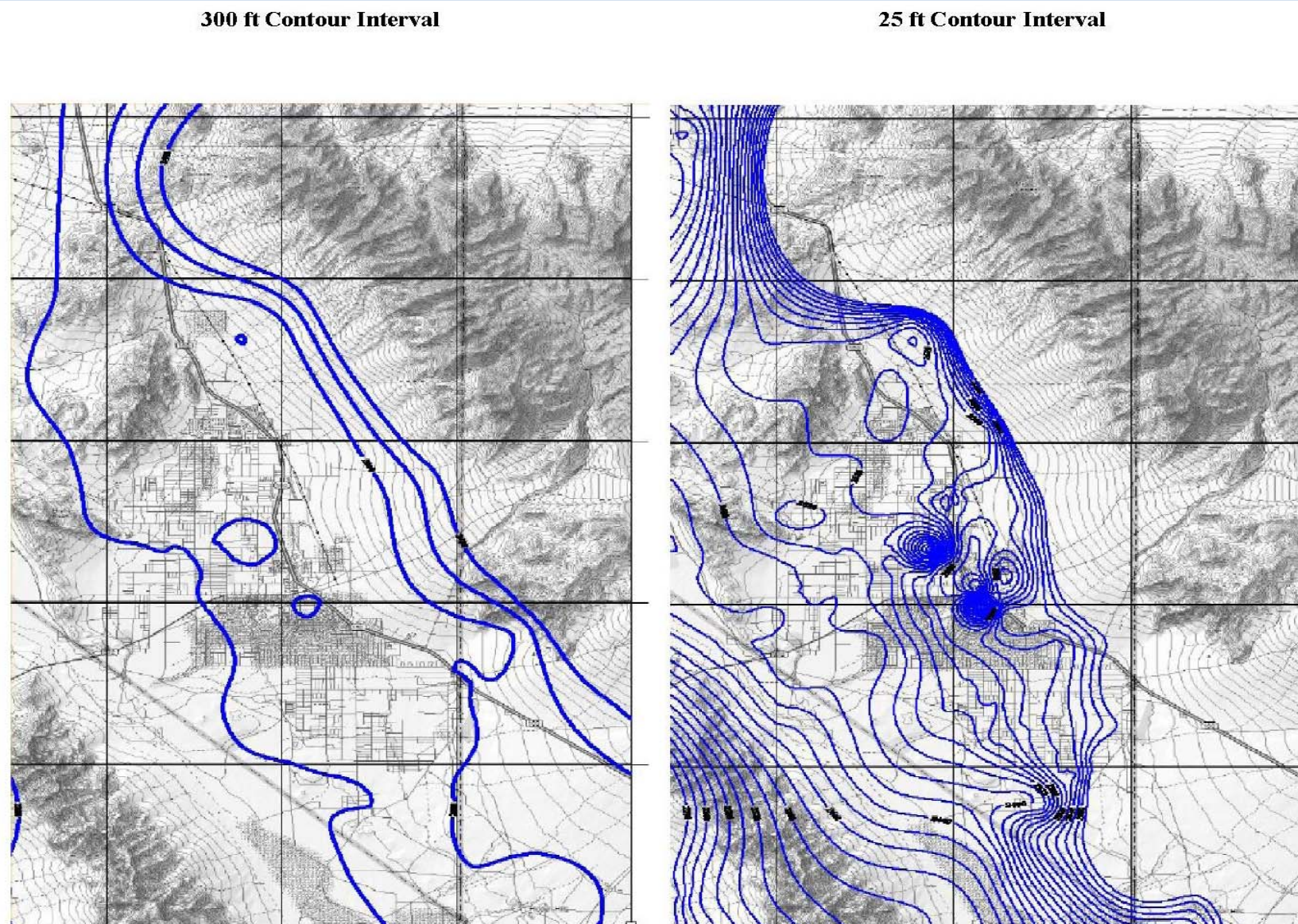


Figure 4.5-3. Pahrump Valley Potentiometric Maps
Decreasing contour intervals provide better definition of pumping centers

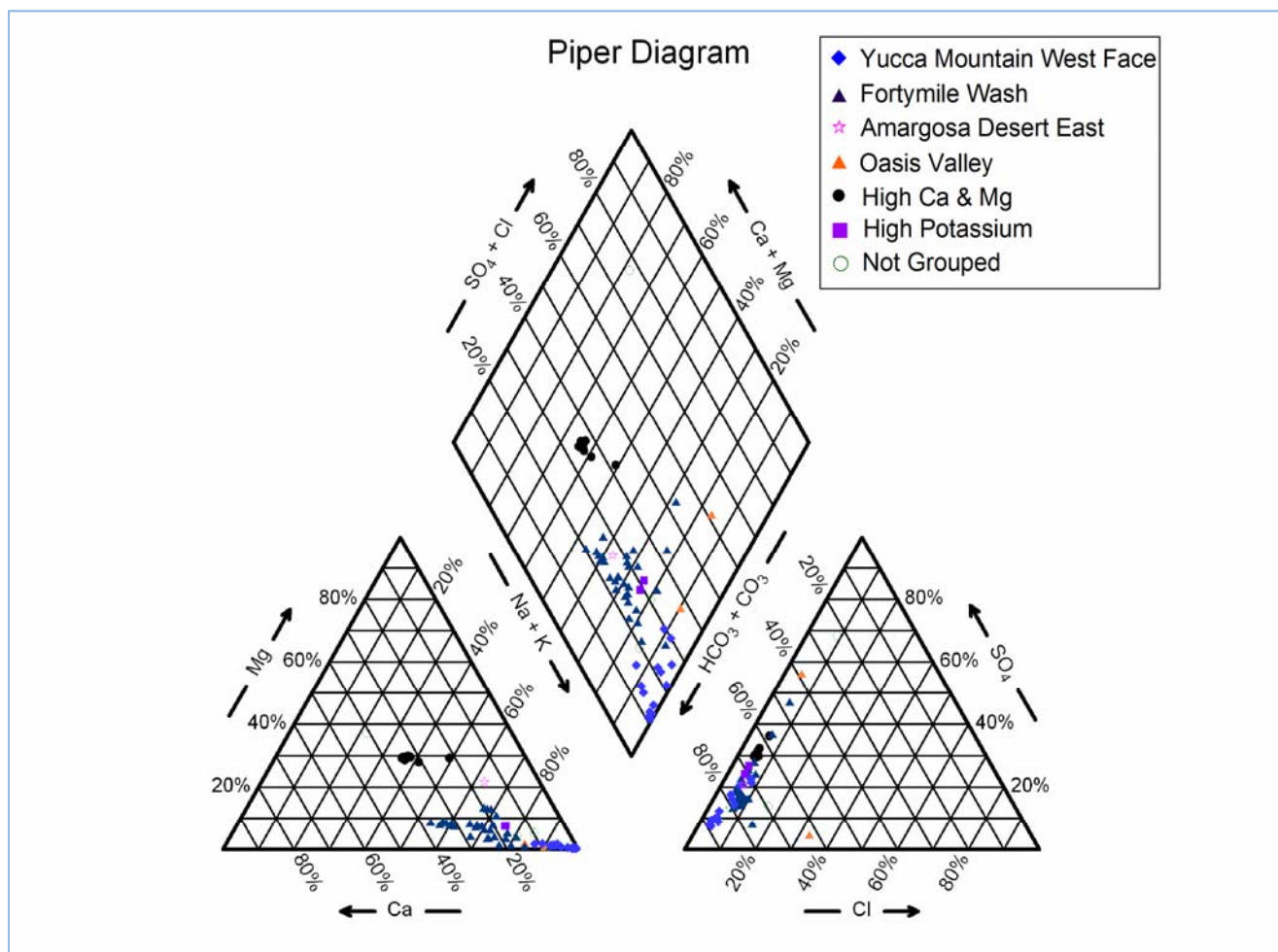


Figure 5.2-1
Piper Plot of Nye County Well Data

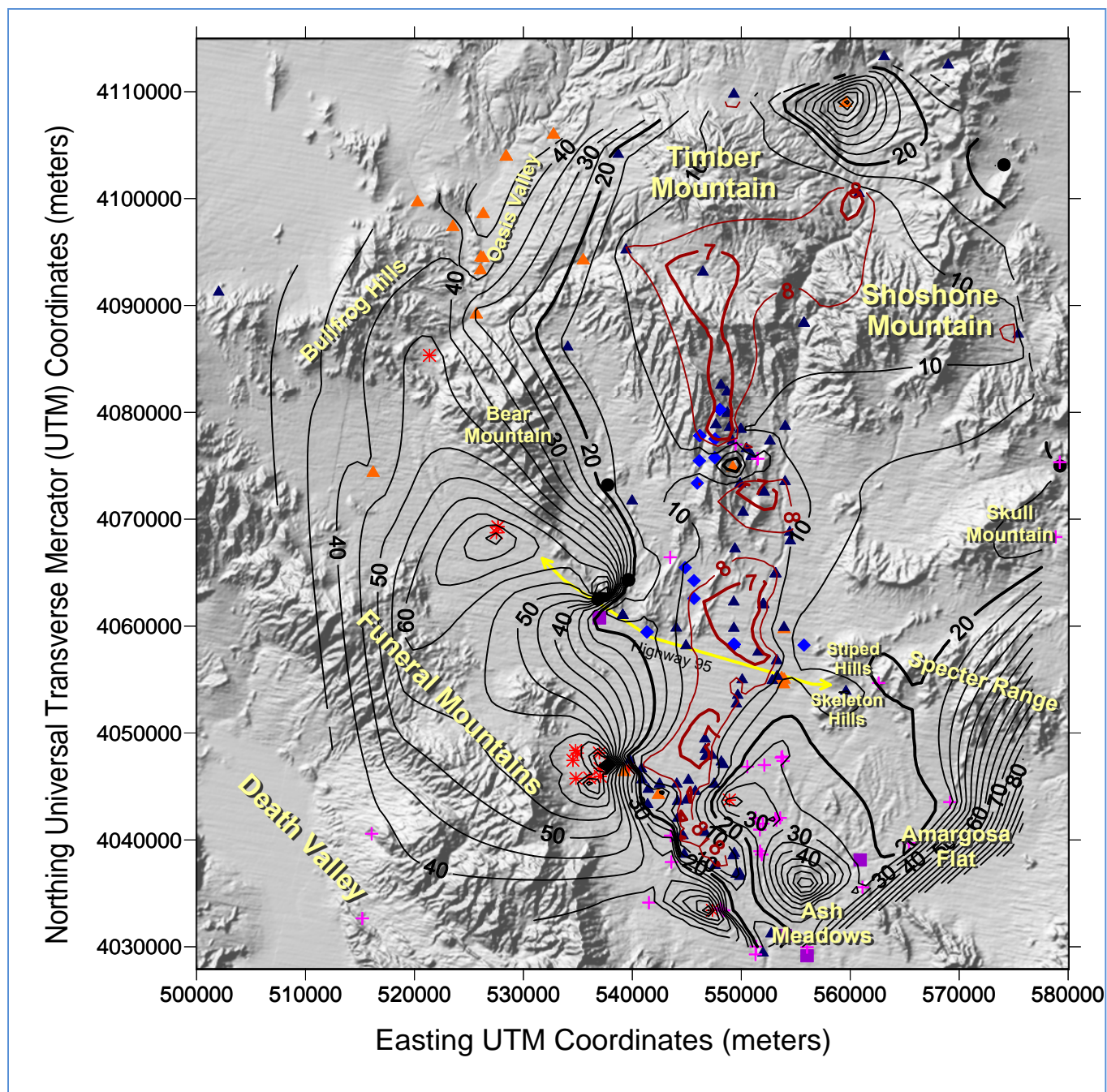


Figure 5.2-2
Contours of concentration in milligrams per liter with a thick contour at the dataset average and with maroon contours over Fortymile Wash. a) Ground water total dissolved solids; b) Ground water chloride.

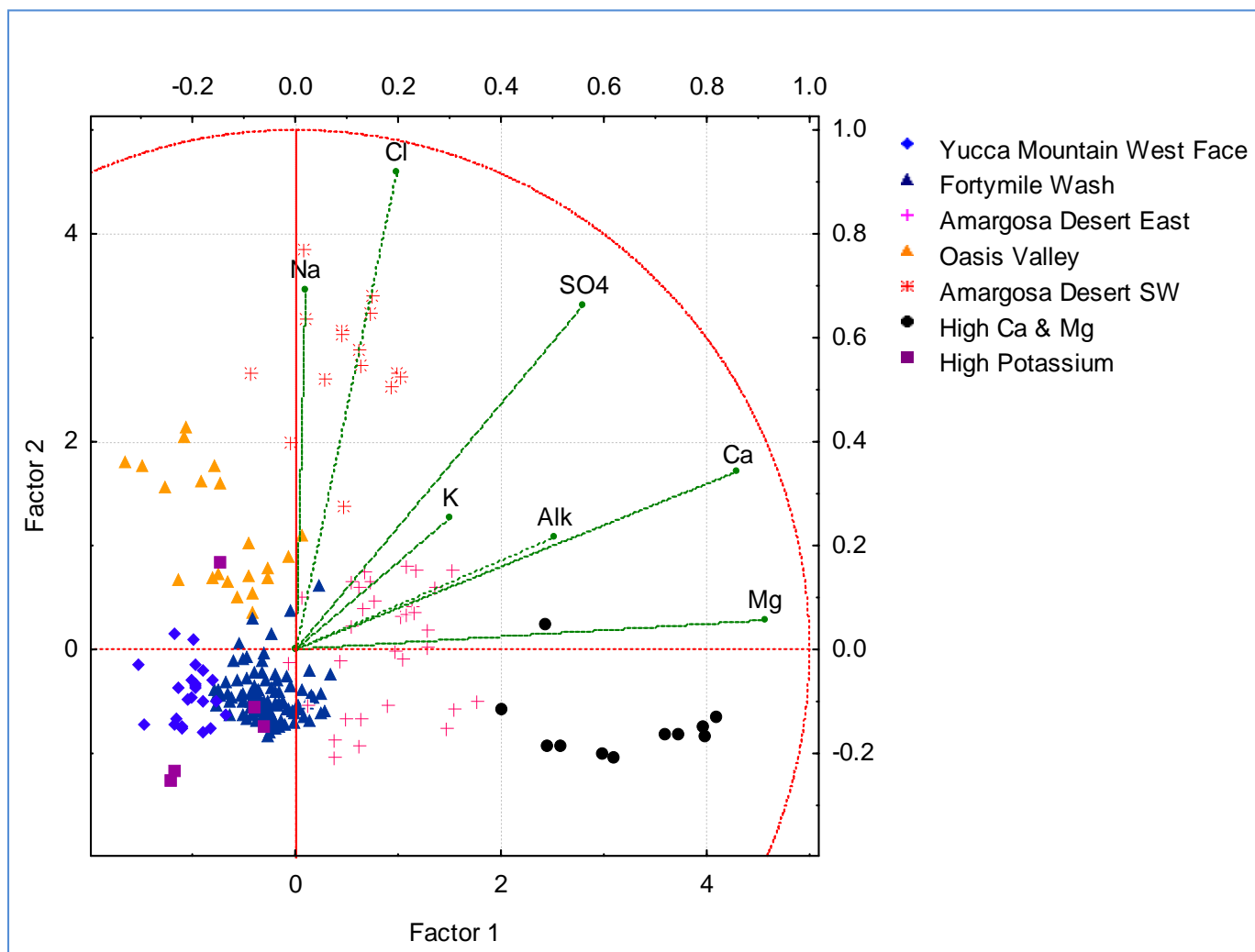


Figure 5.2-3
Principal component analysis biplot with samples grouped into seven hydrochemical facies and relevant major ions.

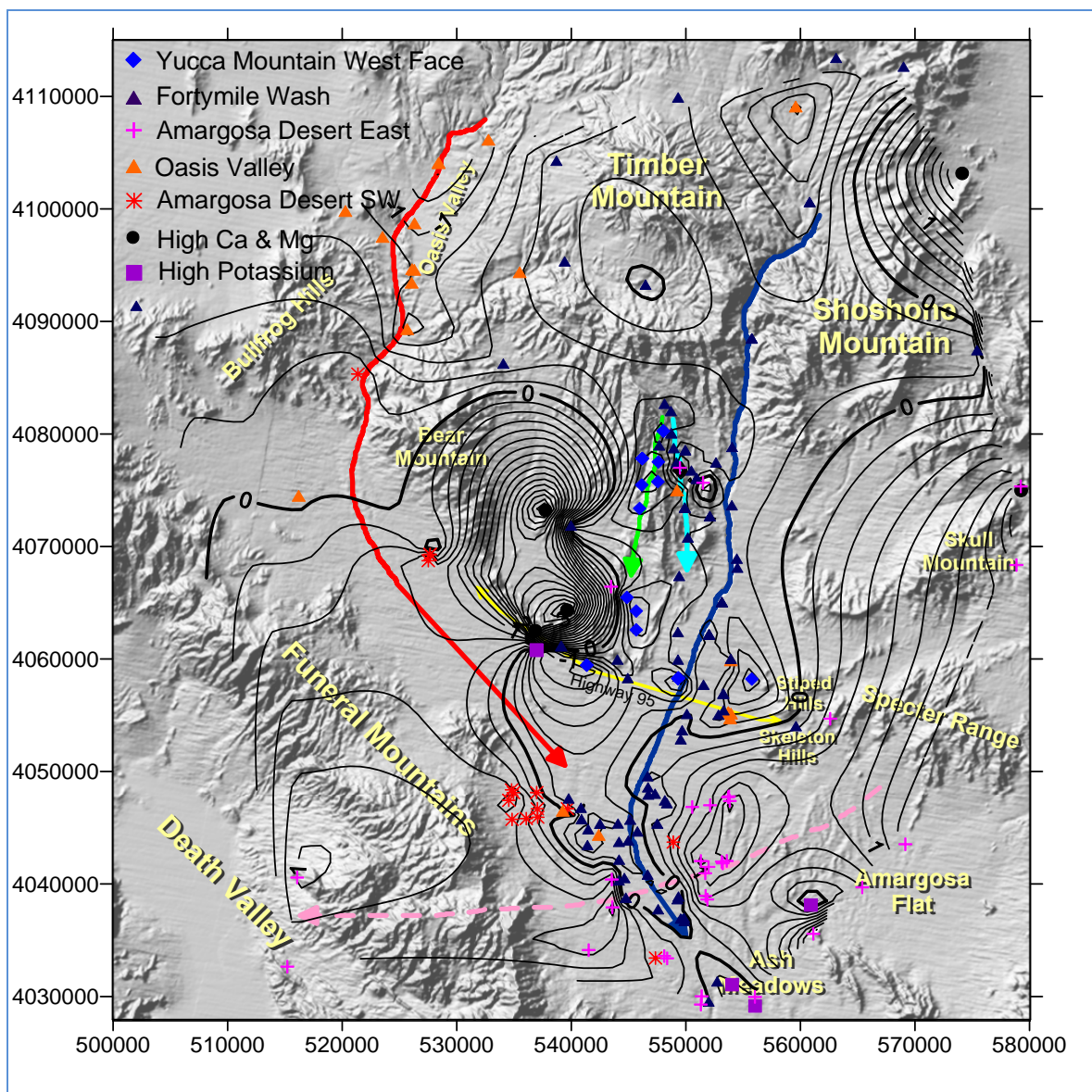


Figure 5.2-4
Factor 1 contours shown with well groupings and potential flow paths

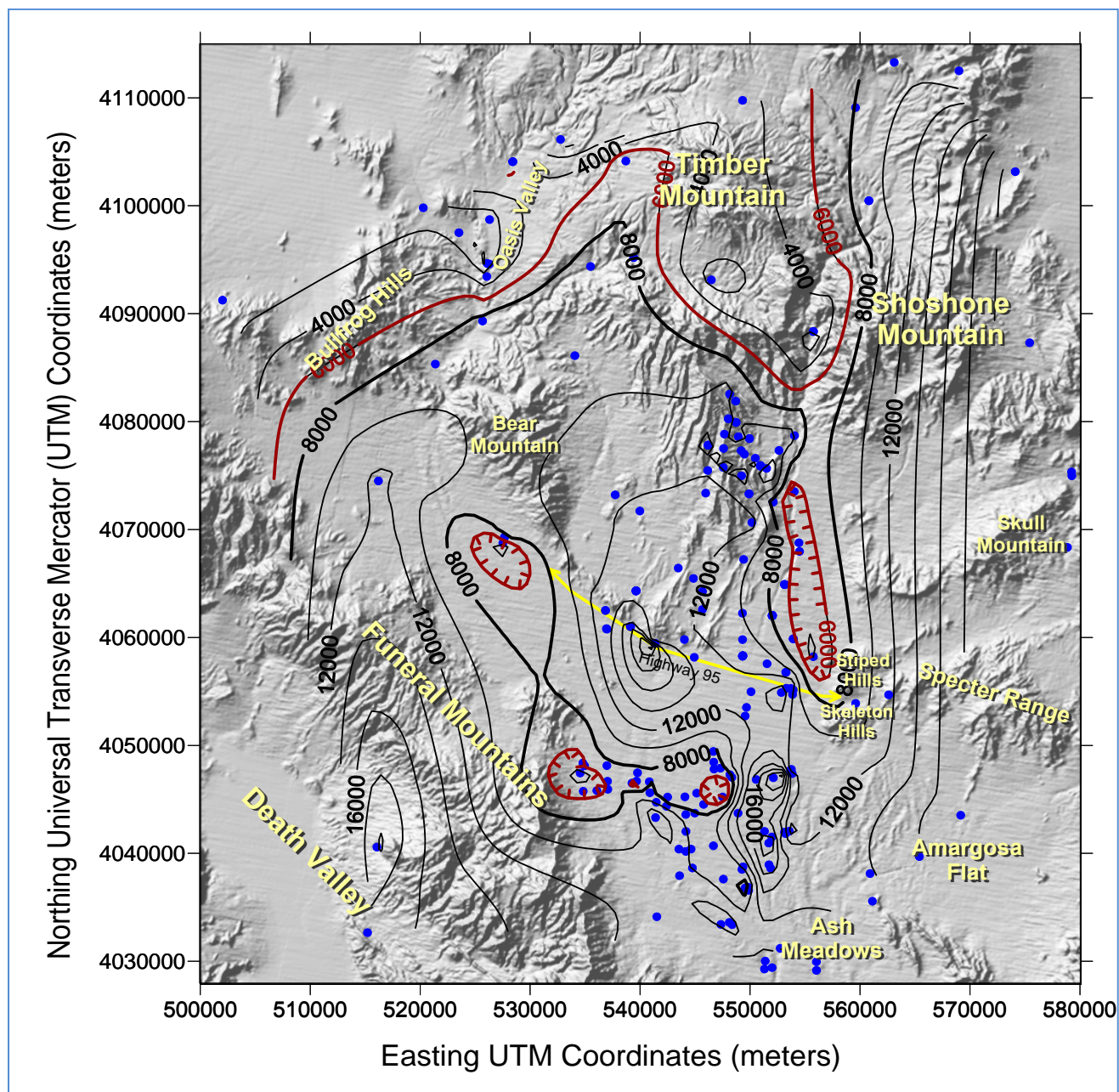


Figure 5.2-5
 ^{14}C age dates adjusted with ^{13}C data

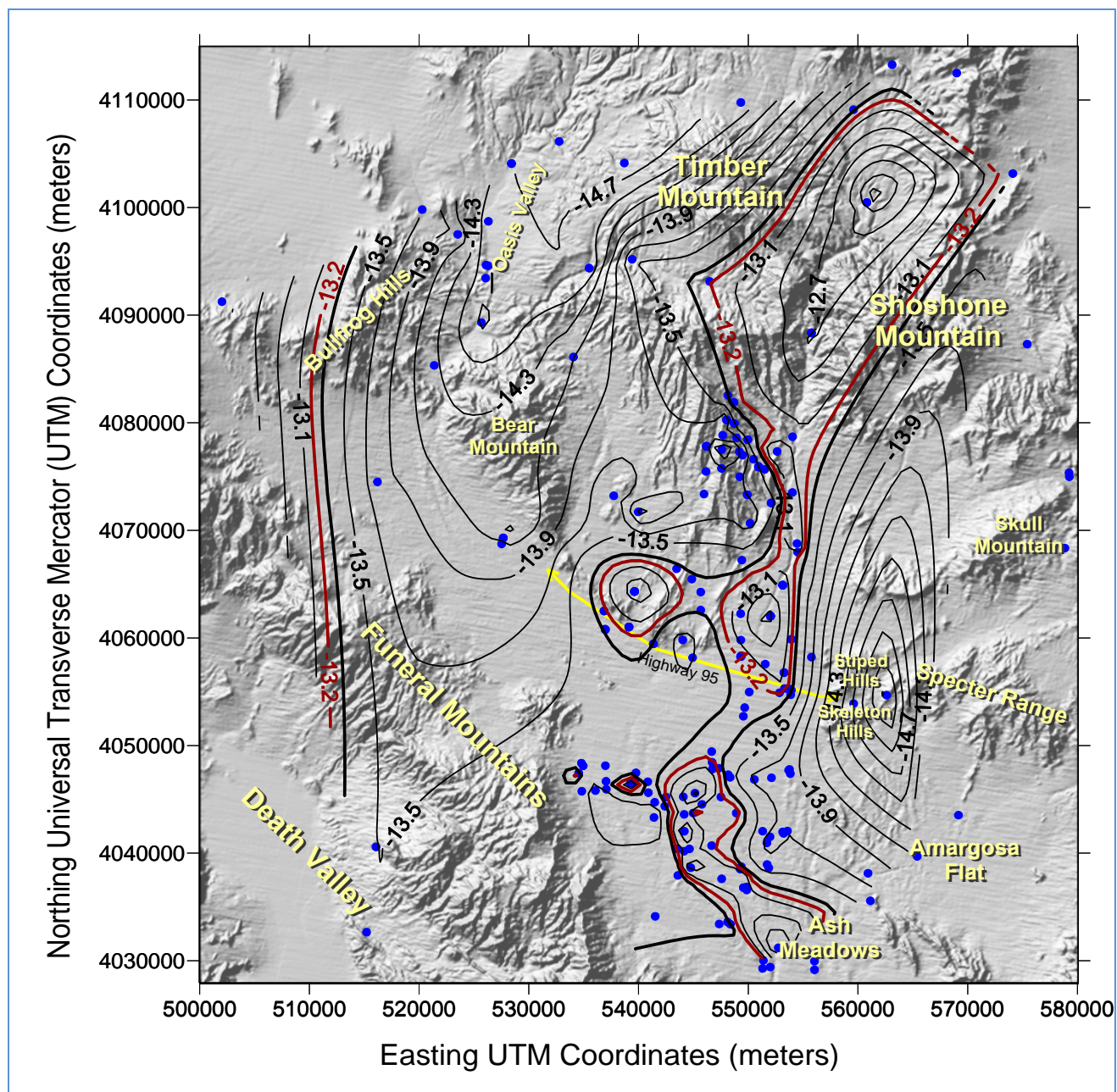


Figure 5.2-6
 $\delta^{18}\text{O}$ data contoured over the Digital Elevation Model

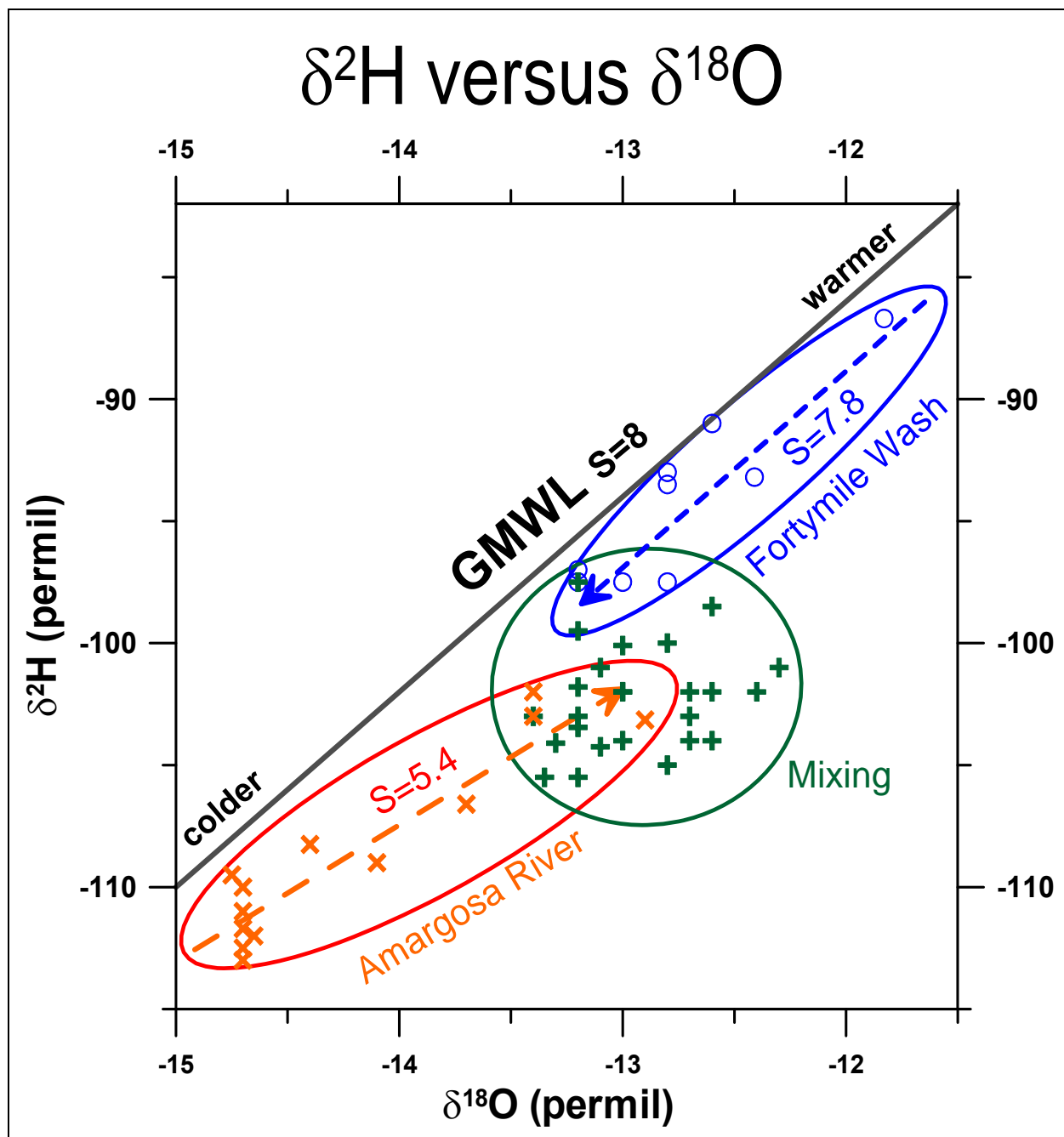


Figure 5.2-7

^2H versus ^{18}O groundwater values beneath Fortymile Wash, the Amargosa River, and the junction of the two, plotted against the GMWL

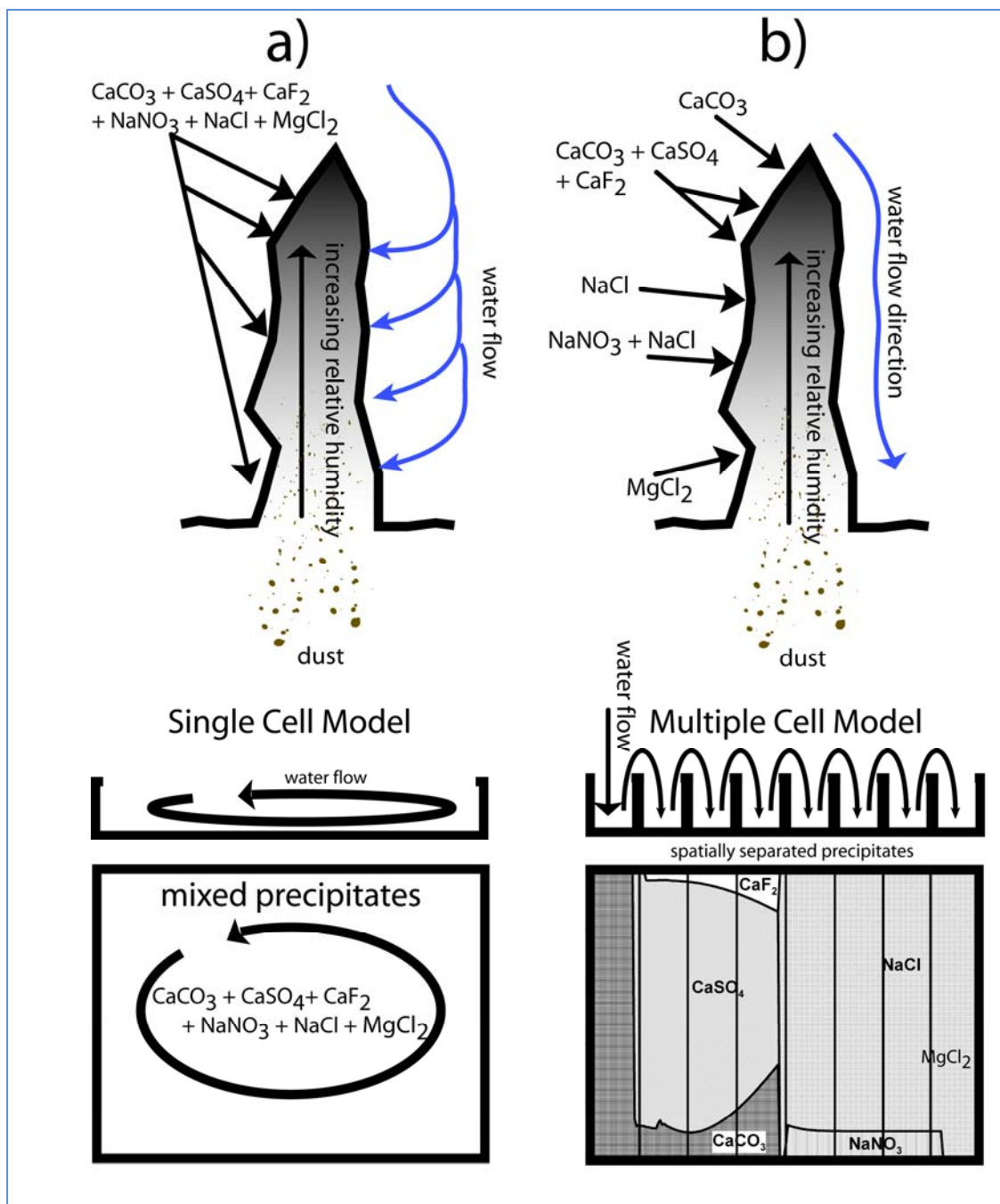


Figure 5.3-1
Flow separation of anion

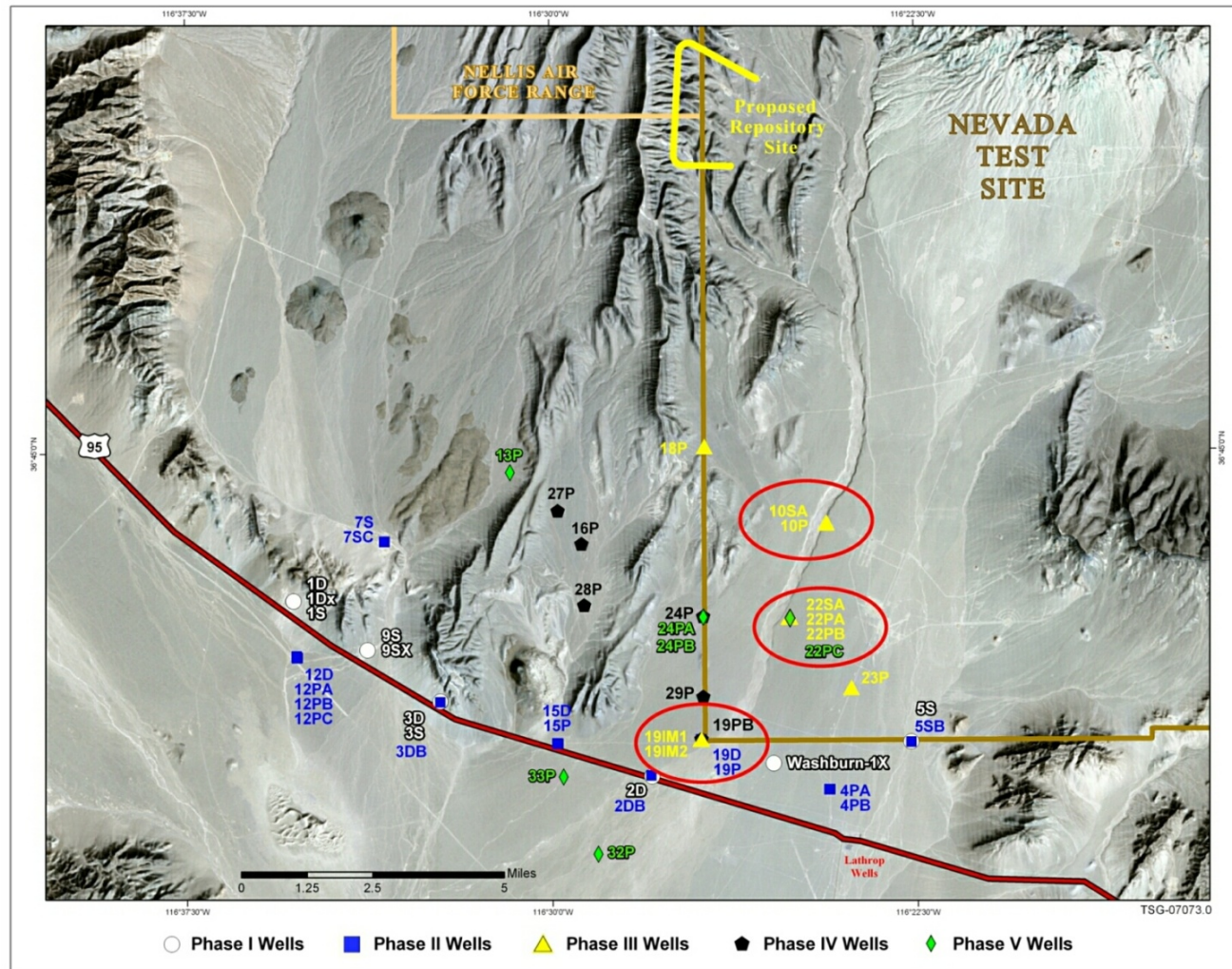


Figure 6.0-1
Location of Sites 19, 10, and 22 in relation to other nearby EDWP wells
and the proposed Yucca Mountain repository site.

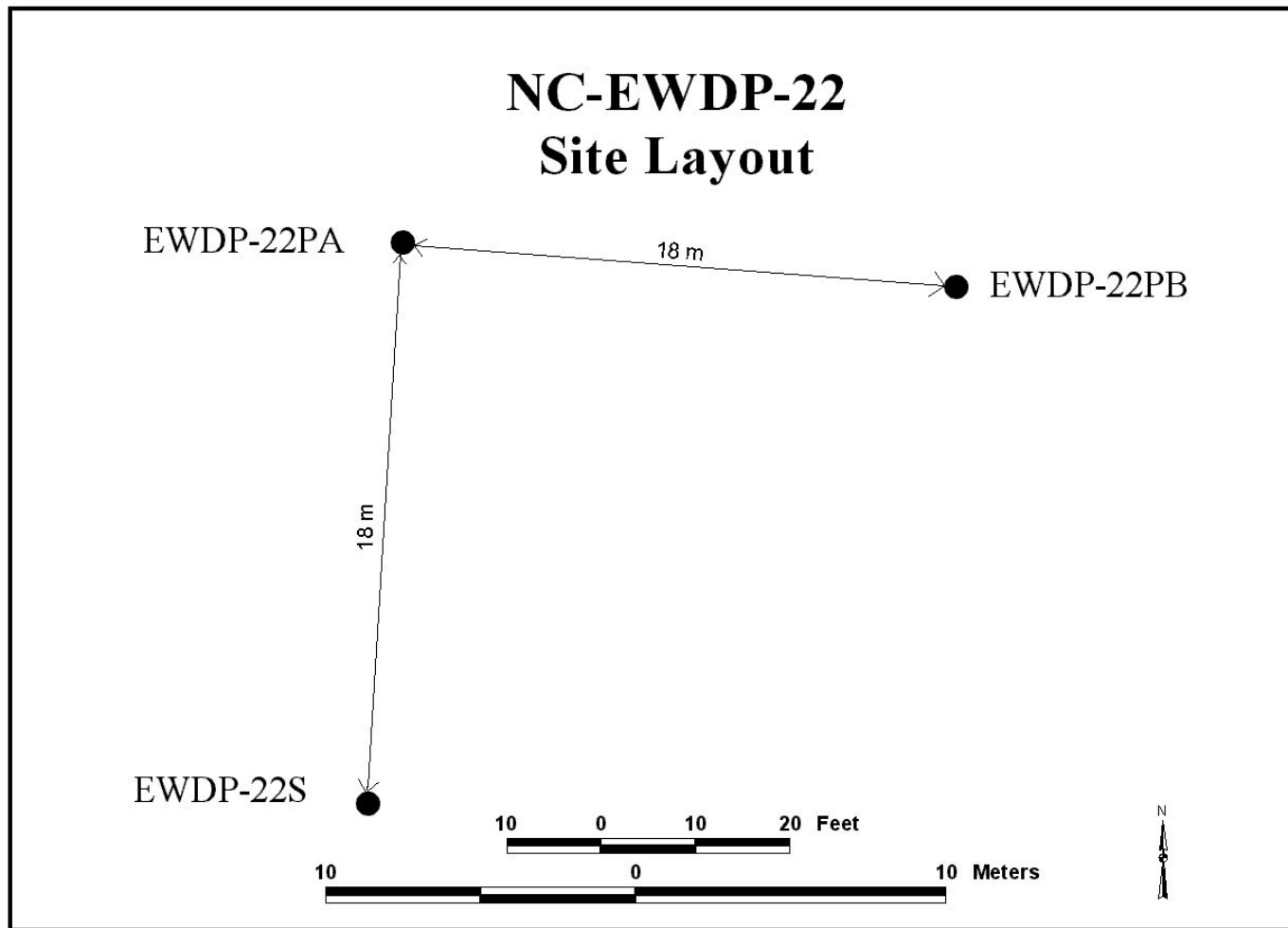


Figure 6.1-1
Site 22 Layout for Aquifer Tests

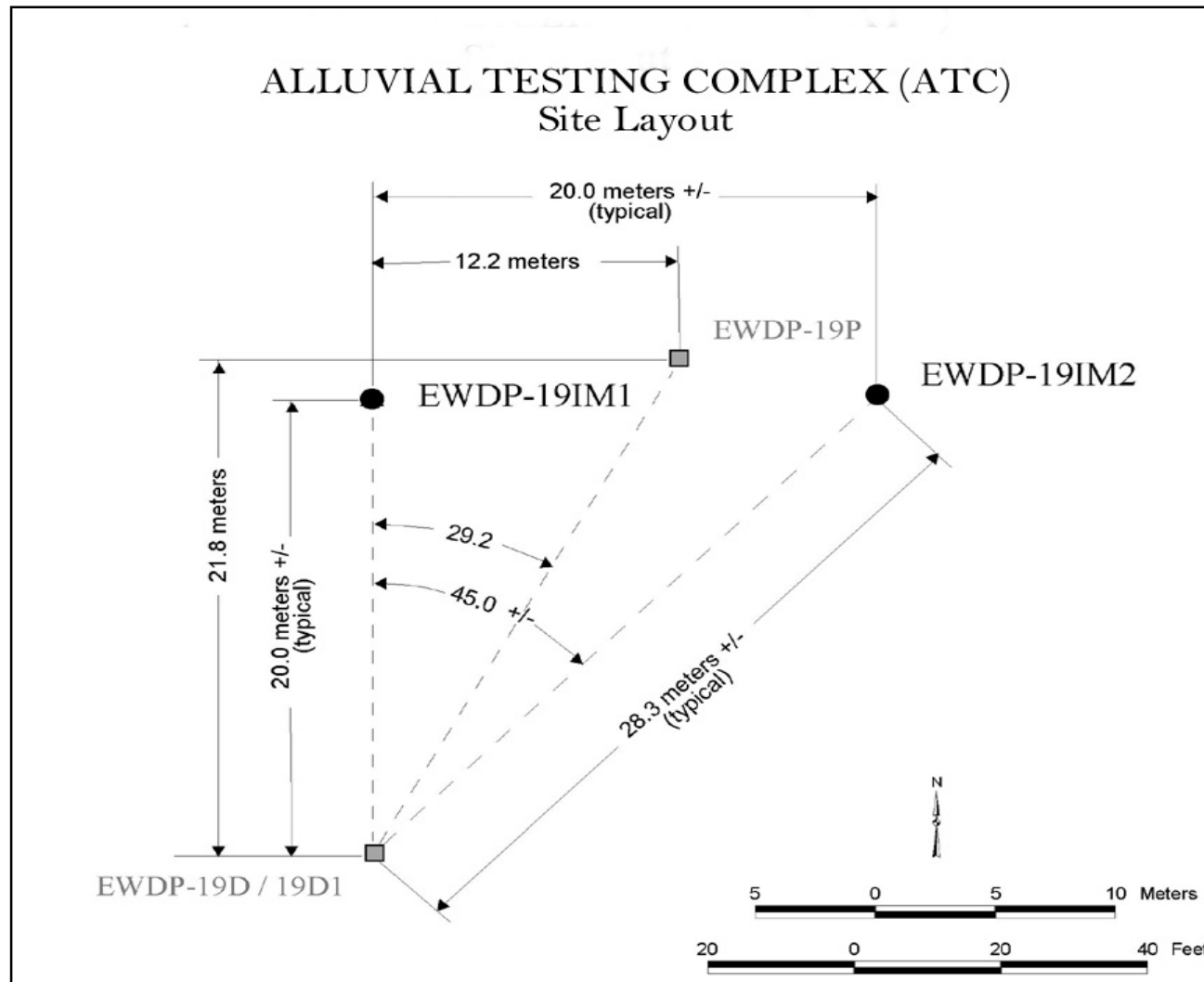


Figure 6.1-2
Location of Pump and Observation Wells at the Site 19 ATC

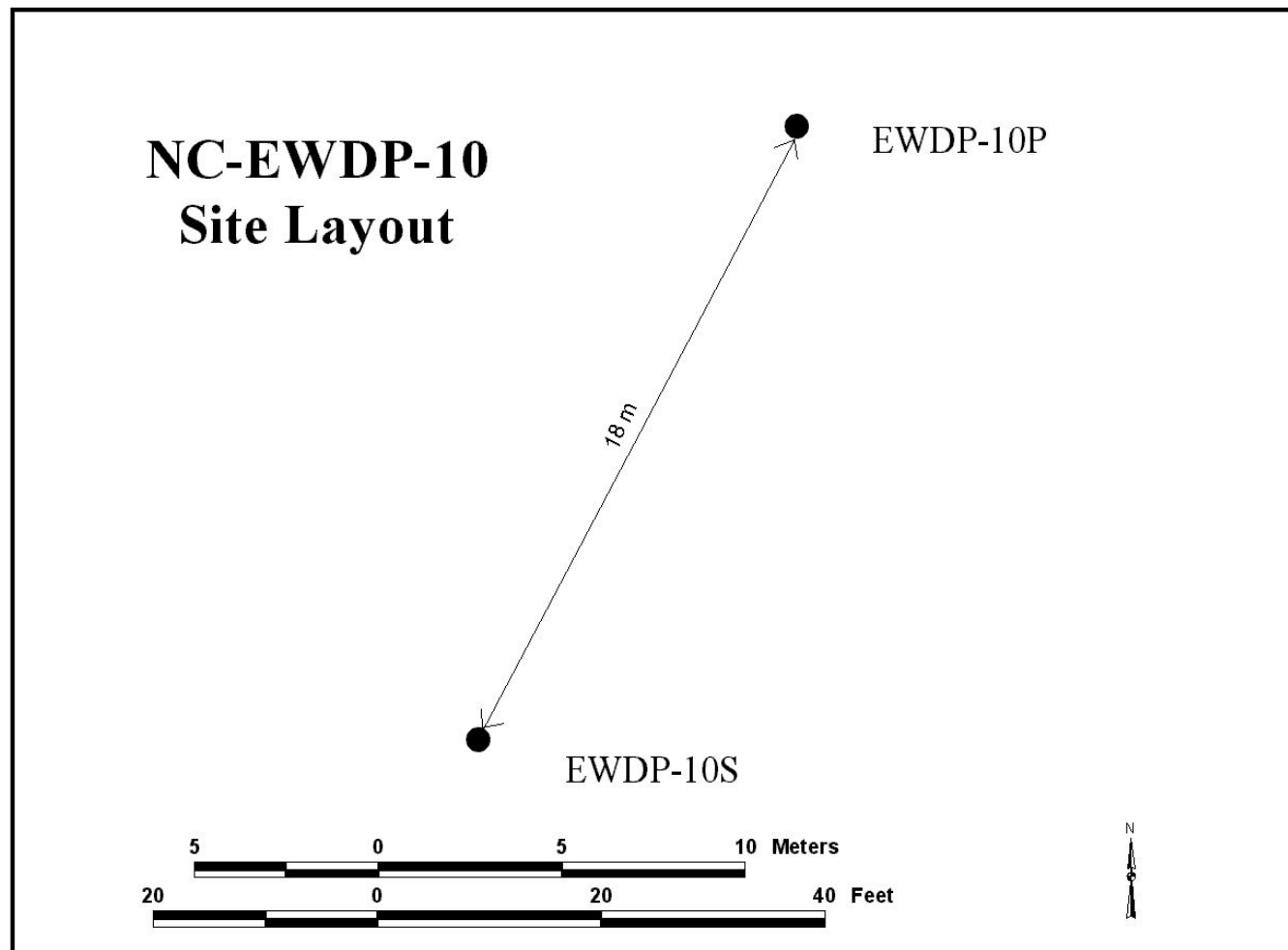


Figure 6.1-3
Location of Pump (10S) and Observation (10P) Wells at Site 10

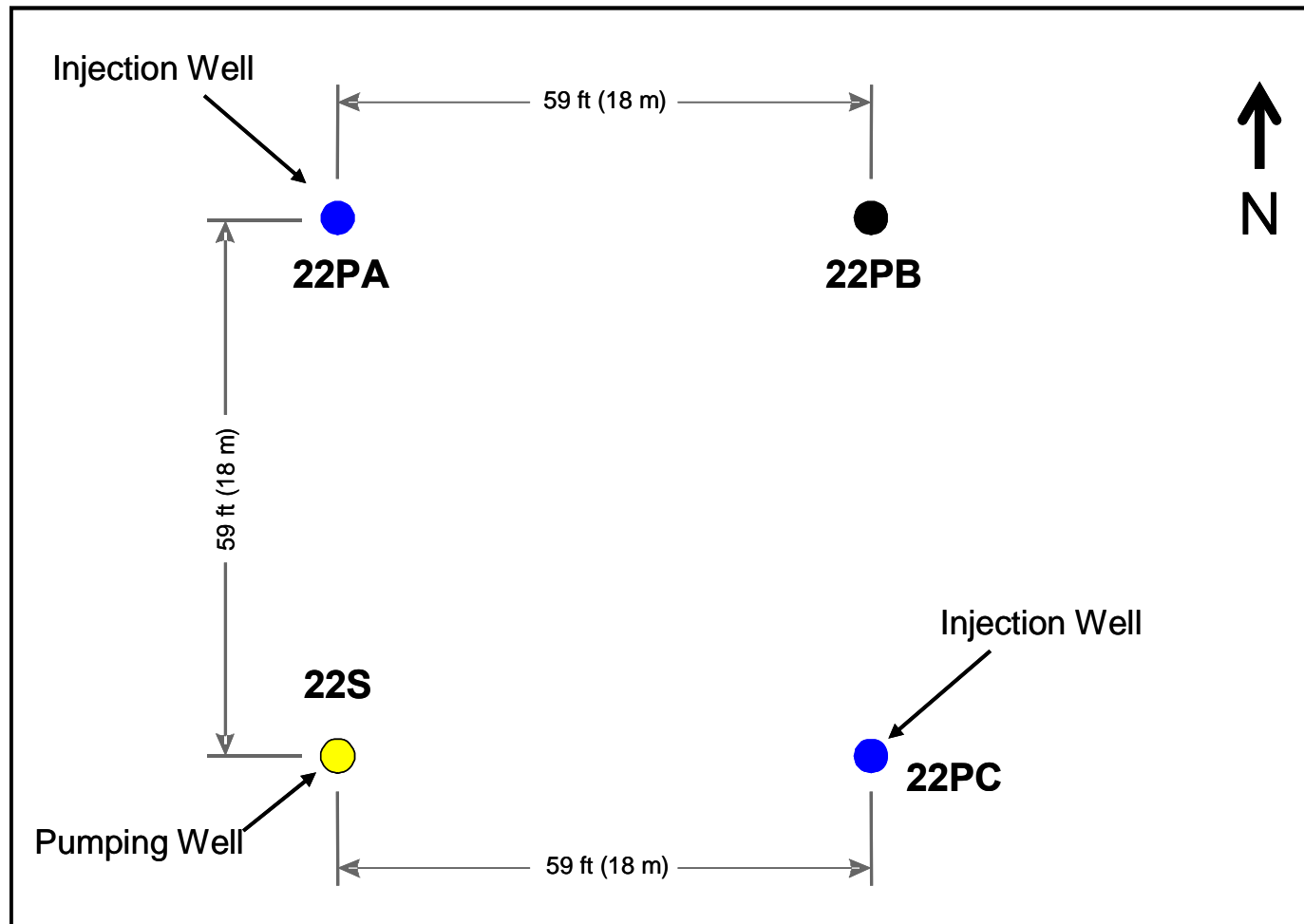


Figure 7.1-1
Surface layout for tracer tests at Site 22

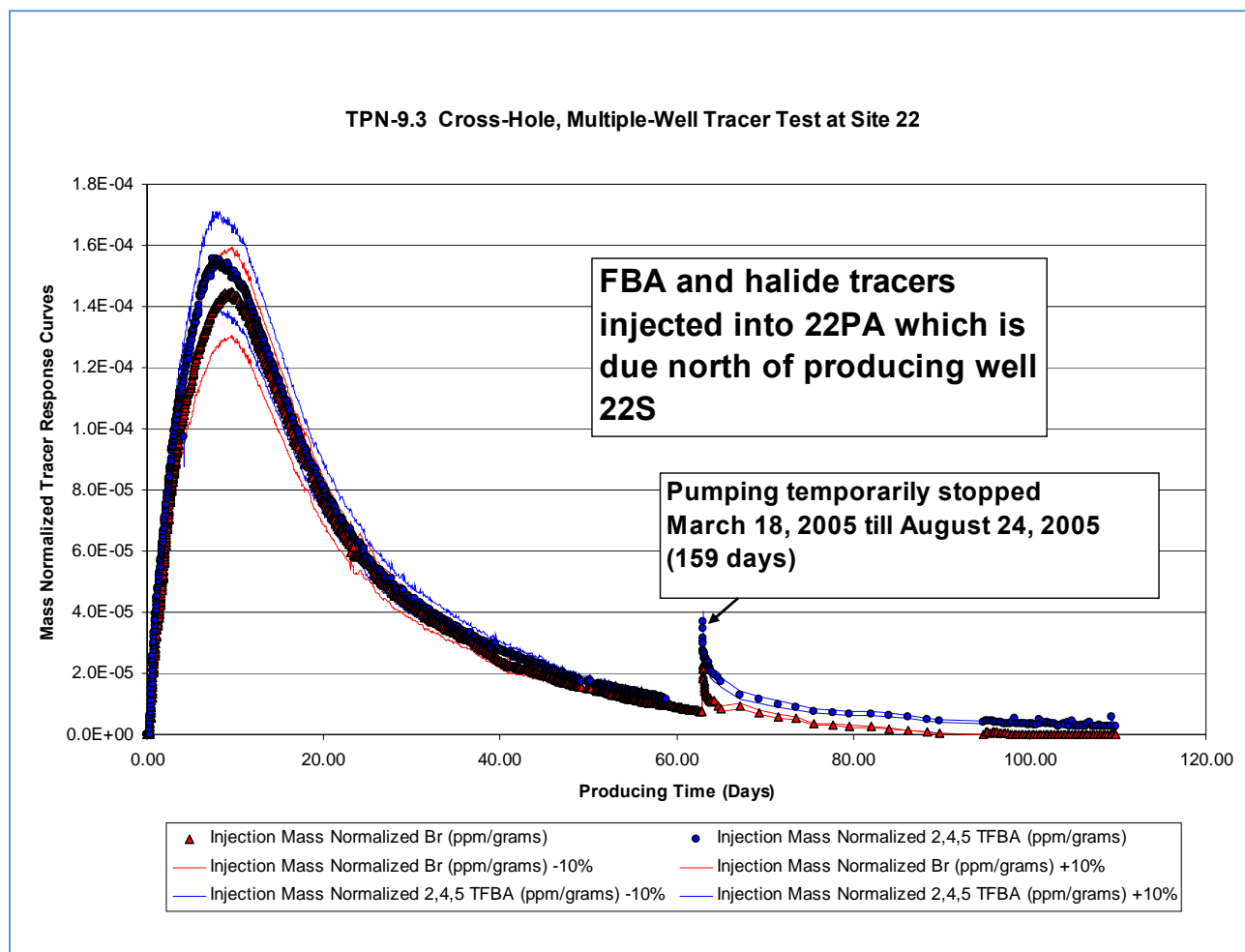


Figure 7.2-1
Alternative calculated injected tracer mass normalized tracer response curves for
injection in 22PA Zone 2.

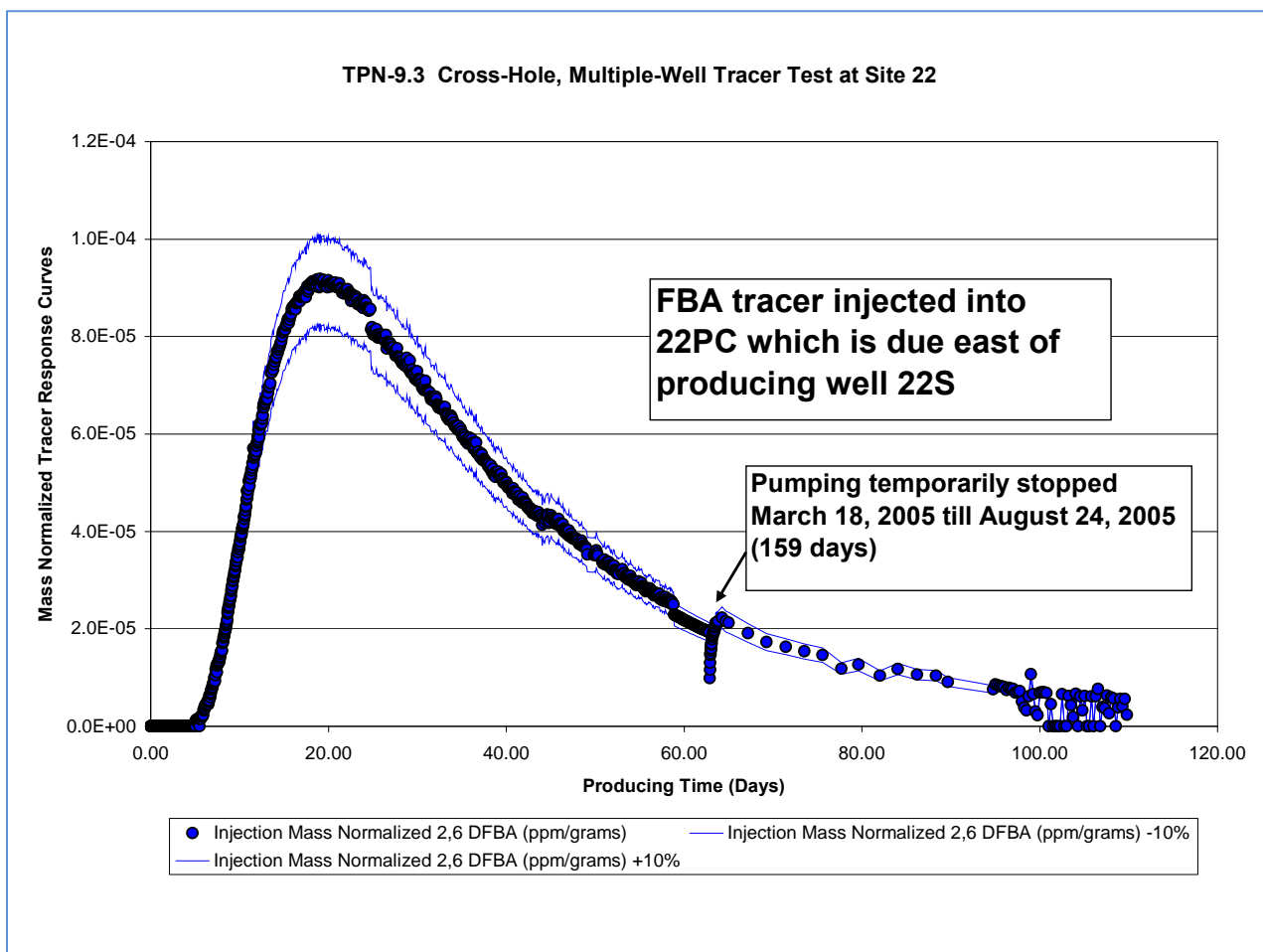


Figure 7.2-2
Mass normalized tracer response curves for injection in 22PC Zone 2.



Figure 7.2-3
Aerial view of Site 22 and the channel system observed in nearby Fortymile Wash

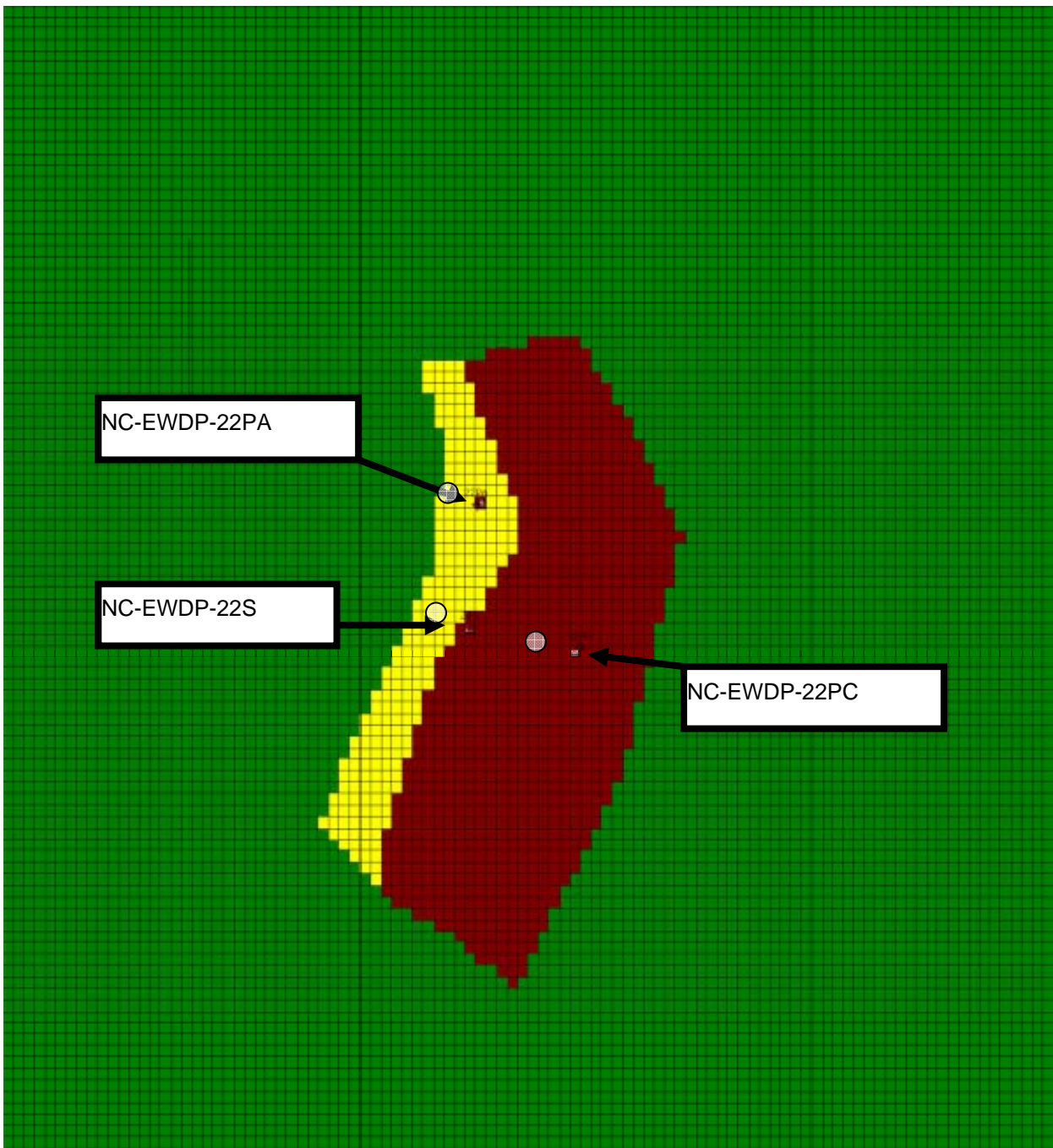


Figure 7.2-4
MODFLOW model geometry for Zone 2 at Site 22 in map view.

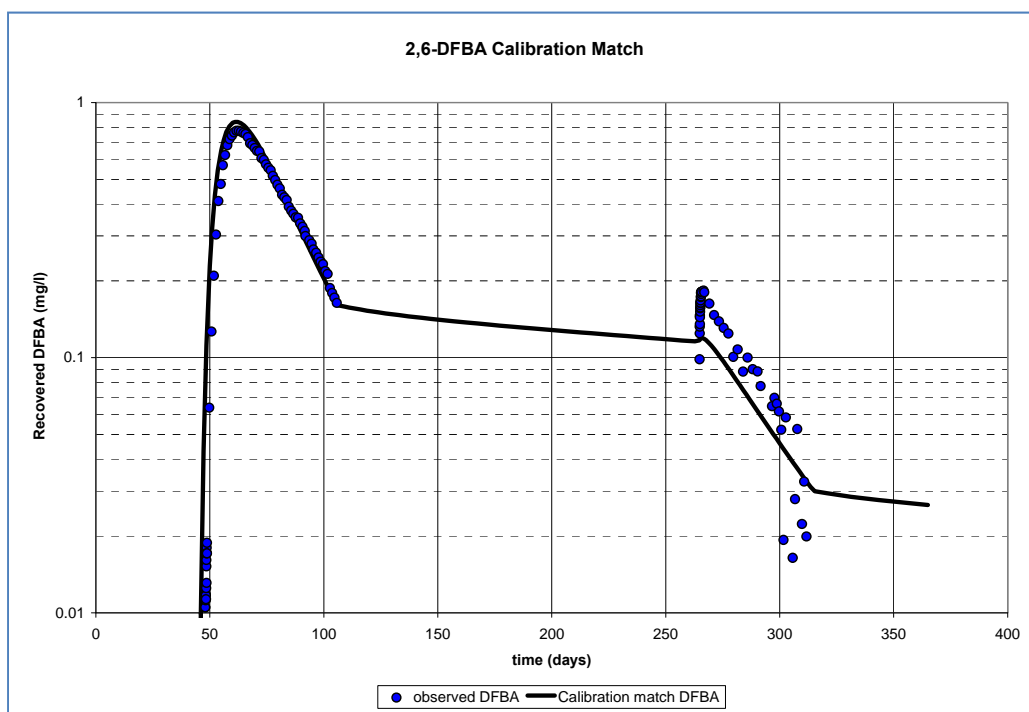


Figure 7.2-5
Calibration match obtained for 2,6-DFBA (cross-hole test 2).

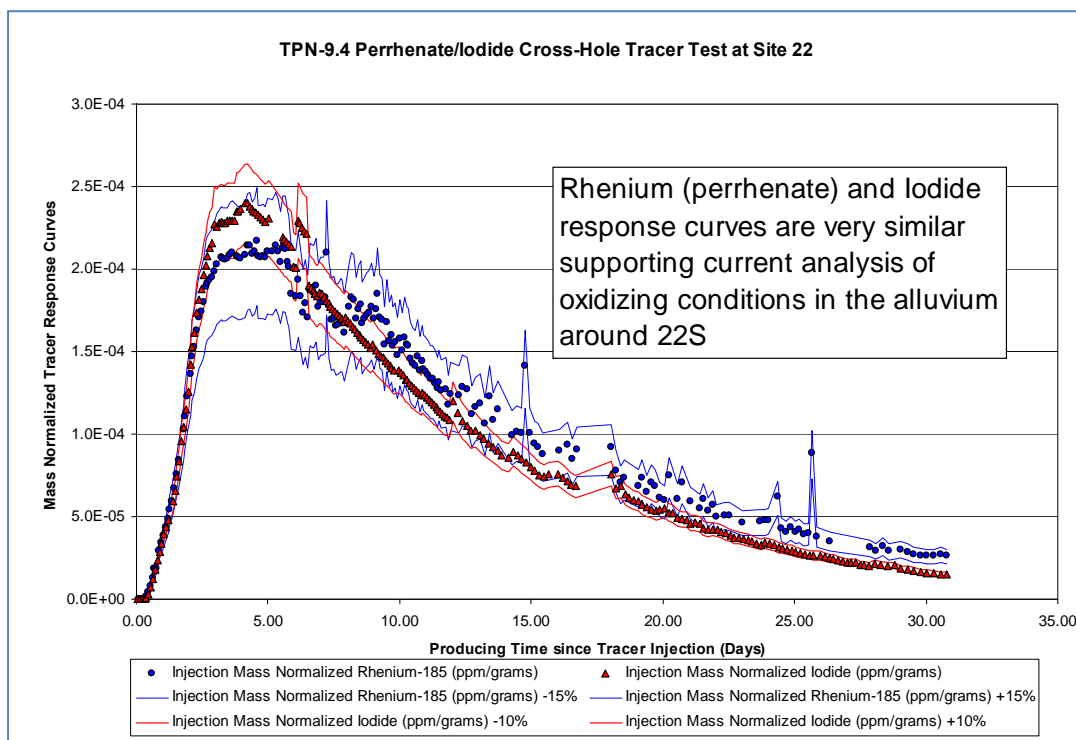


Figure 7.2-6
Mass normalized tracer response curves indicating oxidizing conditions at Site 22.

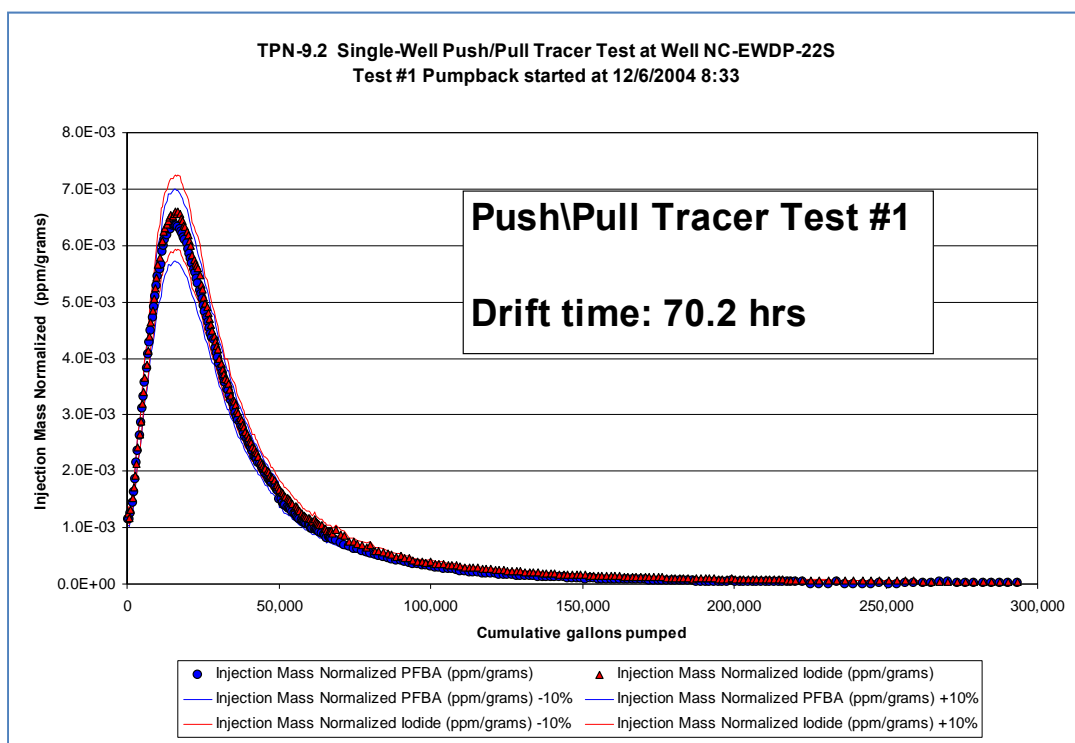


Figure 7.2-7
Nearly identical mass normalized tracer recovery curves indicate no diffusion into stagnant layers.

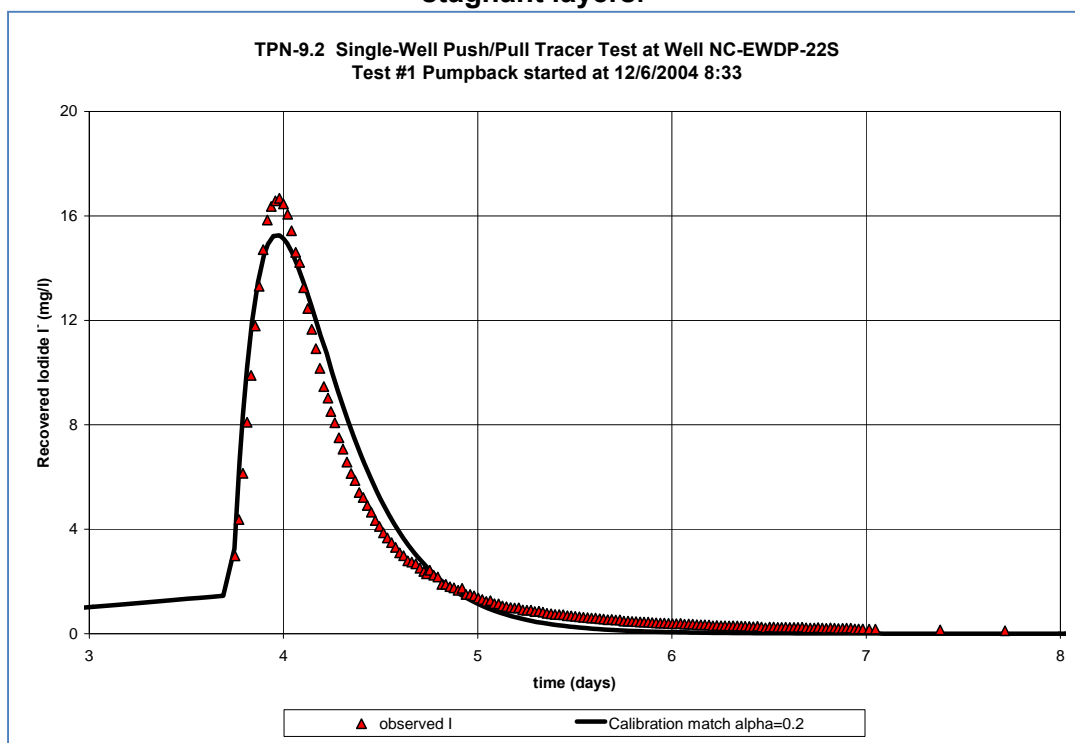


Figure 7.2-8
Calibration match obtained for iodide on first single-well push/pull tracer test.

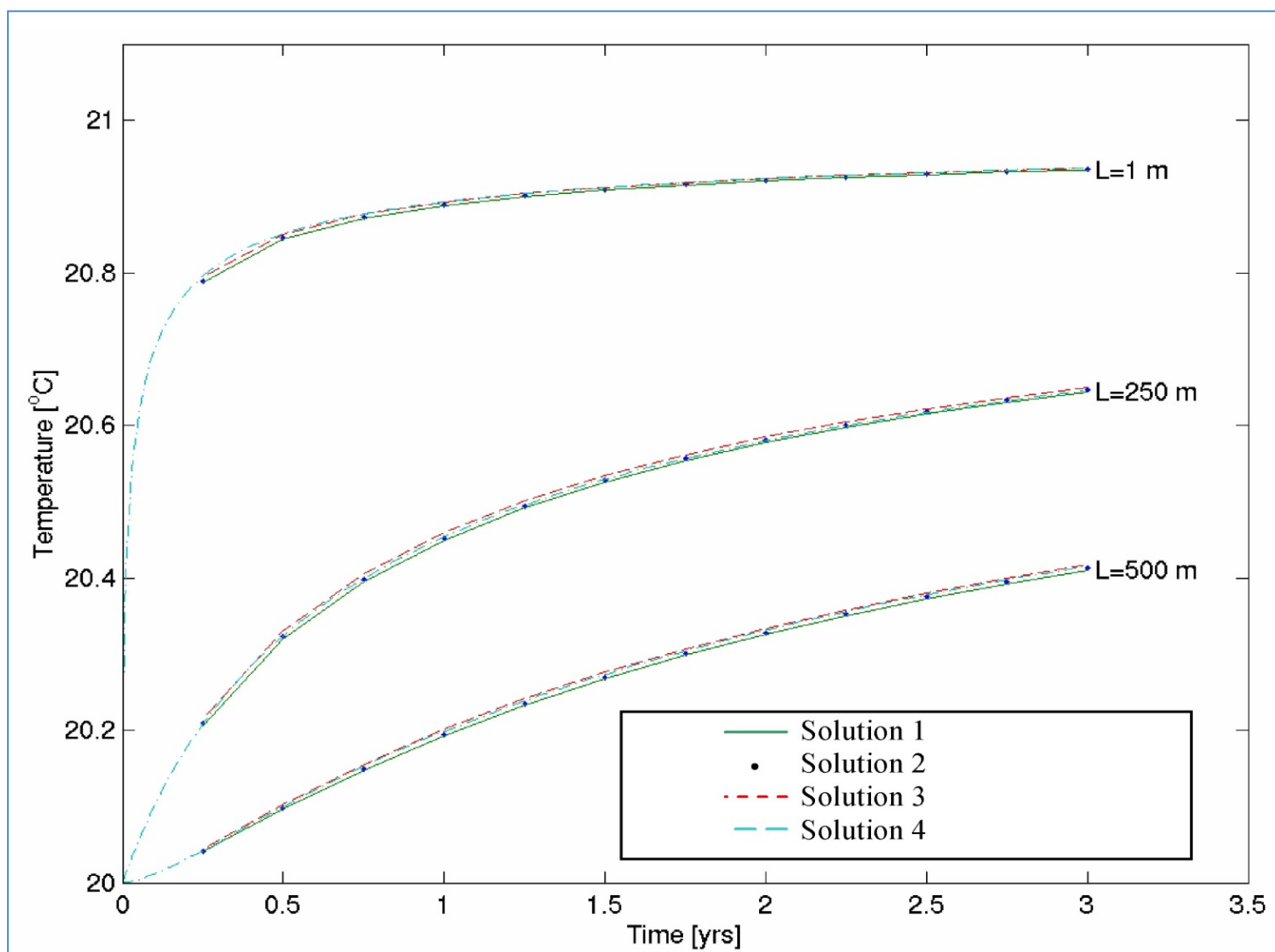


Figure 8.1-1
Wall temperature history comparison for Solutions 1 through 4 at 1m, 250m and 500m distance along the airway.

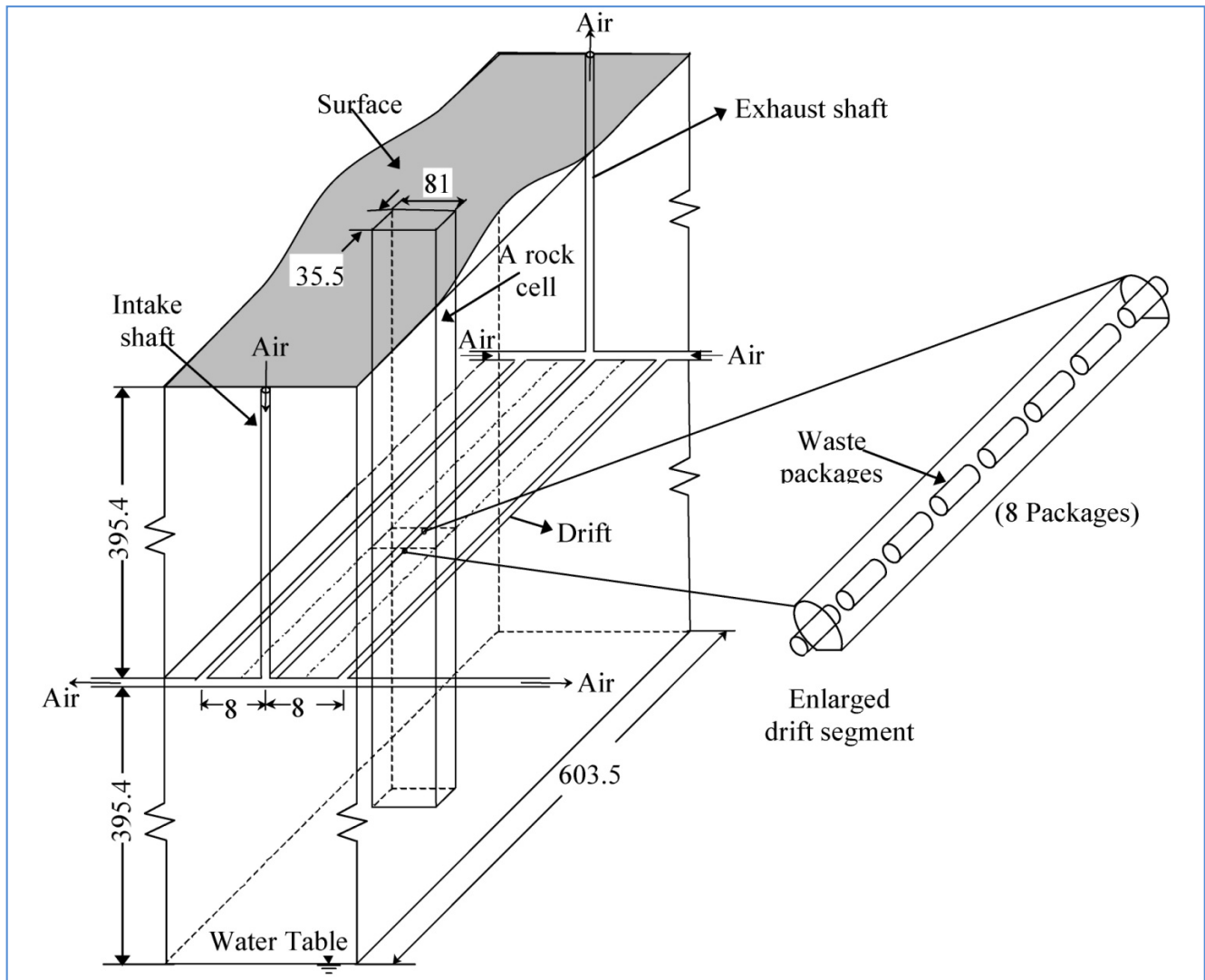


Figure 8.2-1

A three-drift section of an emplacement panel of 26 drifts with the peripheral tunnels, the intake and exhaust shafts, and the surrounding rockmass. The waste packages are shown in one of 17 repeating rock cells in each drift.

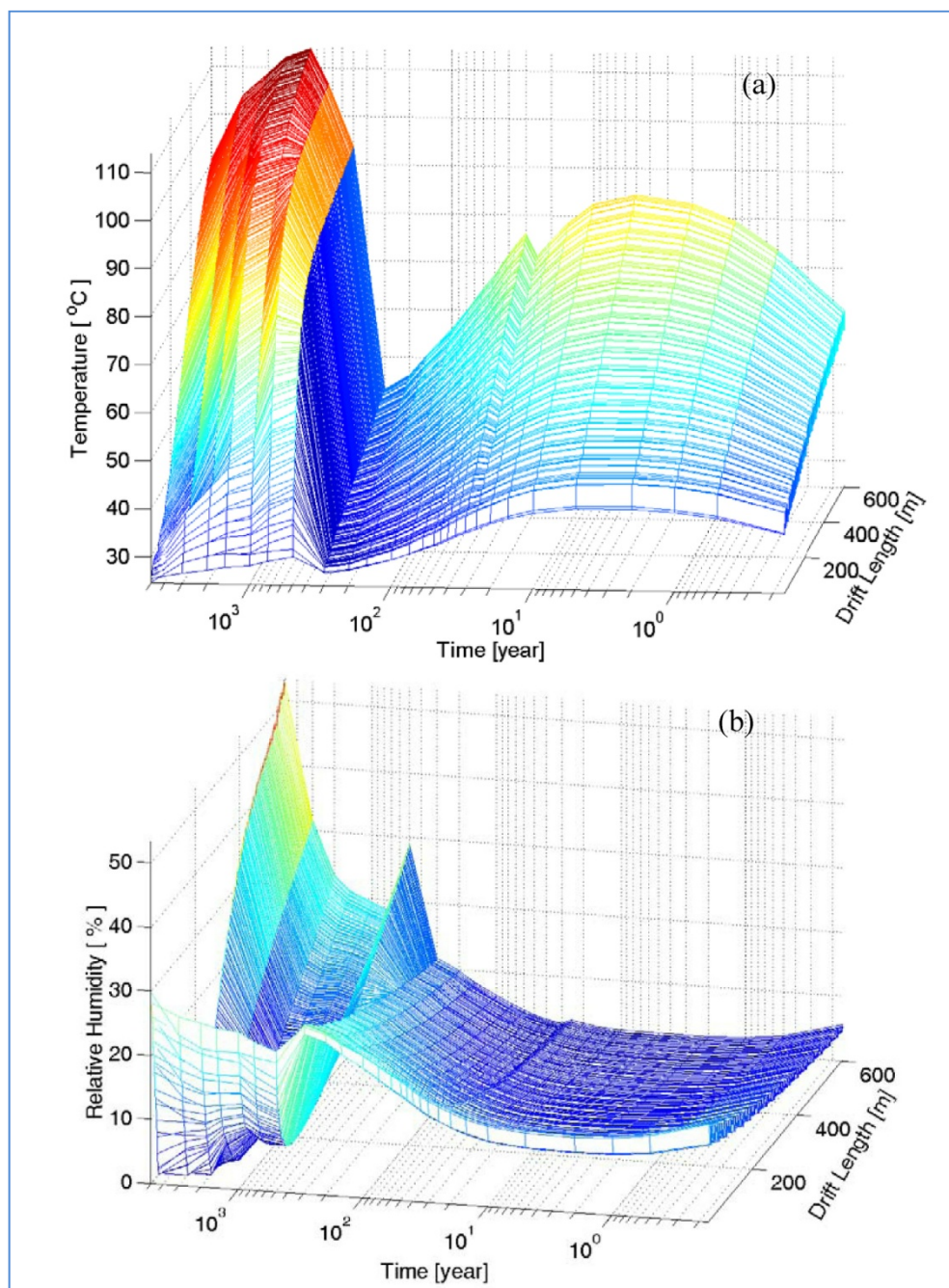


Figure 8.2-2
Pre- and post-closure wall temperature (a) and wall relative humidity (b) distributions in time and space.

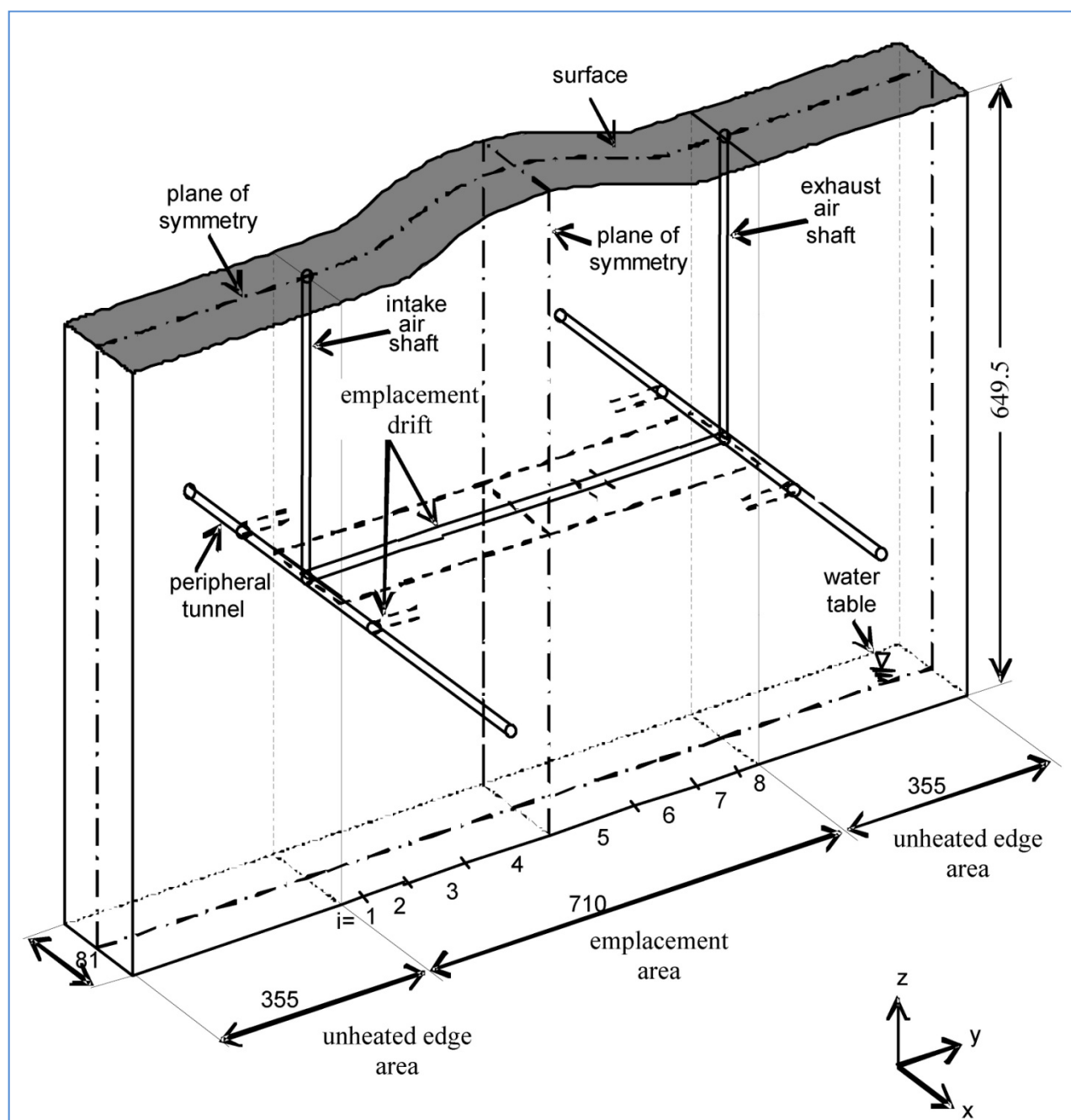


Figure 8.4-1
Rockmass domain around an emplacement drift in Panel 2.

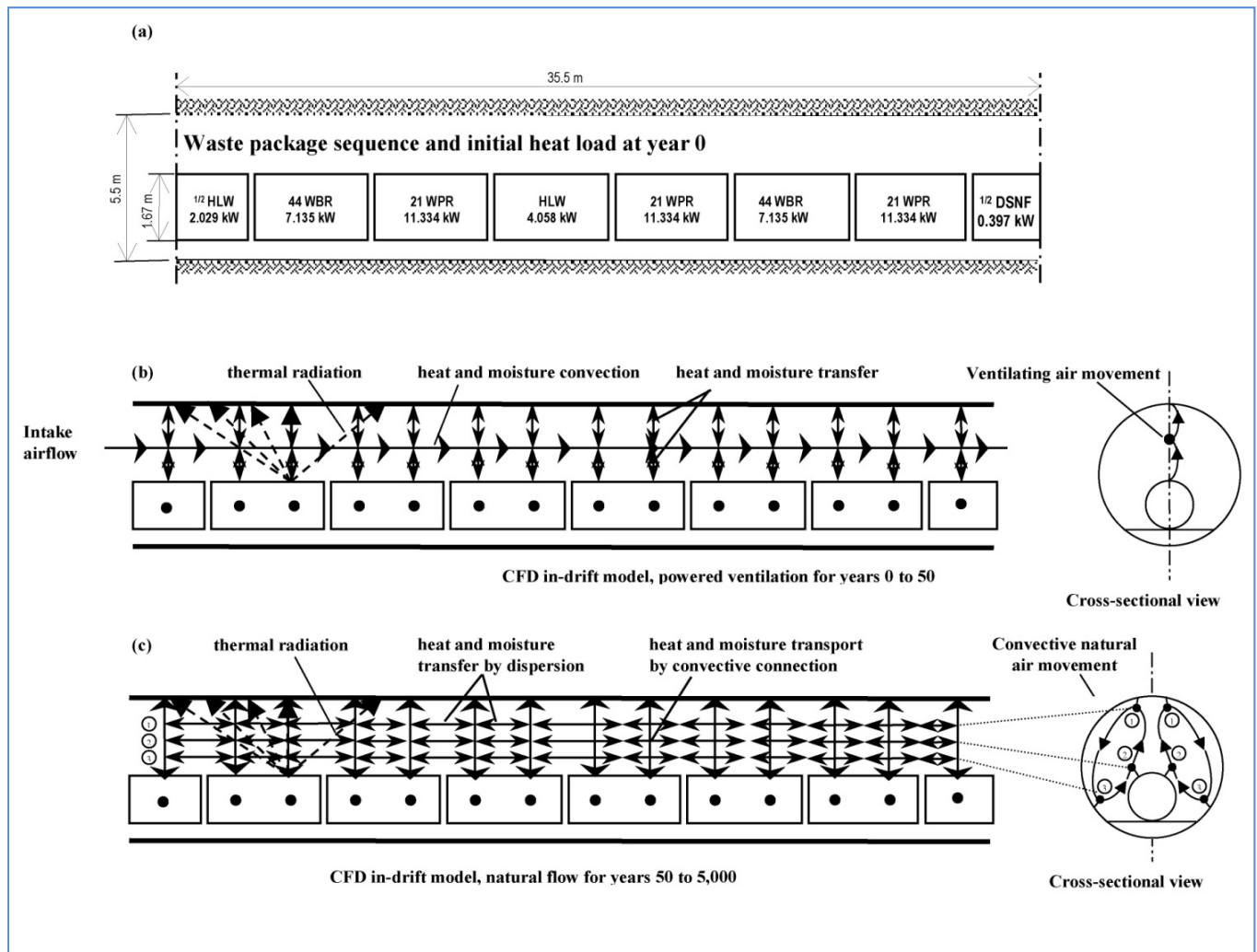


Figure 8.4-2

Computational fluid dynamics model configuration in the airway showing repeated sequence of eight waste packages in an emplacement drift (a), schematic diagram of pre-closure powered ventilation (b), and schematic diagram of post-closure natural air movement with axial dispersion (c).

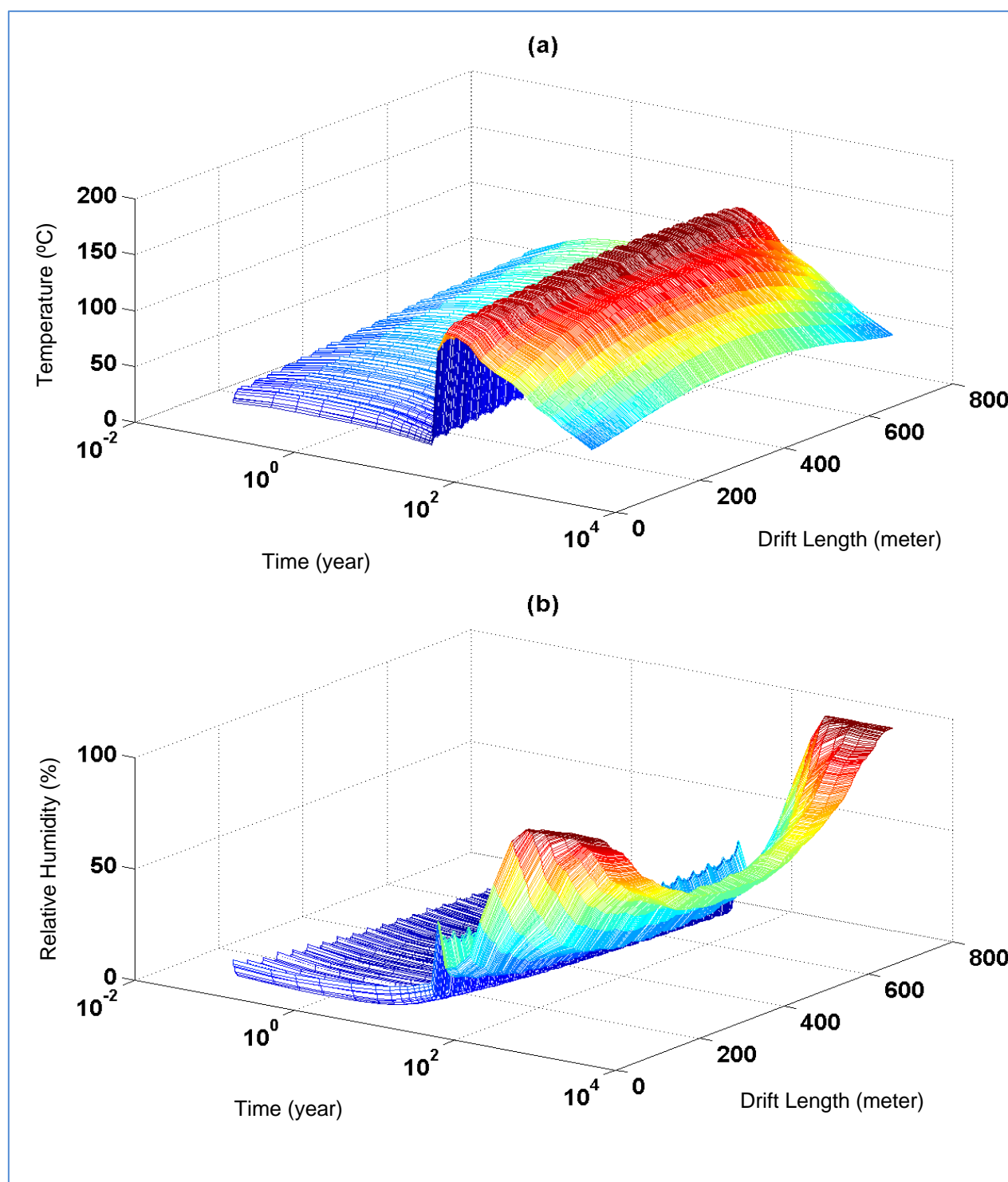


Figure 8.4-3
Drift wall temperature (a) and relative humidity distributions (b) in time and space.

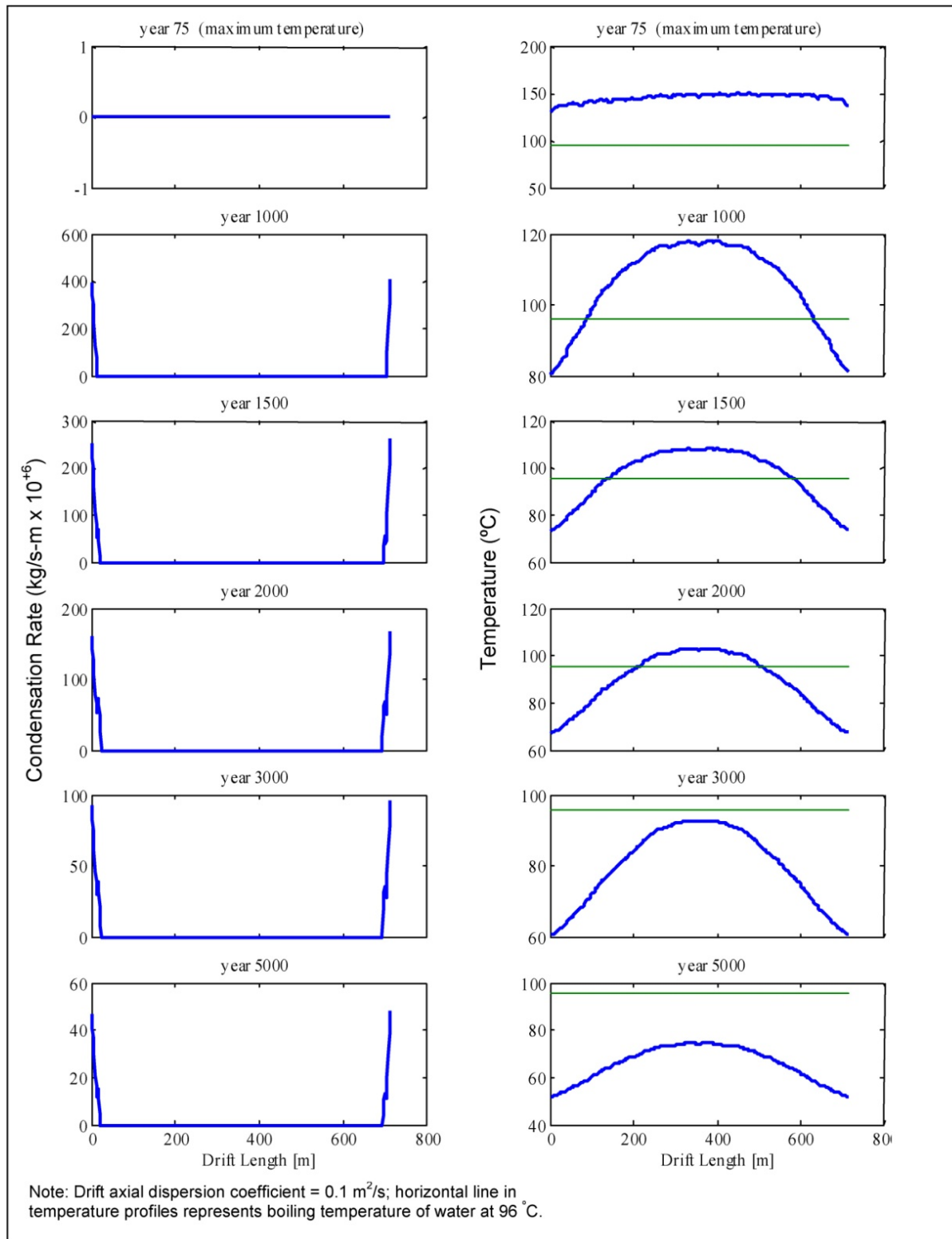


Figure 8.4-4
Axial Distribution of Drift Wall Condensation Rate and Temperature at Selected Post-Closure Time Divisions.

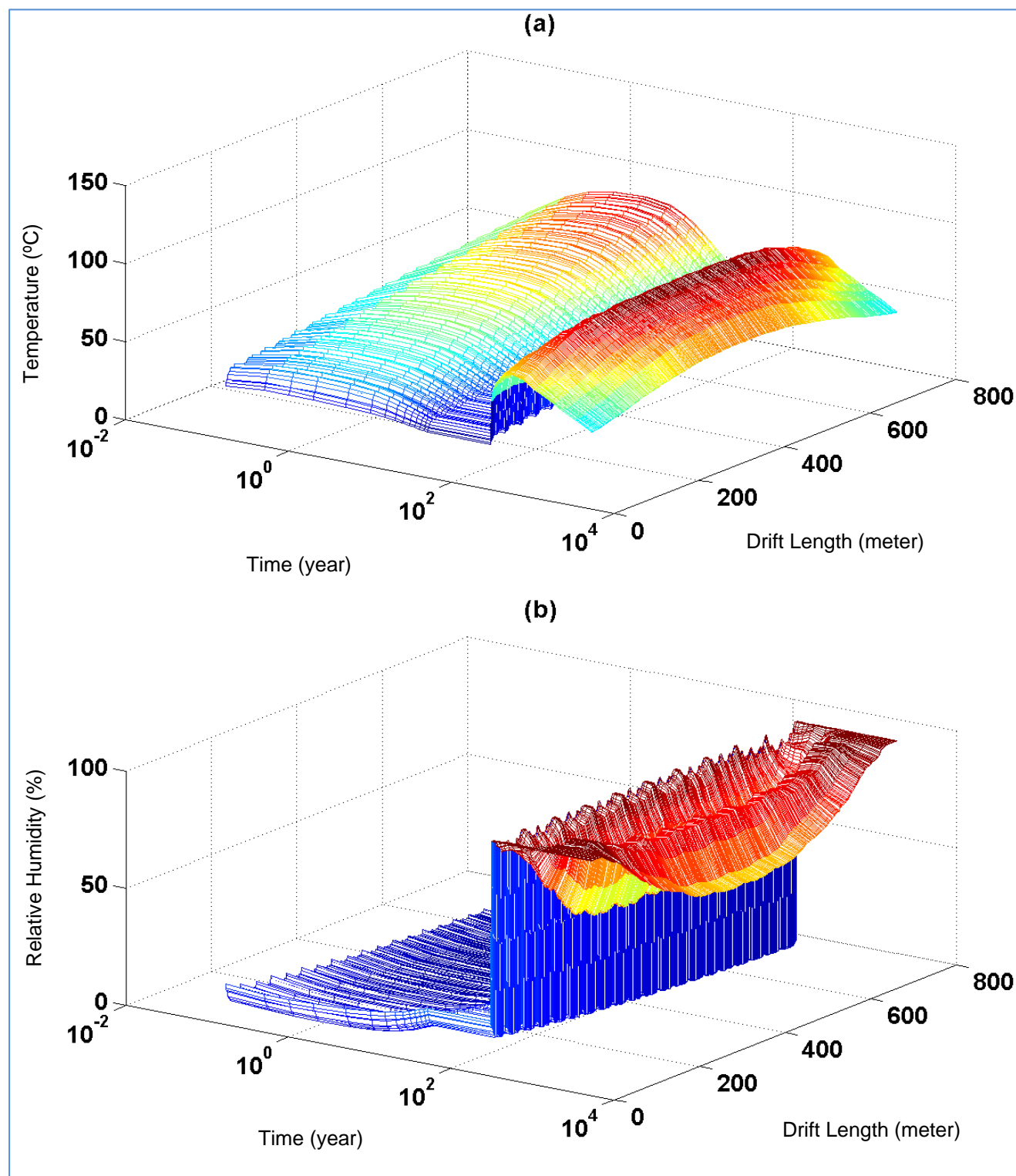


Figure 8.5-1
Drift wall temperature (a) and relative humidity distributions (b) in time and space with 300-year pre-closure.

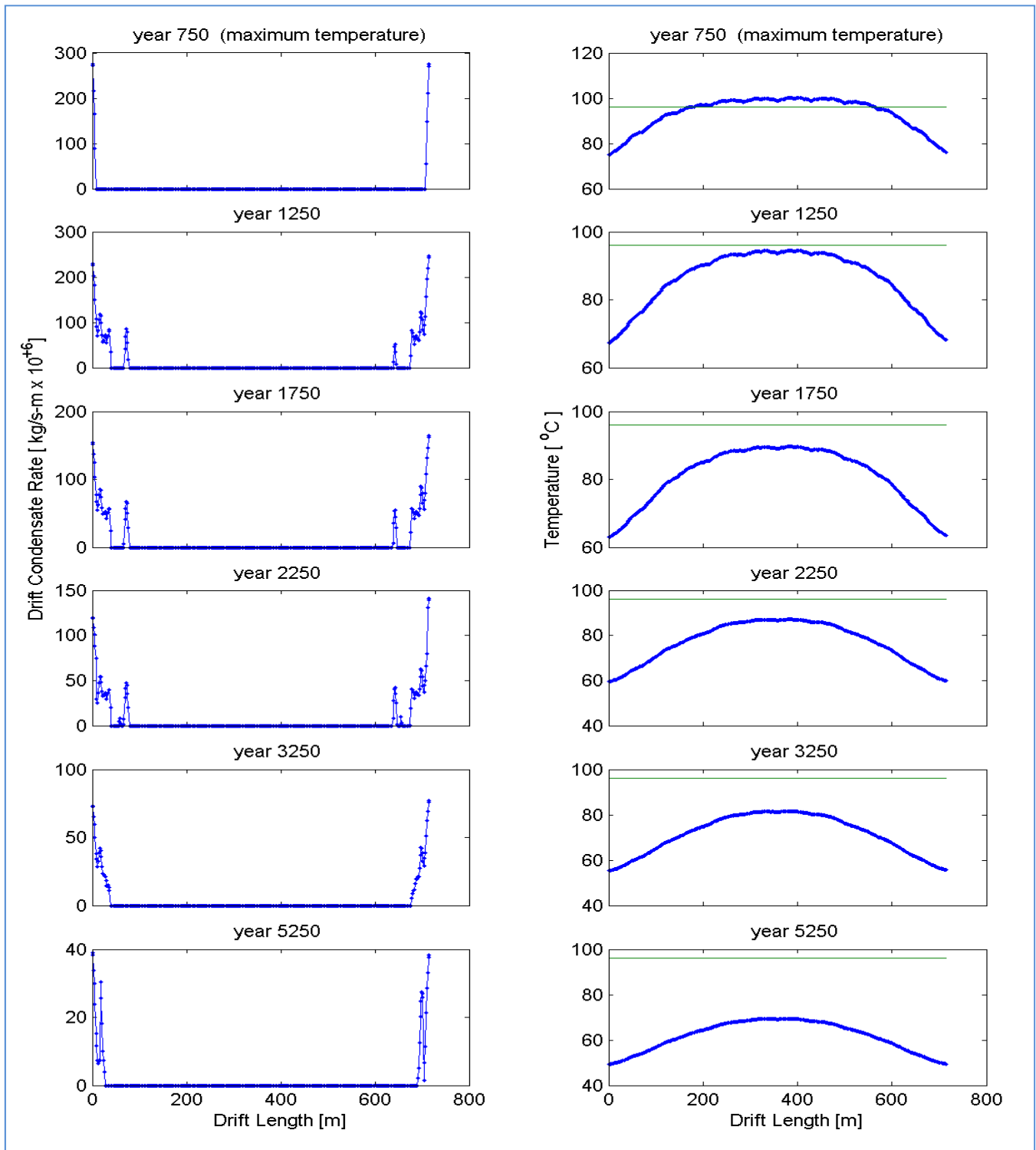


Figure 8.5-2
Axial Distribution of Drift Wall Condensation Rate and Temperature at
Selected Time Divisions for 300-Year Pre-Closure Ventilation.

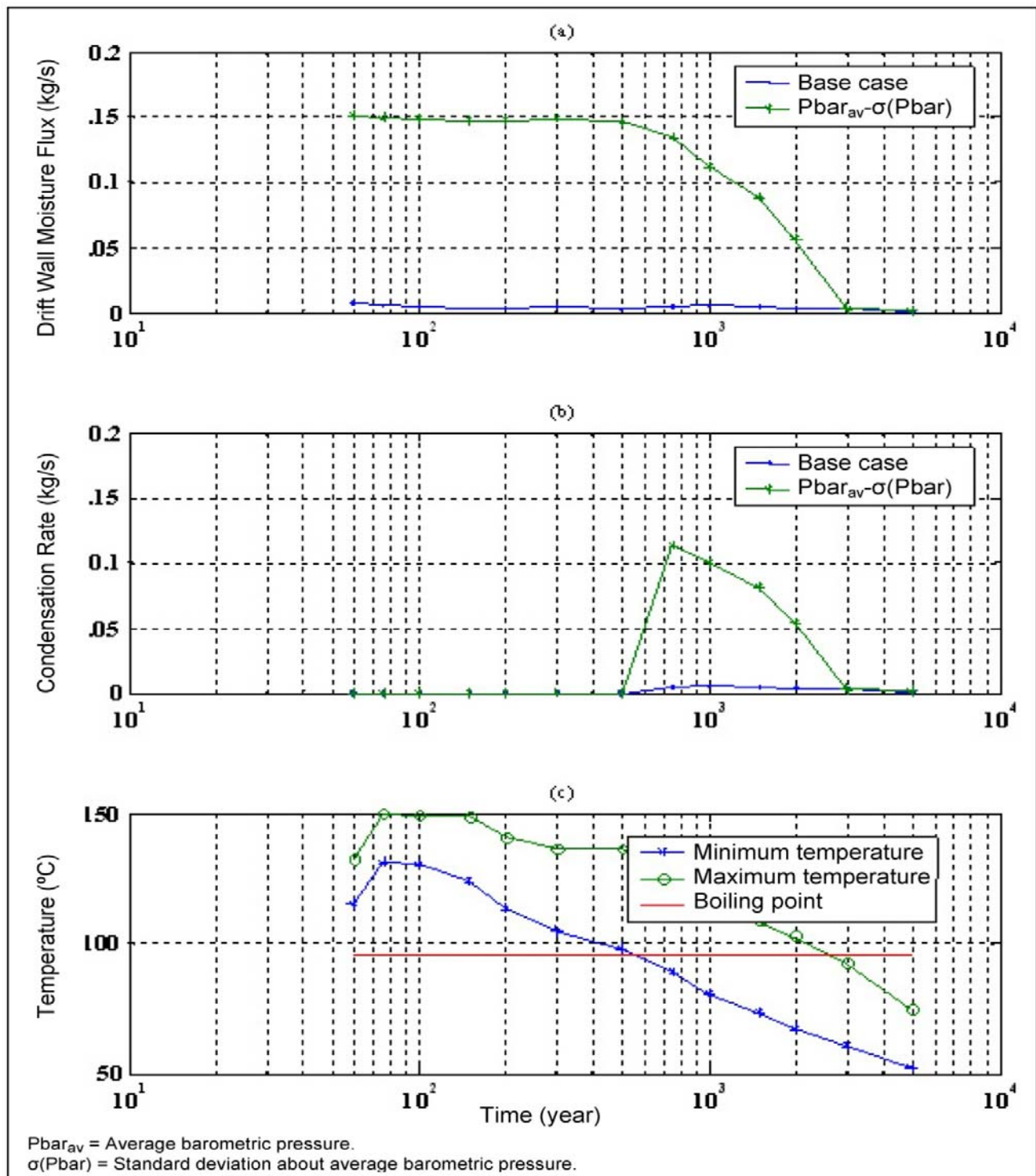


Figure 8.6-1
Effect of Barometric Pressure Fluctuation on Drift Moisture Inflow (a) and Condensation Rate (b) and Maximum and Minimum Temperature (c).

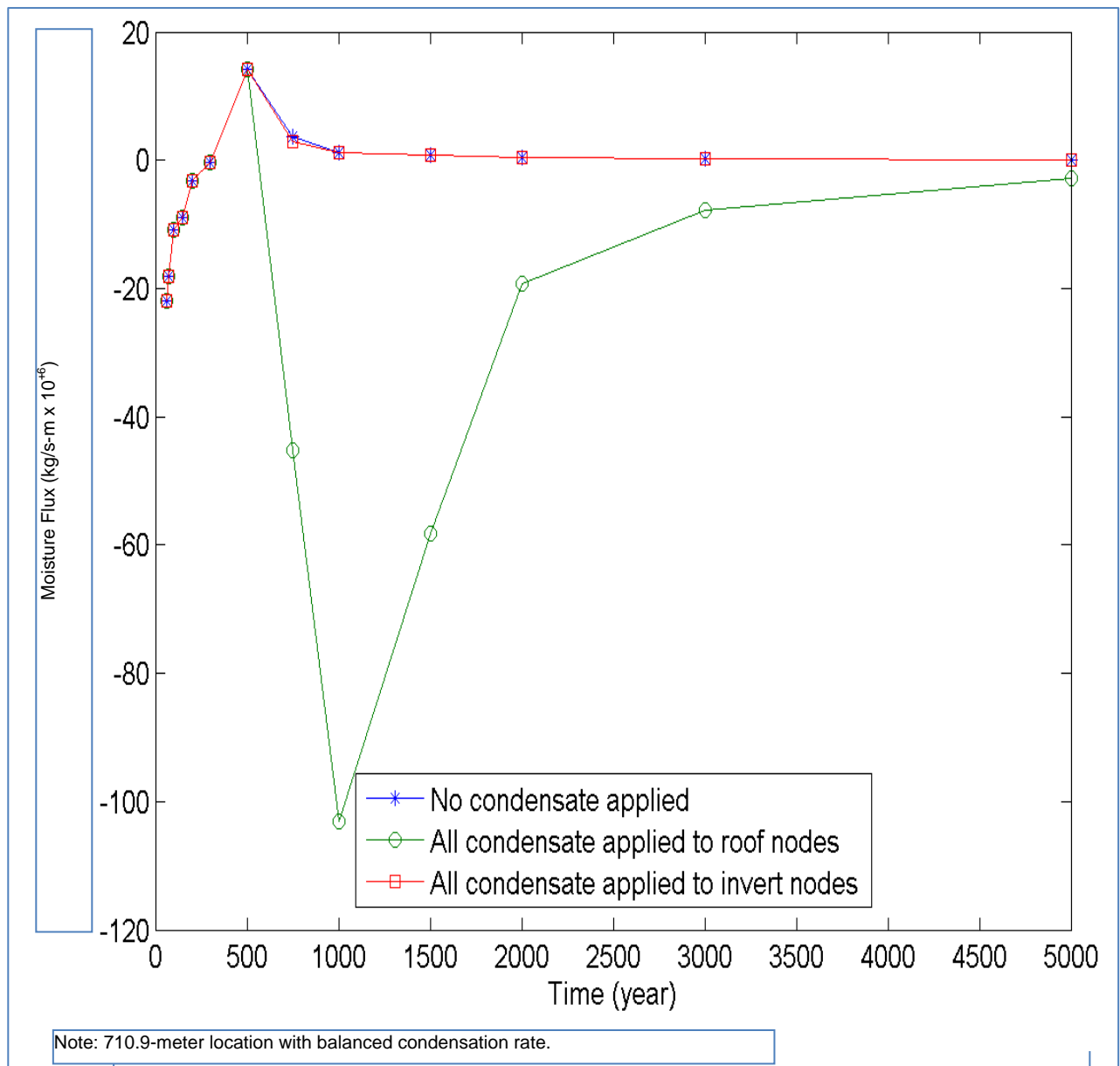


Figure 8.7-1
Comparison of drift wall moisture fluxes

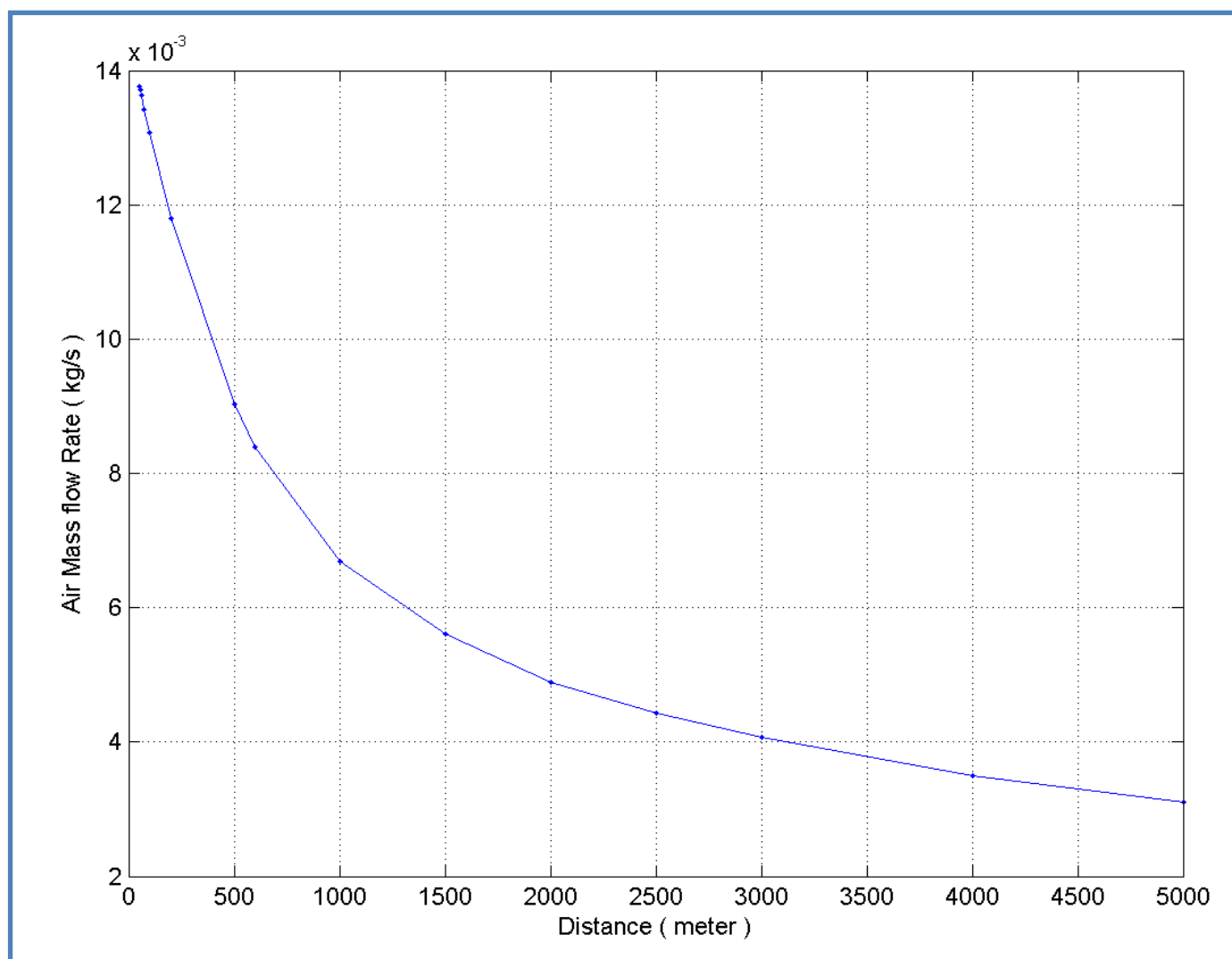


Figure 8.9-1
Air flow variation with time, used in the one-dimensional air flow studies.

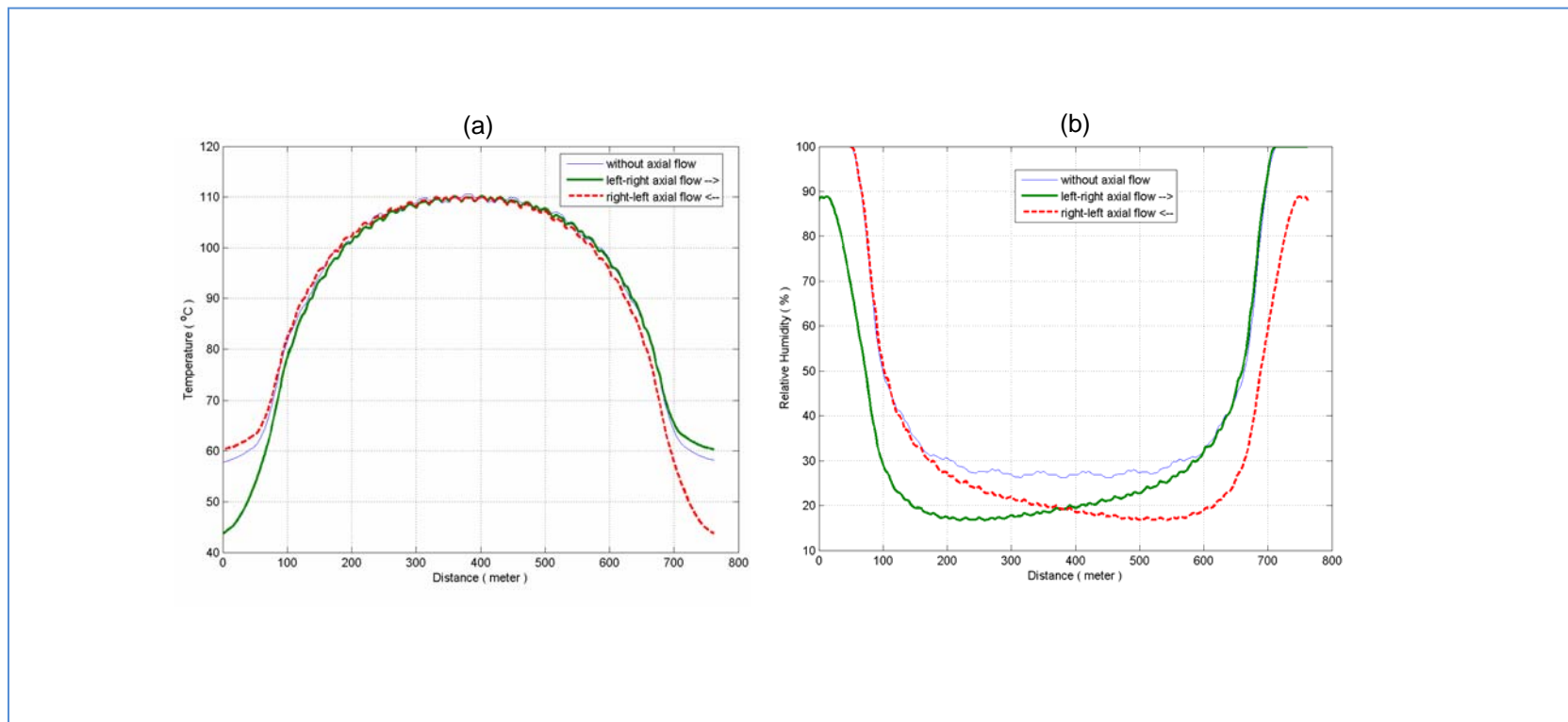


Figure 8.9-2
Temperature and relative humidity variations at year 500 under two different air flow directions in the emplacement drift.

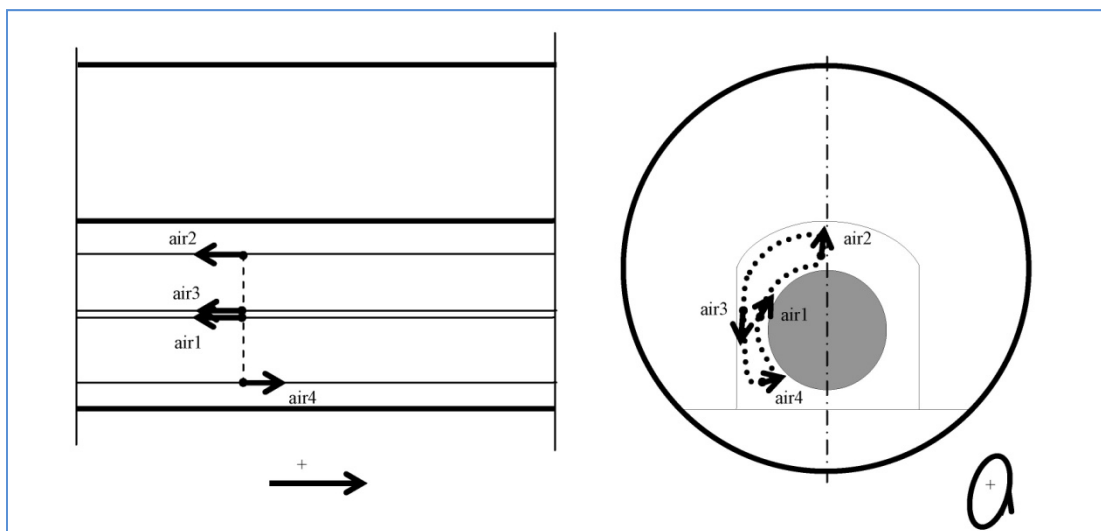


Figure 8.9-3

Definition of horizontal and vertical velocity components at a given cross section under the drip shield.

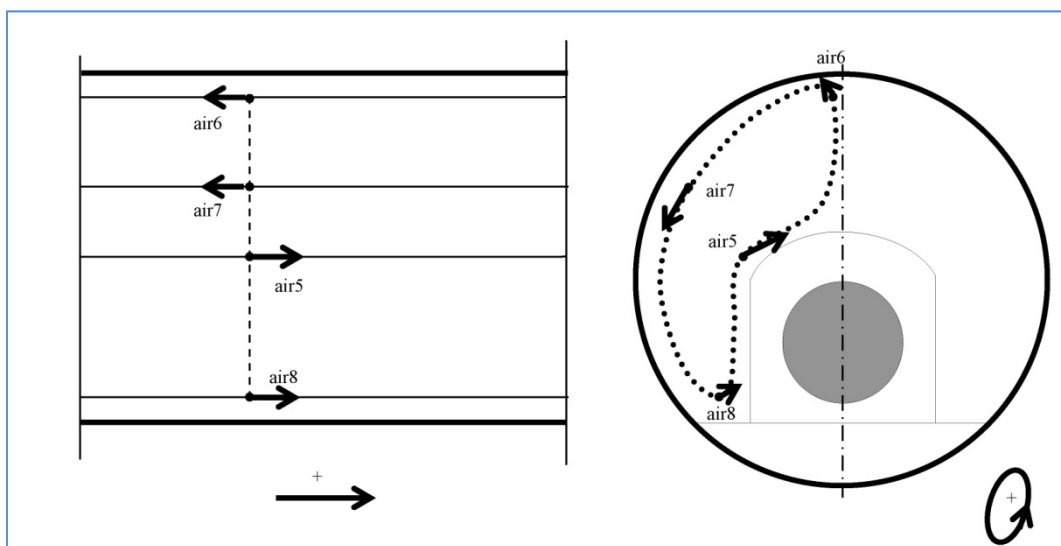


Figure 8.9-4

Definition of horizontal and vertical velocity components at a given cross section outside the drip shield.

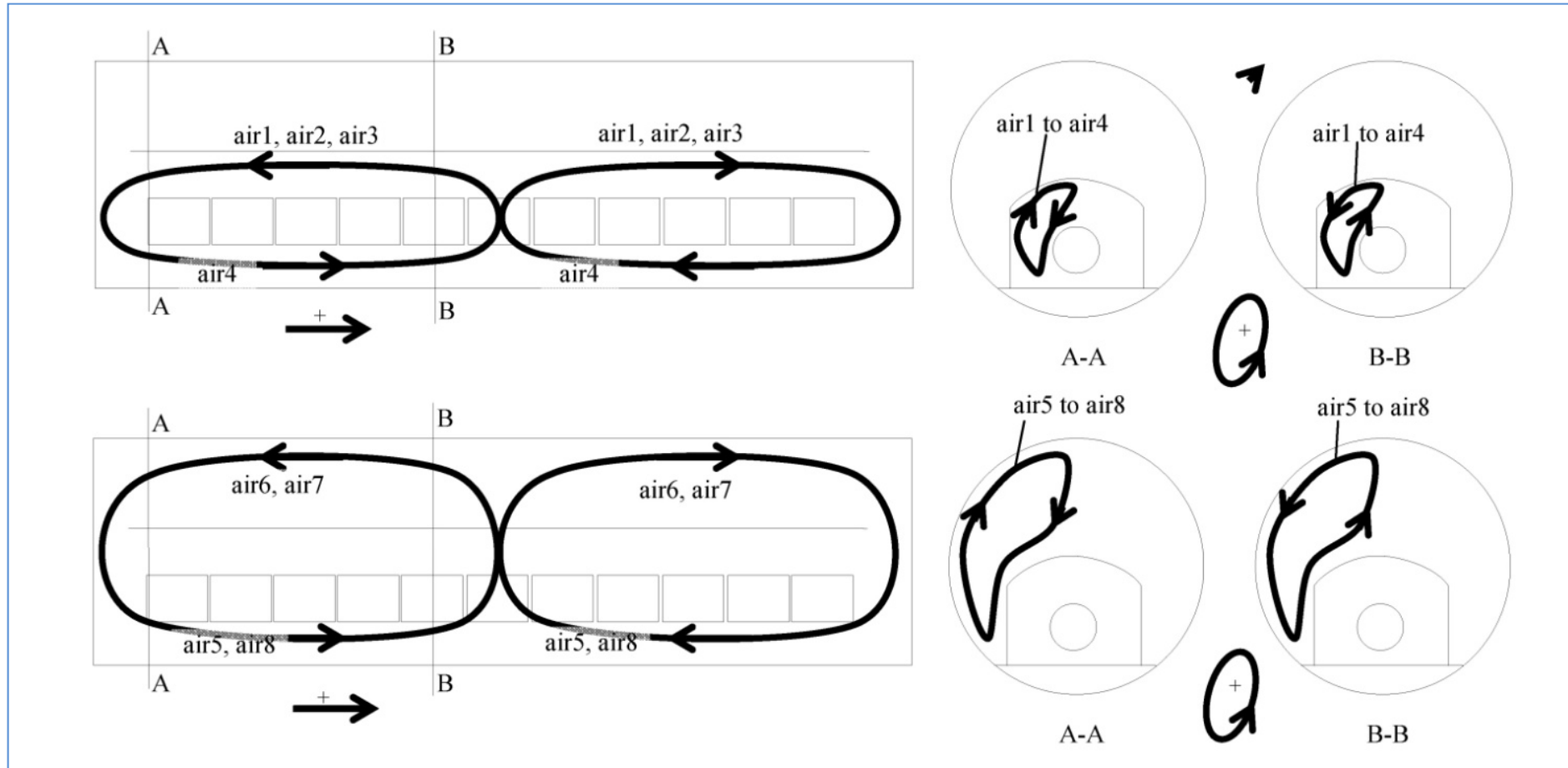
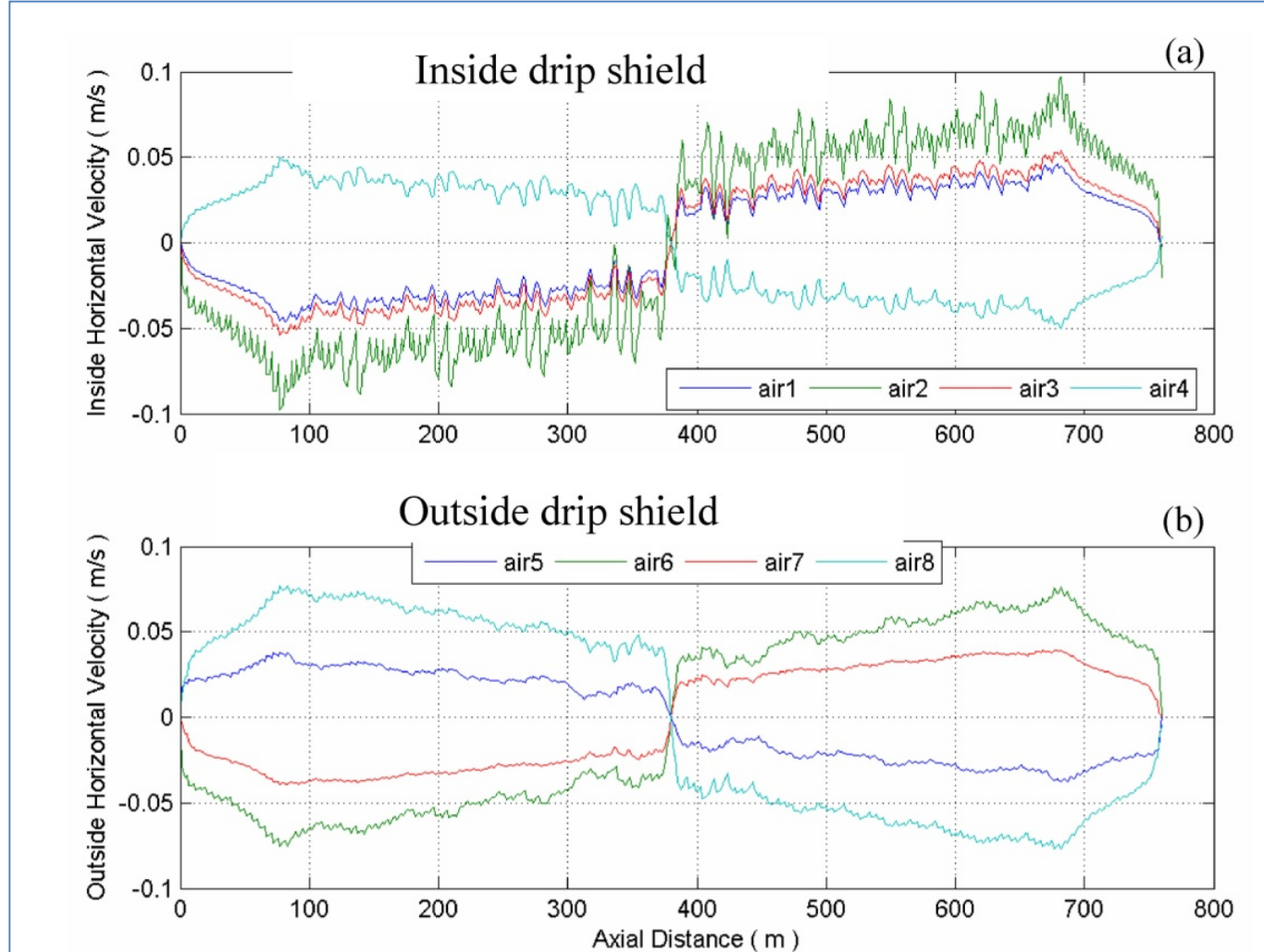


Figure 8.9-5
Drift-scale natural air flow patterns in one emplacement drift.

**Figure 8.9-6**

Air flow velocity variation in the horizontal circulation direction along the emplacement drift (a) inside and (b) outside the drip shield at year 1000.

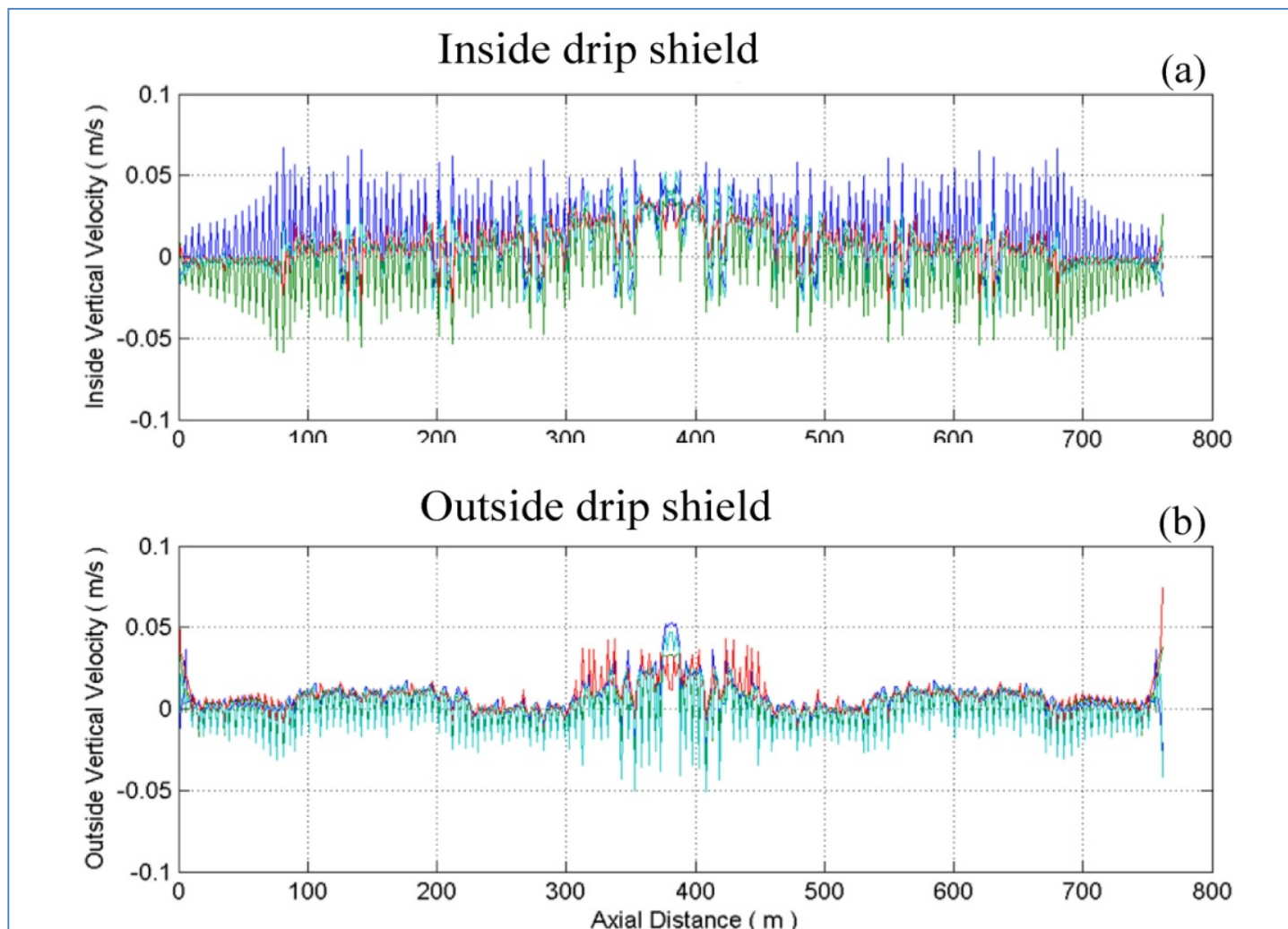


Figure 8.9-7
Vertical in-drift velocities along the drift length (a) inside and (b) outside the drip shield at year 1000.

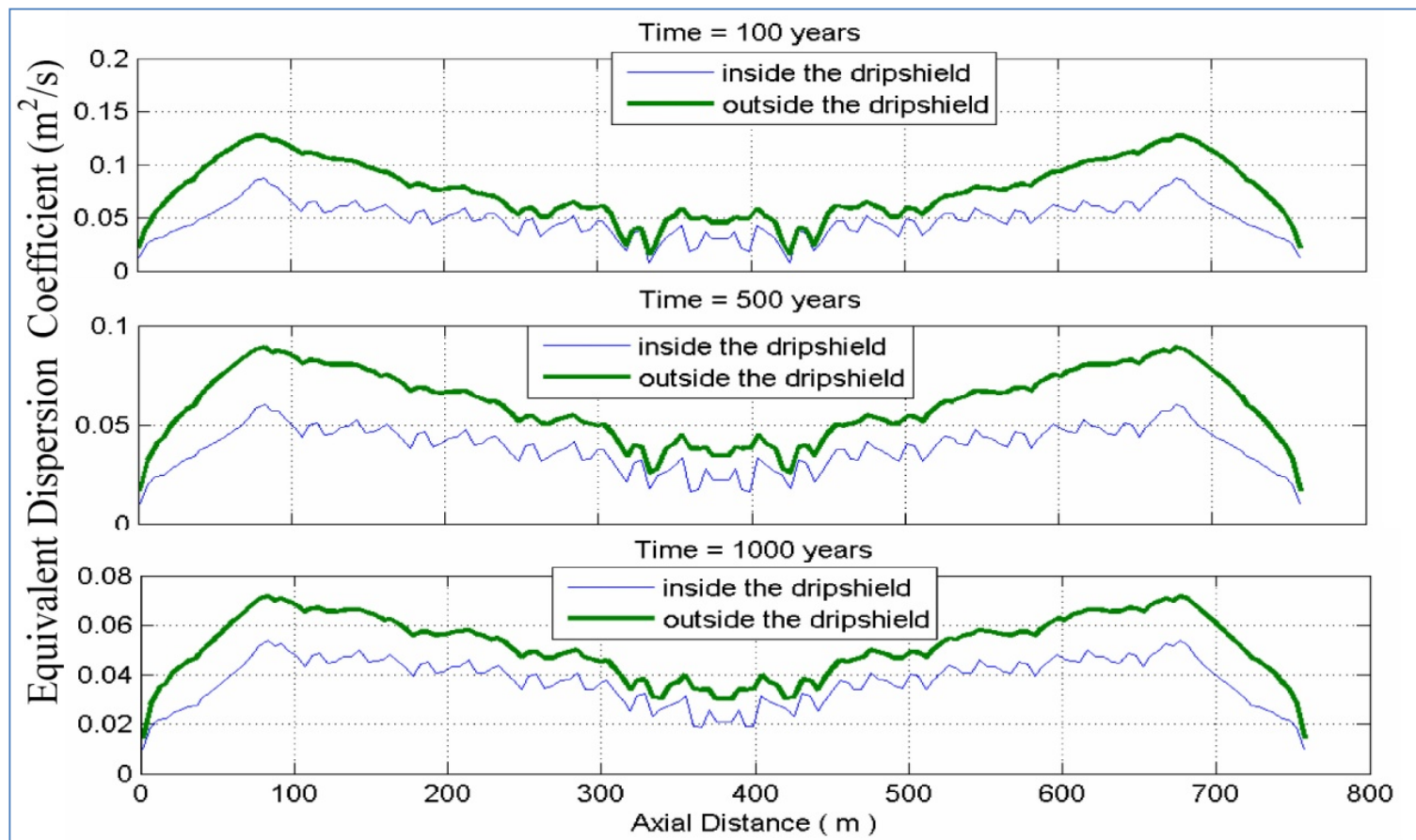
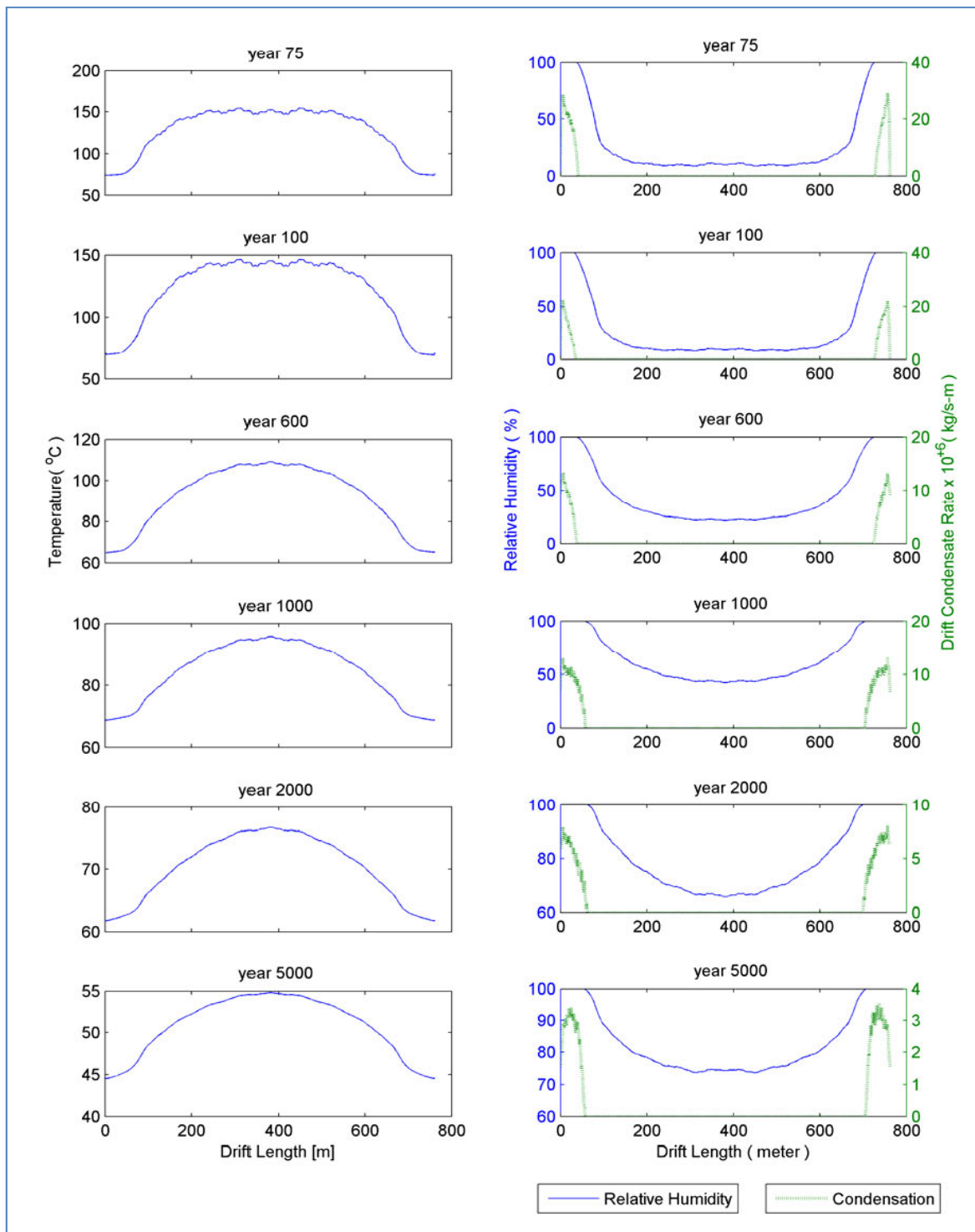


Figure 8.9-8
Equivalent dispersion coefficient at three time periods

**Figure 8.9-9**

Temperature, relative humidity, and rate of condensation distributions along the drift length for selected post-closure time periods at the roof segment of the drift wall.

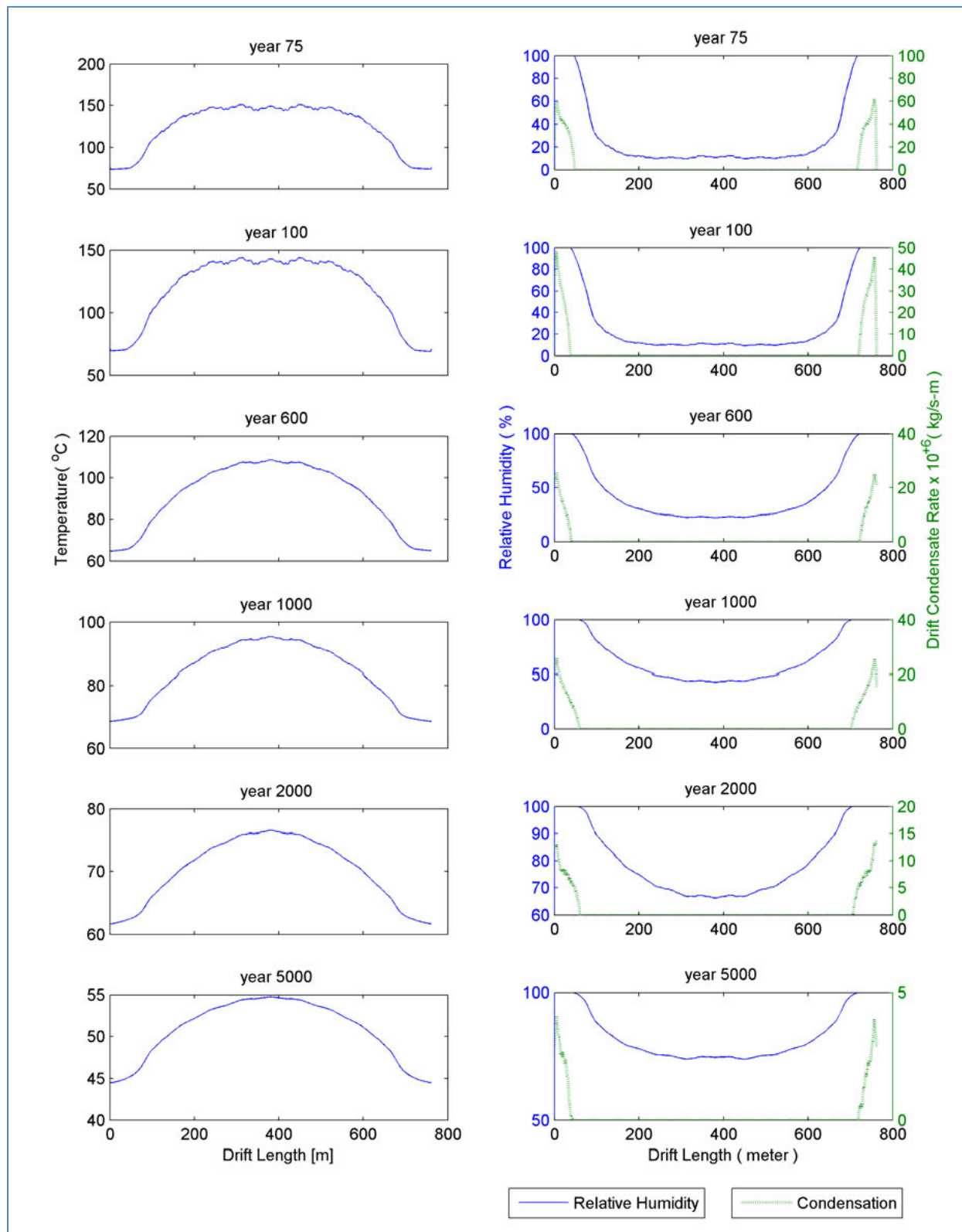
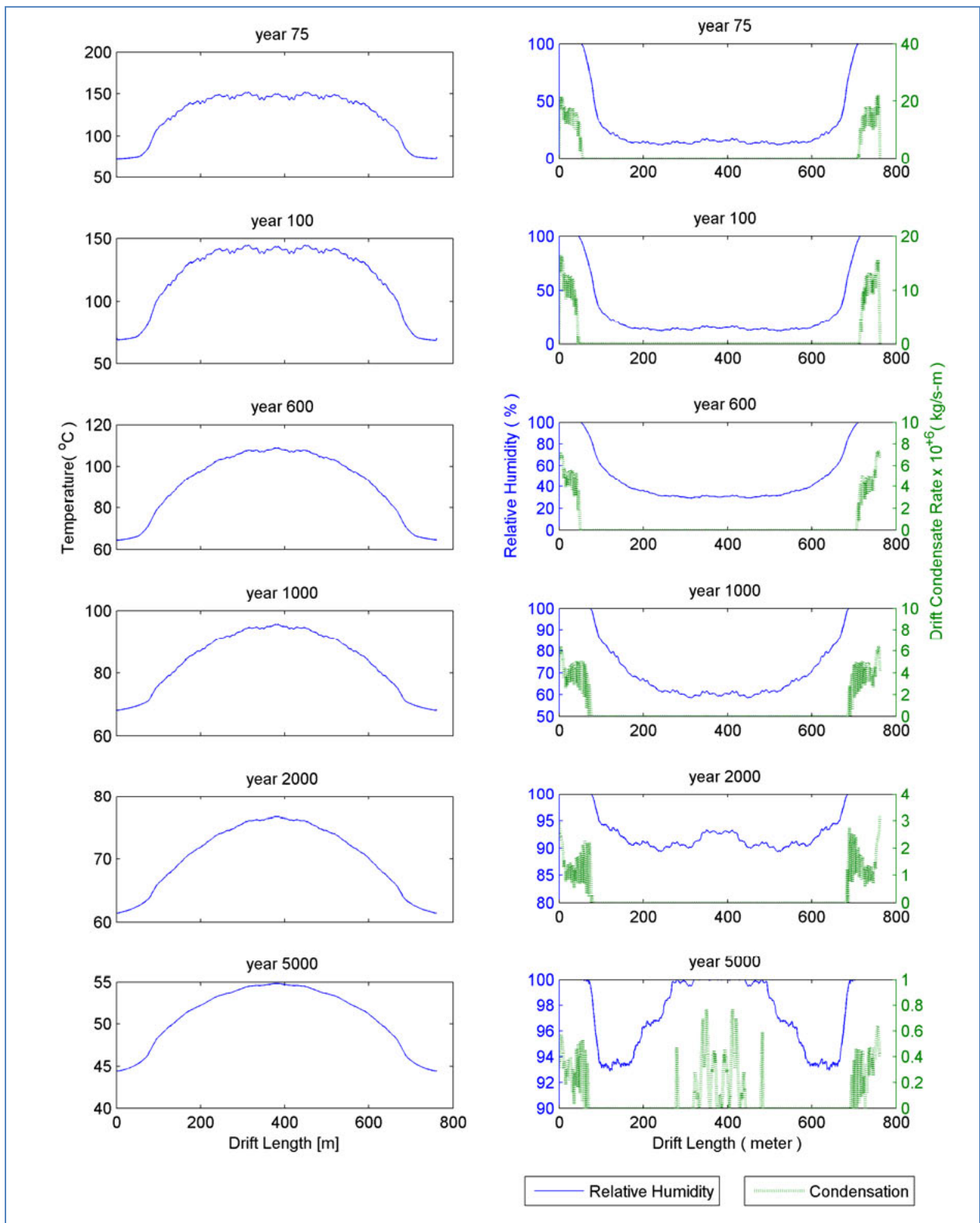
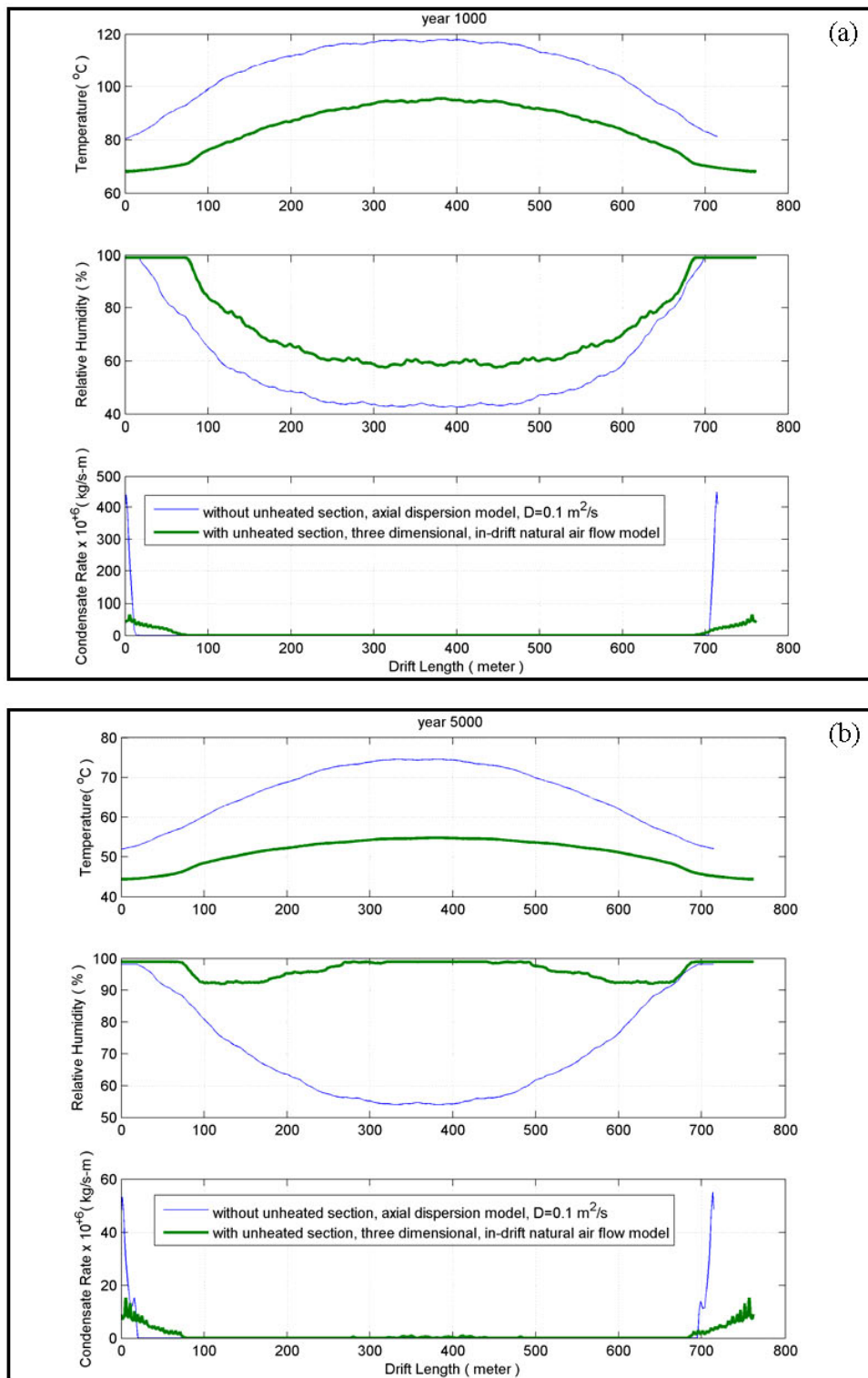


Figure 8.9-10
Temperature, relative humidity, and rate of condensation distributions along the drift length for selected post-closure time periods at the sidewall segment of the drift wall.

**Figure 8.9-11**

Temperature, relative humidity, and rate of condensation distributions along the drift length for selected post-closure time periods at the floor segment of the drift wall over the invert.

**Figure 8.9-12**

Temperature, relative humidity, and rate of condensation distributions along the drift length for the floor segment of the drift wall for two post-closure time periods: year 1000 (a); and year 5000 (b).

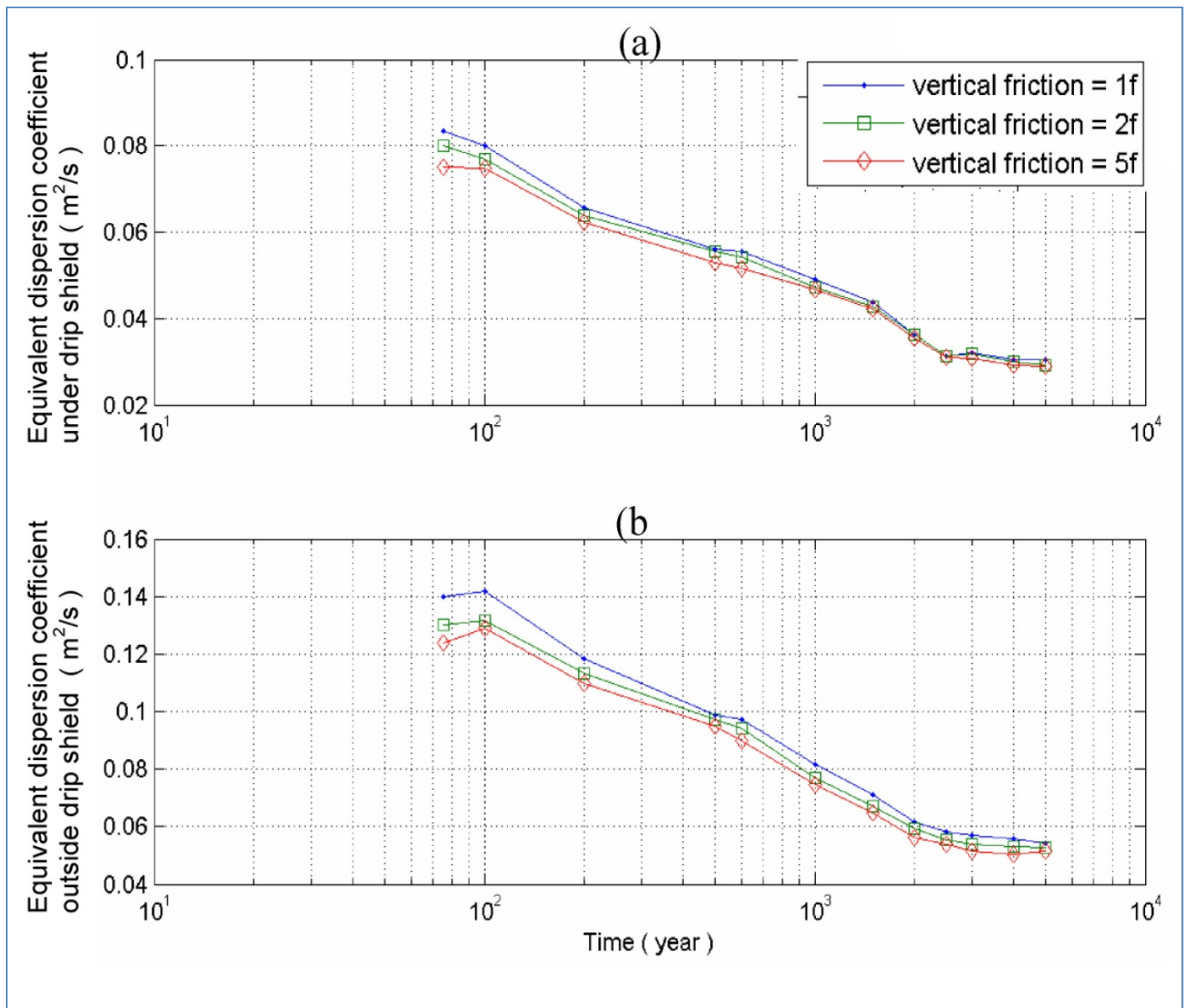


Figure 8.9-13

Sensitivity study of input friction loss coefficient, used in the air flow model, (a) inside and (b) outside the drip shield.

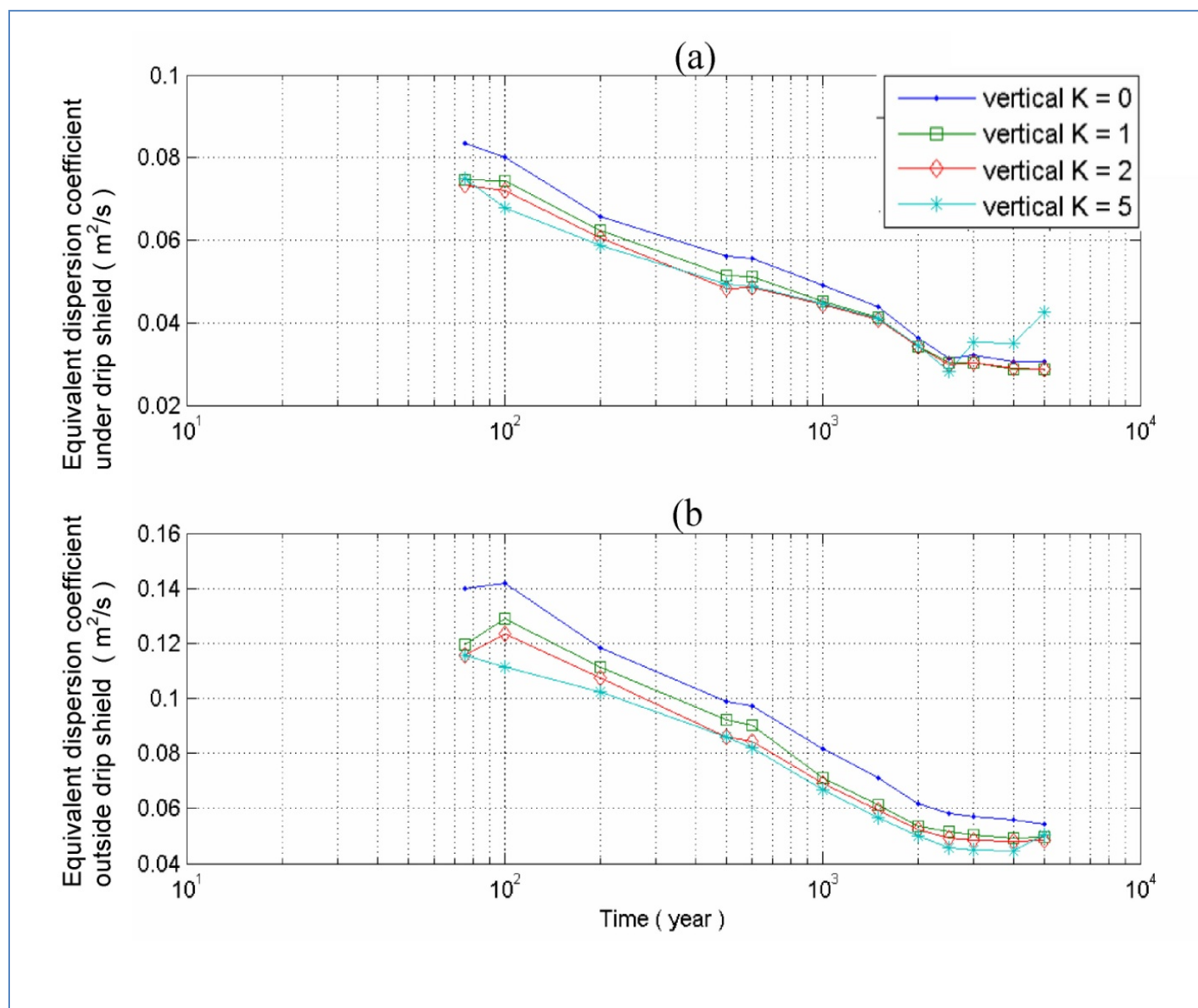


Figure 8.9-14
Sensitivity study of input kinetic shock loss factor, used in the air flow model, inside (a) and outside (b) the drip shield.

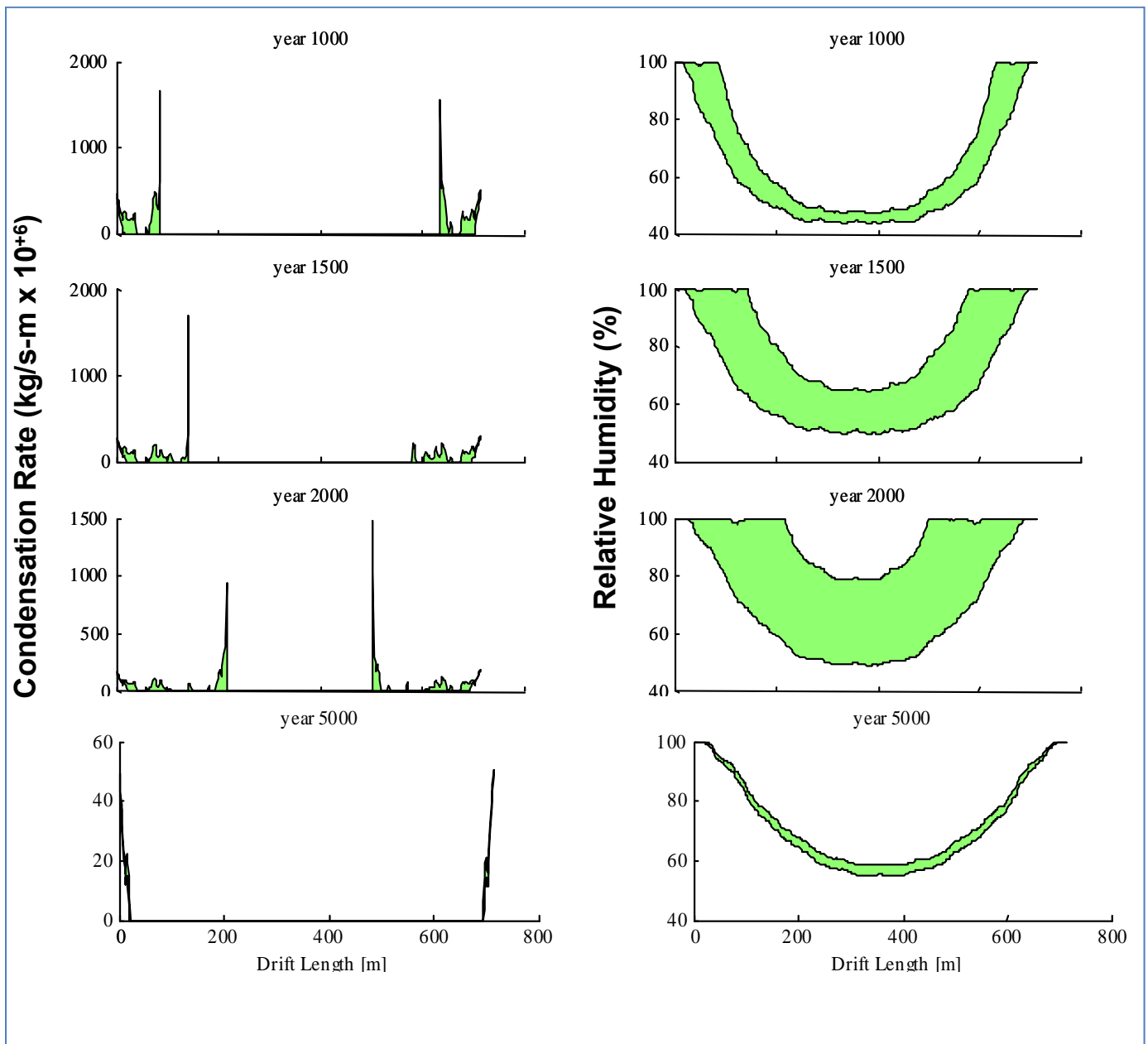


Figure 8.10-1
Barometric pressure fluctuation effects on relative humidity and
condensation rate, FY03 – FY04 model results.

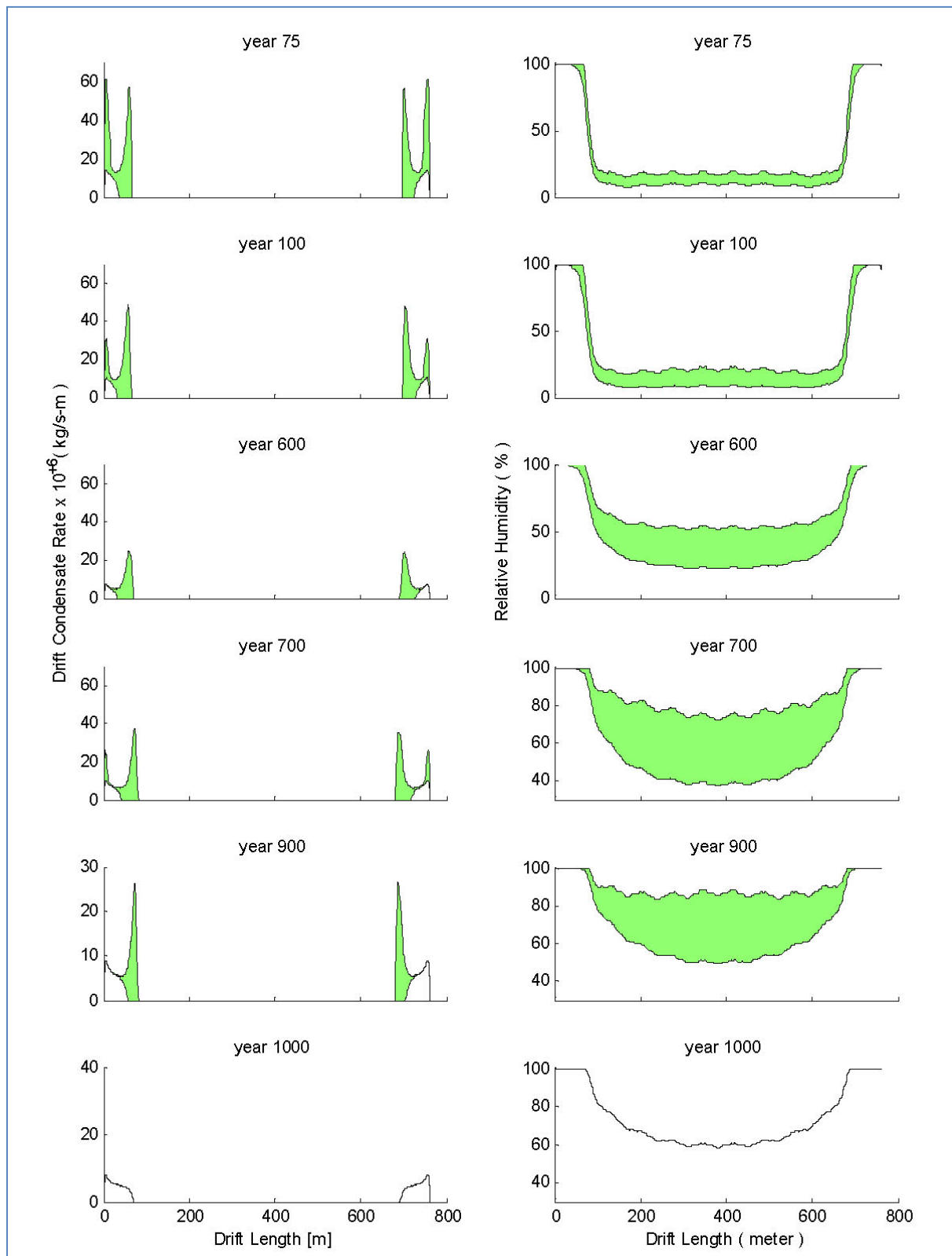


Figure 8.10-2
Barometric pressure fluctuation effects on relative humidity and condensation rate, updated FY06 model results at the roof segment of the drift wall.

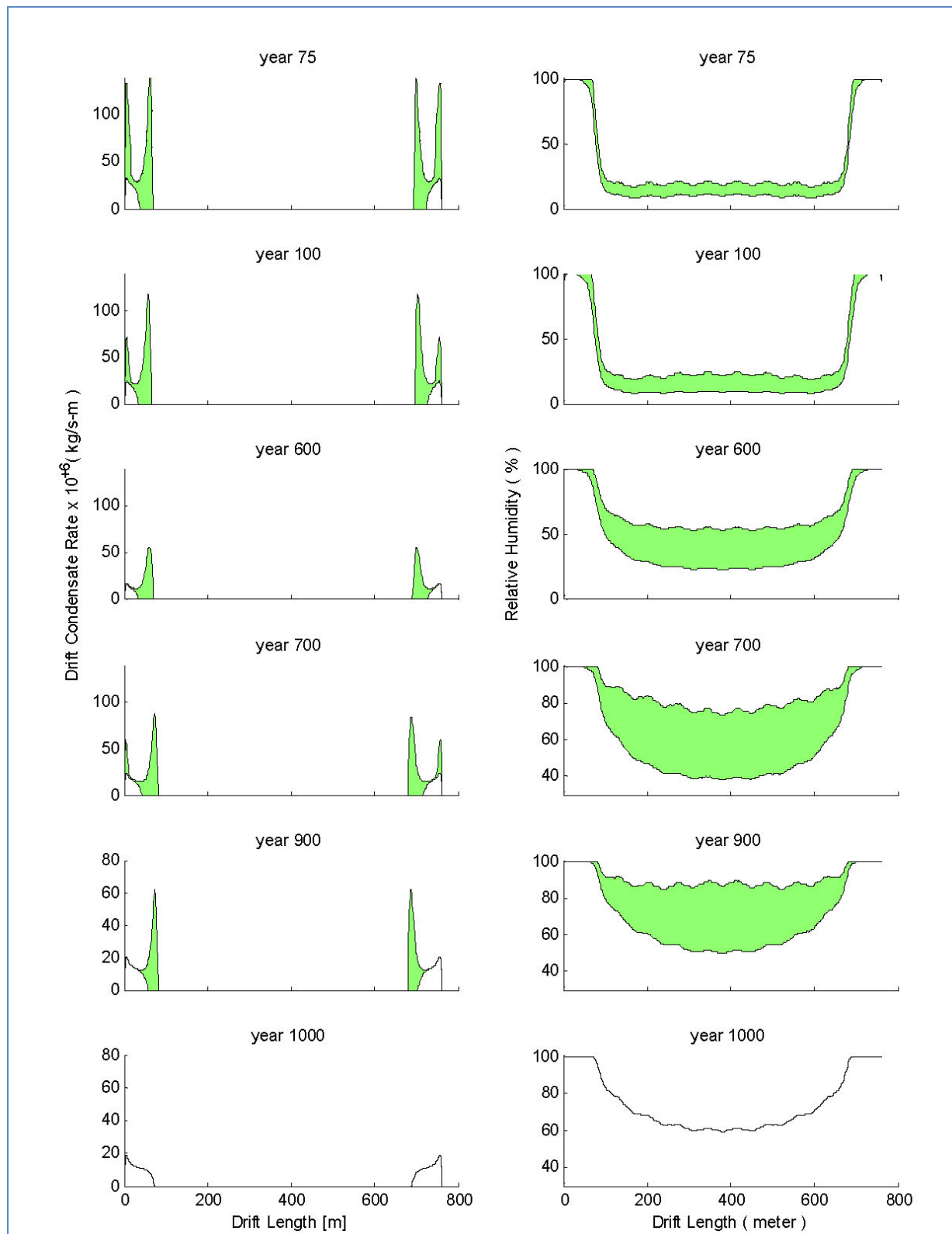


Figure 8.10-3
Barometric pressure fluctuation effects on relative humidity and condensation rate, updated FY06 model results at the sidewalls segment of the drift wall.

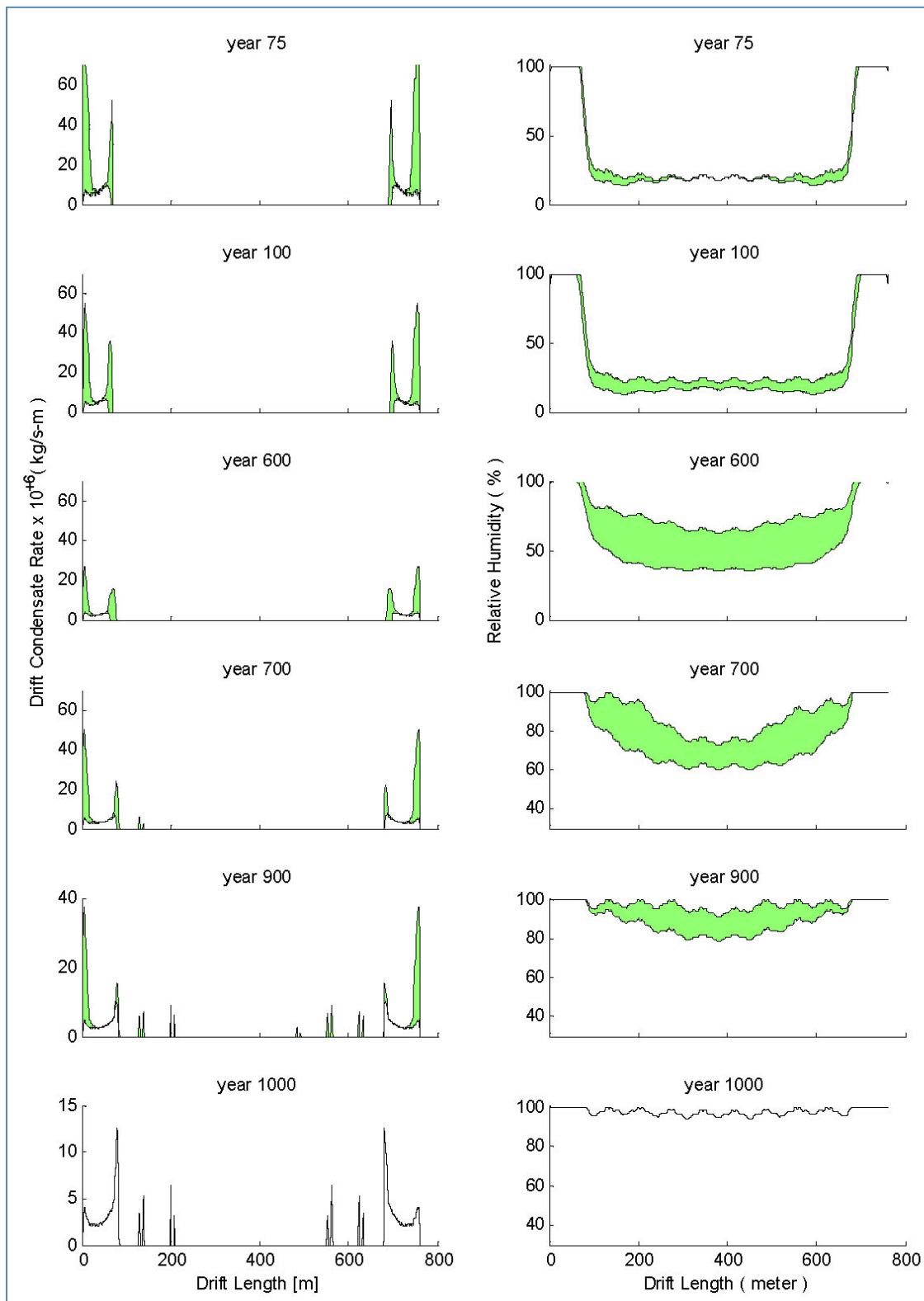


Figure 8.10-4
Barometric pressure fluctuation effects on relative humidity and condensation rate,
updated FY06 model results at the floor segment of the drift wall, over the invert.

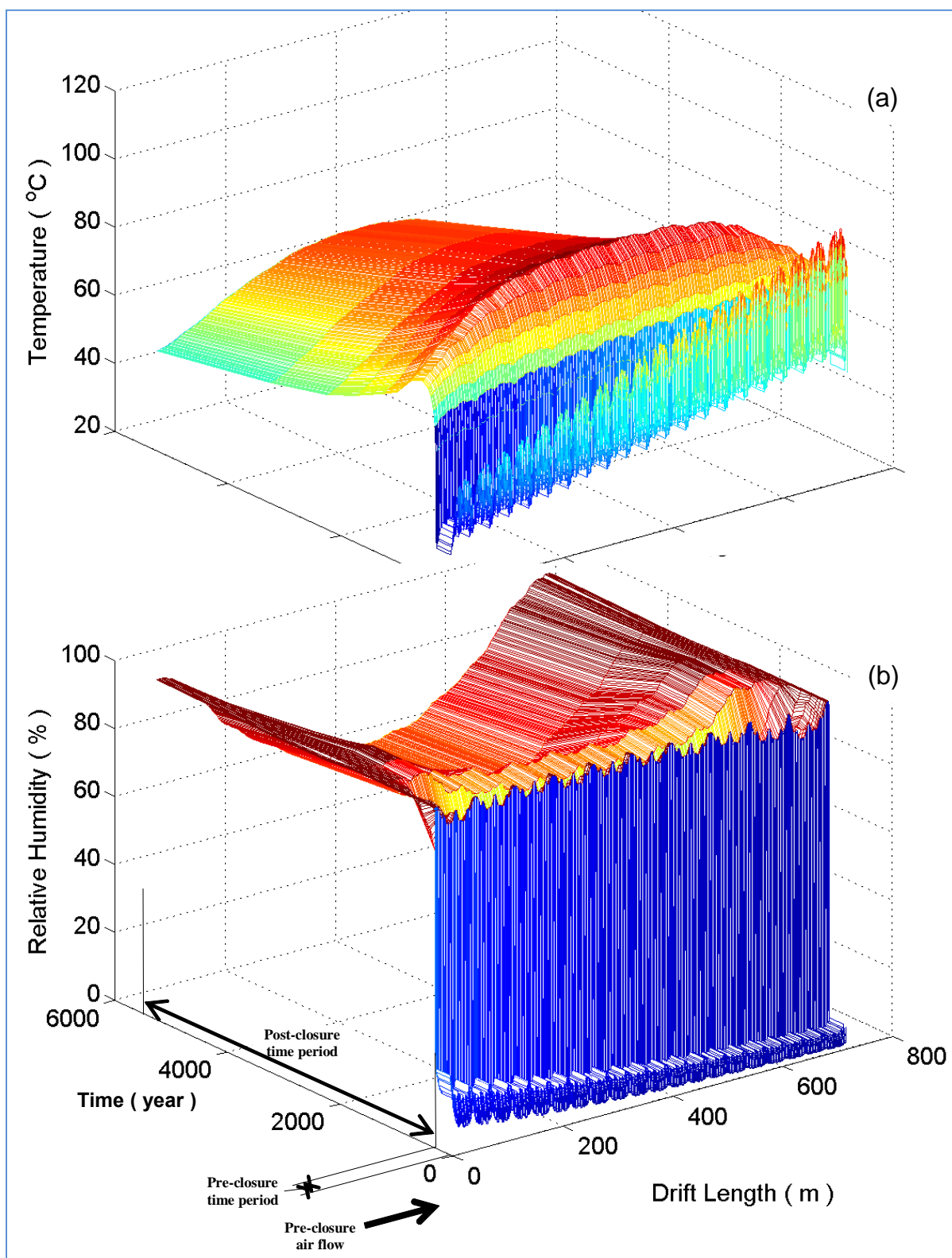


Figure 8.11-1
Long-term, forced ventilation studies (300 years), baseline results.

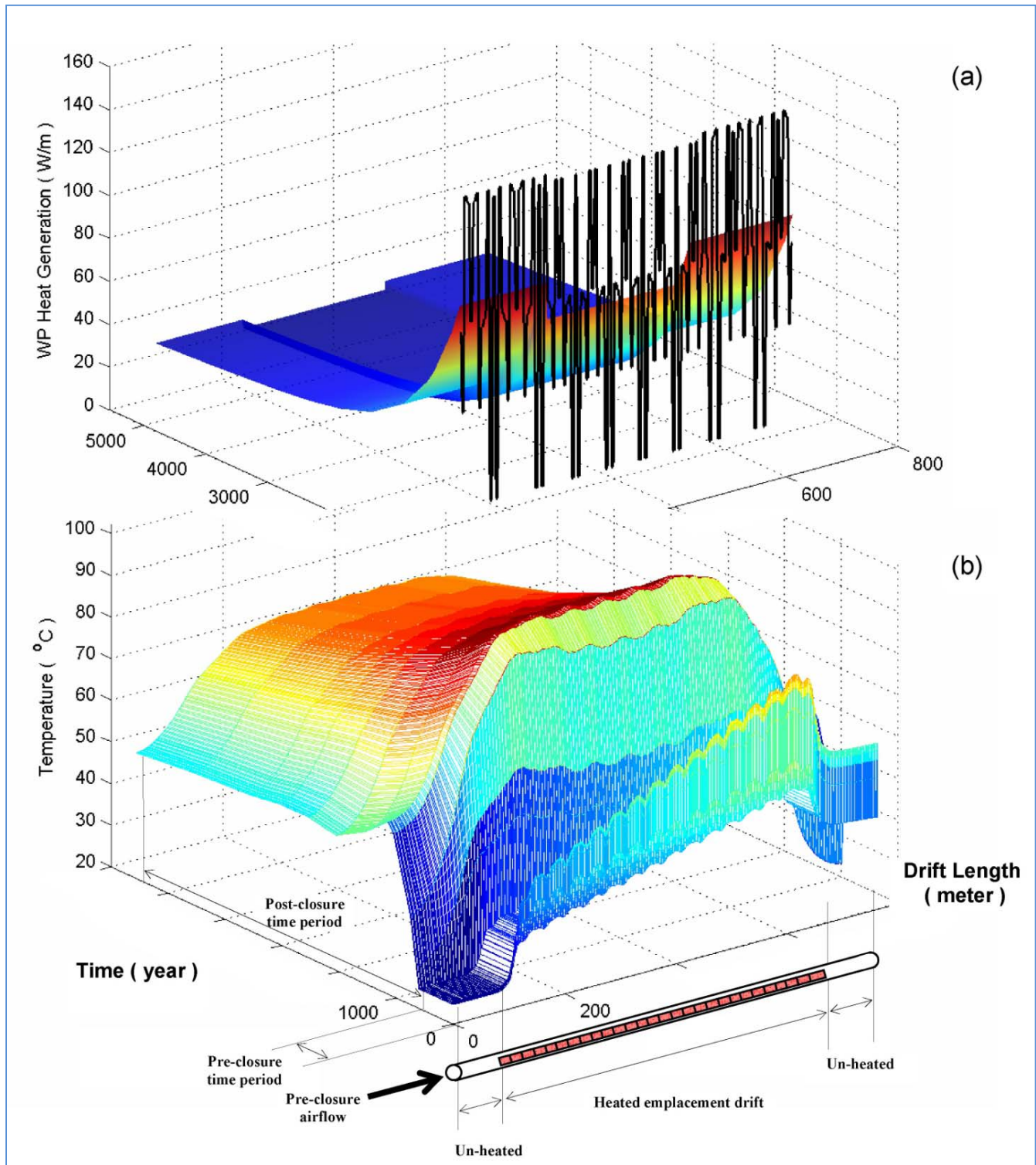


Figure 8.11-2

Variable, optimized post-closure heat load per unit length for individual WPs at year 600 (solid line), and line-averaged load equivalent (smooth surface) (a); temperature variation of a double-capacity, low-temperature, conceptual repository (b).

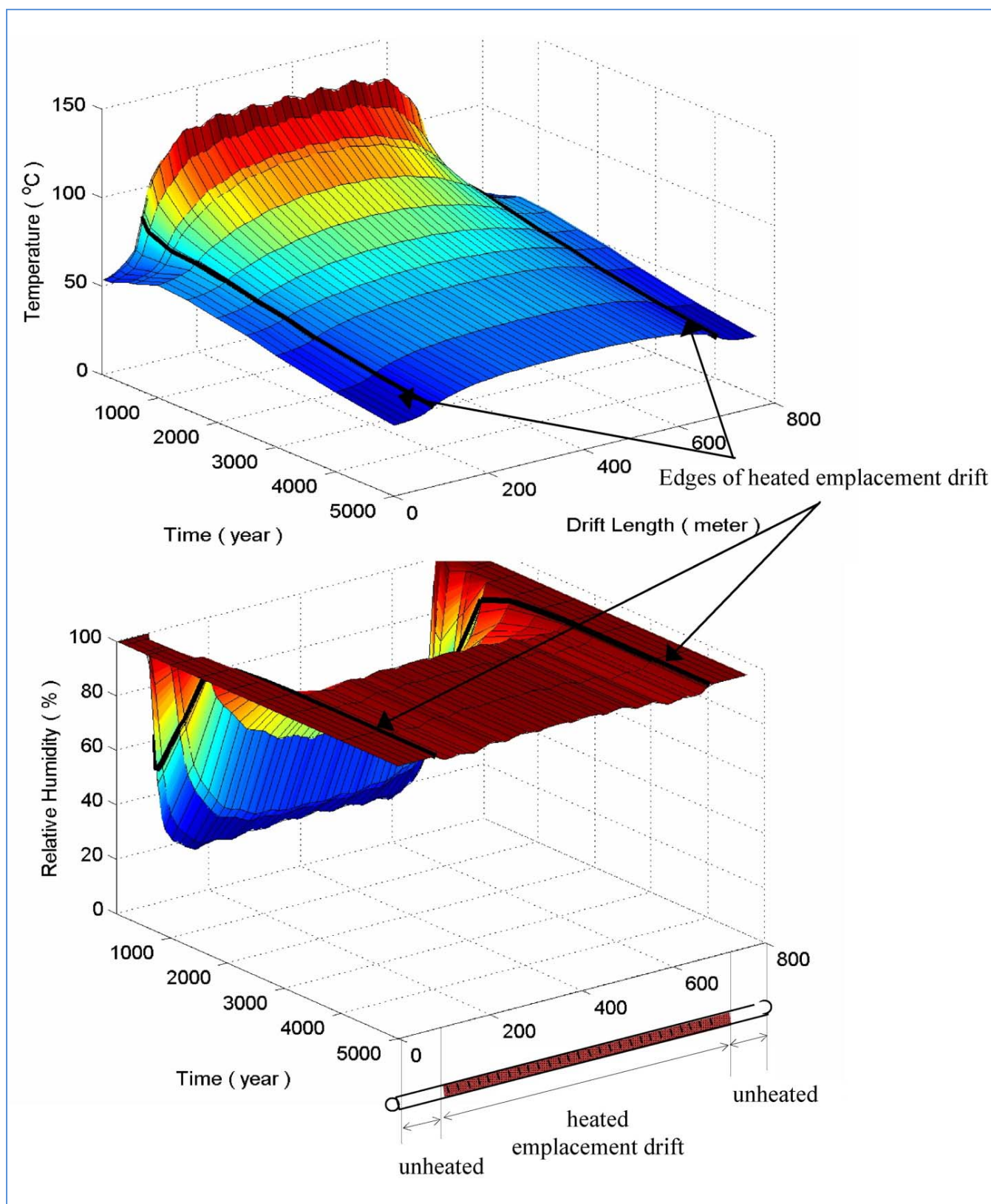


Figure 8.12-1
 In-rock (via drift) vapor flow studies, drift wall temperature (a) and wall relative humidity (b) distribution in time and space.

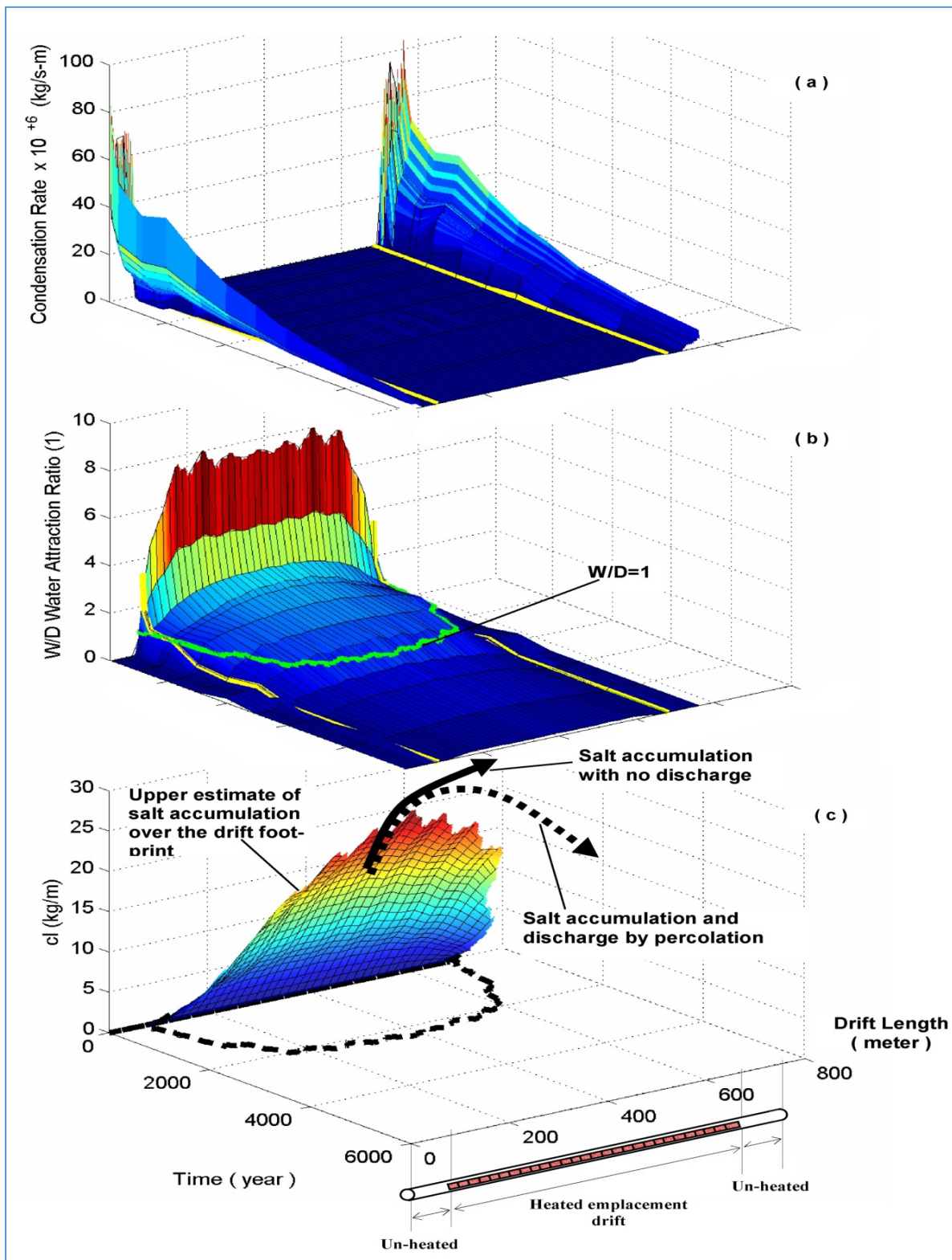


Figure 8.12-2
 Water condensation rate at the emplacement drift wall (a); W/D water attraction ratio (b); chloride accumulation over the drift width D (c); as a hypothesis from the model results.

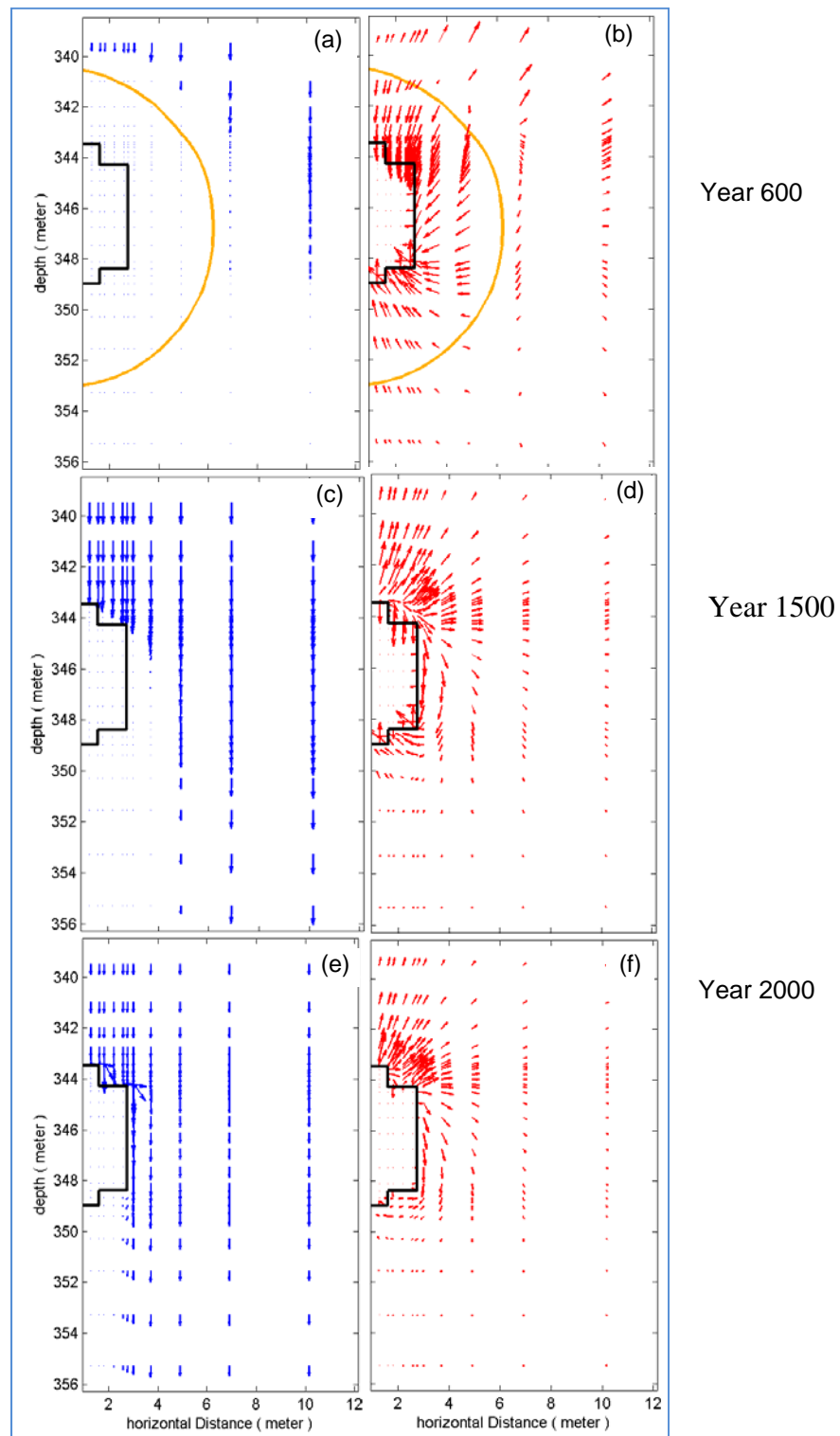


Figure 8.12-3

Water pore velocity in the rock mass surrounding the emplacement drift in liquid phase (left column, a, c, e) and gas phase (right column, b, d, f) at year 600 (a, b); year 1500 (c, d); and year 2000 (e, f); solid line indicates 96 °C contour, the boiling temperature at Yucca Mountain.

Table 2.1-1
Drilling, Coring, and Completion Summary for EWDP Phase III

Well ID ^a	Well Type	Well Status	Preliminary Drilling Method	Coring Method	Start Drilling Date	Drilling Completion Date	Total Depth (feet, bgs ^b)	Survey Coordinates		Ground Elevation (feet, amsl ^c)	Approx Open Hole Water Level at End of Drilling (feet, bgs)	Screened Interval(s) (feet, bgs)	Sand Pack Interval(s) (feet, bgs)	Lithology at Sand Pack Intervals	Westbay Packer Interval(s) (feet, bgs)	Well Casing Type	Well Casing Depth (feet, bgs)	Well Casing Out-side Diameter (in.)
								Latitude	Longitude									
19IM1A	Exploratory Borehole	Abandoned	AR-RC	NA	7/10/01	7/13/01	900	36° 40' 14.615"	116° 26' 56.397"	2687.3	366	NA	NA	NA	NA	NA	NA	NA
19IM1	Monitor Well - Multiple Screen	Completed	FM	NA	8/13/01	8/28/01	1012.5	36° 40' 14.615"	116° 26' 56.397"	2687.3	358	410.0-430.0	394.1-440.6	Alluvium	404-436	Steel	949.3	7
												515.0-535.0	503.3-545.4	Alluvium	508-540			
												574.9-674.9	562.3-689.6	Alluvium	568-680			
												724.9-784.8	715.0-797.7	Alluvium	722-788			
												849.5-949.3	838.8-967.3	Tertiary Tuff	846-949.3			
													967.3-1012.5 ^e	Tertiary Tuff				
19IM2A	Exploratory Borehole	Abandoned	AR-RC	NA	7/13/01	7/17/01	900	36° 40' 14.614"	116° 26' 55.597"	2688.1	369	NA	NA	NA	NA	NA	NA	NA
19IM2	Monitor Well - Multiple Screen	Completed	FM	NA	8/14/01	9/13/01	965.6	36° 40' 14.614"	116° 26' 55.597"	2688.1	358	410.2-430.2	382.7-443.4	Alluvium	NA	Steel	950.1	7
												515.0-534.9	500.5-550.4	Alluvium				
												574.9-674.9	561.2-684.6	Alluvium				
												724.9-784.9	715.8-797.6	Alluvium				
												849.9-950.1	840.1-965.8	Tertiary Tuff				
10SA	Exploratory Borehole	Abandoned	AR-RC	NA	7/18/01	7/28/01	1200	36° 43' 48.339"	116° 24' 20.725"	2963.5	383	NA	NA	NA	NA	NA	NA	NA
10S	Monitor Well - Multiple Screen	Completed	FM	NA	9/20/01	10/3/01	900	36° 43' 48.339"	116° 24' 20.725"	2963.5	579	660.0-700.0	650.5-710.8	Alluvium	652-702	Steel	880	6 5/8
												800.0-860.0	787.2-900.0	Tertiary Volcanic Conglomerate	796-870			
10P	Piezometer	Completed	CA	DC	9/20/01	1/13/02	910.5	36° 43' 48.874"	116° 24' 20.362"	2964.6	580	660.1-699.3 801.2-860.0	145.6-154.4 ^f	Alluvium	NA	PVC	879.9	2 3/8
													247.2-256.8 ^f	Alluvium				
													347.0-350.0 ^f	Alluvium				
													444.7-464.4 ^f	Alluvium				
													530.0-583.8 ^f	Alluvium				
													650.9-706.1	Alluvium				
													776 - 910.5	Tertiary Volcanic Conglomerate				
18P	Piezometer	Completed	AR	NA	9/20/01	10/21/01	890.4	36° 45' 04.797"	116° 25' 50.340"	3164.5	777	835.8-885	830.2-890.4	Tertiary Tuff	NA	PVC	885	2 3/8
22SA	Exploratory Borehole	Abandoned	AR-RC	NA	7/28/01	8/2/01	1200	36° 42' 15.132"	116° 25' 06.636"	2849.0	474	NA	NA	NA	NA	NA	NA	NA
22S	Monitor Well - Multiple Screen	Completed	FM	NA	9/21/01	10/25/01	1196.5	36° 42' 15.132"	116° 25' 06.636"	2849.0	473	521.5-581.3	510.4-590.1	Alluvium	514-582	Steel	1190.1	6 5/8
												661.2-760.6	648.8-770.6	Alluvium	650-766			
												880.2-980.0	866.5-991.0	Alluvium	874-982			
												1140.0-1180.0	1127.5-1196.5	Tertiary Volcanic Conglomerate	1134-1188			
22PA	Piezometer	Completed	CA	DC	1/13/02	2/5/02	779.8	36° 42' 15.712"	116° 25' 06.581"	2849.9	471	520.7-579.7 661.5-759.8	47.3-53.3 ^f	Alluvium	NA	PVC	770	2 3/8
													147.4-153.6 ^f	Alluvium				
													244.2-253.0 ^f	Alluvium				
													346.7-353.9 ^f	Alluvium				
													445.7-455.0 ^f	Alluvium				
													508.7-587.0	Alluvium				
													649.7-779.8	Alluvium				
22PB	Piezometer	Completed	AR-RC	NA	2/21/02	2/27/02	1199.7	36° 42' 15.665"	116° 25' 05.863"	2849.3	474	881.3-979.7	868.7-989.7	Alluvium	NA	PVC	1189.9	2 3/8
												1140.3-1179.7	1125.2-1199.7	Tertiary Volcanic Conglomerate				
23P	Piezometer	Completed	AR-RC	NA	3/9/02	3/20/02	1339.9	36° 41' 05.317"	116° 23' 50.412"	2800.2	426	460.9-519.9	449.1-531.0	Alluvium	NA	PVC	700	2 3/8
												650.5-689.8	635.9-700.0	Alluvium				

^a The official prefix for all new Nye County wells is "NC-EWDP-."
^b Below ground surface.
^c Above mean sea level.
^d Not applicable.
^e Caved interval of the borehole.
^f Air piezometers.

NOTES: All depth data have not been corrected for borehole deviation.
AR-RC = air rotary reverse circulation drilling method.
CA = Casing advance drilling method.
FM = flooded mud drilling method.
AR = air rotary method.
DC = Drive core method.

Table 2.1-2
Drilling, Coring, and Completion Summary for EWDP Phase IV

Well Name	Primary Drilling Method	Coring Method	Drilling Duration		Total Depth (feet bgs ^a)	Yucca Mountain Project Survey Coordinates		Ground Elevation ^b (feet amsl ^c)	Approximate Open-Hole Water Level at End of Drilling (feet bgs)	Screened Interval (feet bgs)		Sandpack Interval (feet bgs)		Lithology at Sandpack Interval	Well Casing Total Depth ^d (feet bgs)
			Start	Completion		North Latitude	West Longitude			To	From	To	From		
16P	AR-RC	NA ^e	12/13/02	1/27/03	2900.0	36° 43' 29.089"	116° 29' 22.219"	2888.9	496	489.4	549.4	474.8	555.3	Tertiary Tuff	559.9
24P	AR-RC	DC	7/16/03	8/19/03	1860.0	36° 42' 16.775"	116° 26' 52.756"	2789.8	404	400.0	440.0	393.2	446.8	Tertiary Tuff	450.0
27P	AR-RC	NA	11/20/02	12/12/02	1900.0	36° 44' 02.072"	116° 29' 51.436"	2973.4	583	580.7	620.6	563.0	626.7	Tertiary Tuff	631.0
28P	AR-RC	NA	10/21/02	11/20/02	2080.0	36° 42' 28.386"	116° 29' 19.390"	2767.2	374	370.0	449.0	365.6	451.5	Tertiary Tuff	459.3
29P	AR-RC	DC	6/25/03	7/15/03	790.7	36° 40' 57.297"	116° 26' 52.884"	2724.3	349	340.0	390.0	333.8	404.8	Tertiary Tuff	395.0
19PB	MR	NA	12/2/03	12/18/03	634.0	36° 40' 15.440"	116° 26' 55.593"	2688.4	368	375.5	395.0	350.0	401.9	Alluvium	405.3
		SC								514.7	534.7	505.1	545.2	Alluvium	545.0

^aBelow ground surface.
^bGround elevations provided by the Yucca Mountain Project and based on a Global Positioning System. The elevations are not known to be precise to one-tenth of a meter.
^cAbove mean sea level.
^dPVC blank well casing and screen with 2¾-inch outside diameter.
^eNot applicable.

NOTES:
AR-RC = air rotary reverse circulation drilling method.
MR = Mud rotary drilling method used to penetrate and case off upper 350 ft of alluvium.
DC = Drive core method.
SC = Somic core method.

Table 2.1-3
Drilling, Coring, and Completion Summary for EWDP Phase V

Well Name	Primary Drilling Method(s)	Coring Method	Construction Duration		Total Depth (feet bgs ^a)	Yucca Mountain Project Survey Coordinates		Ground Elevation (feet amsl ^b)	Approximate Open Hole Water Level at End of Drilling (feet bgs)	Piezometer Screen and U-tube/ Injection Line Interval(s) (feet bgs)		Sand Pack Interval(s) (feet bgs)		Lithology at Sand Pack Interval(s)	Well Casing Type	Well Casing Total Depth (feet bgs)	Well Casing Outside Diameter (inches)
			Start	End		North Latitude	West Longitude			To	From	To	From				
22PC	DR-CA ^c	SC	10/14/04	11/11/04	763.0	36° 42' 15.090"	116° 25' 05.906"	2848.8	472	510.0	579.8	505.2	585.1	Alluvium	PVC	585.3	2 3/8
										665.4	755.0	659.2	763.0			760.5	
13P	AR-RC	NA	6/16/05	7/28/05	1559.0	36° 44' 39.866"	116° 30' 50.235"	2937.5	433	426.0	466.0	419.0	471.0	Tertiary Tuff	PVC	476.1	2 3/8
24PA	DR-CA AR-RC ^d	NA	1/25/06	1/28/06	152.0	36 42' 15.777"	116 26' 52.258"	2788.9	N/A ^e	N/A	N/A	N/A	N/A	N/A	N/A	N/A	N/A
24PB	AR-RC ^f DR-CA	NA	1/29/06	3/26/06	1394.1	36° 42' 15.777"	116° 26' 52.692"	2788.8	404	729.2	769.9	723.1	776.9	Tertiary Tuff	SS	1176.6 ^e	2 3/8
										866.4 ^g	870.5 ^g	865.3	873.7				
										1145.2 ^h	1149.4 ^h	1143.8	1153.6				
33P	NA	NA	N/A	N/A	657.0	36° 39' 38.210"	116° 29' 45.814"	2570.1	204	210.8	249.9	205.0	254.0	Alluvium	PVC	260.1	1 2/3
										484.5	523.6	476.0	528.0	Alluvium		533.8	1 2/3
										600.9	640.0	591.0	657.0	Alluvium		650.2	1 2/3
32P	AR-RC ⁱ DR-CA	NA	3/28/06	4/10/06	1000.0	36° 38' 21.544"	116° 29' 03.381"	2545.3	245	238.7	277.9	233.8	282.5	Alluvium	PVC	287.7	1 2/3
										463.7	483.3	458.4	489.4	Tertiary Basalt		493.0	1 2/3
										697.9	737.0	692.7	764.0	Tertiary Fluvial/ Alluvial Deposits		913.0	1 2/3

^aBelow ground surface.
^bFeet above mean sea level.
^cDrilled and cased alluvium to 460 ft bgs.
^dDrilled and sampled to 57.7 ft bgs. Reamed and drilled ahead with DR-CA Symmetrix™ to approximately 157 ft bgs.
^eNot applicable.
^fDrilled and sampled entire depth of borehole. Reamed and set surface casing using DR-CA Symmetrix to approximately 467 ft bgs.
^gU-tube/injection line intervals from top of intake valve to the bottom of the U-tube.
^hCasing below screen interval used as support casing for instrumentation.
ⁱDrilled and sampled entire depth of borehole. Used DR-CA to set surface at approximately 57.5 ft bgs.

NOTES:
24PA was abandoned due to drilling equipment lost in the borehole at approximately 152 feet.
Nye County completed 33P, which had been drilled previously by the U.S. Department of Energy.
DR-CA = dual rotary casing advance drilling method.
AR-RC = air rotary reverse circulation drilling method.
SC=sonic coring method.

Table 2.4-1
Summary of Phase III Geophysical Logs

Borehole ID (NC-EWDP-)	Date	Log Suite Type ^a	Borehole/Well Depth at Time of Logging (feet)	Logged Interval (feet)	Log Type											Comments
					Gamma	Density	Spectral Gamma	Moisture	Fluid Temperature	Deviation	Resistivity (SPR, R8-R64)	Fluid Resistivity	Spontaneous Potential	Caliper	Acoustic Velocity (Sonic)	
10SA	7/27/01	1	1200	0-1180	x	x	x	x	x	x						Run inside 4.5-in. dual-wall drill pipe in 5.375-in. borehole with approximately 20 ft of 6.625-in. OD steel surface casing.
10S	9/30/01	2	900	0-895	x	x	x	x	x	x	x	x	x	x	x	Run in 14.75-in. flooded mud borehole with 62.5 ft of 18-in. OD steel conductor casing and drilling mud from approximately 5 ft to total depth.
10S	2/18/02	3	880	0-880	x	x		x								Run inside 6.625-in. OD steel well casing.
10S	9/25/02	3	870	0-867						x					x	Run inside 4-in. Schedule 80 PVC riser pipe from 0 to 647 ft and 2.9-in. OD PVC Westbay [®] casing from 647 to 867 ft.
10P	12/27/01	1	910.5	0-900	x					x			x		x	Run in 6.625-in. OD drill casing from 0 to 792 ft, telescoped inside of 9.625-in. drill casing from 0 to 304 ft, and in 5.875 in. open hole from 792 to 900 ft.
10P	12/27/01	2	910.5	790-907	x	x	x	x	x	x	x	x	x	x	x	Run inside 5.875-in. open hole beyond drill casing from 790 to 900 ft.
10P	2/19/02	3	880	0-880	x	x		x		x						Run inside 2-in. Schedule 80 PVC well casing, unable to run deviation tool below 128 ft.
10P	9/25/02	3	880	0-879						x					x	Run inside 2-in. Schedule 80 PVC well casing.
18P	2/20/02	3	885	0-885	x	x		x		x						Run inside 2-in. Schedule 80 PVC well casing.
19IM1A	7/13/01	1	900	0-880	x	x	x	x	x	x						Run inside 4.5-in. dual-wall drill pipe in 5.375-in. borehole with approximately 20 ft of 6.625-in. OD steel surface casing.
19IM1 ^b	10/2/01	3	950	0-935	x	x			x	x						Run inside 7-in. OD steel well casing prior to pump testing.
19IM2A	7/17/01	1	900	0-880	x	x	x	x	x	x						Run inside 4.5-in. dual-wall drill pipe in 5.375-in. borehole with approximately 20 ft of 6.625-in. OD steel surface casing.
19IM2	9/8/02 - 9/9/02	2	965	0-965	x	x	x	x	x	x	x	x	x	x	x	Run in 14.75-in. flooded mud borehole with 75 ft of 18-in. OD steel conductor casing and drilling mud from approximately 12 ft to total depth.
19IM2	10/2/01	3	950	0-925	x	x			x	x		x				Run inside 7-in. OD steel well casing prior to pump testing.
19IM2	9/26/02	3	950	0-917											x	Run inside 7-in. OD steel well casing.
22SA	8/1/01	1	1200	0-1180	x	x	x	x	x	x						Run inside 4.5-in. dual-wall drill pipe in 5.375-in. borehole with approximately 20 ft of 6.625-in. OD steel surface casing.
22S	10/20/01	2	1197	0-1190	x	x	x	x	x	x	x	x	x	x	x	Run in 14.75-in. flooded mud borehole with 75 ft of 18-in. OD steel conductor casing and drilling mud from approximately 5 ft to total depth.
22S	2/19/02	3	1190	0-1180	x	x		x								Run inside 6.625-in. OD steel well casing.
22S	9/26/02	3	1183	0-1181						x					x	Run inside 4-in. Schedule 80 PVC riser pipe from 0 to 508 ft and 2.9-in. OD PVC Westbay [®] casing from 508 to 1183 ft.
22PA	2/19/02	3	770	0-770	x	x		x		x						Run inside 2-in. Schedule 80 PVC well casing, unable to run deviation tool below 229 ft.
22PA	9/25/02	3	770	0-767						x					x	Run inside 2-in. Schedule 80 PVC well casing.
22PB	3/3/02	1	1212	1212	x	x	x	x	x	x	x	x	x	x	x	Run inside 8.5-in. open hole with 15.1 ft of 10.75-in. OD steel surface casing.
22PB	3/18/02	3	1212	0-987			x									Run inside 2-in. Schedule 80 PVC well casing; to total depth in the shallow piezometer and to 271 ft in the deep piezometer.
22PB	9/25/02	3	1190	0-1188						x					x	Run inside 2-in. Schedule 80 PVC well casing in the deep piezometer.
23P	3/26/02	2	702	0-702	x	x		x	x	x	x	x	x	x	x	Run inside 8.5-in. open hole with 16.9 ft of 10.75-in. OD steel surface casing.
23P	9/26/02	3	700	0-691	x	x	x	x								Run inside 2-in. Schedule 80 PVC well casing in the deep piezometer.

NOTES:

NA = not applicable; OD = outer diameter; PVC = polyvinyl chloride

^a1 = logged inside drill pipe or casing (drill-string log); 2 = logged in open borehole (open-hole log); 3 = logged inside well casing (well-completion log).^bNo open-hole logging was conducted in well borehole NC-EWDP-19IM1 due to borehole instability problems at total depth

Table 2.4-2
Summary of Phase IV Geophysical Logs

Well Name	Date	Suite	Interval Logged (feet)		Log Name													Record Identification Desigation (RID) Number	Company Name	Comments
					Gamma (Natural Gamma)	Density	Spectral Gamma	Neutron (Moisture)	Fluid Temperature	Resistivity (SPR, R8-R64)	Fluid Resistivity	Spontaneous Potential	Caliper	Acoustic Velocity (Sonic)	Magnetic Susceptibility	Optical Televiwer	Deviation			
16P	1/20/03	Open-hole	1,980	2,898	X	X	X	X	X		X	X		X				5482	Geophysical Logging Services (GLS)	Run in 6.5- to 5.625-inch borehole with 61.5 feet of 12-inch surface casing.
	1/20/03	Drill-string	0	2,880	X				X		X						X	5481	GLS	Run in 4.5-inch dual-wall drill pipe in 6.5- to 5.625-inch borehole with 61.5 feet of 12-inch surface casing.
	1/8/04	Well-completion	0	559.9	X	X	X	X							X		X	6035	GLS	Run in 2-inch Schedule 80 PVC well casing with 61.5 feet of 12-inch surface casing.
	3/4/04		0	560					X									6209	GLS	Run in 2-inch Schedule 80 PVC well casing with 61.5 feet of 12-inch surface casing.
	1/10/03 to 11/03	Open-hole	0	2,121	X	X		X	X	X	X		X		X		X	5485	GLS	Run in 6.5- to 5.75-inch borehole with 61.5 feet of 12-inch surface casing.
28P	11/2/02	Open-hole	0	1,196.5												X		5340	GLS	Run in 6.5- to 6.125-inch borehole.
	11/2/02		0	1,196.5	X	X	X	X	X	X	X		X	X	X		X	5341	GLS	Run in 6.5- to 6.125-inch borehole.
	11/13/02		1,120	2,064	X		X		X	X	X		X					5321	GLS	Run in 6.5- to 5.625-inch borehole.
	11/13/02	Drill-string	1,120	2,050	X	X	X	X	X	X							X	5337	GLS	Run in 4.5-inch dual-wall drill pipe in 6.5- to 5.625-inch borehole.
	1/8/04	Well-completion	0	459.3	X	X	X	X							X		X	6034	GLS	Run in 2-inch Schedule 80 PVC well casing.
	3/4/04		0	459					X									6213	GLS	Run in 2-inch Schedule 80 PVC well casing.
27P	1/8/04	Well-completion	0	630.3	X	X	X	X							X		X	6036	GLS	Run in 2-inch Schedule 80 PVC well casing with 60.4 feet of 12-inch surface casing.

Table 2.4-2
Summary of Phase IV Geophysical Logs

Well Name	Date	Suite	Interval Logged (feet)		Log Name													Record Identification Desigation (RID) Number	Company Name	Comments
					Gamma (Natural Gamma)	Density	Spectral Gamma	Neutron (Moisture)	Fluid Temperature	Resistivity (SPR, R8-R64)	Fluid Resistivity	Spontaneous Potential	Caliper	Acoustic Velocity (Sonic)	Magnetic Susceptibility	Optical Televiwer	Deviation			
	3/4/04	Open-hole	0	631					X									6212	GLS	Run in 2-inch Schedule 80 PVC well casing with 60.4 feet of 12-inch surface casing.
	12/7/02 to /8/02		0	1,897.7	X	X		X	X	X	X	X	X	X	X		X	5536	GLS	Run in 6.5- to 6-inch borehole with 60.4 feet of 12-inch surface casing.
	12/7/02 to 12/8/02		0	1,880												X		5484	GLS	Run in 6.5- to 6-inch borehole with 60.4 feet of 12-inch surface casing.
29P	7/9/03	Open-hole	0	702	X	X		X	X	X	X		X	X	X		X	5746	GLS	Run in 5-inch steel casing inside 6.25-inch borehole to total depth with 61.5 feet of 12-inch surface casing. Inductive resistivity and inductive conductivity logs run as a test in the unsaturated zone.
	7/9/03		0	700												X		5745	GLS	Run in 6.25-inch borehole with 61.5 feet of 12-inch surface casing.
	7/10/03	Drill-string	0	695.4	X			X										5767	Century Geophysical (Century)	Run in 5-inch steel casing inside 6.25-inch borehole with 61.5 feet of 12-inch surface casing.
	7/10/03		0	695.4	X	X												5766	Century	Run in 5-inch steel casing inside 6.25-inch borehole with 61.5 feet of 12-inch surface casing.
	1/8/04	Well-completion	0	395	X	X	X	X							X		X	6032	GLS	Run in 2-inch Schedule 80 PVC well casing with 61.5 feet of 12-inch surface casing.
	3/4/04		0	395					X								X	6214	GLS	Run in 2-inch Schedule 80 PVC well casing with 61.5 feet of 12-inch surface casing.
24P	8/8/03	Drill-string	0	1,840	X	X	X	X	X	X							X	5831	GLS	Run in 4.5-inch dual-wall drill pipe inside 6.25- to 6.125-inch borehole with 61.5 feet of 12-inch surface casing.
	8/9/03		0	1,658.4	X			X										5830	Century	Run in 5-inch steel casing inside 6.25- to 6.125-inch borehole with 61.5 feet of 12-inch surface casing.
	8/9/03		0	1,659.1	X	X												5829	Century	Run in 5-inch steel casing inside 6.25- to 6.125-inch borehole with 61.5 feet of 12-inch surface casing.

Table 2.4-2
Summary of Phase IV Geophysical Logs

Well Name	Date	Suite	Interval Logged (feet)		Log Name												Record Identification Designation (RID) Number	Company Name	Comments	
					Gamma (Natural Gamma)	Density	Spectral Gamma	Neutron (Moisture)	Fluid Temperature	Resistivity (SPR, R8-R64)	Fluid Resistivity	Spontaneous Potential	Caliper	Acoustic Velocity (Sonic)	Magnetic Susceptibility	Optical Televiwer				Deviation
	8/10/03	Open-hole	0	1,733					X	X	X		X	X				6031	GLS	Run in 6.25- to 6.125-inch borehole with 61.5 feet of 12-inch surface casing.
	8/10/03		728	1,550											X	X	6062	GLS	Run in 6.25- to 6.125-inch borehole with 61.5 feet of 12-inch surface casing.	
	1/9/04	Well-completion	0	450	X	X		X						X		X	6037	GLS	Run in 2-inch Schedule 80 PVC well casing with 61.5 feet of 12-inch surface casing.	
	3/4/04		0	450					X								6211	GLS	Run in 2-inch Schedule 80 PVC well casing with 61.5 feet of 12-inch surface casing.	
	19PB	11/22/03	Open-hole	0	350													X	6269	GLS
12/18/03		Drill-string	0	634	X	X	X	X	X								X	6270	GLS	Run in sonic coring casings within multiple telescoping casings and 18 feet of 17.5-inch surface casing.
12/19/03			0	619.6	X	X		X			X							6102	Century	Run in 5.5-inch steel casing within multiple telescoping casings and 18 feet of 17.5-inch surface casing.
19PB (deep)	1/9/04	Well-completion	0	545	X	X	X	X						X		X	6038	GLS	Run in 2-inch Schedule 80 PVC within multiple telescoping casings and 18 feet of 17.5-inch surface casing.	
	3/4/04		0	545					X									6210	GLS	Run in 2-inch Schedule 80 PVC within multiple telescoping casings and 18 feet of 17.5-inch surface casing.

Table 2.4-3
Summary of Phase V Geophysical Logs

Well Name	Date	Suite	Interval Logged (feet)		Log Name													Record Index Designator (RID) Number	Company Name	Comments
					Gamma	Density	Spectral Gamma	Neutron (Moisture)	Fluid Temperature	Resistivity (SPR, R8-R64)	Fluid Resistivity	Fluid Electrical Conductivity	Spontaneous Potential	Caliper	Acoustic Velocity (Sonic)	Optical Televiwer	Deviation			
13P	7/24/05	Drill-string	0	1,558	X		X		X								X	6698	GLS	Run in 4.5-inch dual-wall drill pipe inside 6.5-inch borehole with 57.8 feet of 8.625-inch surface casing.
	7/24/05	Open-hole	140	709	X				X	X	X		X	X				6788	GLS	Run in open borehole below drill string set at 140 feet. Borehole conditions did not permit logging below 709 feet. Conductivity and induction resistivity logs run for evaluation purposes. Data are contained in RID6698.
	7/24/05	Open-hole	0	140												X		6790	GLS	Video run to observe bridging in borehole during geophysical logging.
	8/4/05	Drill-string	0	1,512.4	X	X		X										6773	Century	Run in 5.5-inch steel casing inside 6.5-inch borehole with 57.8 feet of 8.625-inch surface casing.
	9/21/05	Well-completion	0	477	X		X		X		X						X	6794	GLS	Run in 2-inch schedule 80 PVC well casing with 57.8 feet of 8.625-inch surface casing.
	9/21/05	Well-completion	0	464.7												X		6790	GLS	Video run in 2-inch schedule 80 PVC well casing during completion logging.
22PC	11/11/04	Drill-string	1.2	759	X	X		X										6783	Century	Run in 5.5-inch steel casing within multiple telescoping casings and 460 feet of 10.75-inch surface casing.
	11/12/04	Drill-string	0	762.5	X	X	X	X	X	X	X						X	6787	GLS	Run in sonic core casings within multiple telescoping casings and 460 feet of 10.75-inch surface casing.
	11/17/04	Well-completion	346	710										X				6573	GLS	Caliper run in 2-inch schedule 80 PVC casing to inspect it for cracks or separation of joints.
	11/17/04	Well-completion	0	698												X		6567	GLS	Video run in 2-inch schedule 80 PVC casing to inspect it for cracks or separation of joints.
24PB	2/14/06	Drill-string	0	773.4													X	6868	GLS	Run in 5.5-inch dual-wall drill pipe with 467.3 feet of 10-inch surface casing.
	2/23/06	Open-hole	0	1,395	X					X	X		X	X				6865	GLS	Run in 6.5-inch open borehole with 467.3 feet of 10-inch surface casing.
	3/8/06	Open-hole	0	480												X		6870	GLS	Video log run to observe obstruction in borehole at 480 feet.
	3/8/06	Drill-string	0	1,375													X	6870	GLS	Run in 5.5-inch dual-wall drill pipe with 467.3 feet of 10-inch surface casing.
	3/8/06	Open-hole	0	1,000												X		6870	GLS	Video log run in 6.5-inch open borehole with 467.3 feet of 10-inch surface casing.
	3/8/06	Open-hole	387	1,392											X			6870	GLS	Run in 6.5-inch open borehole with 467.3 feet of 10-inch surface casing.
	3/9/06	Open-hole	464.5	1,395												X	X	6871	GLS	Run in open borehole with 467.3 feet of 10-inch surface casing.
	4/9/06	Well-completion	0	1,175	X		X		X		X						X	6904	GLS	Run inside 2-inch stainless steel casing with 467.3 feet of 10-inch surface casing.
	2/24/06 - 2/28/06	Open-hole	480	1,385 (maximum)								X						6866	GLS	Run in 6.5-inch open borehole with 467.3 feet of 10-inch surface casing. Multiple logs were run as part of Fluid Electrical Conductivity (FEC) testing. Primary FEC data sets.
	2/24/06 - 2/28/06	Open-hole	480	1,386 (maximum)	X				X	X	X		X					6867	GLS	Run in 6.5-inch open borehole with 467.3 feet of 10-inch surface casing. Conventional open-hole logging data collected in conjunction with FEC data.
32P	4/10/06	Open-hole	0	995	X				X	X	X		X	X				6901	GLS	Run in 6.5-inch open borehole with 53.5 feet of 8.625-inch surface casing.
	4/19/06	Open-hole	0	775												X		6903	GLS	Video run in open borehole with 53.5 feet of 8.625-inch surface casing.
	4/19/06	Open-hole	50	775												X		6903	GLS	Optical televiwer run in open borehole with 53.5 feet of 8.625-inch surface casing.
	4/11/06 - 4/12/06	Open-hole	320	960 (maximum)								X						6902	GLS	Run in open borehole with 297.3 feet of temporary steel casing and 53.5 feet of 8.625-inch surface casing. Multiple logging runs made as part of FEC testing. Primary FEC data sets.
33P	2/27/06	Drill-string	0.6	652.7	X	X		X										6862	Century	Run in 5.5-inch steel casing inside 6.25-inch borehole with 55 feet of 10.875-inch surface casing.
	2/28/06	Open-hole	0	637	X		X		X	X	X		X	X	X		X	6864	GLS	Run in 6.25-inch open borehole with 58.9 feet of 10-inch surface casing.

**Table 4.1-1
Summary Table of Nye County Monitoring Wells**

Location	Number of Wells Monitored	Period of Record	Corresponding NWRPO RID
EWDP	51	5/99 - 12/06	7122 (Manual) Multiple RIDS for Westbay Water Levels
Pahrump Valley	70	12/99 - 12/06	7045
Amargosa Desert	25	12/99 - 12/06	7045
Stewart Valley	1	8/03 - 12/06	7045
Chicago Valley	1	4/04 - 12/06	7045
Death Valley	2	5/05 - 12/06	7045
Crystal	1	12/99 - 12/06	7045

Table 5.1-1
Well Sampling History

Well/ Borehole	Private (Public) Well	Sampling Date	Sampling Interval (ft)	Sample Type			Analyses								Comments
				First Water Encountered During Drilling	Pre- Development/Purging	Post Well Development/Purging	Gross Chemistry	Field Electrode/Probe Measurements	Trace Elements	Tritium	Gross Alpha-Beta Activity	Stable Isotopic Ratio Analyses	Carbon 14 & TDIC	Chlorine-36/35 ratio	
Amargosa Valley School	Yes	3/11/2000	unknown			X					X				From pressurized water supply tank.
Bond Gold Mining Well 13	Yes	7/19/1999	1005+				X	X	X	X	X	X	X	X	Submersible centrifugal pump.
McCracken Well	Yes	6/19/2000	100-170			X	X	X	X		X	X		X	Submersible centrifugal pump.
NC-EWDP-12P	No	3/22/2000	177.1	X			X	X			X				Bailed.
NC-EWDP-12PA	No	5/22/2000	325-384			X	X	X	X	X	X	X	X	X	Bennett pumped.
NC-EWDP-12PA	No	10/25/2000	325-384			X	X	X	X	X	X	X	X	X	Bennett pumped.
NC-EWDP-12PB	No	5/22/2000	325-385			X	X	X	X	X	X	X	X	X	Bennett pumped.
NC-EWDP-12PB	No	10/25/2000	325-385			X	X	X	X	X	X	X	X	X	Bennett pumped.
NC-EWDP-12PC	No	5/22/2000	170-230			X	X	X	X	X	X	X	X	X	Bennett pumped.
NC-EWDP-12PC	No	10/25/2000	170-230			X	X	X	X	X	X	X	X	X	Bennett pumped.
NC-EWDP-15P	No	2/27/2000	210		X		X	X			X				Bailed.
NC-EWDP-15P	No	5/23/2000	200-260			X	X	X	X	X	X	X	X	X	Bennett pumped.
NC-EWDP-15P	No	10/26/2000	200-260			X	X	X	X	X	X	X	X	X	Bennett pumped.
NC-EWDP-19D	No	5/13/2000	7 zones			X	X	X	X	X	X	X	X	X	Submersible centrifugal pump.
NC-EWDP-19P	No	3/10/2000	366.4	X			X	X			X				Bailed.
NC-EWDP-19P	No	5/23/2000	359-459			X	X	X	X	X	X	X	X	X	Bennett pumped.
NC-EWDP-1DX	No	12/12/1998	70	X			X	X							Bailed, water level at 70 ft.
NC-EWDP-1DX	No	12/12/1998	240	X			X	X	X	X					Air-lifted from 240 ft.
NC-EWDP-1DX	No	5/24/1999	2160-2240			X	X	X	X	X	X	X	X	X	Bennett pump at 210 ft.
NC-EWDP-1DX	No	5/24/1999	2160-2240			X	X	X	X	X	X	X	X	X	Bennett pump.
NC-EWDP-1DX	No	5/25/2000	2160-2240			X	X	X	X	X	X	X	X	X	Bennett pumped.
NC-EWDP-1S	No	1/27/1999	60	X			X	X	X	X		X			Bailed 3 times.
NC-EWDP-1S	No	5/17/1999	210-270			X	X	X	X	X	X	X	X	X	Bennett pump set at 250 ft.
NC-EWDP-1S	No	5/17/1999	160-180			X	X	X	X	X	X	X	X	X	Bennett pump.
NC-EWDP-1S	No	5/18/1999	160-180			X	X	X	X	X	X	X	X	X	Bennett pump at 150-160 ft.
NC-EWDP-1S	No	11/8/1999	210-270			X	X	X	X	X	X	X	X	X	Bennett pumped.
NC-EWDP-1S	No	11/8/1999	160-180			X	X	X	X	X	X	X	X	X	Bennett pumped.
NC-EWDP-1S	No	5/18/2000	210-270			X	X	X	X	X	X	X	X	X	Bennett pumped.
NC-EWDP-1S	No	5/19/2000	160-180			X	X	X	X	X	X	X	X	X	Bennett pumped.
NC-EWDP-2D	No	1/14/1999	312	X			X	X	X	X		X			Bailed sample, water level at 312 ft.

NC-EWDP-3D	No	1/24/1999	240	X			X	X	X			X			USGS collected 1/23/99, bailed.
NC-EWDP-3D	No	1/24/1999	240	X			X								Duplicate.
NC-EWDP-3D	No	2/17/1999	323		X		X	X	X	X		X			Submersible centrifugal pump in casing at 323 ft.
NC-EWDP-3D	No	2/17/1999	323		X		X								Duplicate.
NC-EWDP-3S	No	5/20/1999	478-520			X	X	X	X	X	X	X	X	X	Bennett pump at 450 ft.
NC-EWDP-3S	No	5/20/1999	338-420			X	X	X	X	X	X	X	X	X	Bennett pump at 390 ft.
NC-EWDP-3S	No	11/15/1999	478-520			X	X	X	X	X	X	X	X	X	Bennett pumped.
NC-EWDP-3S	No	11/15/1999	338-420			X	X	X	X	X	X	X	X	X	Bennett pumped.
NC-EWDP-3S	No	5/17/2000	478-520			X	X	X	X	X	X	X	X	X	Bennett pumped.
NC-EWDP-4PA	No	1/9/2000	398-429	X			X	X	X		X	X			Bailed.
NC-EWDP-4PA	No	2/23/2000	405-485		X		X	X			X				Stainless steel logging bailer.
NC-EWDP-4PA	No	3/2/2000	405-485			X	X	X	X	X	X	X	X	X	Bennett pumped.
NC-EWDP-4PA	No	5/15/2000	405-485			X	X	X	X	X	X	X	X	X	Bennett pumped.
NC-EWDP-4PA	No	10/26/2000	405-485			X	X	X	X	X	X	X	X	X	Bennett pumped.
NC-EWDP-4PB	No	2/23/2000	740-839		X		X	X			X				Stainless steel logging bailer.
NC-EWDP-4PB	No	3/2/2000	740-839			X	X	X	X	X	X	X	X	X	Bennett pumped.
NC-EWDP-4PB	No	5/16/2000	740-839			X	X	X	X	X	X	X	X	X	Bennett pumped.
NC-EWDP-4PB	No	5/26/2000	740-839			X	X	X	X	X	X	X	X	X	Bennett pumped.
NC-EWDP-4PB	No	10/26/2000	740-839			X	X	X	X	X	X	X	X	X	Bennett pumped.
NC-EWDP-5S	No	2/8/1999	378	X			X	X	X	X		X			Bailed.
NC-EWDP-5SB	No	5/16/2000	379-489			X	X	X	X	X	X	X	X	X	Bennett pumped.
NC-EWDP-5SB	No	5/17/2000	379-489			X	X	X	X	X	X	X	X	X	Bennett pumped.
NC-EWDP-5SB	No	5/17/2000	379-489			X	X	X	X	X	X	X	X	X	Duplicate sample for tritium.
NC-EWDP-5SB	No	10/23/2000	379-489			X	X	X	X	X	X	X	X	X	Bennett pumped.
NC-EWDP-7S	No	2/25/2000	21		X		X	X			X				Bailed.
NC-EWDP-7S	No	10/24/2000	28-40			X	X	X	X	X	X	X	X	X	Bennett pumped.
NC-EWDP-9S	No	12/12/1998	99	X			X	X	X			X			Bailed, from about 100 ft.
NC-EWDP-9SX	No	1/15/1999	132		X		X	X	X	X		X		X	Pumped with submersible centrifugal pump during spinner test, open hole.
NC-EWDP-9SX	No	5/18/1999	330-340			X	X	X	X	X	X	X	X	X	Bennett pump at 310.2 ft.
NC-EWDP-9SX	No	5/19/1999	250-290			X	X	X	X	X	X	X	X	X	Bennett pump at 270.4 ft.
NC-EWDP-9SX	No	5/19/1999	140-160			X	X	X	X	X	X	X	X	X	Bennett pump at 150 ft.
NC-EWDP-9SX	No	5/19/1999	90-120			X	X	X	X	X	X	X	X	X	Bennett pump at 111 ft.
NC-EWDP-9SX	No	11/9/1999	330-340			X	X	X	X	X	X	X	X	X	Bennett pumped.
NC-EWDP-9SX	No	11/9/1999	250-290			X	X	X	X	X	X	X	X	X	Bennett pumped.
NC-EWDP-9SX	No	11/10/1999	140-160			X	X	X	X	X	X	X	X	X	Bennett pumped.
NC-EWDP-9SX	No	11/10/1999	90-120			X	X	X	X	X	X	X	X	X	Bennett pumped.
NC-EWDP-9SX	No	5/19/2000	250-290			X	X	X	X	X	X	X	X	X	Bennett pumped.

NC-EWDP-9SX	No	5/20/2000	140-160			X	X	X	X	X	X	X	X	X	Bennett pumped.
NC-EWDP-9SX	No	5/20/2000	90-120			X	X	X	X	X	X	X	X	X	Bennett pumped.
Ponderosa Dairy	Yes	4/25/2000	350-400			X	X	X	X		X	X		X	Submersible centrifugal pump.
UE#25-ONC#1	No	12/15/1994	1458	X			X	X				X			Teflon bailer, saturated zone.
UE#25-ONC#1	No	12/22/1994	1428	X			X	X				X			Air-lifted, collected from cyclone.
NC-EWDP-19IM	No	11/14/2001	410-430			X	X		X	X		X			Bennett pumped.
NC-EWDP-19IM1 (blind field duplicate)	No	11/14/2001	410-431			X	X		X	X		X			Bennett pumped.
NC-EWDP-19IM1	No	11/15/2001	515-535			X	X		X	X		X			Bennett pumped.
NC-EWDP-19IM1	No	11/15/2001	575-675			X	X		X	X		X			Bennett pumped.
NC-EWDP-19IM1	No	11/15/2001	725-785			X	X		X	X		X			Bennett pumped.
NC-EWDP-19IM1	No	11/15/2001	850-950			X	X		X	X		X			Bennett pumped.
J-13 well	No	11/28/2001	996-3488			X	X		X	X		X			Submersible centrifugal pump.
J-13 well (blind field duplicate)	No	11/28/2001	996-3488			X	X		X	X		X			Submersible centrifugal pump.
NC-EWDP-10P	No	8/27/2002	801-860			X	X	X	X	X	X	X			Bennett pumped.
NC-EWDP-10P	No	8/27/2002	660-699			X	X	X	X	X	X	X			Bennett pumped.
NC-EWDP-10S	No	9/12/2002	660-700			X	X	X	X	X	X	X			Bennett pumped.
NC-EWDP-10S	No	9/11/2002	800-860			X	X	X	X	X	X	X			Bennett pumped.
NC-EWDP-18P	No	8/26/2002	835-885			X	X	X	X	X	X	X			Bennett pumped.
NC-EWDP-22PA	No	8/28/2002	661-759			X	X	X	X	X	X	X			Bennett pumped.
NC-EWDP-22PA	No	8/28/2002	520-579			X	X	X	X	X	X	X			Bennett pumped.
NC-EWDP-22PA blind field duplicate	No	8/28/2002	520-579			X	X	X	X		X	X			Bennett pumped.
NC-EWDP-22PB	No	8/30/2002	1140-1179			X	X	X	X	X	X	X			Bennett pumped.
NC-EWDP-22PB	No	8/29/2002	881-979			X	X	X	X	X	X	X			Bennett pumped.
NC-EWDP-22S	No	9/11/2002	521-581			X	X	X	X	X	X	X			Bennett pumped.
NC-EWDP-22S	No	9/10/2002	661-760			X	X	X	X	X	X	X			Bennett pumped.
NC-EWDP-22S	No	9/10/2002	880-980			X	X	X	X	X	X	X			Bennett pumped.
NC-EWDP-22S blind field duplicate	No	9/10/2002	880-980			X	X	X	X		X	X			Bennett pumped.
NC-EWDP-22S	No	9/9/2002	1140-1180			X	X	X	X	X	X	X			Bennett pumped.
NC-EWDP-23P	No	10/1/2002	650-689			X	X	X	X	X	X	X			Bennett pumped.
NC-EWDP-7SC	No	9/13/2002	80-90			X	X	X	X	X	X	X			Bennett pumped.
NC-EWDP-7SC	No	9/13/2002	180-210			X	X	X	X	X	X	X			Bennett pumped.
NC-EWDP-7SC	No	10/3/2002	270-370			X	X	X	X	X	X	X			Bennett pumped.
NC-EWDP-22S-Z1	No	8/5/2003	522 -579.80			X	X				X				
NC-EWDP-22S-Z1	No	8/5/2003	522 -579.80			X	X				X				
NC-EWDP-22S-Z2	No	8/12/2003	662-759.5			X	X	X	X	X	X	X	X		Turbidity was between 0.3 and 2.0.
NC-EWDP-22S-Z3	No	9/9/2003	882-979.5			X	X	X	X	X	X	X	X		DO probe calibrated, greater than 3 well volumes purged.
NC-EWDP-22S-Z4	No	9/23/2003	1142-1179.5			X	X	X	X	X	X	X	X		Greater than 3 well columns purged.

NC-EWDP-27P	No	9/29/2003	580.70-620.60			X	X	X	X	X	X	X	X		Turbidity values not stable.
NC-EWDP-28P	No	9/30/2003	370-449			X	X	X	X	X	X	X	X		Turbidity unstable.
NC-EWDP-24P	No	9/30/2003	400-440			X	X	X	X	X	X	X	X		
NC-EWDP-19P	No	10/1/2003				X	X	X	X		X				Negative ORP; turbidity unstable.
NC-EWDP-29P	No	10/1/2003	340-390			X	X				X				
NC-EWDP-19P	No	10/1/2003				X	X				X				
NC-EWDP-4PB	No	10/2/2003	739.5-839.2			X	X	X	X	X	X	X	X		Turbidity unstable-lots of air in line.
NC-EWDP-10P Shallow	No	10/6/2003	663.5-702.7			X	X	X	X	X	X	X	X		
NC-EWDP-10P-Deep	No	10/7/2003	801.20-860			X	X	X	X	X	X	X	X		
NC-EWDP-22PA Shallow	No	10/7/2003	520.8-579.7			X	X	X	X	X	X	X	X		Air in lines; DO, turbidity and ORP unstable.
NC-EWDP-22PA-Deep	No	10/8/2003	661.4-759.8			X	X	X	X	X	X	X	X		DO=108%.
NC-EWDP-22PB Shallow	No	10/9/2003	881.3-979.7			X	X	X	X	X	X	X	X		No air in line; very stable and matches LANL meter.
NC-EWDP-22PB Shallow	No	10/9/2003	881.3-979.7			X	X				X				
NC-EWDP-22PB-Deep	No	10/10/2003	1140.3-1179.7			X	X	X	X	X	X	X	X		Air in line switched to nitrogen; after 2 hours with nitrogen there is no change in DO.
NC-EWDP-23P Shallow	No	10/13/2003	460-520			X	X	X	X	X	X	X	X		Air in line-DO may be affected; turbidity ranges from 20-30 NTU.
NC-EWDP-23P-Deep	No	10/15/2003	650-690			X	X	X	X	X	X	X	X		
NC-EWDP-18P	No	10/16/2003				X	X	X	X	X	X	X	X		Negative turbidity reading; switch to nitrogen.
NC-EWDP-19IM1A-Z5	No	10/27/2003				X	X	X	X	X	X	X	X		
NC-EWDP-16P	No	10/28/2003				X	X				X				
NC-EWDP-19IM2A	No	10/29/2003				X	X	X	X	X	X	X	X		
NC-EWDP-19D	No	10/29/2003				X	X	X	X						Negative ORP (-252.3).
NC-EWDP-7SC-Z4	No	10/30/2003	429.8-449.8			X	X				X				
NC-EWDP-7SC-Z3	No	10/31/2003	270-370			X	X	X	X	X	X	X	X		Stopped pumping at 1600.
NC-EWDP-7SC-Z2	No	11/3/2003	180-210			X	X	X	X	X	X	X	X		Negative ORP (-76.2).
NC-EWDP-19IM1A-Z1	No	11/3/2003				X	X	X	X						
NC-EWDP-7SC-Z1	No	11/4/2003	80-90			X	X	X	X	X	X	X	X		Negative ORP (-28.1).
NC-EWDP-3S-Z2	No	11/4/2003				X	X				X				
NC-EWDP-10S-Z1	No	11/6/2003	662-699.5			X	X	X	X	X	X	X	X		
NC-EWDP-10S-Z2	No	11/7/2003	802-8659.5			X	X	X	X	X	X	X	X		Negative ORP (-14.1).
NC-EWDP-19PB-Deep	No	5/10/2004	514.7-534.7			X	X				X				
NC-EWDP-19PB Shallow	No	5/11/2004	375-395			X	X				X				
NC-EWDP-19PB Shallow	No	5/11/2004	375-395			X	X				X				
NC-EWDP-4PA	No	11/10/2004	405.3-485.2			X	X				X				
NC-EWDP-4PA	No	11/10/2004	405.3-485.2			X	X				X				
NC-EWDP-4PA	No	12/6/2004	405.3-485.2			X	X				X				
UE-25 WT#3	Yes	4/25/2005			X		X								
UE-25 WT#17	Yes	4/26/2005			X		X								

USW WT#1	Yes	4/27/2005			X		X								
USW WT#1	Yes	4/27/2005			X		X								
NC-EWDP-13P	No	6/21/2005				X	X								
NC-EWDP-27P	No	9/20/2005	580.7-620.6			X	X			X	X		X		
NC-EWDP-16P	No	9/20/2005				X	X			X	X		X		
NC-EWDP-28P	No	9/21/2005	370-449			X	X			X	X		X		
NC-EWDP-28P	No	9/21/2005	370-449			X	X			X	x		X		
NC-EWDP-28P	No	9/21/2005	370-449			X	X								
NC-EWDP-24P	No	9/22/2005	400-440			X	X			X	X		X		
NC-EWDP-29P	No	9/23/2005	340-390			X	X	X	X	X	X		X		
NC-EWDP-12PA	No	9/27/2005	324.7-384.4			X	X			X	X		X		
NC-EWDP-12PA	No	9/27/2005	324.7-384.4			X	X			X	X		X		
NC-EWDP-12PB	No	9/28/2005	325-384			X	X			X	X		X		
NC-EWDP-1DX Deep	No	9/29/2005	2160-2240			X	X	X			X		X		
NC-EWDP-19IM1 zone 1	No	10/4/2006					X	X				X	X		
NC-EWDP-19IM1 zone 5	No	10/4/2006					X	X			X	X	X		
NC-EWDP-1S zone 1	No	10/4/2006					X	X			X	X	X		
NC-EWDP-1S zone 2	No	10/4/2006					X	X			X	X	X		
NC-EWDP-9SX zone 1	No	10/4/2006					X	X			X	X	X		
NC-EWDP-9SX zone 2	No	10/4/2006					X	X			X	X	X		
NC-EWDP-9SX zone 3	No	10/4/2006					X	X			X	X	X		
NC-EWDP-9SX zone 4	No	10/4/2006					X	X			X	X	X		
NC-EWDP-1S zone 2 blind field duplicate	No	10/4/2006					X	X			X	X	X		
NC-EWDP-13P	No						X	X			X	X	X		
NOTE: 1 ft. = 0.3048 meters.															
N/F= not found															

Table 6.0-1: Test Zone Intervals in Multiple Screen Pump Wells and Observation Wells

Well Name	Well Type	Well Zone	Sandpack Depth Interval (ft, bgs)		Sandpack Thickness (ft)	Lithology at Sandpack	Screen Depth Interval (ft, bgs)		Screen Length (ft)
			From	To			From	To	
10S	Pump & Spinner Logging	1	653.4	709.0	55.6	Alluvium (mainly silty sand with gravel)	660.0	700.0	40.0
		2	795.6	900.0	104.4	Tertiary Volcanic Conglomerate	800.0	860.0	60.0
10P	Observation	1	652.0	796.1	144.1	Alluvium (mainly silty sand with gravel)	663.5	702.7	39.2
		2	776.2	910.5	134.3	Tertiary Volcanic Conglomerate	801.2	860.0	58.8
19IM1	Pump and Spinner	1	401.4	438.0	36.6	Alluvium (mainly silty sand with gravel)	410.0	430.0	20.0
		2	506.0	543.0	37.0	Alluvium (mainly silty sand with gravel)	515.0	535.0	20.0
		3	565.8	686.7	120.9	Alluvium (mainly silty sand with gravel)	574.9	674.9	100.0
		4	718.1	795.6	77.5	Alluvium (mainly silty sand with gravel)	724.9	784.8	59.9
		5	843.2	967.3	124.1	Tertiary Tuff	849.5	949.3	99.8
19IM2	Pump, Spinner, and Observation	1	389.4	440.7	51.3	Alluvium (mainly silty sand with gravel)	410.2	430.2	20.0
		2	503.2	547.4	44.2	Alluvium (mainly silty sand with gravel)	515.0	534.9	19.9
		3	565.9	681.1	115.2	Alluvium (mainly silty sand with gravel)	574.9	674.9	100.0
		4	718.9	795.6	76.7	Alluvium (mainly silty sand with gravel)	724.9	784.9	60.0
		5	842.3	965.6	123.3	Tertiary Tuff	849.9	950.1	100.2
19D	Observation	5	834.0	1061.0	227.0	Tertiary Tuff	881.1	981.0	99.9
22S	Pump and Spinner	1	513.4	586.3	72.9	Alluvium (mainly silty sand with gravel)	521.5	581.3	59.8
		2	651.8	766.5	114.7	Alluvium (mainly silty sand with gravel)	661.2	760.6	99.4
		3	870.3	986.9	116.6	Alluvium (mainly silty sand with gravel)	880.2	980.0	99.8
		4	1133.2	1196.5	63.3	Tertiary Volcanic Conglomerate	1140.0	1180.0	40.0
22PA	Observation	1	508.7	587.0	78.3	Alluvium (mainly silty sand with gravel)	520.7	579.7	59.0
		2	649.7	779.8	130.1	Alluvium (mainly silty sand with gravel)	661.5	759.8	98.3
22PB	Observation	3	870.7	989.2	118.5	Alluvium (mainly silty sand with gravel)	881.3	979.7	98.4
		4	1125.2	1199.7	74.5	Tertiary Volcanic Conglomerate	1140.3	1179.7	39.4

Table 6.2-1
Allocation of Constant Rate Pump Test Transmissivity to Zone Intervals Based on Pump Spinner Logging

Pump and Spinner Logging Well 19IM1						
Zone	Zone 1	Zone 2	Zone 3	Zone 4	Zone 5	Total or Average
Thickness (ft)	36.6	37	120.9	77.5	124.1	396.1
Allocated Rate (gpm)	11	11	79	10	12	123
Allocated Percent of Transmissivity	9	9	64	8	10	100
Transmissivity (ft²/day)	288	288	2048	256	320	3200 ^a
Hydraulic Conductivity (ft/day)	7.9	7.8	16.9	3.3	2.6	7.7 ^b
Pump and Spinner Logging Well 19IM2						
Zone	Zone 1	Zone 2	Zone 3	Zone 4	Zone 5	Total
Thickness (ft)	51.3	44.2	115.2	76.7	123.3	410.7
Allocated Rate (gpm)	13	16	83	16	28	156
Allocated Percent of Transmissivity	12	10	51	10	17	100
Transmissivity (ft²/day)	924	770	3927	770	1309	7700 ^a
Hydraulic Conductivity (ft/day)	18.0	17.4	34.1	10.0	10.6	18.0 ^b
Pump and Spinner Logging Well 22S						
Zone	Zone 1	Zone 2	Zone 3	Zone 4	Zone 5	Total
Thickness (ft)	72.9	114.7	116.6	63.3	NA ^c	367.5
Allocated Rate (gpm)	43	53	23	13	NA	132
Allocated Percent of Transmissivity	33	40	17	10	NA	100
Transmissivity (ft²/day)	4868	5900	2508	1475	NA	14750 ^a
Hydraulic Conductivity (ft/day)	66.8	51.4	21.5	23.3	NA	40.6 ^b

^a Calculated from constant rate pump test in open wellbore.

^b Average

^c Not Applicable

Table 6.2-2
Constant Rate Pump Test Data and Analysis Results

Pumping Well Name	Well Type											
	Pumping/Spinner Logging	Observation	Well Zones	Total Zone Thickness (ft)	Pumping Rate (gpm)	Pumping Time (hours)	Recovery Time Monitoring (hours)	Transmissivity (ft ² /day)	Permeability (darcy)	Storage Coefficient (ft/ft)	Apparent Skin Factor	Well Efficiency (%)
19IM1	x		1, 2, 3, 4, 5	409	120	49.5	51	3200	2.2		9	48
19IM2	x		1, 2, 3, 4, 5	412	154	48	94	7700	5.27		37	16
19IM2		x	5	130	120	49.5	51	1015	2.2	0.007		
19D		x	5	130	120	49.5	51	1015	2.2	0.00073		
22S	x		1, 2, 3, 4	369	133	~24	~15	15500	14.5		32	19
22S	x		1	72.9	43.5	11	>10	2600	12	0.00116	12	30
22S	x		2	114.7	44.1	11	>10	4600	14	0.00035	33	16
22S	x		3	116.6	27.1	11	>10	1500	4.5	0.0001	17	27
22S	x		4	63.3	20.5	11	>10	2000	11	0.00021	7	15
22PA		x	1	72.9	44	~24	~15	3400	16	0.0016		
22PA		x	2	114.7	53	~24	~15	5900	17.7	0.00031		
22PB		x	3	116.6	23	~24	~15	2550	7.5	0.00002		
22PB		x	4	63.3	13	~24	~15	2900	15.4	0.00023		
10S	x		1,2	160	107	48	48	920	2		0.9	90
											50	12
10P		x	1	56	102	48	48	650	4.2	0.00063		
10P		x	2	104	5	48	48	270	0.9	0.00084		

Table 7.1-1: Tracer Test Injection and Pumping Summary

Tracer Test Type and Number	Forced or Natural Gradient	Test Number	Cross-Hole Phase	Tracer Injection Information							Chase Water Information	Chase Water Injection Start Date/Time	Chase Water Injection Rate (gpm)	EC and Temp Monitored Injection Well or Piezometer	Pumping Well Information					
				Injection Well or Piezometer No.	Injection Zone	Tracers	Tracer Mass (Kg)	Tracer Solution Volume (gals)	Tracer Injection Start (date/time)	Tracer Injection Rate (gpm)	Chase Water Volume (gals)				Pumping Well	Pumping Zone	Pumping Start (Date/Time)	Pumping Stop (Date/Time)	Average Pumping Rate (gpm)	Recovery Volume (gals)
Single-Well Push/Pull	Forced	1		22S	2	NaI	3	1.054	12/2/04 14:51	17.3	19,842	12/2/04 15:52	17.9	Yes	22S	2	12/6/2004	12/10/2004	47.3	295,060
						PFBA	1													
						NaI	3	1032	12/13/04 14:42	15.4	19,534	12/13/04 15:49	16.3	Yes	22S	2	1/13/2005	3/20/2005	47.8	4,408,166
Cross-Hole	Forced	1	1	22PA Deep	2	LiBr	25	256.7	1/14/05 10:27	11.7	95.5	1/14/05 10:49	6.8	Yes	22S	2	1/13/2005 8:51	10/13/2005 9:41	48.0	7,765,074
						LiCl	97													7,765,074
						2,4,5-TFBA	8.5													7,765,074
	Forced	2	1	22PC Deep	2	2,6-DFBA	8.5	275.9	1/14/05 11:10	11.7	98.6	1/14/05 11:32	6.8	Yes	22S	2	1/13/2005 8:51	10/13/2005 9:41	48.0	7,765,074
	Forced	3	1	22PA Shallow	1	2,5-DFBA	1.5	278.5	1/14/05 11:59	9.0	32.8	1/14/05 12:30	4.7	Yes	22S	2	1/13/2005 8:51	10/13/2005 9:41	48.0	7,765,074
	Forced	4	1	22PA Deep	2	Micro-sphere Colloids	2.E-03	271.8	1/24/05 13:12	15.0	87.9	1/24/05 13:25	12.8	Yes	22S	2	1/13/2005 8:51	10/13/2005 9:41	48.0	4,408,166
	Forced	5	2	22PA Deep	2	NaI	5	254.5	8/25/05 12:06	11.2	95.4	8/25/05 12:29	10.0	Yes	22S	2	8/24/2005 11:03	10/13/2005 9:41	49.3	3,567,936
						NaReO ₄	1.E-01													3,567,936

Table 7.2.-1: Summary of Final Calibration Parameters for Tracer Tests at Site 22

Tracer Test	Tracer Response Calibrated	Effective Porosity %	Dispersivity (longitudinal) ft	Dispersivity (transverse) ft	Dispersivity (vertical) ft	Hydraulic Conductivity ft/day	Diffusivity Coefficient ft ² /day
Cross-hole test 1	Bromide	8.2	20	4	0.2	35	0.0002
Cross-hole test 2	2,6-DFBA	24	7	1.4	0.07	65	0.0002
Single-well test 1	Iodide	0.24	0.2	0.02	0.002	65	0.0002
Single-well test 2	Iodide	0.24	1	0.1	0.01	65	0.0002